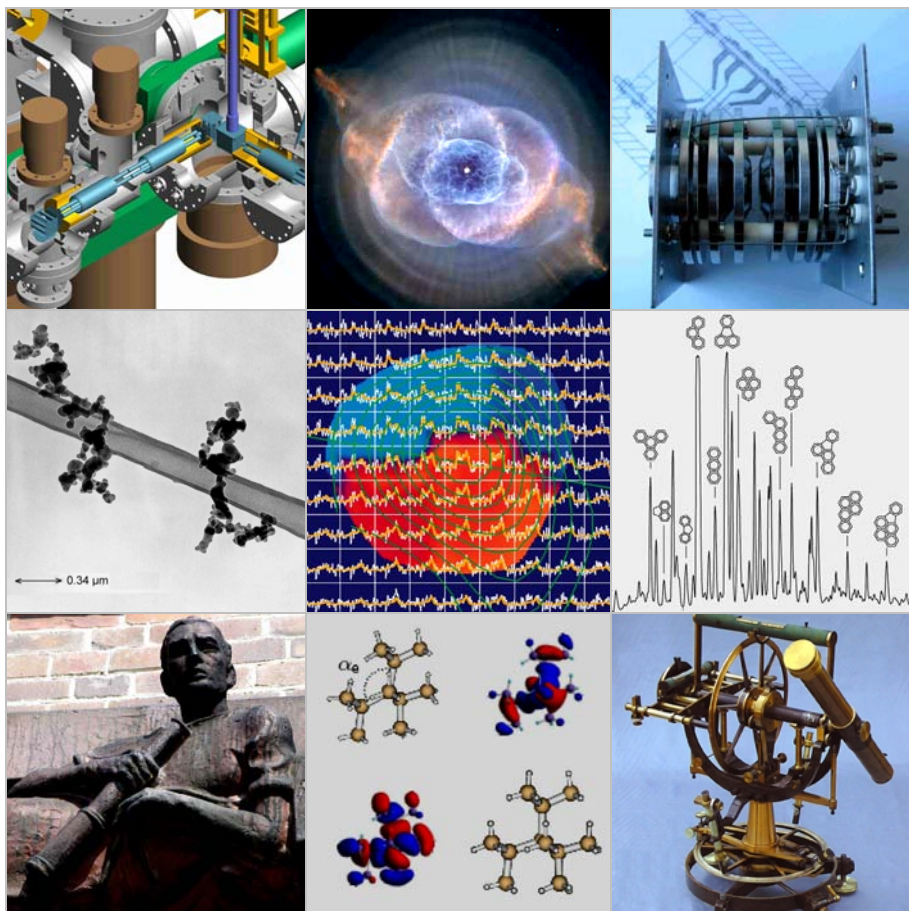


TU Chemnitz

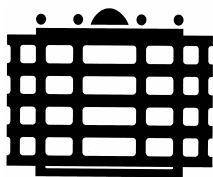
Laboratory Astrophysics



FSU Jena



DFG-Forschergruppe 388, Report 2003 - 2006
Dieter Gerlich and Thomas Henning



TU Chemnitz



FSU Jena

Structure, Dynamics and Properties of Molecules and Grains in Space

FOR 388
Report 2003 - 2006

Dieter Gerlich and Thomas Henning

Figures shown on the title page

1a Next generation ion trapping machine for astrochemistry (TP 5, Fig. 10)

1b Cat's Eye Nebula (NGC 6543), constellation of Draco (Hubble 2004).

1c Quadrupole trap for studying interstellar dust analogues (TP 7, Fig. 4)

2a TEM image of soot (TP 8, Fig. 9)

2b Dense protoplanetar disc, simulation (TP 3, Fig. 2)

2c Liquid chromatogram of carbonaceous powder (TP 11, Fig. 5)

3a Georgius Agricola Gymnasium, Chemnitz

3b Calculated orbital for $\text{Si}_{17}\text{H}_{36}$ (TP 2, Fig. 2)

3c Meridian circle (Pistor & Martins 1862), Lohrmann Observatory, Dresden

Inhalt / Contents

Vorbemerkung / Preface	1
1. Allgemeine Angaben / General information	3
2. Gesamtkonzept / Basic concept	7
3. Darstellung der Teilprojekte / Individual projects	43
TP 1 Molecular dynamics simulation of formation and reactivity of molecules and clusters <i>G. Seifert, R. Scholz</i>	43
TP 2 Theoretical investigations of the spectroscopic properties of silicon nanocrystals <i>R. Scholz, M. Schreiber</i>	67
TP 3 Astrophysical modeling – chemistry in protoplanetary disks <i>T. Henning</i>	83
TP 4 Infra-red and far infra-red spectroscopy of molecular ions: from the hydronium ion (H_3O^+) via clusters to ice <i>S. Schlemmer</i>	95
TP 5 Reactions of stored cold ions with H atoms and molecules of interstellar relevance <i>D. Gerlich, A. Luca</i>	115
TP 6 Photophysics and Photochemistry at Interfaces of Silicon Nanoparticles <i>F. Cichos, C. von Borczyskowski</i>	139
TP 7 Growth and destruction of carbon-rich molecules and clusters under inter- and circumstellar conditions <i>D. Gerlich</i>	159
TP 8 Gas phase condensation of carbon nanoparticles and their structural characterization <i>H. Mutschke</i>	181
TP 9 Infrared spectroscopy and light scattering of dust agglome- rates <i>H. Mutschke, J. Blum</i>	213
TP 11 Spectroscopy of astrophysically relevant molecules in the gas phase and in ultracold helium droplets <i>F. Huisken</i>	229
TP 12 Silicon nanocrystals in matrices and their relation to the Extended Red Emission <i>F. Huisken, W. Witthuhn</i>	249

First funding period (2000 - 2003)

- TP1 Molecular dynamics simulation of structure, formation and reactivity of molecules and clusters*
R. Scholz, M. Schreiber, G. Seifert
- TP2 Theoretical study of the electron transfer between adsorbed molecules and the substrate*
U. Kleinekathöfer, M. Schreiber
- TP3 Astrophysical modeling - the chemical evolution of protoplanetary disks*
T. Henning
- TP4 The role of fine structure, rotational and zero point energy in slow collisions*
S. Schlemmer, D. Gerlich
- TP5 Reactions of H atoms with ions and nanoparticles*
D. Gerlich, S. Schlemmer, I. Čermák
- TP6 Single molecule spectroscopy of aromatic hydrocarbons on silicon crystalline nanoparticles*
F. Cichos, C. von Borczyskowski
- TP7 Growth dynamics of carbon-containing nanostructures*
I. Čermák, D. Gerlich
- TP8 Gas-phase condensation of carbonaceous nanoparticles and their structural characterization*
H. Mutschke, T. Henning
- TP9 Infrared spectroscopy of isolated sub-micron oxide particles*
H. Mutschke
- TP10 Agglomerates and light scattering*
J. Dorschner, G. Wurm

Vorbemerkungen / Preface

From 2000 to 2006 the Deutsche Forschungsgemeinschaft has supported the Forschergruppe *Laboratory Astrophysics: Structure, Dynamics and Properties of Molecules and Grains in Space*, briefly called **FGLA**. Laboratory astrophysics and astrochemistry belongs to an interdisciplinary research area covering the physics and chemistry of molecules, clusters, nanoparticles, and grains under the conditions of interstellar space, ranging from low temperature and low density molecular clouds to hot environments of stars. It was our aim to study the microphysics which control the formation and destruction of interstellar matter and to use the results for understanding observational facts and for predicting new astrophysical features.

In this final report we briefly review the overall achievements ranging from the proposal written in December 1999 which was based on a very efficient exchange of ideas from research groups in Chemnitz and Jena to the perspectives where our research is going to. A vital part of the scientific life of the Forschergruppe was the close interaction with the guest researchers. In addition, the regular joint **FGLA** seminars and special symposia were very important for all of us. One of the highlights was the international meeting *Interstellar Reactions: from Gas Phase to Solids*, we have organized in 2005 in Pillnitz.

As usual in such a group where many young and active researchers are project leaders, there are changes due to promotion, habilitation and new appointments. These alterations are summarized in chapter 2.3. Everything started in Chemnitz and Jena, but projects and people moved to Dresden, Heidelberg, Köln, Leiden, and München. The changes also can be seen by comparing the list of projects and project leaders from the first and the second funding period.

The activities of the individual projects are summarized in the main part of this report with emphasis on the second funding period (2003-2006). These contributions reveal that the theoretical and experimental projects have made major contributions to the field of laboratory astrophysics and -chemistry: worldwide, the FGLA has become an attractive center in its field. We thank our universities and institutions for their help and especially the DFG for the generous financial support.

Chemnitz, Dresden, Heidelberg, Jena, Köln

January 2007

Dieter Gerlich

Preface

1 Allgemeine Angaben / General information

1.1 Chairman

Gerlich, Dieter Prof. Dr. Dipl. Phys., Universitätsprofessor,
Institut für Physik, Technische Universität
09107 Chemnitz

gerlich@physik.tu-chemnitz.de
<http://www.tu-chemnitz.de/FGLA/>

Henning, Thomas, Prof. Dr., Institutsdirektor und Professor an der
Friedrich-Schiller-Universität Jena
Max-Planck-Institut für Astronomie
69117 Heidelberg, Königstuhl 17

1.2 Title

*Laboraastrophysik: Struktur, Dynamik und Eigenschaften von
Molekülen und Staubteilchen im Weltraum*

*Laboratory astrophysics: Structure, dynamics and proper-
ties of molecules and grains in space*

1.3 Keyword

Laboratory astrophysics

1.4 Field of research

Laboratory astrophysics, physics and chemistry of cosmically
relevant molecules and grains, *ab initio* calculations, reaction dy-
namics, spectroscopy, modeling of complex systems

1.5 Berichtszeitraum / reported period

01.07.2003 - 31.12.2006 and summary of the 6 years

1.6 Zusammenfassung Abschlussbericht/ Summary final report

Wie in den beiden ersten Anträgen und in dem Zwischenbericht wird auch in diesem Berichtsband zunächst einiges an allgemeiner Information zusammengetragen. In Kapitel 2.1 wird noch einmal kurz auf den wissenschaftlichen Hintergrund eingegangen, in dem unsere Initiative einzuordnen ist. Das Forschungsgebiet, das man kurz als *Astrochemie* bezeichnen kann, erfordert verschiedene interdisziplinäre Aktivitäten. Dies wird z.B. an der Liste der Konferenzen illustriert, die Forscher der *FGLA* besucht haben. Eine Übersicht der wissenschaftlichen Ergebnisse in Kap. 2.2 erfolgt diesmal nicht, sondern statt dessen wird dort auf einen geplanten Sonderband hingewiesen, in dem unter anderem die astrophysikalisch relevanten Resultate der *FGLA* in einem größeren Rahmen zusammengestellt werden sollen. Der Arbeitstitel ist *New Frontiers in Laboratory Astrophysics – Understanding basic processes*. Im Kapitel 2.3 werden die Projektleiter der ersten und zweiten Förderperiode aufgelistet und die große Zahl von Wissenschaftlern, mit denen wir enge Kooperationen hatten. 2.4 geht auf das wissenschaftliche Leben der *FGLA* ein. Neben den Seminaren und Workshops spielte das Gästeprogramm eine sehr große Rolle. In 2.5 unterstreicht die Zusammenstellung der *FGLA* - Publikationen die Vielfalt unserer Aktivitäten in den vergangenen drei Jahren. Im Hauptteil dieses Berichtsbandes finden sich die einzelnen Beiträge der 11 Teilprojekte zur zweiten Förderperiode.

Similar to the previous proposals and to the intermediate report in 2003, this final report first summarizes some general information related to the *FGLA*. In chapter 2.1 a few remarks are made to the scientific background of the initiative we have started 7 years ago. The research field which can be briefly called *astrochemistry*, requires a lot of interdisciplinary activities. This can be seen, for example, from the variety of conferences *FGLA* researchers participated on. In this report, chapter 2.2 does not give an overview of the scientific achievements as in the previous one. Instead of that we refer to the aim to edit a special issue summarizing both results from the *FGLA* and from related activities. The working title is *New Frontiers in Laboratory Astrophysics – Understanding basic processes*. In chapter 2.3 the project leaders from the first and the second funding period are listed as well as the researchers we cooperated with. Besides the seminars and work shops which are summarized in 2.4, the guest researchers have significantly influenced the scientific life of the *FGLA*. The long list of publications given in 2.5 corroborates the diversity of scientific activities of our research group. The main part 3 contains the final reports of the 11 projects covering the second funding period.

1.7 Zusammenfassung Antrag 2002 / Summary proposal 2002

Die Deutsche Forschungsgemeinschaft (DFG) fördert seit dem 01.07.2000 die Forschergruppe *Laborastrophysik: Struktur, Dynamik und Eigenschaften von Molekülen und Staubteilchen im Weltraum*. Die Initiative, gemeinsam das Gebiet der Laborastrophysik (daher *FGLA*) zu bearbeiten, ging von der Technischen Universität Chemnitz und der Friedrich-Schiller-Universität Jena aus. In den vergangenen Jahren wurden in den zehn Teilprojekten wesentliche Beiträge zu diesem Forschungsgebiet geleistet. Obwohl eine Reihe von Veränderungen Umorganisationen in fast allen Projekten erforderte, ist dieser Verlängerungsantrag in vollem Einklang mit den Zielen des Erstantrags. In jetzt 11 Projekten sollen auf mikrophysikalischer Ebene die Zusammensetzung, die Eigenschaften sowie die Mechanismen der Bildung und Zerstörung von Bestandteilen des interstellaren Mediums bestimmt werden. Die experimentellen Projekte benutzen moderne Methoden wie Speicherapparaturen für Ionen und Nanopartikel, moderne optische und spektroskopische Methoden sowie spezielle Verfahren zur Untersuchung von Analoga der interstellaren Staubteilchen. Die theoretischen Projekte beinhalten sowohl Berechnungen zur Struktur und Dynamik von Molekülen und Nanoteilchen als auch die Modellierung der dichteren Phasen des interstellaren Mediums.

Since summer 2000, the Deutsche Forschungsgemeinschaft (DFG) supports the Forschergruppe *Laboratory Astrophysics: Structure, Dynamics and Properties of Molecules and Grains in Space*. The initiative to start a joint effort on laboratory astrophysics - therefore *FGLA* - has started from the Chemnitz University of Technology and the Friedrich Schiller University in Jena. In the last years, significant contributions to this field of research have been made within 10 projects. Although a variety of alterations have required a reorganization of most projects, this proposal, to renew the Forschergruppe, is in full accordance with the aim of the first one. In now 11 projects, we intend to study in detail the microphysics which control the formation and destruction of interstellar matter in order to understand observational facts and to predict new astrophysical features. The experimental projects encompass modern state-of-the-art techniques such as traps for ions and nanoparticles, modern optical and spectroscopic techniques, and unique methods for studying interstellar dust analogues. The theoretical activities include calculations of the structure and dynamics of molecules and nanoparticles as well as modeling of dense phases of the interstellar medium.

1.8 Zusammenfassung Antrag 1999 / Summary proposal 1999

Dieser Antrag beschreibt eine Initiative von mehreren Gruppen der Technischen Universität Chemnitz und der Friedrich-Schiller-Universität Jena für eine gemeinsame Forschergruppe auf dem Gebiet *Laborastrophysik*, (*FGLA*). Es ist das Ziel, auf mikrophysikalischer Ebene die Zusammensetzung, Eigenschaften sowie die Bildung und Zerstörung von Bestandteilen des interstellaren Mediums zu bestimmen. Hierdurch werden astrophysikalische Daten besser verständlich und neue Beobachtungen gezielter vorbereitet. Die experimentellen Projekte benutzen moderne Methoden wie die Einzelmolekülspektroskopie, Speicherapparaturen für Ionen und Nanopartikel und spezielle Verfahren zur Untersuchung von Analoga der interstellaren Staubeilchen. Die theoretischen Projekte beinhalten sowohl Berechnungen zur Struktur und Dynamik von Molekülen und Nanoteilchen als auch die Modellierung der dichteren Phasen des interstellaren Mediums.

This proposal describes an initiative of research groups from the Chemnitz University of Technology and the Friedrich Schiller University in Jena to start a joint effort on *laboratory astrophysics*, (*FGLA*). It is the aim to study in detail the microphysics, e.g. elementary collision processes, which control the formation and destruction of interstellar matter in order to understand observational facts and to predict new astrophysical features. The experimental projects encompass modern state-of-the-art techniques such as single molecule spectroscopy, traps for ions and nanoparticles, and unique methods for studying interstellar dust analogues. The theoretical activities include calculations of the structure and dynamics of molecules and nanoparticles and modeling of dense phases of the interstellar medium.

2 Gesamtkonzept / Basic concept

2.1 Astrophysical background

It is more than 7 years ago that we have started to collect ideas for the *FGLA*. Motivations came from questions raised in the fields *astrophysics* and *astrochemistry*. We knew that it was timely to start dedicated experiments for characterizing fundamental processes which occur in the interstellar medium as part of the lifecycle of matter. A typical document describing the situation at that time was the German decadal report on astronomy (*Denkschrift für Astronomie*) which recommended to support research in this field. There have been many other strategic papers for preparing new missions and observations and summaries such as the *NASA Laboratory Astrophysics White Paper* (Salama *et al.* 2002).

Meanwhile there have been various research initiatives which use the keyword *astro* for stimulating the interdisciplinary exchange between various communities (often instead of *nano* or *bio*). Universities in the US recognize more and more *astrochemistry* being an attractive interdisciplinary field emerging at the intersection of the traditional disciplines of chemistry, physics, and astronomy. In the *capital of astronomy*, Tucson, the chemistry department has started a related initiative. Other universities in the US advertise that they become *a leader in this young field*. Seminar series are started with support from the NSF. In Europe there are several related activities. Very close to the basic idea of the *FGLA* was and still is the French network PCMI (Physique et la Chimie du Milieu Interstellaire), a national cooperation which has been started more than a decade ago and which is still very active. Many European groups working in the field are members of the Research Training Network *Molecular Universe*. A comparable activity has been proposed recently in the US to the National Science Foundation with the title *Molecules in the Cosmos*.

Another evidence that the field of astrochemistry has been gaining prominence is the growing number of international scientific conferences, meetings and sessions dedicated to this area. In 2003 a large conference was devoted to cosmic dust, the 2005 Pacifichem concentrated on astrochemistry and also the American Chemical Society organized in 2006 a special session. Members of the Forschergruppe have participated and contributed to many of those meetings as can be seen from the list below (on the other hand, this list also indicates the need to stay in contact with many other communities). Project leaders of the *FGLA* have actively contributed to the organization of international conferences, the 2006 Royal Society Science Meeting *Physics, Chemistry and Astronomy of H₃⁺*

is just one example. The highlight of the *FGLA* conference activities was certainly the international 2005 *Symposium Interstellar Reactions: from the Gas phase to Solids* we have organized in Schloss Pillnitz close to Dresden. This event has been summarized separately in a *Book of Abstracts* and in a DFG report.

What is the future of laboratory astrophysics and -chemistry? In Pillnitz we have organized a round table discussion to give some answers. A lot of topics have been raised by internationally recognized researchers including program scientists from the NASA and the DFG. Certainly there is a huge demand for data which enable astronomers to analyze and interpret observations from the new instruments; however, filling larger and larger databases with spectroscopic parameters, properties of dust, ices, grains etc. is not sufficient. It is certainly true that high resolution spectra of astrophysically important molecules are the key for identifying them; however, it is of basic importance to learn more about their formation and destruction, i.e. their chemistry. The challenges are to study them under conditions which are of relevance for the early universe, for the interstellar medium, or for atmospheres of stars, planets, and comets. Moreover, there is a huge need for specific laboratory activities which help to understand the transition from the atomic scale via nanoparticles (interstellar dust) to macroscopic structures and finally to star formation.

Astronomy always has attracted the interest of young people. Lets hope that this curiosity can be transferred to *astrochemistry* or may be also *astro-material-science*. An important contribution the *FGLA* has made was to educate young researchers in this interdisciplinary field.

Conference participations of *FGLA* researchers

2003

- Gaseous Ions: Structures, Energetics & Reactions, Ventura, CA
- Workshop on solid state Astrochemistry, Lorentz Centre, Leiden, University, Netherlands
- International Symposium on Cosmic Dust, Estes Park , Colorado, U.S.A.
- XX International Symposium on Molecular Beams, Lisboa, Portugal
- XVIII International Conference on Molecular Energy Transfer
- XIXth Conference on the Dynamics of Molecular Collisions, Granlibakken Conference Center and Resort at Lake Tahoe
- XXIII ICPEAC, Stockholm

- Ion chemistry meeting (HS-60 Symposium) Schloss Blankensee bei Berlin
- The Dense Interstellar Medium in the Galaxies, 4th Cologne-Bonn-Zermatt-Symposium
- SPP Workshop in Aachen, Neuere Entwicklungen zur Generierung und Charakterisierung von Nanostrukturen
- Royal Astronomical Society Meeting “Polyatomics and DIB’s in Diffuse Interstellar Clouds”, Manchester, England, January 8-9, 2003
- 7th International Conference ROMOPTO 2003, Conference on Optics, Constanta, Romania, September 8-11, 2003
- 18th Colloquium on High Resolution Molecular Spectroscopy, Dijon, France, September 8-12, 2003

2004

- XIV Symposium on Atomic, Cluster and Surface Physics, La Thuile (Aosta), Italy.
- ECAMP VIII: 8th European Conference on Atomic and Molecular Physics, Rennes
- Sixth international conferences on dissociative recombination: Theory, experiments, and applications. Mosbach (near Heidelberg), Germany
- MOLEC XV. Nunspeet, Netherlands
- 85th International Bunsen Discussion Meeting
- 44th Sanibel Symposium, Florida, U.S.A.
- 103rd Bunsentagung, Dresden, Germany
- STC2004 Symposium on Theoretical Chemistry: Quantum Chemistry - Methods and Applications, Suhl, Germany
- 24th International Symposium on Rarefied Gas Dynamics, Bari, Italy, July 10 – 16, 2004, in combination with a 3-days satellite meeting on Highlights of Molecular Beams
- International Conference on Advanced Laser Technologies (ALT04), Rome, Italy, Sept. 10 – 15, 2004
- 2004 MRS Fall Meeting, Boston, USA, Nov. 29 – Dec. 3, 2004

2005

- GRC on Gaseous Ions, Ventura, California
- Symposium Interstellar Reactions: from the Gas phase to Solids, Schloss Hotel Pillnitz, Dresden
- 12th RACI Convention, Royal Australian Chemical Institute
- XXIV ICPEAC, Rosario, Argentina

2 Basic concept

- Astrochemistry throughout the Universe: Recent Successes and Current Challenges, Asilomar, California,
- Clustertreffen 2005: CFN-Symposium: Cluster als Molekulare Nanostrukturen, Bad Herrenalb, Germany
- IRSIB Interdisciplinary Research with Slow Ion Beams , Caen / France
- Cold Polar Molecules Ringberg castle, lake Tegernsee
- Molecular Universe Network Meeting Leiden Lorentz Center
- Pacificchem 2005 Astrochemistry - From Laboratory Studies to Astronomical Observations, Honolulu, Hawaii
- International Conference on the Physics and Chemistry of Matrix-Isolated Species (Matrix2005), Funchal, Madeira, July 24 – 29, 2005

2006

- Royal Society Science Division Meeting, Physics, chemistry and astronomy of H_3^+
- NASA Laboratory Astrophysics Workshop, Las Vegas, USA, February 14 – 16, 2006
- 53rd annual conference of the Western Spectroscopy Association
- American Chemical Society, Spring 2006 National Meeting, Atlanta, Georgia,
- Carbon in Space, Villa Vigoni, Lago di Como
- 22PT meeting TU Chemnitz
- Nobel Symposium 133 on Cosmic Chemistry and Molecular Astrophysics, Sodertuna, Schweden, June 2006.
- EXCON 2006, Winston Salem NC, USA, 26 - 30 June 2006
- Molecular universe, RTN Summer school on Molecular Astrophysics, Ile de Berder, France
- SPIG 2006 23rd Summer School and International Symposium on the Physics of Ionized Gases
- XVI MOLEC 2006: International Conference on Dynamics of Molecular Systems, Trento, Italy
- 59th GEC Gaseous Electronics Conference at Ohio State, Columbus, OH
- ISSPIC XIII - International Symposium on small particles and inorganic clusters, Gothenburg, Sweden
- STC2006 Symposium on theoretical chemistry: quantum chemistry - methods and applications, Erkner, Germany

2.2 Scientific concept of the research group

As emphasized in the two proposals and in the 2003 report, the *FGLA* has selected a few topics from the wide field of laboratory astrophysics and astrochemistry. In accord with challenges of modern astronomy, the special scientific experience of the *FGLA* researchers, and the potentials of the involved groups and laboratories, contributions have been made to the fields

- Basic theory
- Modeling
- Gas phase collisions
- Grains and surfaces
- Carbon and Silicon particles
- Spectroscopy and optical properties

As can be seen from the long list of publications (see 2.5), invited contributions to conferences etc., the overall concept turned out to be rather fruitful. A large number of collaborators supported the projects of the *FGLA*. In addition, members of the *FGLA* also have started new co-operative projects with other laboratories and groups. As a result, some members of the *FGLA* proposed that it may be a good time to review results obtained within the last years. Two related activities are planned, and a special issue. As proposed by Stephan Schlemmer, the working title for both initiatives is *New Frontiers in Laboratory Astrophysics – Understanding basic processes*.

International final meeting of the *FGLA*

The international meeting is planned for 2008. It should involve present and previous project leaders, guest researchers and collaborators of the *FGLA*. Presently two possibilities are under discussion. One is to combine it with the Research and Training Network *Molecular Universe*. This European activity intends to organize a conference in Arcachon, May 5 - 8, 2008. This idea has the advantage that most European groups of our field will be represented; also the French activity PCMI will participate.

An alternate idea is to combine the final *FGLA* meeting with an RTN summer school on *Laboratory Astrochemistry*, which will be organized by the Köln group, also in 2008.

2007 Special issue

In spring 2006 in Dresden, the project leaders have decided at an *FGLA* meeting to write (i) a final report summarizing the *FGLA* activities and (ii) to edit until summer 2007 a special issue covering not only the scientific fields of the *FGLA* but including also other important contributions, especially made by our guest researchers or in collaboration with *FGLA* members. Originally we intended to include into this final report already a list of authors and subjects; however, the ambitious idea needs more work and interaction between potential contributors. Therefore the following list of articles is rather preliminary.

Modern experimental techniques in laboratory astrophysics:

Among the many scientific contributions of the *FGLA* a number of main topics developed over the last six years. One is related to laboratory instruments. Given the very special conditions of astrophysical environments, several experimental techniques were developed or further improved to meet the conditions relevant for the astrophysical questions raised in the projects. It is planned that a number of review articles shall summarize these developments. Tentative titles of the articles in this first section are:

- Specific analysis of trapped ions using collisional probing
- Grain analogues in quadrupole traps
- Laser induced reactions: Ultrasensitive spectroscopy and state-to-state reactions
- Transient molecules in supersonic jets

Isotope fractionation and the role of radicals

Deuterium and its fractionation became the focus of many observational, theoretical and laboratory investigations also within the *FGLA* over the last six years. Atomic hydrogen which is much harder to supply in laboratory experiments also became an important target within the *FGLA*. As a result the second very important section deals with:

- The role of H atoms in astrochemistry
- Nuclear spin restrictions in astrochemistry
- Deuteration in cold dense protostellar clouds

Carbon based materials

Carbon has been one main target of the *FGLA*. Due to the chemical diversity of this atom many different species can be formed. This led to a number of rather different laboratory approaches which shall be summarized in the third section:

- Pure carbon molecules, low bending vibrations
- Carbon structures, from low to high temperatures
- Polycyclic aromatic hydrocarbons
- Growth and destruction of small hydrocarbons

Interstellar dust and nanoparticles

Another focus of the *FGLA* deals with dust analogues and their properties. Triggered by the extended red emission (ERE) phenomenon and its possible relation to silicon nanoparticles, great efforts have been put in this field during the last couple of years. Moreover, also several other research activities within *FGLA* covered a wide spectral range and brought together theory and experiment. This section is characterized by the following collection of titles:

- Spectroscopic properties of silicon nanocrystals
- Si-nanoparticles and the ERE phenomenon
- Interstellar extinction and the UV spectra of carbon and silicate condensates
- IR extinction of nanoparticles and aggregates

Outside expertise

Beside the tentative articles which are indicated by the bulleted list, it is intended to round up the topics of this special issue by outside expertise. Some of the world leading scientists in the field have already indicated their interest in participating in this effort. Nonetheless it is clear that such a project cannot cover the complete field of astrophysics and astrochemistry. Thus topics like molecule formation on grain surfaces, the role of interstellar ices or neutral-reactions may be left out, although they are of great importance to the field as well.

In any case it should be emphasized that the main scope of the special issue and of the final conference is set by the activities of the *FGLA*. This position shall be described in an introductory section.

2.3 Participating groups, cooperations

2.3.1 List of project leaders (alphabetic order)

First funding period (2000 - 2003)

Prof. Christian von Borczyskowski	C4	IfP TU Chemnitz
Dr. Ivo Čermák	Wiss. Ass.	IfP TU Chemnitz
Dr. Frank Cichos	Wiss. Ass.	IfP TU Chemnitz
Dr. Johann Dorschner	Wiss. Ang.	AIU Jena
Prof. Dieter Gerlich	C4	IfP TU Chemnitz
Prof. Thomas Henning	C4	AIU Jena
Dr. Ulrich Kleinekathöfer	Wiss. Ang.	IfP TU Chemnitz
Dr. Harald Mutschke	Wiss. Ass.	AIU Jena
Dr. Stephan Schlemmer	Wiss. Ass.	IfP TU Chemnitz
Dr. Reinhard Scholz	Wiss. Ass.	IfP TU Chemnitz
Prof. Michael Schreiber	C4	IfP TU Chemnitz
Prof. Gotthard Seifert	Wiss. Ang.	IFP UGH Paderborn
Dr. Gerhard Wurm	Wiss. Ang.	AIU Jena

Second funding period (2003 - 2006)

Prof. Christian von Borczyskowski	C4	IfP TU Chemnitz
PD Dr. Jürgen Blum	OA	AIU Jena
Dr. Frank Cichos	Wiss. Ass.	IfP TU Chemnitz
Dr. Johann Dorschner	Wiss. Ang.	AIU Jena
Prof. Dieter Gerlich	C4	IfP TU Chemnitz
Prof. Thomas Henning	C4	MPIA/AIU Jena
Prof. Friedrich Huiskens	Wiss. Ang.	MPIA/FSU Jena
Dr. Alfonz Luca	Wiss. Ass.	IfP TU Chemnitz
Dr. Harald Mutschke	Wiss. Ang.	AIU Jena
PD Dr. Stephan Schlemmer	OA	IfP TU Chemnitz
Dr. Reinhard Scholz	Wiss. Ass.	IfP TU Chemnitz
Prof. Michael Schreiber	C4	IfP TU Chemnitz/ IUB
Prof. Gotthard Seifert	C4	TU Dresden
Prof. Wolfgang Witthuhn	C4	FSU Jena

2.3.2 Changes in the second funding period

Also during the second funding period a variety of changes occurred in the scientific staff. Most of them have been due to promotions of project leaders or young researchers and changes to other universities and research institutions. Details can be found in the following overview.

TP 1 and TP 2

- **Scholz, Dr. R.** In March 2006 he accepted a position as Oberassistent in the Walter Schottky Institut, TU München (with Prof. P. Vogl)

TP 4

- **Schlemmer, Prof. Dr. S.** From May 2003 until September 2004 he was associate professor at the Leiden Observatory and head of the Raymond & Beverly Sackler Laboratory for Astrophysics. The 22PT-apparatus of TP 4 was transferred to Leiden in order to continue work on laser induced reactions (LIR). In October 2004 he accepted an appointment as associate professor (C3) at the Universität zu Köln. In the I. Physikalisches Institut, he heads the laboratory spectroscopy group. The major work concentrates on high-resolution spectroscopy of molecules of astrophysical interest. Also work on low temperature collision dynamics is conducted. As a part of these efforts the LIR work is continued in Köln and efforts are made to extend LIR to the far infrared range using the 22PT-apparatus.

TP 5

- **Luca, A. Dr.** He got his PhD during the first funding period at the TU Chemnitz. In the second funding period he has taken over the responsibility for TP 5. His position as scientific assistant ends on 30.11.2007.

TP 6

- **Cichos, Dr. F.** In Nov. 2006 he accepted an appointment (W2) at the Institute for Experimental Physics of the University of Leipzig.

TP 7

- **Čermák, Dr. I.** He joined the TUC in 1999 and has stimulated the ambitious proposal of TP 7. Unfortunately, he became sick in summer 2002. He could not come back to work until his contract as assistant ended in February 2005. He did not contribute at all to

the report in 2003 and to the proposal for the second funding period.

TP 9

- **Blum, Prof. Dr. J.,** In 2004 he accepted an appointment at the Technische Universität Carolo-Wilhelmina zu Braunschweig

TP 11 and TP 12

- **Huiskens, Prof. Dr. F.** In 2003 he moved from the Max-Planck-Institut für Strömungsforschung Göttingen to the FSU Jena and became head of the Laboratory Astrophysics and Cluster Physics Group which is jointly operated by the Max-Planck-Institut für Astronomie Heidelberg and the FSU Jena. In 2005 he was appointed apl. Professor for experimental physics at the Faculty for Astronomy and Physics of the FSU Jena.

2.3.3 Cooperations

All groups have many cooperations and scientific exchange with groups from all over the world. The following list has been updated from the last overview; however, it is rather sure that it is not complete (see also our guest program).

Cooperations in Germany

Bertholdi, F. (MPIfR Bonn): H_2 and HD emission from PDRs and shocks.

Dopfer, O. (Institut für Optik und Atomare Physik, Technische Universität Berlin): Solvation of molecular ions

Gail, H.-P. (ITA Heidelberg): Chemistry in accretion disks. The Heidelberg group is well-known for their theoretical contributions to astrochemistry and grain formation. The Jena group has strong contacts to Dr. Gail and works presently together with him on theoretical aspects of grain annealing and the formation of crystalline solids under circumstellar conditions.

Giesen, T. (Universität zu Köln): Absorption spectroscopy of transient molecules in jets and beams

Jaquet, R. (GH Siegen): PES and dynamics for the H_3^+ system.

Krätschmer, W. (MPI-K Heidelberg): Absorption and emission spectroscopy of matrix-isolated carbon molecules, sublimation of carbon.

Menten, K. (MPIfR Bonn): Millimeter Interferometry. The Jena group has traditionally strong connections to the MPI for Radioastronomy and will continue with these contacts to the submillimeter/millimeter astronomy group.

Niedner-Schatteburg, G. (Universität Kaiserslautern): Experiments in ICR traps, protonated and deprotonated water clusters

2 Basic concept

- Pflaum, J.** (Universität Stuttgart, Germany). Spectroscopy of molecular crystals
- Schnaiter, M.** (FZ Karlsruhe): Dr. Martin Schnaiter is a former Ph.D. student of the Jena group who now applies his knowledge of carbonaceous materials to aerosol science.
- Schreiber, F.** (Universität Tübingen, Germany). Spectroscopy of molecular crystals
- Troe, J.** (Göttingen): Capture theory in low temperature collisions. The Chemnitz group is associated with the present work of Prof. Troe in the Astrophysical Chemistry.
- Weitzel, K.-M.** (Physical Chemistry, University of Marburg): Chemical reactions in and with molecular ions and cluster ions, state selective ion molecule reactions, synchrotron experiments.
- Wurm, G.** (Universität Münster): is a former leader of TP 10. We will collaborate with him on the subject from light scattering by dust particles.

International Cooperations

- Allamandola, L.** (NASA-Ames Research Center, Moffet Field, USA): Spectral features of PAHs, ice layers.
- Chan, Y.** (Brandeis University, USA): ODMR measurements on silicon nanocrystals.
- Cherchneff, I.** (UMIST, Manchester): Chemistry and dust formation in carbon-star outflows.
- de Andrade e Silva E.** (Instituto Nacional de Pesquisas Espaciais, Sao Jose dos Campos, Brasil), Band structure and spin splittings in inorganic semiconductors.
- Mc Cullough, R.W.**, The Queen's University of Belfast, UK, H-atom source development, collisions with multiply charged ions
- Duley, W. W.** (University of Waterloo, Canada): Laser applications in material science, physics of interaction of laser radiation with condensed matter, laser processing of materials in space, physics and chemistry of interstellar matter, synthesis and characterization of carbonaceous materials.
- Ehrenfreund, P.** (Leiden Observatory, Holland): Astrobiology
- Glosík J.**, Charles University Prague, Ion molecule reactions in a flowing after-glow plasma, spectroscopy, structure and reactivity of H_3^+
- Herbst, E.** (Ohio State University, Columbus, USA): Chemical networks, ammonia formation, reactions involving H_3^+ , radiative association, modeling of grain chemistry.
- Hutson, J.** (Durham, England): Prof. Hutson is a world leading theoretician working in the field of weakly interacting ion-molecule and neutral-neutral system.
- Jancu, J.-M.** (Laboratoire de Photonique et de Nanostructures, CNRS, Marcoussis, France), Band structure and spin splittings in inorganic semiconductors.

- Joblin, C.** (CERS Toulouse, France): Connections between PAHs and hydrogen (H_2), laboratory experiments in the temperature variable ICR trap *PIRENEA* and observations, Photophysics of interstellar molecules, photodissociation of PAHs.
- Kaiser, R.** (University of Hawai'i at Manoa, Department of Chemistry): Habilitation 2002 in Chemnitz. His field of research is Reaction Dynamics, Planetary Chemistry, Astrochemistry.
- Kroes, J.-G.** (University of Leiden, Holland): Theoretical chemistry of elementary processes in water ices and in gas-phase collisions.
- La Rocca, G. C.** (Scuola Normale Superiore, Pisa, Italy). Band structure and spin splittings in inorganic semiconductors.
- Linnartz, H.** (Freie Universität Amsterdam, Niederlande): Cavity ring-down spectroscopy, molecular beam experiments
- Maier, J.P.** (Department of Chemistry, University of Basel, Switzerland): Exploring the potential of low temperature 22-pole trap for spectroscopy studies of astrophysical relevance, multiple photon fragmentation of cold trapped ions, spectroscopy of carbon ions, e.g. C_3^+ and C_{60}^+
- Meijer, G.** (HMI Berlin): Cold Molecules: Formation, Trapping, and Dynamics, ultracold molecules and collisions.
- Millar, T.J.** (Department of Physics, UMIST, Manchester): Chemical networks. T. Millar is one of the experts in the field of chemical networks the Jena group will continue the collaboration with the UMIST group in the field of chemical modeling of dense phases of the ISM.
- Nemecek, Z., Šafránková, J.** (Charles University, Prague): Charging of microparticles by ions and electrons.
- Oka, T.** (University of Chicago, USA): Formation and excitation of H_3^+ . Prof. Oka's group is the leading team in molecular spectroscopy.
- Patchkowski, S.** (Ottawa, now Univ. of Calgary, Canada) Theory of hydrogen carbon interaction.
- Rizzo, T.** (EPFL, CH-1015 Lausanne, Switzerland, together with O. Boiarkine), Electronic and vibrational spectroscopy of cold, biomolecular ions, coupling an electrospray ion source to a cold 22-pole ion trap.
- Reynaud, C.** (SPAM/CEA Saclay): Laboratory simulations and spectroscopy of carbonaceous dust, correlation of optical and structural grain properties, interpretation of astronomical observations, photoluminescence of silicon nanocrystals, Extended Red Emission.
- Roueff, E.** (Observatory Paris-Meudon, France): Modeling of chemical networks, Observations.
- Rowe, B.** (University of Rennes, France): Low energy reactions in CRESU, reactions with H atoms. The low temperature flow reactor technique developed by Prof. Rowe is a complimentary technique as compared to the trapping experiments of Prof. Gerlich's group for the investigation of low energy collisions.

2 Basic concept

Salama, F. (NASA Ames): The collaboration between Th. Henning and F. Salama was sponsored in the past by the German-American Academic Council and led to an invited review paper about Carbon in the Universe in Science. The group of F. Huisken has a collaboration with F. Salama on the electronic spectroscopy of PAHs.

Saykally, R.J. (Department of Chemistry, University of California, Berkeley): Infrared spectroscopy. The Berkeley group of Prof. Saykally has a very unique IR detector which has been used also by Dr. Schlemmer for the emission detection of highly excited PAHs.

Smith, M. (Tucson, Arizona, USA): Ion-molecule and neutral-neutral reactions at low temperatures, experiments in free expansions, reactions with radicals, infrared laser induced reactions. Prof. Smith has been an Alexander von Humboldt fellow with Prof. Gerlich. In 2004/2005 Prof. Gerlich spent his sabbatical in Tucson. One of the results was a joint NSF application for the construction of the *next generation* trapping machine for astrochemical studies. Since spring 2006 this machine is under construction. More details see TP 5.

Valenta, J (Charles University Praha, Czech Rep.) Blinking dynamics of Si nanoparticles.

Van Dishoek, E. (Leiden Observatory, Holland): Reactions populating rotational states of H_2 , chemistry on the surface of grains, observations, the HD/ H_2 abundance, millimeter interferometry. There are and will be well-established contacts between the Leiden Astrochemistry group and the *FGLA*.

Voicu, I. (National Institute for Lasers, Plasma and Radiation Physics, Bukarest, Romania): Synthesis of polycyclic aromatic hydrocarbons by CO_2 laser pyrolysis of hydrocarbons and species characterization.

von Helden, G. (FOM Rijnhuizen, Holland): Infrared absorption spectroscopy of PAH, Metal cluster dynamics, infrared absorption spectroscopy of jet-cooled weakly bound clusters ions.

Wagner, H.-P. (University of Cincinnati, Ohio, USA), Spectroscopy of molecular crystals

Zaifman, D. (Max-Planck-Institut für Kernphysik, Heidelberg, Germany, together with A. Wolf and H. Kreckel) Preparation and characterization of state selected H_3^+ ions for injection into a storage ring, electron-ion recombination.

2.4 Experiences and activities

2.4.1 Overview

It was the main goal of the *FGLA* initiative to provide a stimulating scientific environment for developing new ideas in studying interstellar matter and for extending the present state of the art experiments and theories to new frontiers of *laboratory astrophysics*. We are convinced that we have made a big step forward, may be less than hoped since in some projects problems occurred due to problems in finding good graduate students. Also changes in the personal and some financial or administrative restrictions caused friction.

This section summarizes all those experiences and activities from the last funding period which can be summarized with the keywords scientific communication, personal interactions and education. Communication via internet and transfer of information via the public and internal homepage of the *FGLA* was quite efficient. Nonetheless personal exchanges and contacts cannot be replaced by that. Very important for all of us was the guest program. Many scientists came visiting and working with us for a few days, weeks and in some cases also for months. Another central activity was the organization of regular joint seminars, discussion meetings and special workshops. The list of contributors and subjects reveal that the *FGLA* activity has provided an attractive scientific forum for experimentalist, theorists, modelers and astronomers from all over the world.

The *FGLA* has also made remarkable contributions to the education of young people. The list of Diploma and PhD students and the titles of their thesis corroborate this. We have started with several young researchers as project leaders, which have succeeded with their habilitation, got appointments as group leaders or a position as Juniorprofessor, full professor or director of the MPIA.

2.4.2 Communication and interactions

In the first funding period, the regular contacts and exchanges were just localized between Chemnitz and Jena. In the second one, the activities spread out more and more. Finally five locations were involved. On one side the exchange of people and joint seminars became somewhat more complicated because of distances; however the new scientific environments also provided new insights and stimulated new ideas and cooperations.

2. Basic concept

As already pointed out in the first report, the flexible guest program has been very important for the *FGLA*. Although in some cases, especially for leading figures in their fields, the visits were rather short, they have been always very stimulating. Our innovative experimental and theoretical methods in the field of laboratory astrophysics have attracted many researchers. Many close cooperations have been started partly initiated by the Forschergruppe. Some details to the visits are given in the individual final reports.

Per semester we have organized usually four regular Friday afternoon seminars with discussions, laboratory visits and a common diner. Usually more than 80 % of the members of the *FGLA* could participate. In addition several specific meetings and workshops have been organized.

2.4.3 Guest program

During the first funding period, 69 guest researchers came visiting (see *FGLA* report 2003, p37 - 39). The number even increased during the second one to 86! Between 2003 and 2006, the following scientists were visiting the *FGLA* (chronological order)

- Dr. Helen Fraser**, Leiden Observatory, 06.01. – 09.01.2003
Prof. Michael Grewing, IRAM Grenoble, 18.03. – 20.03.2003
Prof. Gerhard Hensler, Universität Kiel, 18.03. – 20.03.2003
Prof. Wolfgang Domcke, TU München, 18.03. – 20.03.2003
Prof. Philippe Brechignac, Laboratoire de Photophysique Moleculaire Orsay, France, 18.03. – 20.03.2003
Prof. Louis d'Hendecourt, Institut d'Astrophysique Spatiale-CNRS Orsay, France, 18.03. – 20.03.2003
Prof. Thomas Leisner, TU Ilmenau, 18.03. – 20.03.2003
Serge, Krasnokutski, MPI für Astronomie Heidelberg, 19.03 – 20.03.2003
Dr. Martin Stübiger, MPI Heidelberg, 03.04. – 30.06.2003
A. Dzhonson, Universität Basel, Schweiz, 27.04. – 29.04.2003
Dr. P. Kolek, Universität Basel, Schweiz, 27.04. – 29.04.2003
Dr. A. T. Mostefaoui, Cornell University Ithaca, USA, 28.04. – 30.09.2003
Dr. R. Plasil, Karls-Universität Prag, 12.05. – 14.05.2003
Dr. P. Votava, Heyrovsky Institut Prag, 12.05. – 14.05.2003
Dr. Juraj Glosik, Karls-Universität Prag, 12.05. – 14.05.2003
Prof. R. Mauersberger, IRAM Granada, 15.05. – 18.05.2003
Dr. Ulrich Ott, MPI für Kosmologie, 16.05. – 17.05.2003
Dr. Tom Govers, Universite Rennes, Frankreich, 22.10. – 25.10.2003
Prof. Liv. Hornekaer, University of Southern, Denmark, 23.10. – 25.10.2003
Prof. V. Pirronello, Universita di Catania, Italien, 23.10. – 26.10.2003
Prof. Rainer Johnson, University of Pittsburg, USA, 03.11. – 05.11.2003
Dr. Gerhard Wurm, Universität Münster, 20.01.2004
Dr. Marcus Behnke, Universität Köln, 19.01. – 25.01.2004
Prof. Adolf N. Witt, University of Toledo, USA, 21.01. – 25.01.2004
Dr. Marcus Behnke, Universität Köln, 12.01. – 14.01.2004
Dr. Ference Glück, Universität Mainz, 10.02. – 11.02.2004
Dr. Glosik, Charles University Prag, 09.02. – 16.02.2004
Dr. Radek Plasil, Charles University Prag, 09.02. – 16.02.2004
Prof. Scott Anderson, University of Salt Lake City, USA, 07.02. – 13.02.2004

2. Basic concept

Dr. Axel Pramann, PtB Braunschweig, 22.03. – 23.03.2004
Dr. K. Strobel, Universität der Bundeswehr München, 22.03.2004
Alexander Uhl, TU Kaiserslautern, 24.03.2004
Dr. H. Nahler, University of Bristol, 24.03.2004
Dr. H.-J. Deyerl, Technical University of Denmark, 25.03. – 27.03.2004
Dr. Ivan Mistrik, Penn State University, USA, 29.03. – 31.03.2004
Prof. Zdenek Herman, Heyrovski Institut Prag, 30.04.2004
Dr. Glosik, Charles University Prag, 27.04. – 05.05.2004
Dr. Radek Plasil, Charles University Prag, 27.04. – 05.05.2004
Prof. Dr. Rodica Alexandrescu, National Institute for Lasers, Plasma and Radiation Physics, Bukarest, Romania, 17.05. – 16.06.2004
Dr. Radek Plasil, Charles University Prag, 15.07. – 14.09.2004
Prof. Cheuk Ng, UCLA Davis, USA, 26.07. – 02.08.2004
Prof. K.-M. Weitzel, Universität Marburg, 26.07. – 27.07.2004
Prof. Mark Smith, University of Arizona, Tucson USA, 01.08. – 07.08.2004
Dr. Jan Fulara, Polish Academy of Sciences, Warszawa, Poland, 31.10. – 28.11.1004
Dr. W. D. Geppert, University Stockholm, Nova, 06.12. – 31.12.2004
Prof. R. E. Continetti, University of California, San Diego, 11.12. – 18.12.2004
Dr. W. D. Geppert, University of Stockholm, 02.01. – 16.01.2005
Davous Pouladzaz, University of Iran, Januar/ Februar
Dr. Kutepov, Universität München, 01.02. – 08.02.2005
Prof. R. Gredel, Centro Astronomico Hispano-Aleman, 03.02. – 05.02.2005
Dr. Patchkowski, Steacie Institute for Molecular Sciences, 01.03. – 31.03.2005
Prof. Armin Hansel, Universität Innsbruck, 20.04.2005
Dr. Evan Bieske, University of Melbourne, 30.04.2005
Dr. Thierry Stöcklin, Universite de Bourdeaux, France, 01.05. – 04.05.2005
Dr. Juraj Glosik, Charles-University Prag, Mai 2005
Dr. Radek Plasil, Charles-University Prag, Mai 2005
Dr. Jun-Ya Kohno, Genesis Research Institute, Inc. Japan, Mai 2005
Prof. N. Sathyamurthy, Indian Institute of Technology, 08.05. – 10.05.2005
Prof. Mark N. Smith, University of Arizona, Tucson USA, 02.06. – 30.06.2005
Dr. Igor Savic, University of Novi Sad, 02.06. – 16.06.2005
Prof. Juraj Glosig, Charles-University Prag, 01.08. – 30.09.2005
Dr. Radek Plasil, Charles-University Prag, 01.08. – 30.09.2005
Dr. Steven Horning, Thermo Electron Bremen, 25.08. – 26.08.2005

- Dr. R. Rapacioli**, Universite Paris, 19.09. – 25.09.2005
- Dr. Jacek Krelowski**, University of Torun Polen, 27.10. – 29.10.2005
- Prof. Baoshan Wang**, Wuhan University PR China, 23.10. – 22.11.2005
- Dr. Eva Kovacevic (Hon)**, Ruhr-Universität, 27.10. – 29.10.2005
- Dr. Johann Berndt**, Ruhr-Universität, 27.10. – 29.10.2005
- Prof. Christine Joblin**, CESR Toulouse, Dezember 2005
- Dr. D. Ascenzi**, University of Trento, 15.12. – 17.12.2005
- Dr. Ion Voicu**, National Institute of Lasers, Plasman and Radiation Physics, Bukarest, 16.01. – 15.02.2006
- Prof. Albert Viggiano**, NASA Hanscom, USA, 30.04. – 11.05.2006
- Prof. Mark Smith**, University of Arizona, Tucson USA, 28.05. – 11.06.2006
- Dr. Igor Savic**, University of Nvi Sad, 26.06. – 25.07.2006
- Prof. C. Koike**, Kyoto Japan, 10.07. – 23.07.2006
- Prof. Louis d'Hendecourt**, IAS Orsay, 06.07. – 08.07.2006
- Prof. Gail**, Universität Heidelberg, 06.07. – 08.07.2006
- Dr. M. Min**, University of Amsterdam, 07.07. – 08.07.2006
- Dr. J. Bouwman**, MPI Heidelberg, 07.07. – 08.07.2006
- Dr. T. Stephan**, Universität Münster, 06.07. – 08.07.2006
- Dr. Igor Savic**, University of Novi Sad, 26.07. – 25.08.2006
- Xianwen Quan**, Universität Bielefeld, 27.08. – 03.09.2006
- Prof. A. Sherman**, University of Tartu, Estland, 05.09. – 20.09.2006
- Dr. Juraj Glosik**, Charles- University Prag, 05.09. – 13.09.2006
- Dr. Radek Plasil**, Charles- University Prag, 05.09. – 13.09.2006
- Prof. Krätschmer**, Universität Heidelberg, 02.10. – 07.10.2006

2. Basic concept

2.4.4 Workshops and symposia

Chemnitz 24.10.2003

H₂ - formation on surfaces and on interstellar dust

V. Pirronello, *Results on surfaces of astrophysical interest and theoretical modeling*

L. Hornekaer, *The surface experiment in Odense*

T. Govers, *Bolometric detection of the energy release*

Leiden, 16.04.2004

Dutch Activities in Laboratory Astrophysics

J.-Ch. Augereau, *On the Dynamics of Planet-Formation in Disks*

S. Ingemann, *Experimental Determination of Thermodynamic Properties of Simple Molecules with FTICR*

J. Oomens, *IR-Spectroscopy of Astrophysically Relevant Molecular Ions using FELIX*

W. van der Zande, *Collisions of Low Energy Electrons with Molecular Ions: Mechanisms and Astrophysical Implications*

H. Fraser, *Solid State Chemistry on Interstellar Dust*

O. Asvany, *Laser Induced Reactions using FELIX*

D. Bodewits, *EUV and soft X-Ray Emission from the Interaction of Ions (Groningen) with Neutrals*

H. Linnartz, *Planar Plasma Expansions as a Tool for Spectroscopy of Molecular Radicals of Astrophysical Interest*

Heidelberg 11. - 13.10.2004

Chemie in Scheiben

Symposium organized by the MPI für Astronomie Heidelberg

Köln 25.11.2005

THz-Spectroscopy of Molecules in Space

Jürgen Stutzki, *New Instruments for Observation: SOFIA and Herschel*

Carsten Kramer, *From Observations to Modelling*

Frank Lewen, *Development and Application of THz Sources in the Laboratory*

Thomas Giesen, *Jet cooled Carbon Chains*

Oskar Asvany, *Laser Induced Reactions with FELIX and other IR Sources*

Chemnitz 08. - 10.06.2006

RF ion traps: technique and applications in reaction dynamics and spectroscopy

- D. Gerlich**, *History of rf based ion guides and traps*
M. Smith, *From 10 to 1000 K: thermochemistry in traps*
A. Dzhonson, *Two-photon fragmentation of cold trapped ions: recent progress*
H. Kreckel, *Preparing a state selected H_3^+ beam using a storage ion source and a 22PT*
J. Glosik, *State specific probing of H_3^+ and deuterated analogues using overtone excitation*
T. Rizzo, *Electronic and vibrational spectroscopy of cold, biomolecular ions*
A. Knut, *Structure and stability of stored gas phase cluster ions*
S. Schlemmer, *Combination of THz spectroscopy and LIR in a 22PT*
J. Maier, *Potential of a 10 K 22PT for spectroscopy studies of astrophysical relevance*
A. Luca, *Reactions of cold ions with a slow H-atom beam*
D. Gerlich, *The role of ortho- H_2 in cold traps and in pre-protostellar collapse*
R. Wester, *Quantum reactive scattering of ions and neutrals*
O. Boiarkine, *Coupling an electrospray ion source to a cold 22-pole ion trap*
F. Windisch, *Combination of a 4K-22PT and an effusive or supersonic beam*
J. Mikosch, *Interactions of trapped negative ions*
D. Kunte, *Construction details of traps*

Heidelberg 29.05.2006

Highlights in Astrochemistry and Astrobiology

- E. Herbst**, *The Production of Complex Molecules in the Interstellar Medium*
E. van Dishoeck, *Astrochemical Evolution from Low-mass YSOs to Protoplanetary Disks*
G.A. Blake, *High-Resolution Spectroscopy and Imaging of Circumstellar Disks*
A. Dutrey, *Physico-Chemistry in Proto-planetary Disks: A next Step Towards Planetary Formation*
E. Bergin, *Interstellar Chemistry: Exploring Links to Comets and Meteorites*
J. Kastning, *The Early Earth as an Analogue for Possible Extrasolar Planets*

Jena 07.07.2006

Silicon-based dust in space

- J. Bouwman**, *Mineralogy results from “Spitzer” observations*
M. Min, *Models for optics of grains and aggregates*
A. Tamanai, *IR spectroscopy of grains in aerosol*
H. Mutschke, *Silicate properties at UV and FIR wavelengths*
T. Stephan, *Fire and ice – first results from stardust*

2. Basic concept

L. d'Hendecourt, *Structural modifications of silicates upon irradiation: a comprehensive guide to interstellar grain evolution?*

C. von Borczyskowski, *Photophysical processes in Si nanocrystals*

F. Huysen, *Si nanocrystals embedded in silica matrices*

H.-P. Gail, *What is needed from the laboratories*

2.4.5 Seminars

17.01.2003, *Characterization of iron- and carbon-based nanostructures produced by CO₂ laser pyrolysis*, **Rodica Alexandrescu**, National Institute for Lasers, Plasma, and Radiation Physics, Bucharest, Romania

07.01.2003, *CO'ded messages: Just what we learn about the ISM with surface chemistry*, **Helen Fraser**, Leiden Observatory, Niederlande

04.04.2003, *Reaction rates: Accurate quantum dynamical calculations for polyatomic systems*, **Uwe Manthe**, Theor. Chemie TU München

04.04.2003, *Theoretical investigations of formation of interstellar hydrocarbons*, **Robert Barthel**, TU Dresden

04.04.2003, *Photochemistry of hydrocarbon radicals*, **Ingo Fischer**, University of Wuerzburg

08.04.2003, *Simulation of cosmic dust in the laboratory*, **Martin Stübiger**, MPI - K Heidelberg

16.05.2003, *Observing Molecules in Space Clouds*, **Rainer Mauersberger**, IRAM, Granada

16.05.2003, *Reduction Schemes for Chemical Networks*, **Dimitri Semenov**, AIU Jena

16.05.2003, *Primitive Matter in Meteorites*, **Ulrich Ott**, MPI für Chemie, Mainz

20.06.2003, *Cluster-Beam Deposition and in situ Characterization of Carbyne-Rich Carbon Films*, **Paolo Milani**, University of Milano

20.06.2003, *Spectral and Structural Properties of Carbon Nanoparticles as Cosmic Dust Analogues*, **Cornelia Jäger**, (TP 8)

20.06.2003, *Spectroscopy and reactions of water clusters*, **Udo Buck**, MPI-S Göttingen

24.06.2003, *Laser Spectroscopy of Non-covalent Interactions in Molecular Clusters*, **Klaus Müller-Dethlefs**, Department of Chemistry, The University of York

11.07.2003, *Ion-Molecule Collisions: Cross Sections and Fragmentation Products*, **John R. Sabin**, University of Florida

11.07.2003, *Radiative Association in CH₃⁺ + H₂O and CO Collisions: Experimental Studies of Ion-Molecule Collisions*, **A. Luca**, (TP 5)

04.11.2003, *Dissociative recombination of molecular ions with thermal electrons*, **Rainer Johnson**, University of Pittsburgh

- 21.11.2003, *Disk chemistry and the perspectives of ALMA*, **Anne Dutrey**, Observatoire de Bordeaux
- 21.11.2003, *CO Depletion and extreme deuterium fractionation in pre-stellar cores*, **Aurore Bacmann**, Observatoire de Bordeaux
- 12.12.2003, *Infrared Spectroscopy of Molecular Particles*, **Ruth Signorell**, Universität Göttingen
- 12.12.2003, *Aggregates and Light Scattering (final report TP10)*, 2., **Gerhard Wurm**, Universität Münster
- 12.12.2003, *Scattering-type Near-field Microscopy for Optical Nanospectroscopy*, **Rainer Hillenbrand**, MPI für Biochemie, Martinsried
- 13.01.2004, *Design and new applications of a high resolution microwave spectrometer*, **Marcus Behnke**, I. Phys. Institut zu Köln
- 23.01.2004, *Optical Photoluminescence from Interstellar Nanoparticles*, **Adolf N. Witt**, University of Toledo
- 23.01.2004, *Spectroscopy of CdSe nanocrystals: size, shape and surface effects*, **Ulrike Woggon**, Universität Dortmund
- 23.01.2004, *Photophysics of Individual Silicon Nanocrystals*, **Jörg Martin**, Chemnitz
- 23.01.2004, *UV spectroscopy of carbon nanoparticles produced by laser pyrolysis*, **Isabel Llamas**, Jena
- 10.02.2004, *Low temperature tritium gas, hydrogen ions and the neutrino mass*, **J. Glosik and R. Plasil**, University Prag, F. Glück, Universität Mainz
- 11.02.2004, *Experimental and Trajectory Study of Vibrational Effects on Ion-Molecule Reactions*, **Scott Anderson**, University of Salt Lake City, USA
- 30.04.2004, *Dynamics of chemical reactions of dications(crossed beam scattering experiments)*, **Zdenek Herman**, Heyrovski Institut Prag
- 11.06.2004, *Quantum dynamical calculation on the surface catalysed formation of H₂ in interstellar space*, **Anthony Meijer**, University of Sheffield
- 11.06.2004, *Spectroscopic properties of interstellar molecules: Theory and experiment*, **Peter Botschwina**, Georg-August-Universität Göttingen
- 11.06.2004, *First Principle simulations of hydrogen on graphitic platelets*, **Thomas Heine**, TU Dresden
- 02.07.2004, *Exogenous and endogenous contributions to the origin of life*, **Pascale Ehrenfreund**, Leiden
- 02.07.2004, *Biomarkers and their observability*, **Daniel Apai**, MPIA
- 02.07.2004, *Chemical evolution of the circumstellar gas and dust in the AB Auriga system*, **Dimitri Semenov**, MPIA
- 22.10.2004, *Carbon nanotubes and spheres - how they grow, look like, and behave*, **Andreas Schaper**, Universität Marburg

2. Basic concept

- 22.10.2004, *Carbon onions and related nanoparticles: structure formation under irradiation*, **Florian Banhart**, Universität Mainz
- 12.11.2004, *Asteroidenforschung*, **Michael Soffel**, Institut f. Planetare Geodaesie, TU Dresden
- 12.11.2004, *Structure, Electronic Structure and Stability of PAH*, **A. Kuc**, TU Dresden
- 12.11.2004, *Minimum energy path calculations of hydrocarbon formation*, **Robert Barthel**, TU Dresden
- 17.12.2004, *Charge-exchange of H_3^+ and its isotopomers*, **R. E. Continetti**, University of California, San Diego
- 17.12.2004, *New data on dissociative recombination reactions and their influence on the chemistry of interstellar clouds*, **W. D. Geppert**, University Stockholm
- 17.12.2004, *Experimental results on the reaction of $CH_5^+ + H$* , **G. Borodi**, TUC
- 04.02.2005, *Optical absorption line studies of interstellar molecules*, **Roland Gredel**, Director of Calar Alto Observatory, Centro Astronomico Hispano-Aleman, Almeria, SPAIN
- 04.02.2005, *Non-local thermodynamic equilibrium diagnostics of the infra-red observations of planetary atmospheres*, **Alexander Kutepov**, Institut für Astronomie und Astrophysik, Universität München
- 29.04.2005, *Infrared probing of negatively charged complexes*, **Evan Bieske**, University of Melbourne, Australia
- 29.04.2005, *New aspects of PAH formation*, **R. Barthel**, TU Dresden
- 29.04.2005, *Spectroscopy of single molecules and molecular materials*, **R. Scholz**, TU Chemnitz
- 03.05.2005, *Low and ultra low temperature quantum rate coefficient calculations for atom diatom collisions of astrochemical interest*, **Thierry Stoecklin**, University of Bordeaux, France
- 03.05.2005, *Dynamics of Certain Ion-Molecule Processes*, **N. Sathyamurthy**, Indian Institute of Technology, Kanpur
- 24.06.2005, *Exploration of Titan: Laboratory Studies of an Astrobiological Hot Spot*, **Mark A. Smith**, University of Arizona, USA
- 26.08.2005, *Modern MS applications in ion chemistry: LTQ FT and LTQ Orbitrap*, **Stevan Horning**, Thermo Electron GmbH (Bremen)
- 28.10.2005, *DIBs and problems in observing them*, **Jacek Krelowski**, University of Torun, Poland
- 28.10.2005, *Carbonaceous IS dust analog : Formation by reactive plasma polymerization*, **Eva Kovacevic**, Universität Bochum
- 28.10.2005, *Aerosol infrared spectroscopy of SiO₂ particles*, **Akemi Tamanai**, Universität Jena

- 01.11.2005, *Implication of Quantum Mechanics in chemical thermodynamics and kinetics*, **Baoshan Wang**, College of Chemistry and Molecular Sciences, Wuhan University PR CHINA
- 08.11.2005, *High-level computational studies of some ion-molecule reactions: towards mechanisms, kinetics, thermochemistry, and dynamic*, **Baoshan Wang**, Wuhan University PR CHINA
- 16.12.2005, *Chemistry of interstellar PAH candidates in the PIRINEA set-up*, **Christine Joblin**, CESR Toulouse
- 16.12.2005, *Reactivity of aromatic hydrocarbon ions with small molecule*, **Daniela Aszenci**, Università di Trento
- 16.12.2005, *Silicon nanoparticles: The carriers of the Extended Red Emission?*, **Davoud Pouladsaz**, TU Chemnitz
- 21.04.2006, *Photodissociation of small molecules*, **Reinhard Schinke**, MPI DS Göttingen
- 21.04.2006, *Development of algorithms and methods for the prediction of molecular properties*, **Alexander Auer**, TU Chemnitz
- 21.04.2006, *Modeling Polycyclic Aromatic Hydrocarbons clusters in photodissociation regions*, **Mathias Rapacioli**, TU Dresden
- 02.05.2006, *Reexamination of ionospheric chemistry: High temperature kinetics, internal energy dependences, unusual isomers, and corrections*, **Al Viggiano**, AFRL/VSXT
- 31.05.2006, *Exploration of Titan: Laboratory Studies of an Astrobiological Hot Spot*, **Mark Smith**, University of Arizona, Tucson
- 30.08.2006, *LIF detection of ions trapped in an ICR cell*, **Xianwen Guan**, Department of Organic Chemistry ETHZ
- 05.10.2006, *Spectroscopic Studies of Carbon Chain Molecules and Oxides*, **Wolfgang Krätschmer**, MPI Heidelberg

2. Basic concept

2.4.6 Qualifications (since 2000)

Habilitationen, Berufungen, Ernennungen

Dr. Stephan Schlemmer: *Molecular Reaction Dynamics: Gas Phase, Clusters and Nanoparticles*, Habilitation, TU Chemnitz, 2001

Prof. Thomas Henning: 2002 Berufung zum Direktor des MPI für Astronomie

Dr. Ralf Kaiser: *Crossed Molecular Beam Studies on the Formation of Carbon-Bearing Molecules in the Interstellar Medium via Neutral-Neutral Reactions* Habilitation, TU Chemnitz, 2002

Dr. Ulrich Kleinekathöfer: *Structure and Dynamics in Molecular Systems: Electron and Exciton Transfer*, TU Chemnitz, Habilitation, 2002

Dr. Stephan Schlemmer: 2003 associate professor, Leiden Observatory

Dr. Frank Cichos, Juniorprofessur, TU Chemnitz, 2003

Prof. Stephan Schlemmer: C3 Professur, I. Physikalisches Institut, Universität zu Köln, 2004

Dr. Reinhard Scholz, *Spectroscopic Properties of Perylene Derivatives*, Habilitation, TU Chemnitz, 2004

Dr. Reinhard Scholz, Ernennung zum Oberassistenten TU München, 2006

Dr. Frank Cichos, Ruf auf eine W2 Stelle, Universität Leipzig, 2006

PhD-Thesis

Jens Illemaann, Präzisionsmassebestimmung einzelner Partikel im Femtogrammbereich und Anwendungen in der Oberflächenphysik, TU Chemnitz July 2000

Emmanuelle Lescop, *Laserinduzierte Prozesse im System $C_2H_2^+ + H_2$* , TU Chemnitz August 2000

Alfonz Luca, *Neuartige Speicherexperimente zur Untersuchung der Bildung atomarer und molekularer Strukturen*, TU Chemnitz April 2001

Raquel Torrents Martin, *Untersuchung elementarer, plasma-relevanter Ion-Molekül-Reaktionen mit einer GIB-Apparatur*, TU Chemnitz April 2001

Michael Reyman, *Ionenaarbildung bei Multiphotonenanregung von HCl*, TU Chemnitz November 2001

Jörg Schuster, *Untersuchungen der Diffusion in dünnen Flüssigkeitsfilmen mit Methoden der Einzelmoleküldetektion*, TU Chemnitz Januar 2002

Jan von Richthofen, *Untersuchung der Bildung, des Isotopenaustausches und der Isomerisierung des Ionensystems HCO^+/HOC^+* , TU Chemnitz August 2002

Dominik Clement, *Infrarot-Matrixisolationsspektroskopie an SiC- und SiC:N-Nanopartikeln*, AIU Jena August 2002

- Dirk Fabian**, *Optische Eigenschaften und strukturelle Umwandlungen ausgewählter Silikate und Oxide als Analoga des kosmischen Staubes*, AIU Jena November 2002
- Christophe Nicolas**, *Astrophysically relevant reactions of N^+ and C^+ : the role of finestructure*, Verteidigung in Orsay, September 2002
- Ivan Kondov**, *Numerical studies of electron transfer in systems with dissipation*, TU Chemnitz, Februar 2003
- Stefan Wellert**, *Wechselwirkung von Elektronen und Molekülen mit einzelnen SiO_2 -Nanopartikeln: Massenanalyse in einer Vierpolfalle*, TU Chemnitz, April 2003
- Oskar Asvany**, *Isotope fractionation in carbon containing molecules*, TU Chemnitz, Juni 2003
- Igor Vragovic**, *Frenkel exciton model of excitation and recombination processes in crystalline alpha-PTCDA*, TU Chemnitz, 2003
- Oleksandr Sukhorukov**, *Spectroscopy of polycyclic aromatic hydrocarbons for the identification of the diffuse interstellar bands*, Friedrich-Schiller-Universität Jena, July 2004
- Igor Savic**, *Formation of Small Hydrocarbon Ions Under Inter- and Circumstellar Conditions: Experiments in Ion Traps*, TU Chemnitz, August 2004
- Jörg Martin**, *Orts- und zeitaufgelöste optische Spektroskopie an Silizium-Nanokristallen*, TU Chemnitz, Dezember 2004
- Serge Krasnokutski**, *Electronic Spectroscopy of Polycyclic Aromatic Hydrocarbons*, University of Kharkov, Kharkov, Ukrain, July 2005
- Alexander Victorovich Terentyev**, *Theoretical investigation of excited states of C_3 and pathways for the reaction $C_3 + C_3 \rightarrow C_6$* , TU Chemnitz, 2005
- Isabel Llamas Jansa**, *Experimental study of the optical and structural properties of carbon nanoparticles*, FSU Jena, Februar 2006
- Abey Issac**, *Photoluminescence Intermittency of Semiconductor Quantum Dots in Dielectric Environments*, TU Chemnitz, August 2006
- Arne Schob**, *Die Dynamik einzelner Moleküle in eingeschränkten und gescherten Flüssigkeiten*, TU Chemnitz, September 2006
- Akemi Tamanai**, *Experimental Mid-Infrared Spectroscopic Extinction Measurements of Agglomerate Dust Grains in Aerosol*, FSU Jena, eingereicht Dezember 2006
- Olivier Debieu**, *The photoluminescence of silicon nanocrystals embedded in quartz and silicates*, Friedrich-Schiller-Universität Jena, to be submitted in April 2007
- Robert Barthel**, *Computational study of interstellar hydrocarbon formation*, TU Dresden, planned for 2007
- Gheorghe Borodi**, *Reactions of stored ions with H and D atoms*, TU Chemnitz, planned for summer 2007

2. Basic concept

Silvio Decker, *Glühender Kohlenstoff: von C_{60}^+ über Russ bis Stäben*, TU Chemnitz, planned for 2007

Diploma-Thesis

Falk Windisch, *Optische Untersuchungen an laserlevitierten Nanopartikeln*, TU Chemnitz, November 2001

Isabel Llamas Jansa, *Spectroscopy and Structural Characterization of Carbon Nanoparticles*, Produced by Laser Pyrolysis of Acetylene", März 2002

Eckart Vogelsberger, *Aufbau und Optimierung einer Teilchenfalle für mikrometergroße Staubteilchen*, Fachhochschule Jena November 2002

Markus Schröder, *Wellenpaketdynamik in molekularen Systemen*, TU Chemnitz Januar 2003

Robert Barthel, *Theoretische Untersuchungen zur Bildung von Kohlenwasserstoffen unter astrophysikalischen Bedingungen*, TU Dresden, April 2003

Silvio Decker, *Temperaturbestimmung von elektrisch- und lasergeheizten Kohlenstoff-Teilchen*, Diplomarbeit TU Chemnitz, Dezember 2003

Michel Barth, *Mikroskopie und Spektroskopie an Farbstoffmolekülen in photonischen Kristallen*, Diplomarbeit, TU Chemnitz, Oktober 2004

Ruben Schmidt, *Zeitaufgelöste Mikroskopie an einzelnen Molekülen zur Untersuchung der Polymerdynamik in dünnen Filmen*, Diplomarbeit, TU Chemnitz, November 2005

Susann Hummel, *Gasphasen-Kondensation von Silikatpartikeln und spektroskopische sowie analytische Untersuchungen*, FSU Jena, März 2006

Mike Vieluf, *Nanolithographische Strukturierung an selbstassemblierten organischen Monolagen zur selektiven Modifizierung*, TU Chemnitz, September 2006

Jörg Brabandt, *Reversibles und irreversibles Photobleichen von einzelnen Molekülen und im Ensemble*, TU Chemnitz, November 2006

Romy Radünz, *Photothermische Detektion einzelner Quantenobjekte*, TU Chemnitz, Dezember 2006

Rebecca Wagner, *Optische Mikroskopie an einzelnen Quantenpunkten in photonischen Kristallen*, TU Chemnitz, Dezember 2006

2.5 Publications from the FGLA (since 2003)

- Andersen, A.C., Mutschke, H., Posch, Th., Min, M., Tamanai, A.: *Infrared extinction by homogeneous particle aggregates of SiC, FeO and SiO₂: Comparison of different theoretical approaches*, J. Quant. Spectr. Rad. Transfer **100** (2006) 4.
- Asvany, O., Giesen, T., Redlich, B. and Schlemmer, S., *Laser Induced Reaction: the antisymmetric bending vibration of C₂H₂⁺*, Physical Review Letters, **94** (2005), 073001.
- Asvany, O., Kumar, P., Hegemann, I., Redlich, B., Schlemmer, S., and Marx, D., *Understanding the LIR Infrared Spectrum of Bare CH₅⁺*, Science **309**, (2005) 1219-1222.
- Asvany, O., Savic, I., Schlemmer, S., and Gerlich, D.: *Variable temperature ion trap studies of CH₄⁺ + H₂, HD and D₂: negative temperature dependence and significant isotope effect*, Chem. Phys. **298** (2004a) 97-105.
- Asvany, O., Schlemmer, S., and Gerlich, D.: *Deuteration of CH_n⁺ (n=3-5) in collisions with HD measured in a low temperature ion trap*, Astrophys. J., **617** (2004b) 685-692.
- Barth, M. Gruber, A. Cichos, F.: *Spectral and spatial redistribution of photoluminescence near a photonic stop band*, Phys. Rev. B. **72** (2005) 85129.
- Barthel, R., Heine, T., Joblin, C., Seifert, G.: *Photoinduced dissociation of hydrocarbons: coronene, corannulene and isomers*, (2007b), in preparation.
- Barthel, R., Scholz, R., Seifert, G.: *Growth mechanisms of interstellar polycyclic hydrocarbons: reactions with methyldine*, Astron. Astrophys. (2007a), in preparation.
- Barthel, R., Seifert, G.: *Growth mechanism of interstellar polycyclic hydrocarbons: reactions with di- and trivalent polyatomic molecules*, Astron. Astrophys. (2007c), in preparation.
- Barthel, R.: *Computational study of interstellar hydrocarbon formation*, Ph.D. Thesis, TU Dresden (2007), under preparation.
- Barthel, R.: *Theoretische Untersuchung zur Bildung von Kohlenwasserstoffen unter astrophysikalischen Bedingungen*, Master Thesis, Technische Universität, (2003).
- Binette, L., Magris C., G., Krongold, Y., Morisset, C., Haro-Corzo, S., Antonio de Diego, J., Mutschke, H., Andersen, A.C.: *Nanodiamond dust and the far-ultraviolet quasar break*, Astrophys. J., **631** (2005) 661.
- Binette, L., Andersen, A.C., Mutschke, H., Haro-Corzo, S.: *Nanodiamond dust and the energy distribution of quasars*, Astron. Nachr. **327** (2006) 151.
- Borodi, G., Geppert, W.D., Luca, A., Mogo, C., Gerlich, D.: *Formation and destruction of CH⁺ in interstellar space*, in preparation (2007)
- Borodi, G., Luca, A., Gerlich, D.: *Collisions of cold trapped CH₅⁺ ions with a slow H atom beam*, in preparation (2007)

- Borodi, G., Luca, A., Gerlich, D.: Reactions of $\text{CO}_2^+ + \text{H} / \text{H}_2$ and deuterated analogues, in preparation (2007)
- Cichos, F., Martin, J., von Borczyskowski, C.: *Characterizing the non-stationary blinking of silicon nanocrystals*, J. Luminesc. **107** (2004a) 160-165.
- Cichos, F., Martin, J., von Borczyskowski, C.: Emission intermittency in silicon nanocrystals, Phys. Rev. B **70** (2004b) 1153141- 11543149.
- Dai, D., Wang, C.C., Wu, G., Harich, S. A., Song, H., Hayes, M., Skodjes, R.T., Wang, X., Gerlich, D., Yang, X.: *State -to-State Dynamics of High-n Rydberg H-Atom Scattering with D_2* , Phys. Rev. Lett. **95**, (2005) 13201-1 - 4.
- Delerue, C., Allan, G., Reynaud, C., Guillois, O., Ledoux, G., Huisken, F.: *Multiexponential photoluminescence decay in indirect-gap semiconductor nanocrystals*, Phys. Rev. B **73** (2006) 235318.
- Dzhonson, A., Gerlich, D., Bieske E.J., and Maier, J.P.: *Apparatus for the study of electronic spectra of collisionally cooled cations: para-dichlorobenzene*, J. Mol. Struc. **795** (2006) 93 - 97.
- Fischer, G., Barthel, R., Seifert, G. *Molecular dynamics study of the reaction $\text{C}_3 + \text{H}_3^+$* , Eur. Phys. J. D **35** (2005), 479.
- Gerlich, D.: *Molecular ions and nanoparticles in RF and AC traps*, Hyperfine Interactions, **146/147** (2003) 293-306.
- Gerlich, D.: *Rf Ion Guides*, in "The Encyclopedia of Mass Spectrometry", Vol 1, Ed. by P. B. Armentrout, Elsevier Ltd., (2003) 182-194.
- Gerlich, D.: *Applications of rf fields and collision dynamics in atomic mass spectrometry*, J. Anal. At. Spectrom., **19** (2004) 581-590.
- Gerlich, D.: *Probing the structure of CH_5^+ ions and deuterated variants via collisions*, Phys. Chem. Chem. Phys. **7** (2005) 1583- 1591.
- Gerlich, D., Smith, M.: *Laboratory astrochemistry: studying molecules under inter- and circumstellar conditions*, Phys. Scr. **73** (2006) C25-C31.
- Gerlich, D., Windisch, F., Hlavenka, P., Plašil, R., Glosik, J.: *Dynamical constraints and nuclear spin caused restrictions in H_mD_n^+ collision systems and deuterated variants*, Phil. Trans. R. Soc. Lond. **A 364** (2006) 3007–3034.
- Glosík, J., Hlavenka, P., Plašil, R., Windisch, F., Gerlich, D., Wolf, A., Kreckel, H.: *Action spectroscopy of H_3^+ using overtone excitation*, Phil. Trans. R. Soc. Lond. **A 364** (2006) 2931–2942.
- Grimm, M., Langer, B., Schlemmer, S., Lischke, T., Becker, U., Widdra, W., Gerlich, D., Flesch, R., Rühl, E.: *Charging mechanisms of trapped element-selectively excited nanoparticles exposed to soft X-rays*, Phys. Rev. Lett. **96** (2006) 066801-066805.
- Hlavenka, P., Plašil, R., Bánó, G., Korolov, I., Gerlich, D., Ramanlal, J., Tennyson, J., Glosík, J.: *Near infrared second overtone cw-cavity ringdown spectroscopy of D_2H^+ ions*, Int. J. Mass Spectrometry, **255** (2006) 170-176.

- Hummel, S., *Gasphasen-Kondensation von Silikatpartikeln und spektroskopische sowie analytische Untersuchungen*, Diplomarbeit, FSU Jena, März 2006
- Issac, A., Cichos, F., von Borczyskowski, C.: Correlation between photoluminescence intermittancy of CdSe quantum dots and self-trapped states in dielectric media, *Phys. Rev. B* **71** (2005) 1613021-1613024 (R).
- Jäger, C., Dorschner, J., Mutschke, H., Posch, Th., Henning, Th.: *Steps toward interstellar silicate mineralogy VII. Spectral properties and crystallization behaviour of magnesium silicates produced by the sol-gel method*, *Astron. Astrophys.* **408** (2003) 193.
- Jäger, C., Krasnokutski, S., Staicu, A., Huiskens, F., Mutschke, H., Henning, Th., Poppitz, W., Voicu, I.: *Identification and spectral properties of PAHs in carbonaceous soot produced by laser pyrolysis*, *Astrophys. J. Suppl. Ser.* **166** (2006) 557 .
- Jäger, C., Mutschke, H., Henning, Th., *Spectral and structural properties of carbon nanoparticles produced by laser ablation*, *Astrophys. J.*, (2007b), in preparation.
- Jäger, C., Mutschke, H., Huiskens, F., Henning, Th., Voicu, I., Poppitz, W.: *Spectral characterization of soot by-products obtained by CO₂ laser pyrolysis of benzene/hydrocarbon vapors*, *Carbon* (2007a), in preparation
- Krasnokutski, S., Rouillé, G., Huiskens, F.: *Electronic spectroscopy of anthracene molecules trapped in helium nanodroplets*, *Chem. Phys. Lett.* **406** (2005) 386-392.
- Kreckel, H., J. Mikosch, R. Wester, J. Glosik, R. Plasil, M. Motsch, D. Gerlich, D. Schwalm, D. Zajfman and A. Wolf: *Towards state selective measurements of the H₃⁺ dissociative recombination rate coefficient*, *Journal of Physics: Conference Series* **4** (2005) 126 -133.
- Kreckel, H., Motsch, M., Mikosch, J., Glosik, J., Plasil, R., Altevogt, S., Andrianarijaona, V., Buhr, H., Hoffmann, J., Lammich, L., Lestinsky, M., Nevo, I., Novotny, S., Orlov, D. A., Pedersen, H. B., Sprenger, F., Terekhov, A. S., Toker, J., Wester, R., Gerlich, D., Schwalm, D., Wolf, A., and Zajfman D.: *High-Resolution Dissociative Recombination of Cold H₃⁺ and First Evidence for Nuclear Spin Effects*, *Phys. Rev. Lett.* **95** (2005) 263201.
- Llamas Jansa, I., Jäger, C., Mutschke, H., Henning, Th.: *Far-ultraviolet to near-infrared optical properties of carbon nanoparticles produced by pulsed-laser pyrolysis of hydrocarbons and their relation with structural variations*, *Carbon*, (2007), submitted
- Llamas Jansa, I., Mutschke, H., Clément D., Jäger, C., Henning, Th.: *IR spectroscopy of carbon nanoparticles from laser-induced gas pyrolysis*, In: *Exploring the ISO Data Archive-Infrared Astronomy in the Internet Age*, ed. C. Gry et al., ESA SP-511 (2003) 69.
- Llamas Jansa, I.: *Experimental study on the optical and structural properties of carbon nanoparticles*. Ph. D. Thesis, Friedrich Schiller Universität Jena, (2006)

2 Basic concept

- Luca, A., Borodi, G., Gerlich, D.: *Interactions of ions with Hydrogen atoms*, Progress report in XXIV ICPEAC 2005, Rosario, Argentina, July 20-26, 2005, Edited by F.D.Colavecchia, P.D.Fainstein, J.Fiol, M.A.P.Lima, J.E.Miraglia, E.C.Montenegro, and R.D.Rivarola
- Luca, A., Borodi, G., Mogo, C., Smith, M., Gerlich, D.: On the combination of a temperature variable H/D atom beam with a multipole ion trap, to be submitted to Rev. Sci. Instr. (2007)
- Martin, J., Cichos, F., Chan, I. Y., Huisken, F., von Borczyskowski, C.: Photoinduced processes in silicon nanoparticles, *Isr. Journ. Chem.* **44** (2004) 341-351
- Martin, J., Cichos, F., von Borczyskowski, C.: Confocal microscopy of electrostatic properties of Si-quantum dots and silica surfaces by charge sensitive dye molecules, *Opt. Spectr.* **99** (2005) 281- 288 and **99** (2005) 297-303.
- Martin, J., Cichos, F., von Borczyskowski, C.: Spectroscopy of single silicon nanoparticles, *J. Luminesc.* **108** (2004) 347-350.
- Mikosch, J., Kreckel, H., Plasil, R., Gerlich, D., Glosik, J., Schwalm, D., Wolf, A.: *Action spectroscopy and temperature diagnostics of H_3^+ by chemical probing*, *J. Chem. Phys.*, **121** (2004) 11030 - 11037.
- Mirzov, O., Cichos, F., von Borczyskowski, C., Scheblykin, I. G.: *Fluorescence blinking in MEH-PPV single molecules at low temperature*, *J. Lumin.* **112** (2005) 353.
- Mirzov, O., Cichos, F., von Borczyskowski, C., Scheblykin, I.G.: *Direct exciton quenching in single molecules of MEH-PPV at 77 K*, *Chem. Phys. Lett.* (2004) 286-290.
- Mirzov, O., Pullerits, T., Cichos, F.: von Borczyskowski, C., Scheblykin, I. G.: *Large spectral diffusion of conjugated polymer single molecule fluorescence at low temperature*, *Chem. Phys. Lett.* **408** (2005) 317-321.
- Mutschke, H., Andersen, A.C., Jäger, C., Henning, Th., Braatz, A.: *Optical data of meteoritic nano-diamonds from far-ultraviolet to far-infrared wavelengths*, *Astron. Astrophys.* **423** (2004) 983.
- Mutschke, H., Tamanai, A., Min, M.: *Experimental infrared spectroscopy of dust grains in aerosol: Modeling of forsterite spectra*, Poster at the Workshop: From Dust to Planetesimals, Ringberg, Sept. 2006.
- Nicolas, C., Torrents, R., and Gerlich, D.: *Integral and differential cross section measurements at low collision energies for the $N_2^+ + CH_4 / CD_4$ reactions*, *J. Chem. Phys.* **118** (2003) 2723-2730.
- Perez, N., Heine, T., Barthel, R., Seifert, G., Vela, A., Mendez-Rojas, M., Merino, G., *Planar tetracoordinate carbons in cyclic hydrocarbons*, *Org. Lett.* **7**, (2005) 1509.
- Petrov, E.P., Cichos, F., Zenkevich, E.I., Starukhin, D., von Borczyskowski, C.: Time resolved photoluminescence anisotropy of CdSe/ZnS nanoparticles in toluene at room temperature, *Chem. Phys. Lett.* **402** (2005) 233–238.

- Petrov, E.P., Cichos, F., Spange, S., von Borczyskowski, C.: Investigation of thetherable distilbazolium compounds as fluorescent probes in nanostructured silica sol-gel materials, *Photochem. Photobiol.* **81** (2005) 898-907.
- Petrov, E.P., Cichos, F., von Borczyskowski, C.: Intrinsic photophysics of semiconductor nanocrystals in dielectric media: formation of surface states, *J. Luminesc.* **119-120** (2006) 412-417.
- Posch, Th., Kerschbaum, F., Fabian, D., Mutschke, H., Dorschner, J., Tamanai, A., Henning, Th.: *Infrared properties of solid titanium oxides: Exploring potential primary dust condensates*, *Astrophys. J. Suppl. Ser.* **149** (2003) 437.
- Posch, Th., Mutschke, H., Andersen, A.C.: *Reconsidering the origin of the 21 micron feature: oxides in carbon-rich protoplanetary nebulae?*, *Astrophys. J.* 616 (2004) 1167.
- Posch, Th., Mutschke, H., Trieloff, M., Henning, Th.: *Infrared spectroscopy of calcium-aluminium-rich inclusions – analog material for protoplanetary dust?*, *Astrophys. J.*, accepted.
- Pouladsaz D., thesis: *Density functional studies of the spectroscopic properties of Si nanocrystals* (2007) in preparation.
- Rouillé, G., Arold, M., Staicu, A., Krasnokutski, S., Huiskens, F., Henning, Th., Tan, X., Salama, F.: *The $S_1 \leftarrow S_0$ transition of benzo[ghi]perylene probed by cavity ring-down spectroscopy in supersonic jets*, *J. Chem. Phys.*, submitted for publication.
- Rouillé, G., Sukhorukov, O., Staicu, A., Krasnokutski, S., Huiskens, F., Henning, Th.: *Ultraviolet spectroscopy of pyrene in a supersonic jet and in liquid helium droplets*, *J. Chem. Phys.* **120** (2004) 028-6034.
- Savić, I., Cermak, I., Gerlich, D.: *Reactions of C_n ($n=1-3$) with ions stored in a temperature-variable radio frequency trap*, *Int. J. Mass Spectrom.*, **240** (2005) 139 - 147.
- Savić, I., Gerlich, D.: *Temperature variable ion trap studies of $C_3H_n^+$ with H_2 and HD* , *Phys. Chem. Chem. Phys.* **7** (2005) 1026 – 1035.
- Savić, I., Schlemmer, S., Gerlich, D.: *Low-temperature laboratory measurements of forming deuterated $C_3H_3^+$* , *Ap. J.* **621** (2005) 1163-1170.
- Savić, I., Lukic, S.R., Guth, I., Gerlich, D.: *Test measurement on ion-molecule reactions in a ring electrode ion trap*, *Astr. Obs. Belgrade* **80** (2006) 207-210.
- Savić, I., and Gerlich, D.: *Some routes in forming $C_3H_n^+$ ions and deuterated variants under interstellar conditions* AIP Conference Proceedings **876** (2006) 415-422.
- Schlemmer, S., Luca, A. and Gerlich, D.: *Reactions of Ions with Metal Atoms: $O_2^+ + Ni$ and $NiN_2^+ + Ni$* , *Int. J. Mass Spectrom.*, **223-224** (2003) 291-299.
- Schlemmer, S., Wellert, S., Windisch, F., Grimm, M., Barth S., and Gerlich, D.: *Interactions of electrons and molecules with a single trapped nanoparticle*, *Appl. Phys. A*, **78** (2004) 629-636.

2 Basic concept

- Schlemmer, S., Asvany, O., and Giesen, T., *Comparison of the cis-bending and C-H stretching vibration on the reaction of $C_2H_2^+$ with H_2 using laser induced reactions*, Phys. Chem. Chem. Phys. **7** (2005) 1592-1600.
- Schlemmer, S., and Asvany, O., *Laser induced Reactions in a 22-pole ion trap*, Journal of Physics: Conf. Ser. **4** (2005) 134–141.
- Schlemmer, S., Asvany, O., Hugo E., and Gerlich, D.: *Deuterium fractionation and ion-molecule reactions at low temperatures*, Proceedings of the International Astronomical Union, Symposium, Cambridge University Press, **S231** (2006) 125-134.
- Schnaiter, M., Gimmmler, M., Linke, C., Jäger, C., Llamas Jansa, I., and Mutschke, H.: *Strong spectral dependence of light absorption by organic particles formed by propane combustion*, Atmospheric Chemistry and Physics Discussions, **6** (2006) 1841.
- Scholz R., Pouladsaz D. and Schreiber M., *Influence of the Jahn-Teller effect on absorption and photoluminescence spectra of Si nanocrystals*, phys. stat. sol. (c) **3** (2006) 3561.
- Schuster, J. Brabandt , J., von Borczyskowski, C.: *Discrimination of Photoblinking and Photobleaching on the Single Molecule Level*, J. Luminescence 2007, in print.
- Schuster, J., Cichos, F., von Borczyskowski, C.: Blinking of single dye molecules in various environments, Opt. Spectr. **98** (2005) 712-717.
- Schuster, J., Cichos, F., von Borczyskowski, C.: Influence of self-trapped states and photoproducts on the intermittency of single molecules, Appl. Phys. Lett. **87** (2005) 5195.
- Schuster, J., Cichos, F., von Borczyskowski, C.: Variation of power-law dynamics caused dark state recovery of single molecule fluorescence intermittency, SPIE **6358** (2006) 6258041-8.
- Schuster, R., Barth, M., Gruber, A., Cichos, F.: *Defocused Wide Field Fluorescence Imaging of Single CdSe/ZnS Quantum Dots*, Chem. Phys. Lett. **413** (2005) 280-283.
- Shamirzaev, T.S., Gilinsk, A.M., Toropov, A.I., Bakarov, A.K., Tenne, D.A., Zhuravlev, K.S., von Borczyskowski, C., Zahn, Model of Photoluminescence of InAs quantum dots embedded in dielectric band gap AlGaAs matrices, Material Science (2004) 157- 1160.
- Shamirzaev, T.S., Gilinsky, A.M., Bakarov, A.K., Toropov, A.I., Tenne, D.A., Zhuravlev, K.S., von Borczyskowski, C., Zahn, D.R.T.: Millisecond photoluminescence kinetics in a system of direct-bandgap InAs quantum dots in an AlAs matrix, JETP Letters **77** (2003) 459-463.
- Shamirzaev, T.S., Gilinsky, A.M., Toropov, A.I., Bakarov, A.K., Tenne, D.A., Zhuravlev, K.S., von Borczykowski, C., Zahn, D.R.T.: Millisecond fluorescence in InAs quantum dots embedded in AlAs, Physica E **20** (2004) 282-285.

- Song, H., Dai, D., Wu, G., Wang, C.C., Harich, S. A., Hayes, M. Y., Wang, X., Gerlich, D., Yang, X., Skodje, R. T.: *Chemical reaction dynamics of Rydberg atoms with neutral molecules: A comparison of molecular-beam and classical trajectory results for the $H(n)+D_2 \rightarrow HD+D(n')$ reaction*, Journal of Chem. Phys. **123** (2005) 074314-1 - 10.
- Staicu, A., Krasnokutski, S., Rouillé, G., Henning, Th., Huiskens, F.: *Electronic spectroscopy of polycyclic aromatic hydrocarbons (PAHs) at low temperature in the gas phase and in helium droplets*, J. Molec. Struct. **786** (2006) 105-111.
- Staicu, A., Krasnokutski, S., Rouillé, G., Huiskens, F., Henning, Th., Scholz, R.: *Cavity ring-down spectroscopy of 2,3-benzofluorene in supersonic jets and liquid helium droplets*, Chem. Phys. Lett., to be submitted.
- Staicu, A., Rouillé, G., Sukhorukov, O., Henning, Th., Huiskens, F.: *Cavity ring-down laser absorption spectroscopy of jet-cooled anthracene*, Molec. Phys. **102** (2004b) 1777-1783.
- Staicu, A., Sukhorukov, O., Rouillé, G., Huiskens, F., Henning, Th.: *Cavity ring-down spectroscopy of carbon-containing molecules*, in: ROMOPTO 2003: Seventh Conference on Optics, edited by V. I. Vlad, Proc. SPIE **5581** (2004a) 670-676.
- Sukhorukov, O., Staicu, A., Diegel, E., Rouillé, G., Henning, Th., Huiskens, F.: $D_2 \leftarrow D_0$ transition of the anthracene cation observed by cavity ring-down absorption spectroscopy in a supersonic jet, Chem. Phys. Lett. **386** (2004) 259-264
- Tamanai, A., Mutschke, H., Blum, J., Meeus, G.: *The 10 μm infrared band of silicate dust: A laboratory study comparing the aerosol and KBr pellet techniques*, Astrophys. J. Letters **648** (2006a) L147.
- Tamanai, A., Mutschke, H., Blum, J., Neuhauser, R.: *Experimental infrared spectroscopic measurement of light extinction for agglomerate dust grains*, J. Quant. Spectr. Rad. Transfer **100** (2006b) 373.
- Tamanai, A., Mutschke, H., Blum, J.: *Experimental Infrared Spectroscopic Extinction Measurements of Agglomerate Dust Grains in Aerosol: Silicates*, Contributed talk, 25th Grain Formation Workshop, Kyoto, Jan. 2006
- Tamanai, A., Mutschke, H., Blum, J.: *Experimental Infrared Spectroscopic Extinction Measurements of Agglomerate Dust Grains in Aerosol*, Contributed talk at the Workshop: From Dust to Planetesimals, Ringberg, Sept. 2006.
- Tamanai, A.: *Experimental Mid-Infrared Spectroscopic Extinction Measurements of Agglomerate Dust Grains in Aerosol*, Ph. D. Thesis, Friedrich Schiller Universität Jena, submitted.
- Terentyev, A., Scholz, R., Schreiber, M., Seifert, G.: *Theoretical investigation of excited states of C_3* , J. Chem. Phys. **121** (2004), 5767.
- von Borczyskowski, C., Cichos, F., Martin, J. Schuster, J., Issac, A., Brabandt, J.: *Common luminescence fluctuations of single particle and single molecules in non-conducting matrices*, Europ. Phys. Journ., 2007, in print.

- Wang, Y.-S., Tsai, C.-H., Lee, Y. T., and Chang, H.-C., Jiang, J. C., Asvany, O., Schlemmer, S. and Gerlich, D.: *Investigations of protonated and deprotonated water clusters using a low-temperature 22-pole ion trap*, J. Phys. Chem. A **107** (2003) 4217-4225.
- Wolf, A., Kreckel, H., Lammich, L., Strasser, D., Mikosch, J., Glosik, J., Plašil, R., Altevogt, S., Andrianarijaona, Buhr, H., Hoffmann, J., Lestinsky, M., Nevo, I., Novotny, S., Orlov, D. A., Pedersen, H. B., Terekhov, A. S., Toker, J., Wester, R., Gerlich, D., Schwalm, D., and Zajfman, D.: *Effects of molecular rotation in low-energy electron collisions of H_3^+* , Phil. Trans. R. Soc. Lond. A **364** (2006) 2981–2997.
- Zenkevich, E.I. , Blaudeck, T., Abdel-Mottaleb, M., Cichos, F., Shulga, A.M., von Borczyskowski, C.: *Photophysical properties of self-aggregated porphyrin-semiconductor nanoassemblies*, Int. Journ. Photoenergy, in print.
- Zenkevich, E.I., Blaudeck, T., Shulga, A.M., Cichos, F., von Borczyskowski, C.: *Identification and assignment of porphyrin-CdSe hetero-nanoassemblies*, J. Luminesc. **122-123** (2007) 784-788.
- Zenkevich, E.I., Shulga, A., Blaudeck, T., von Borczyskowski, C.: *Fabrication and primary photoevents in self-assembled nanocomposites on semiconductor quantum dots and tetrapyrrole Chromophores*, SPIE, in print.
- Zenkevich, E.I., Shulga, A., Cichos, F., Petrov, E., Blaudeck, T., von Borczyskowski, C.: *Nanoassemblies designed from quantum dots and molecular arrays*, J. Phys. Chem. B **109** (2005) 8679-8692.
- Zenkevich, E.I., Shulga, A.M., Petrov, E.P., Cichos, F., von Borczyskowski, C.: *Key-Hole principles and photochemistry of porphyrin self-organization on semiconductor quantum dots*, J. Porphyrins and Phthalocyanines **8** (2004) 4583.
- Zenkevich, E.I., von Borczyskowski, C.: *Photoinduced electron transfer and relaxation in selforganized multiporphyrin nanoassemblies* , In: “Fundamental Photoprocesses and Inhomogeneous Broadening of Electronic Spectra of Organic Molecules in Solution”, Ed. V.I. Tomin, Slupsk (2006).
- Zenkevich, E.I., von Borczyskowski, C.: *Structure and excited state relaxation dynamics in nanoscale self-assembled arrays: Multiporphyrin Complexes, Porphyrin-Quantum Dot Composites.*, SPIE **5849** (2005) 29-40.
- Zenkevich, E.I., Shulga, A.M., Blaudeck, T., Cichos, F., von Borczyskowski, C.: *Competition in the formation of nanosize multiporphyrin complexes and porphyrin-quantum dot heterocomposites*, In: “Physics, Chemistry and Applications of Nanostructures. Reviews and Short Notes to Nanomeeting-2005” (V.I. Borisenko, S. V. Gaponenko, V. S. Gurin, Eds.), World Scientific Publishing Co., New Jersey, London, Singapore, Beijing, Shanghai, Hong-Kong, Taipei, Chennai. 367-370 (2005).

3.1 Bericht Teilprojekt 1

3.1.1 Titel / Title

Molekuldynamik-Simulation von Struktur, Bildung und Reaktivität von Molekülen und Clustern

Molecular dynamics simulation of structure, formation and reactivity of molecules and clusters

3.1.2 Berichtszeitraum / reported period

01.08.2003 - 31.07.2006

3.1.3 Projektleiter / principle investigator

Seifert, Gotthard, Prof. Dr., Dipl.-Chem. Universitätsprofessor,
Institut für Physikalische Chemie, Technische Universität Dresden

Scholz, Reinhard, Dr., Dipl.-Phys., Oberassistent,
Technische Universität Chemnitz (bis Dezember 2006)
Technische Universität München (seit März 2006)

3.2 Zusammenfassung / Abstract

3.2.1 Wortlaut des Antrags / abstract of the proposal

Das vorliegende Projekt soll zum Verständnis der Elementarschritte beitragen, welche die dynamische Evolution der interstellaren Materie kontrollieren. Dazu werden Verfahren der Dichte-Funktional Theorie (DFT) und die Dichte-Funktional basierte „tight-binding“ Methode angewendet, die eine hohe Genauigkeit und eine herausragende numerische Leistungsfähigkeit kombinieren. Die Reaktionen der Moleküle und Cluster werden mit statischen Rechnungen des optimalen Reaktionsweges und durch dynamische Simulationen der Kollisionen zwischen Molekülen, Clustern und den entsprechenden Ionen untersucht. Insbesondere soll die Bildung kleiner Kohlenwasserstoffspezies durch Simulation der Stöße zwischen Kohlenstoffclustern und Clusterionen mit CH_x und mit H_2 untersucht werden. Weiterhin soll die Bildung von zyklischen Kohlenwas-

serstoffen als Elementarschritt für die Bildung von PAH's aufgeklärt werden.

The present project shall contribute to an understanding of the elementary steps controlling the dynamical evolution of interstellar matter. The methods applied will be the density-functional theory (DFT) and the density-functional based tight-binding (DFTB) method, combining a high precision with an outstanding numerical performance. The reactions of molecules and clusters will be investigated by static calculations of the optimum reaction path and by dynamical simulations of the collisions between molecules, clusters, and the corresponding ions. Especially the formation of small hydrocarbon species by simulations of collisions between carbon clusters and cluster ions with CH_x and with H_2 will be studied. Furthermore, the formation of cyclic hydrocarbons as elementary steps for the formation of polycyclic aromatic hydrocarbons (PAH) shall be clarified.

3.2.2 Zusammenfassung des Berichts / abstract of the report

In the course of the present project, we have studied formation processes of carbon clusters and hydrocarbons restricted to ultra-low temperatures and densities. The method used for these studies is the density functional theory (DFT).

Our approach is based on quantum molecular dynamic simulations of the collisions between molecular reactants within a statistical framework. In particular, the simulations were conducted by a modification of the DFT, the density-functional based tight binding (DFTB) method, which combines a high precision with an outstanding numerical performance.

On the other hand, the characteristics of single reaction channels were studied by the nudged elastic band method (NEB). The properties of the reactants and the products, as well as the intermediates and the transition states of the reaction channels were refined by modest levels of quantum chemistry.

The investigations comprised ion-molecule reactions of mono-, di-, tri- and tetravalent small interstellar hydrocarbon molecules with carbon clusters and hydrocarbons (CH , HCCC , H_2CC , H_2CCC , H_2CCCC , $\text{C}_2 + \text{C}_x\text{H}_y^+$ and $\text{HCCCCH}_2^+ + \text{C}_x\text{H}_y$, with $x=5-24$ and $y=0-12$). Special emphasis was put in the study of the formation channels of aromatic structures .

Additionally, for a small reference system (C_3), the excited states were analysed with time-dependent density functional theory. The suitability of different excited electronic configurations for the reaction $C_3 + C_3 \rightarrow C_6$ was investigated for selected highly symmetric relative orientations of the reactants.

3.3 Ausgangsfragen, neuster Stand der Forschung / Initial goals, current status of the field

The project was established to contribute to an understanding of the elementary steps which control the dynamical evolution of interstellar matter. The focus was set on the polycyclic hydrocarbon, especially polycyclic aromatic hydrocarbon (PAH), growth mechanisms.

These molecules are known to be part of the interstellar and circumstellar matter. Evidences of their presence comes the infrared (IR) emission bands of different astronomical objects [*Leger1984, Allamandola1985*]. Moreover, interstellar PAHs are considered to be an intermediate stage between the gas and the dust phases of interstellar matter [*Duley1981, Leger1989*]. They are expected to exist in a complex statistical equilibrium of different charge and hydrogenation states. In addition, due to IR fluorescence and photoelectric heating processes, PAH account for a substantial fraction of the total interstellar carbon budget and contribute to the energy balance of the galaxy [*Bakes1994, Habart2001*].

Different formation mechanisms can be responsible for the abundance of polycyclic hydrocarbons and PAHs: a) circumstellar chemistry [*Allamandola1989*], b) shattering of carbonaceous dust grains [*Jones1996*], c) photo-induced destruction of carbonaceous cluster [*Brechignac2005*], and d) interstellar chemistry. In hot carbon-rich circumstellar shells, for example, the dominant chemical pathway to the formation of PAHs and hydrocarbons is the successive addition of C_2H_2 [*Allamandola1989*]. Similar processes are assumed and investigated under the condition of the interstellar ultra-low densities and temperatures [*Smith1992, Millar1997*].

Under constraints of high unsaturation and charged states of hydrocarbons some mechanisms still work (see reaction rates of [*Millar1997*]), but the addition of C_2H_2 to (charged) PAHs show distinctive reaction barriers. Without the proper photo-induced activation, like in the case of dark clouds, C_2H_2 additions are not favoured.

One of the aims of this project was to study growth mechanisms for PAHs and analogues from highly abundant interstellar species. Under the constraints imposed by the ISM, the molecular growth reactions are supposed to be dominated by binary gas-phase collisions.

In order to study dynamic effects of collisions, we focused on the calculations of collision trajectories. However, static calculations were considered for the analysis of important molecular states, such as transition states or local minima. The collision trajectory calculations were based on a quasi-classical molecular dynamics (MD) approach combined with Density-Functional Theory (DFT) methods [Harris1985]. To sample the potential energy surface (PES) of collisions within a statistical framework, we used the Density-Functional Tight-Binding (DFTB) method. This method provides superior computational efficiency and also reasonable accuracy. The characteristic mechanisms of single reaction channels were solved by the nudged elastic band method (NEB). The properties of the reactants and the products, as well as the intermediates and the transition states of the reaction channels, were refined by modest levels of quantum chemistry methods, e.g. post-Hartree-Fock methods.

3.4 Angewandte Methoden / Experimental methods

Quasi-classical trajectories to sample the potential energy surface (PES)

The approach to study large reaction systems, without a reaction PES parameterisation, is based on earlier works by Seifert and Porezag [Seifert1996, Seifert1992, Porezag1995]. Under the adiabatic approximation, molecular dynamic trajectories $R_i(t)$ can be obtained by solving the coupled set of Newton-type equations,

$$M_i \ddot{R}_i = - \frac{\partial}{\partial R_i} E(R_1, \dots, R_N)$$

where N represents the number of nuclei with masses M_i ($i=1, \dots, N$) and $E(R_1, \dots, R_N)$ represents the energy of the electronic ground state of the Born-Oppenheimer surface. The energies are calculated by the DFTB method [Seifert1996, Porezag1995, Seifert1992].

The above set of equations of motion is integrated numerically by a Verlet algorithm. To fulfil the total energy conservation condition, the time step for all quantum MD simulations was restricted to 10 a.u.

Each collision trajectory between the two reactants was started at a quasi interaction-free distance. After the collision or the point of minimal encounter, the trajectories were propagated for a further timer interval of 6 picoseconds (ps). Additionally, the total momentum of the collision system was considered to be conserved.

The statistics were set up by randomisation of the initial trajectory conditions (such as relative orientation). The impact parameter \mathbf{b} was varied systematically, allowing the calculation of the capture cross section σ by integrating the capture/reaction probabilities $P(\mathbf{b})$ over the impact parameter \mathbf{b} . To achieve a representative integration over the reaction probabilities, 50 to 100 trajectories had to be propagated for each range of impact parameter ($\Delta b < 0.4$ a.u.). This high number of calculated trajectories also guaranteed a good sampling of the local reaction potential energy surface as well as a pre-selection of important reaction channels. Finally, thermal rate coefficients $k(T)$ were derived from the proper average $\langle \sigma(\varepsilon) \varepsilon \rangle$.

Minimum energy path (MEP) calculations of reaction channels (RCs)

The lowest reaction paths corresponding to pre-selected reaction channels were refined and re-optimised using the NEB method [Henkelman2000, Henkelmann2000a]. Chain-of-state methods, such as NEB, allow a search of transition states (TS) between unconnected local minima on the reaction PES. The optimisation to the MEP by the NEB method follows a force projection scheme:

$$F_i = F_i|_{\parallel} - \nabla E(R_i)|_{\perp}$$

Forces and total energies were computed in combination with the DFTB (DeMon package [Köster2004]) and with the B3LYP method (Gaussian package [Frisch2004]).

Comparison of different approaches

In addition, the geometry of reactants, product isomers as well as intermediates and transition states of importance were re-optimised using the hybrid B3LYP method. For the optimization and the analysis of the harmonic frequencies we have used B3LYP in the 6-31G(d) basis set. Total energy values were refined by single point calculations with larger basis sets such as 6-311++G(3df,3pd). Furthermore, results were compared with post-Hartree-Fock methods such as G3 [Curtiss1998, Baboul1999] and MP2. Finally, the harmonic frequency analysis was revised at MP2/6-

31G(d) level. For all calculations the Gaussian quantum chemistry package was used.

3.5 Ergebnisse und ihre Bedeutung / Results and their importance

Reactions of interstellar hydrocarbons with methyldine (CH)

a) monocyclic hydrocarbons

Reactive collisions of methyldine with different hydrocarbons were studied in order to check the suitability of methyldine as a precursor of hydrocarbon growth under the constraints of the ISM. Photochemical processes were not considered.

CH addition at arbitrary hydrocarbon positions was found to release of a high amount of reaction energy (5-8 eV). This fact can be related to the trivalent and strong electron donating character of the CH molecule. Its three valence electrons allowed the formation of three new bonds.

CH addition to monocyclic hydrocarbons can lead to an extension of the ring. The results of the CH ring extension of $C_xH_y^+$ are summarized in Table 1 (corresponding structures are shown in Fig. 1).

Table 1: Reaction energies in eV. Isomers are taken from Fig. 1.

$X + CH \rightarrow Y$	DFTB	B3LYP	G3
$\alpha\text{-C}_5\text{H}_5^+, \alpha\text{-C}_6\text{H}_6^+$	-7.3710	-7.7536	-7.2775
$\alpha\text{-C}_6\text{H}_6^+, \alpha\text{-C}_7\text{H}_7^+$	-6.1458	-7.3951	-7.0827
$\alpha\text{-C}_7\text{H}_7^+, \alpha\text{-C}_8\text{H}_8^+$	-4.6859	-4.3160	-4.2443
$\alpha\text{-C}_8\text{H}_8^+, \alpha\text{-C}_9\text{H}_9^+$	-5.8525	-5.8260	-6.1804
$\alpha\text{-C}_9\text{H}_9^+, \alpha\text{-C}_{10}\text{H}_{10}^+$	-6.1156	-5.4932	-

Information about the product distribution was obtained by an analysis of the reactions between $C_xH_x^+$ and CH. Thermodynamic properties of important products were investigated (see Fig.1).

Table 2: Capture rate constants at 100 K and canonical capture cross sections at total collision energy of 0.01 eV.

$X + CH \rightarrow Y$	$k_{100\text{ K}}/10^{-10}\text{ cm}^3\text{ s}^{-1}$	$\sigma_{0.01\text{ eV}}/10^{-20}\text{ m}^2$
$\alpha\text{-C}_5\text{H}_5^+, \alpha\text{-C}_6\text{H}_6^+$	6.3	181.0
$\alpha\text{-C}_6\text{H}_6^+, \alpha\text{-C}_7\text{H}_7^+$	6.1	180.1
$\alpha\text{-C}_7\text{H}_7^+, \alpha\text{-C}_8\text{H}_8^+$	6.9	206.5
$\alpha\text{-C}_8\text{H}_8^+, \alpha\text{-C}_9\text{H}_9^+$	7.7	222.6
$\alpha\text{-C}_9\text{H}_9^+, \alpha\text{-C}_{10}\text{H}_{10}^+$	8.4	239.4






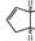


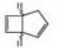
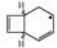

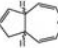
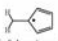
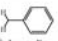

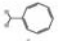
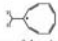


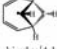




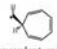
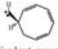
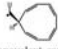
C_xH_x cations	C_xH_x cations	C_xH_x cations	C_xH_x cations	$\text{C}_{10}\text{H}_{10}$ cations
abbr., name	abbr., name	abbr., name	abbr., name	abbr., name
DFTB/B3LYP/G3	DFTB/B3LYP/G3	DFTB/B3LYP/G3	DFTB/B3LYP/G3	DFTB/B3LYP
 α , benzeniumyl 0.0 / 0.0 / 0.0	 α , tropylum 0.0 / 0.0 / 0.0	 α , cyclooctatetraeniumyl 0.7391 / 0.9035 / 1.1501	 α , cyclononatetraeniumyl 1.1290 / 0.7150 / 0.9858	 α , cyclodecapenteniumyl 1.3626 / 0.8743
		 β , dihydropentaleniumyl 0.8072 / 1.3595 / 1.1285		 β , dihydronaphthaleniumyl 0.0 / 0.0
 γ , bicyclo[3.1.0]- hexenyl cation 3.0249 / 2.5627 / 2.3681	 γ , bicyclo[3.2.0]- heptadienyl 2.1562 / 2.2640 / 1.9801	 γ , bicyclo[4.2.0]- octatrienyl 1.3423 / 1.6442 / 1.4093	 γ , dihydro- indenyl 0.0 / 0.0 / 0.0	 γ , dihydro- azulenyl 0.6558 / 0.3756
 δ , fulveniumyl 0.7192 / 0.5039 / 0.5665	 δ , benzylum 0.3842 / 0.3685 / 0.2997	 δ , heptafulveniumyl 0.0 / 0.0 / 0.0	 δ , nonafulveniumyl 0.7058 / 0.3441 / 0.6667	 δ , monafulveniumyl 1.2753 / 0.7121
 ϵ_1 , bicyclo[2.1.1]- hexenyl cation 2.9336 / 2.3683 / 2.1731	 ϵ_1 , bicyclo[2.2.1]- heptadienyl 2.7666 / 2.2764 / 1.6912	 ϵ_1 , bicyclo[4.1.1]- octatrienyl 2.7704 / 2.3081 / -	 ϵ_1 , bridged complex 0.3832 / 1.5405 / 1.4048	 ϵ_1 , triquieniumyl ϵ_2 , bridged complex ϵ_3 , bridged complex 0.0280 / 0.4008 0.4442 / 0.5092 1.5821 / 1.3279
 ξ , monovalent complex 3.8530 / 4.5353 / 4.4657	 ξ , divalent complex 3.8530 / 4.5353 / 4.4657	 ξ , monovalent complex 3.8530 / 4.5353 / 4.4657	 ξ , divalent complex 3.8530 / 4.5353 / 4.4657	 ξ , monovalent complex - / 4.2031

Fig. 1: Products of the reaction $\text{C}_x\text{H}_x^+ + \text{CH}$ to $\text{C}_{x+1}\text{H}_{x+1}^+$ ($x=5-9$). The first row shows the monocyclic products (α), second (β) and third row (γ) show the even and uneven sized bicyclic fused ring products. The fourth row (δ) sketches fulvene derivatives, the fifth row (ϵ_i) bridged polycyclic fused ring isomers whereas the last row (ξ) shows intermediate structures of initial association. For convenience, the hydrogen atoms of sp^2 hybridised carbon atoms are not shown. Relative total energies of products are given at the SCC-DFTB, B3LYP/6-311++G(3df,3pd)//B3LYP/6-31G(d) and G3 level, respectively.

Due to the absence of an entry barrier, almost the entire low-energy collisions were reactive. The cross sections and rate constants of the reactions were found to be close to the capture values of the Langevin model (Table 2.). The results will be described elsewhere in more detail [Barthel2007a].

Zero-point vibration, entropy, and enthalpy corrections of the products were calculated at different temperatures in order to calculate the product distribution/population in thermodynamic equilibrium. The basics of population calculations were described elsewhere in more detail [Slanini2003]. Our results for temperatures ranging between 0 and 5000 K are shown in Fig. 2, revealing that up to 1000 K the product distribution is dominated by the most stable isomers (Fig. 1).

As a function of the number of carbon atoms (and of ring size), the most stable reaction product changes from monocyclic isomers of $C_6H_6^+$ and $C_7H_7^+$ systems (solid lines in Fig. 2), over methylenide structures of $C_8H_8^+$ systems (dashed lines) to bicyclic structures of $C_9H_9^+$ and $C_{10}H_{10}^+$ system (dotted lines). Except for the $C_8H_8^+$ reaction system, the energetic estimates agree with the product distribution of the MD simulations.

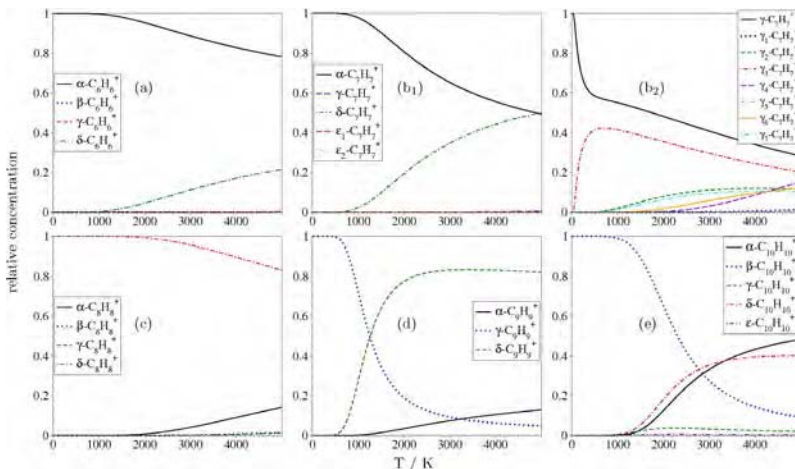


Fig. 2: Population analysis of products of the reactions $C_xH_y^+ + CH$ to $C_{x+1}H_{y+1}^+$: a) $x=5$ b1) $x=6$ b2) $x=6$ (different γ -isomers) c) $x=7$ d) $x=8$ and e) $x=9$ at the B3LYP/6-311++G(3df,3pd)//B3LYP/6-31G(d) level

The origin of the product distribution found by MD simulations and the formation of bicyclic bridged and fused ring systems (see β - and γ -isomers of Fig. 1) were studied by reaction channel mechanisms. The

NEB method was used in combination with DFTB and B3LYP methods. The successive formation of polycyclic isomers was found to be a feature of the CH electron trivalence. The first order association products (A-isomers of Fig. 1) were observed to form further bonds. The reaction dynamics often forced the formation of a second bond with non-adjacent carbon atoms. This led to the formation of the ε -isomers (Fig. 3).

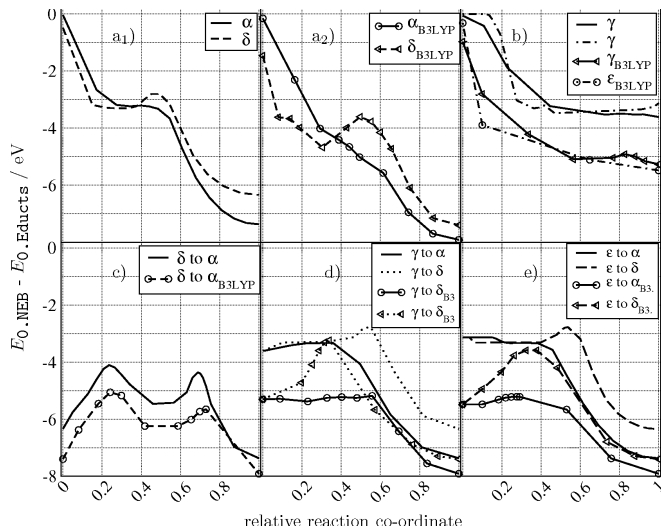


Fig. 3: Reaction channels in a₁) and a₂) represent the association of α -C₆H₆⁺ and δ -C₆H₆⁺, b) the associations of γ -C₆H₆⁺ and ε -C₆H₆⁺. In c), d) and e) isomerisations of all isomers into each other are shown. The reference point is set to α -C₅H₅⁺ + CH.

In Fig. 3, the different mechanisms for the formation and depletion of the C₆H₆⁺ isomers are shown. Certain aspects of the formation and stability / depletion of isomers were found to repeat independently of the system size. The formation of the δ -isomers was found to be always hindered due to a common reaction barrier. For reaction systems C_xH_x⁺ + CH with x=8-9, the formation of the δ -isomers was not observed. The barrier-less reaction channels with broad entrances on the potential energy surface were often found to suppress the δ -isomer channel. The α - and some ε -isomer channels were found to be barrier-less [Barthel2007a].

The reaction energy can be dissipated in the form of molecular dissociation. In particular, dissociation channels of molecular hydrogen (H₂) and acetylene (C₂H₂) were investigated. The latter dissociation channels were

occasionally observed (fraction less than 1/100 within 6 ps) for systems such as $C_xH_x^+ + CH$ with $x=8,10$. A dissociation channel producing H_2 was not found. However, the study of such dissociation channels indicated that bicyclic isomers of $C_9H_9^+$ and $C_{10}H_{10}^+$ have a high tendency to lose H_2 . On the other hand, bicyclic systems of $C_7H_7^+$ and $C_8H_8^+$ were found to have high barriers for H_2 -dissociation (Fig. 4).

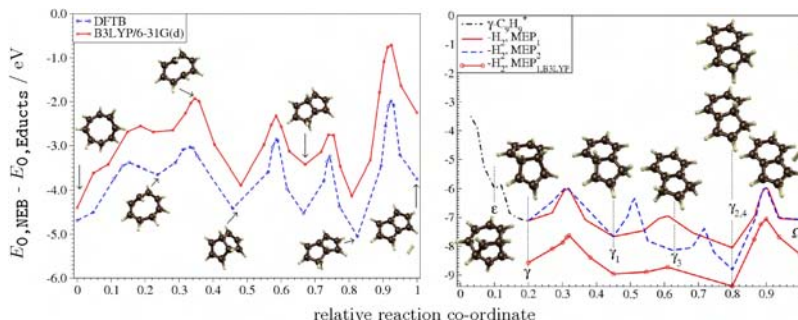


Fig. 4: H_2 dissociation channels of the bicyclic β - $C_8H_8^+$ and γ - $C_9H_9^+$.

Based on these results, we can conclude that the addition of CH to monocyclic hydrocarbons leads to extended ring structures and transformation of monocyclic ring to bicyclic rings, so that it can lead to reaction channels for the formation of aromatic fused ring structures (naphthalene, indene).

The very high energetic impact of reactions with CH could produce radiative emission features similar to processes that follow UV absorption. Therefore, observed interstellar IR-emission features could also be assigned to chemical reactions.

b) bicyclic hydrocarbons

The study of CH addition reactions was extended to larger hydrocarbon molecules in order to develop a general reaction scheme for growth of polycyclic aromatic hydrocarbons. The pathway from naphthalene to phenanthrene was investigated (Fig. 5).

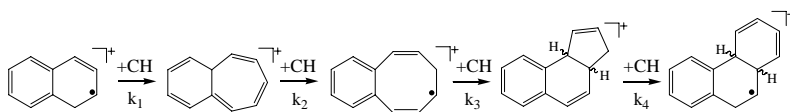


Fig. 5: Reaction path of naphthalene to 4a,10a-dihydrophenanthrene.

Investigations about the reaction energetics and the MD aspects are summarized in Table 3 and Table 4.

Table 3: Reaction energies in eV. Isomers are taken from Fig. 5.

X + CH \rightarrow Y	DFTB	B3LYP	MP2
α -C ₁₀ H ₈ ⁺ , α -C ₁₁ H ₉ ⁺	-6.1369	-6.6199	-7.3086
α -C ₁₁ H ₉ ⁺ , α -C ₁₂ H ₁₀ ⁺	-4.9606	-4.5902	-
α -C ₁₂ H ₁₀ ⁺ , α -C ₁₃ H ₁₁ ⁺	-6.0782	-6.7278	-
γ -C ₁₃ H ₁₁ ⁺ , α -C ₁₄ H ₁₂ ⁺	-6.1661	-5.9271	-

Table 4: Canonical capture cross sections at 0.01 eV total collision energy and capture rate constants at 100 K.

X + CH \rightarrow Y	k _{100 K} /10 ⁻¹⁰ cm ³ s ⁻¹	$\sigma_{0.01 \text{ eV}}$ /10 ⁻²⁰ m ²
α -C ₁₀ H ₈ ⁺ , α -C ₁₁ H ₉ ⁺	8.43	240.2
α -C ₁₁ H ₉ ⁺ , α -C ₁₂ H ₁₀ ⁺	7.56	237.9
α -C ₁₂ H ₁₀ ⁺ , α -C ₁₃ H ₁₁ ⁺	9.39	260.1
γ -C ₁₃ H ₁₁ ⁺ , α -C ₁₄ H ₁₂ ⁺	9.35	264.3

The product distribution of all reactions is depicted in Fig. 4. The product variety was found to be increased compared to monocyclic hydrocarbons, simply by the increase of positions that can be attacked by CH.

It was found that tri- and tetracyclic structures are easily formed either by transformation of bridged product structures or via intermediates with extended ring structures. The methylenyl substituted isomers (δ isomers of Fig. 1) were not formed within the applied simulation time of 6 ps, in agreement with the study of monocyclic hydrocarbons.

Despite CH addition reactions, we observed in particular H abstraction reaction of the kind C_xH_{x-3}⁺ + CH₂ or C_xH_{x-4}⁺ + CH₃. It was found that weakly bound H atoms of sp³ hybridised carbon atoms, in particular at bridging positions, were most efficient in transferring hydrogen to the CH molecule. These reaction channels are highly exothermic and lead to aromatic systems. Additionally, the H transfer to CH was most efficient in cases where the CH insertion is sterically hindered.


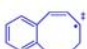
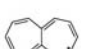
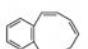
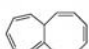
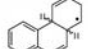
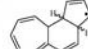
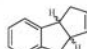
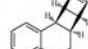
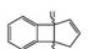
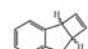
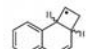
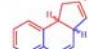
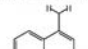
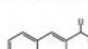
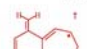
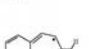
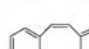
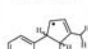
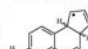
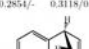
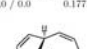
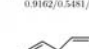

$C_{11}H_9$ cations	$C_{12}H_{10}$ cations	$C_{13}H_{11}$ cations	$C_{14}H_{12}$ cations
(abbr.) name	(abbr.) name	(abbr.) name	(abbr.) name
DFTB/B3LYP/MP2	DFTB/B3LYP/MP2	DFTB/B3LYP/MP2	DFTB/B3LYP/MP2
 (α) benzo[7]annulenylium 0.0 / 0.0 / 0.0	 (α ₁) benzo[8]annulenylium 0.6492/0.8121/-  (α ₂) heptalenylium 0.4825/0.5458/-	 (α ₁) benzo[9]annulenylium 1.0549/0.6775/-  (α ₂) homo-α ₁ -C ₁₂ H ₁₀ 1.0580/0.6651/-	 (α ₁) dihydrophenanthrenylium -0.0751/0.1409/-  (α ₂) homo-γ-C ₁₃ H ₁₁ 0.7582/0.5127/-
	 (β) benzo[5]indolopyrenylium 0.4093/0.7724/-		 (β) tetracyclic cation 1.6406/1.4610/-
 (γ ₁)	 (γ ₂)	 (γ ₃)	 (γ ₄) benzo[6]indolenylium 0.0 / 0.0 / 0.0
2.1120/2.2286/2.1592/1.9063/1.9613/1.9488	1.4404/1.4198/-	0.1338/0.1130/-	
 (δ ₁) methylenyl-naphthylidene 0.2175/0.2854/-	 (δ ₂) methylenyl-naphthylidene 0.3118/0.2930/0.4348	 (δ ₃) 8-methylenylbenzo[7]annulenylium 0.0 / 0.0 / 0.0	 (δ ₄) 3-methylenylbenzo[7]annulenylium 0.1771/0.3027/-
		 (δ ₅) methylenylbenzo[8]annulenylium 0.9162/0.5481/-	 (δ ₆) methylenyl-γ-C ₁₃ H ₁₁ 0.0 / 0.0 / 0.0
			 (δ ₇) methylenyl-γ-C ₁₃ H ₁₁ 0.6977/0.6033/-
 (ε ₁) bridged naphthylidene 2.7299/2.0519/1.4564	 (ε ₂) bridged [9]annulenylium 2.0435/2.0492/-	 (ε ₃) bridged benzo[9]annulenylium 3.5496/2.9067/-	 (ε ₄) bridged benzo[9]annulenylium 1.9084/1.7747/-

Fig. 6: Products of the reaction $C_xH_{x-2}^+ + CH$ to $C_{x+1}H_{x-1}^+$ ($x=10-13$). The first row (α) shows products of ring extension, second (β) and third row (γ) products of ring constriction (new ring condensation), the fourth row (δ) methylene derivatives whereas the fifth row (ε_i) shows monovalent metheno-bridged polycyclic isomers. Total energies of products at SCC-DFTB, B3LYP/6-311++G(3df,3pd)//B3LYP/6-31G(d) and MP2/6-31G(d) level are reported with respect to the most stable isomer.

c) polycyclic hydrocarbons

Reactions of CH with large fused polycyclic hydrocarbon were studied from the point of view of peripheral vs. centred attack as well as steric hindrances. Three different reaction systems were considered (see first row of Fig. 7. The reaction energies (0 K) are given in Table 5.

The reactions of both $C_{20}H_{10}^+$ isomers with CH were highly exothermic and resulted in ring expansion. Ring expansion of $C_{24}H_{12}^+$ releases less energy due to an increase of tension inside the molecular system during the expansion process.

The stability of first order association products (A_{Xj} , last row of Fig. 7) depends on the geometric configuration. It was found that CH attachment at a peripheral pentagon results in ring extension without any reaction barrier. However, at centred pentagons, such as in corannulene,

insertion or bridging was found to exhibit significant barriers. Peripheral hexagon ring extension was found to have barriers below 0.5 eV. The bridging and extension of interior hexagons had barriers above 1 eV.

Table 5: Reaction energies in eV. Isomers are taken from Fig. 1.

X + CH \rightarrow Y	DFTB	B3LYP
$\text{C}_{20}\text{H}_{10}^+(\text{a}), \alpha_{\text{A1}}\text{-C}_{21}\text{H}_{11}^+$	-7.5527	-7.5771
$\text{C}_{20}\text{H}_{10}^+(\text{b}), \alpha_{\text{B1}}^-$	-7.1379	-7.8004
$\text{C}_{24}\text{H}_{12}^+, \alpha_1\text{-C}_{25}\text{H}_{13}^+$	-5.7679	-

Table 6: Canonical capture cross sections at 0.01 eV total collision energy and capture rate constants at 100 K.

X + CH \rightarrow Y	$k_{100\text{ K}}/10^{-10}\text{ cm}^3\text{ s}^{-1}$	$\sigma_{0.01\text{ eV}}/10^{-20}\text{ m}^2$
$\text{C}_{20}\text{H}_{10}^+(\text{a}), \alpha_{\text{A1}}\text{-C}_{21}\text{H}_{11}^+$	11.6	313.7
$\text{C}_{20}\text{H}_{10}^+(\text{b}), \alpha_{\text{B1}}^-$	10.5	312.8
$\text{C}_{24}\text{H}_{12}^+, \alpha_1\text{-C}_{25}\text{H}_{13}^+$	12.5	343.3

Additionally, it was found that the CH is often weakly bound and drifts towards the periphery during the MD simulations. This was also noticed for the $\text{C}_{25}\text{H}_{13}^+$ system. We conclude that despite an attack of CH at arbitrary molecular positions, the systems grow in the periphery. In particular, the ring extension will follow the growth scheme of mono- and bicyclic hydrocarbons. Further implications for the reaction mechanisms will be discussed elsewhere [Barthel2007a].

Reactions of interstellar aromatic hydrocarbons with di- and trivalent polyatomic reactants

Within the project, the suitability of small polyatomic molecules as precursors for hydrocarbon growth mechanisms was investigated in detail. Reactant candidates were selected according to their interstellar abundances. A further pre-selection of suitable candidates was deduced from our own MD calculations of the respective reactivity. The final scheme for the growth process was designed by various combinations of the selected precursors. An overview of the investigated systems is depicted in Fig. 8.

Collisions of non-activated aromatic hydrocarbon cations with C_2H_2 (acetylene) were mostly non-reactive whereas for substituted and activated aromatic species a moderate reactivity with acetylene was found. We conclude that acetylene plays only a minor role for hydrocarbon growth at temperatures below 50 K. Further details can be found in a forthcoming publication [Barthel2007c].

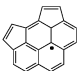


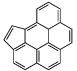
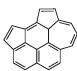
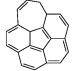
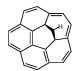
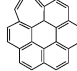
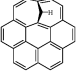
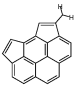
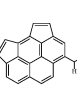
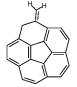
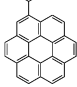
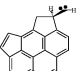
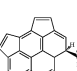
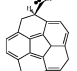
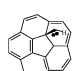
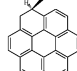
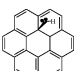
A- $C_{21}H_{11}$ cations		B- $C_{21}H_{11}$ cations		$C_{25}H_{13}$ cations	
(abbr.) name DFTB/B3LYP		(abbr.) name DFTB/B3LYP		(abbr.) name DFTB/B3LYP	
 dicyclopentapyrenylium + CH 8.2921 / 7.1143		 corannulenylium + CH 8.2867 / 7.2392		 coronenylium + CH 6.6979 / 5.5400	
 (α_{A1}) benzo-cyclopentapyrenylium 0.0 / 0.0		 (α_{A2}) azulene analogue of α_{A1} 0.9839 / 0.8914		 (α_{B1}) cyclohepta-analogue 0.0 / 0.0	
		 (α_{B2}) bridged corannulenylium 2.7181 / 3.1904		 (α_1) cyclohepta-analogue 0.1766 / 0.1266	
				 (α_2) bridged coronenylium 2.9523 / 3.1414	
 (δ_{A1}) methylenyl-dicyclopentapyrenylium 1.2937 / 1.1223		 (δ_{A2}) methylenyl-dicyclopentapyrenylium 1.6288 / 1.5162		 (δ_{B1}) methylenyl-corannulenylium 1.2297 / 1.2771	
				 (δ) methylenyl-coronenylium 0.0 / 0.0	
 (A_{A1}) methylenyl dicyclopentapyrenylium 4.5052 / 4.8361		 (A_{A2}) methylenyl dicyclopentapyrenylium 4.9931 / 5.3850		 (A_{B1}) methylenyl corannulenylium 4.5971 / 5.1883	
		 (A_{B1}) methylenyl corannulenylium 4.4104 / 4.9780		 (A_1) methylenyl coronenylium 3.2778 / 3.5412	
				 (A_2) methylenyl coronenylium 4.0404 / 4.3897	

Fig. 7. Products of the reaction $C_xH_{x/2}^+ + CH$ to $C_{x+1}H_{x/2+1}^+$ ($x=20,24$). The first row shows the educts + CH, the second row (α) products of ring extension and ring bridging, the third row (δ) methylene derivatives whereas the fourth row (e_i) shows the first order association products. Total energies of products at SCC-DFTB, B3LYP/6-311++G(3df,3pd)/B3LYP/6-31G(d) and MP2/6-31G(d) level are reported with respect to the most stable isomer.

High reactivity at very low temperature was obtained from reactions between non-activated hydrocarbons and small molecules with multiple electron valences such as cummulene carbenes and derivatives, in particular H_2C_2 (vinylidene), H_2C_3 , H_2C_4 and C_3H .

a) Reactions with C_3H

The studies of C_3H -based reactions include a complete set of growth reactions from $C_7H_7^+$ to $C_{14}H_{10}^+$ (see right part of Fig. 9). The analysis of the MD simulations is given in Table 7. It was found that under a suitable orientation of the reactants the addition of C_3H pass through a barrier-less channel. However, ring condensations (e.g. hexagons at 3-carbon bays) were connected with reaction barriers which were found to be smaller than the total amount of released reaction energy (see Fig. 9).

Despite the electron trivalence of C_3H , the addition rates at ring structures were found to be moderate compared with the trivalent CH based reactions. A substituted hydrocarbon ring such as δ - $C_7H_7^+$ was found to show a higher reactivity than α - $C_7H_7^+$. Additionally, non-substituted ring structures such as tropylium (α - $C_7H_7^+$) and naphthalene cations were found to have large deviations between the capture and association based reaction cross sections. This phenomenon is caused by the formation of H-bridged and orbiting complexes.

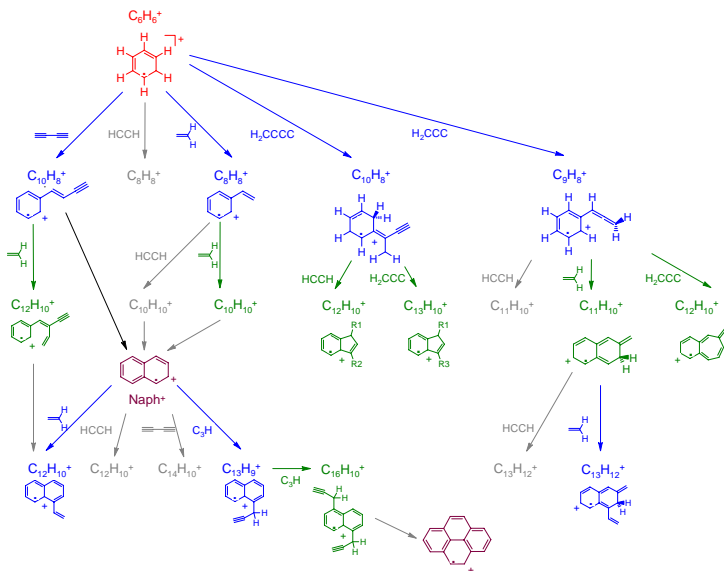


Fig. 8: Schematic overview of investigated reaction system of hydrocarbons with not-valent reactants such as C_2H_2 as well as with divalent and trivalent reactants such as H_2C_2 , H_2C_3 , H_2C_4 and C_3H .

It was found that under a suitable orientation of the reactants the addition of C_3H pass through a barrier-less channel. However, ring con-

densations (e.g. hexagons at 3-carbon bays) were connected with reaction barriers which were found to be smaller than the total amount of released reaction energy (see Fig. 9).

Table 7: Reaction cross sections at 0.01 eV total collision energy and reaction rate constants at 100 K evaluated after 6 ps simulation (t_0 =initial collision hit). Values of the capture process are given in brackets.

$X + C_3H \rightarrow Y$	$k_{100\text{ K}}/10^{-10}\text{ cm}^3\text{ s}^{-1}$	$\sigma_{0.01\text{ eV}}/10^{-20}\text{ m}^2$
$\alpha\text{-C}_7\text{H}_7^+, \alpha\text{-C}_{10}\text{H}_8^+$	1.509 (5.562)	67.2 (244.3)
$\delta\text{-C}_7\text{H}_7^+, \alpha\text{-C}_{10}\text{H}_8^+$	4.348 (6.460)	182.6 (266.0)
$\alpha\text{-C}_{10}\text{H}_8^+, \alpha\text{-C}_{13}\text{H}_9^+$	2.276	98.0
$\alpha\text{-C}_{13}\text{H}_9^+, \alpha\text{-C}_{16}\text{H}_{10}^+$	2.987	125.8

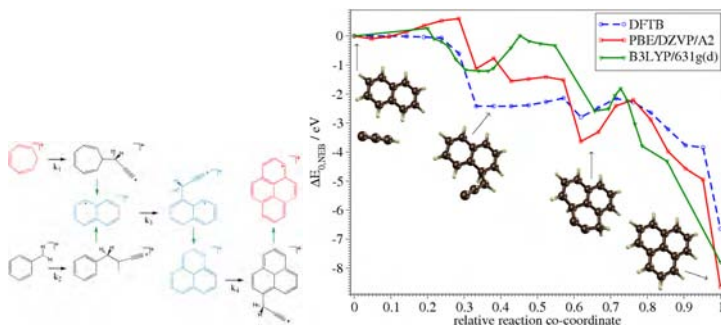


Fig. 9: Left: formation path with C_3H precursor, right: addition of C_3H to $C_{10}H_8^+$ and ring closure mechanisms of the product.

b) Reactions with H_2C_2 , H_2C_3 and H_2C_4

H_2C_2 (vinylidene) based collisions with non-activated aromatic hydrocarbons cation, such as benzene and naphthalene, were studied. The activated products as well as products of other cummulene carbenes were exposed to further collision reactions with H_2C_2 (Fig. 8), resulting in a high reactivity for H_2C_2 addition to hydrocarbons. Inelastic scattering of H_2C_2 often triggered an isomerisation to acetylene. The analysis showed that a ring condensation requires at least 2 H_2C_2 addition steps. However, the low selectivity of H_2C_2 did not favour ring condensation. Without activated sidegroups (such as allenyl groups), the growth with a H_2C_2 precursor leads to tree-like structures rather than ring fused structures.

H_2C_3 and H_2C_4 based collisions with aromatic hydrocarbon cations were found to be dominated by the formation of cummulenyl sidegroups. High ring closure barriers were obtained which hinder cummulenyl sidegroups undergo ring condensation. However, after H_2C_2 addition, cummulenyl can condensate to 6-membered rings.

Reactions of interstellar hydrocarbons with non-valent polyatomic molecules

In this project, we also investigated the ability of non-valent precursors to induce growth of hydrocarbons at ultra-low temperature.

a) C_4H_2

Condensation reactions with diacetylene and (poly)aromatic hydrocarbon cations were investigated, including a detailed analysis of the products with respect to ring condensation processes of the sidegroups. Barriers for rotation and ring closure (see Fig. 10) were found to be reduced due to the charged state. Moreover, the released reaction energy is sufficient for providing the required internal motion. More implications were discussed elsewhere [Barthel2003].

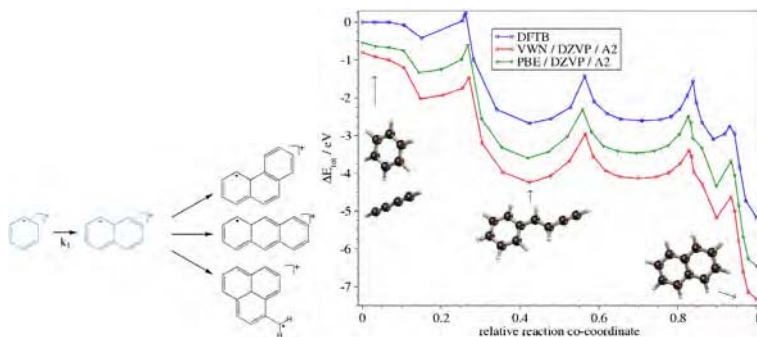


Fig. 10: Left: formation path with C_4H_2 precursor, right: addition of C_4H_2 to C_6H_6^+ and ring closure mechanisms of the product.

c) C_3H_3 (allyl) cations

The possibility to obtain ring condensation from the addition of the allyl cation to small hydrocarbons was investigated, in particular the formation of benzene. According to the reviews by [Smith1992, Millar1997], a single step addition of an allyl cation to C_3H_4 should lead to benzene. Collision MD simulations were performed for two isomers of C_3H_4 : Allene and methylacetylene. Reactive collisions with allene were found to result in cyclisation within less than 3.5 ps. In contrast, for methylacety-

lene, no cyclisation of the reaction products was found. The calculations of the reaction path are depicted in Fig. 11.

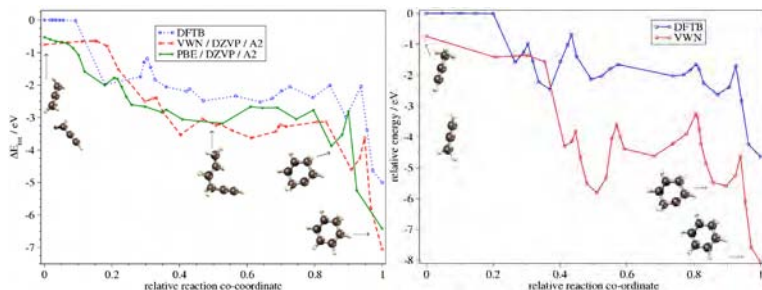


Fig. 11: Ring formation process by two different processes: a) $\text{C}_3\text{H}_3^+ + \text{H}_2\text{CCCH}_2$ b) $\text{C}_3\text{H}_3^+ + \text{H}_3\text{CCCH}$

Reactions of hydrocarbons with tetravalent C_2

In collaboration with the group of C. Joblin, France, we have investigated the formation and the photoinduced oxidation of coronone ($\text{C}_{24}\text{H}_{12}^+$) and its derivatives.

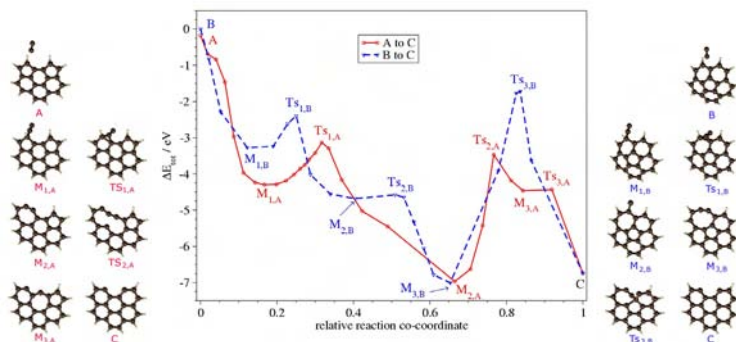


Fig. 12: C_2 addition reaction with dicyclopentapyrene cation (right, red solid line) and corannulene cation (left, blue dashed line) at PBE/DZVP level.

In particular, the mechanisms of C_2 and CO fragmentation during the photoinduced oxidation of coronene was studied [Barthel2007b]. Additionally, a retrosynthesis by C_2 addition reactions was sketched. Pathways of the reorganisation of the C_2 -addition products are shown in Fig. 12.

Excited states of C_3

In this part of the project, it was demonstrated that the lowest excited state of C_3 is a triplet state in the geometry of an equilateral triangle, compare the FGLA report 2000 – 2003. By applying time-dependent density functional theory (TD-DFT) to the lowest singlet and triplet states, we have mapped the lowest single-electron excitations up to an energy of about 10 eV above each initial state.

As an example for the results obtained in a comprehensive study of the lowest excited states of C_3 [Terentyev2004], we report the lowest triplet states obtained via excitations from the singlet ground state (Fig. 13) and from the lowest triplet configuration at large bond angles (Fig. 14).

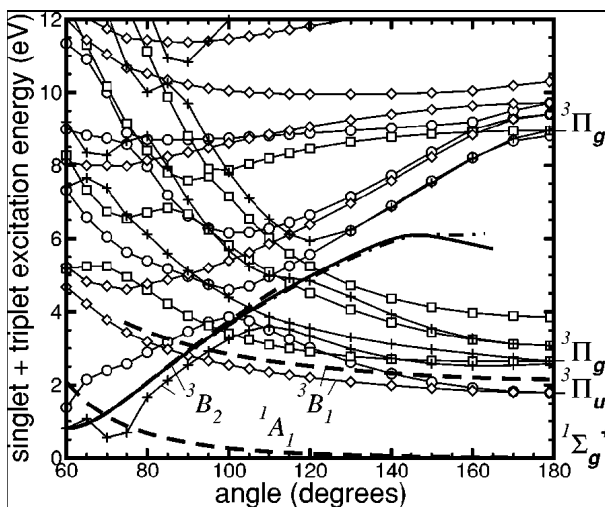


Fig. 13: Total energy of the lowest triplet states, calculated as the sum of the B3LYP/6-31G(d) energy of the singlet ground state with optimized bond length and the B3LYP/6-31G(d) TD-DFT excitation energies. Total energy curves resulting from calculations based on B3LYP/6-31G(d) (dashed), QCISD/6-311G(d) (solid) and QCISD/6-311+G(d) (dot-dashed) are included for comparison. Symbols: circles 3A_1 ; squares 3A_2 ; diamonds 3B_1 ; crosses 3B_2 .

In order to assess the total energy of the lowest triplet states, we add the energy of the singlet ground state and the triplet excitation energies calculated with TD-DFT, Fig. 13. For linear C_3 , the calculated excitation energy of the triplet energy is 1.8 eV, giving an estimate of about -0.35 eV for systematic deviations between the TD-DFT excitation ener-

gies and a total energy calculation excluding corrections due to zero point motion. As can be seen from the low-energy region of Fig. 13, this systematic deviation for the lowest triplet of 3B_1 symmetry does not depend much on the bond angle. For bond angles below 90° , the deviation between the TD-DFT result and the total energy of the lowest 3B_2 triplet is somewhat larger, including some scatter close to the inter-system crossing around 70° . Interestingly, for linear C_3 the calculated difference of 0.86 eV between the two lowest triplet states $^3\Pi_u$ and $^3\Pi_g$ is in good agreement with the experimental value of 0.80 eV [Sasada1991, Tokaryk1995].

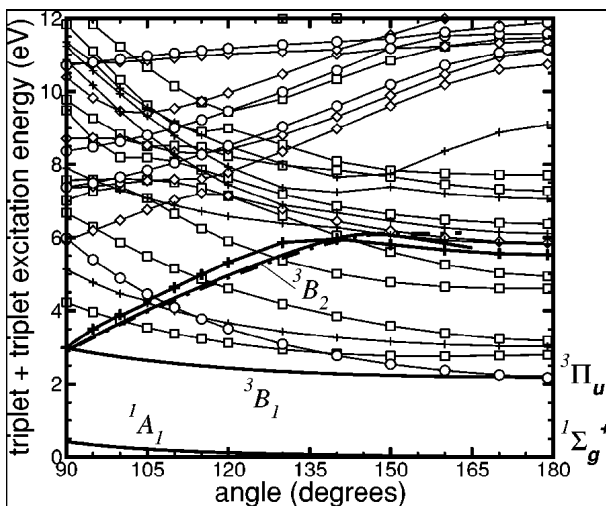


Fig. 14: Total energy of the lowest triplet states, calculated as the sum of the B3LYP/6-31G(d) energy of the lowest 3B_1 triplet state with optimized bond length and the B3LYP/6-31G(d) TD-DFT excitation energies to higher lying triplets. The total energy curves of the B3LYP/6-31G(d) calculation for the 1A_1 singlet and the 3B_1 triplet are superimposed (solid line). The total energy curves of the QCISD calculations of the 3B_2 triplet (thick lines) are included for comparison, based on the 6-311G(d) (solid) and 6-311+G(d) (dash-dotted) variational basis sets. The lowest 3B_2 triplet state is highlighted with heavy symbols. Symbols are defined as in Fig. 13.

Triplet energies defined by excitations starting from the 3B_1 triplet ground state are shown in Fig. 14. As the starting electronic configuration 3B_1 contains already two unpaired electrons, three kinds of excitations can occur. First, excitations between different valence states will result in

low-lying excitations between different triplet configurations. Second, one of the remaining 7 electrons in the four highest occupied valence states can be promoted into a virtual orbital, resulting in electronic configurations which cannot be reached via a single excitation out of the singlet ground state. The third possibility is an excitation of the unpaired electron in the LUMO into higher virtual orbitals, resulting in some of the triplet states displayed in Fig. 13. Nevertheless, these excitations of a single electron starting from the triplet ground state still do not cover all the excited states, as some double excited are still excluded.

These TD-DFT investigations give a comprehensive map of all the low-lying states of C_3 which can be reached via single excitations from the singlet or triplet ground states. However, due to restrictions in the final configurations, some states in the energetic range of interest cannot be reached.

3.6 Zusammenfassung und Ausblick / Summary and future

In this project, ultra-low temperature based growth processes of hydrocarbons with various kinds of precursors were investigated. The precursors were selected according to the known interstellar abundances and reactivities based on previous calculations. The investigated reaction mechanisms provide new insight into growth processes of PAHs in interstellar objects such as dense clouds. The results also strengthen the PAH hypothesis. Calculated cross sections and rate coefficients are a useful support for calculation-based modelling of interstellar chemical reaction networks.

The results and the comparison with DFT and post-Hartree-Fock methods demonstrate that the DFTB in combination with quantum MD simulations and NEB calculations are very useful methods to study reactions dynamics and mechanisms. DFTB based results are applicable for B3LYP and post-Hartree-Fock based calculations. As a perspective for future work, the good qualitative agreement between DFTB and B3LYP/post-Hartree-Fock based results opens up new strategies for reliable studies of very large reaction systems. Formation of hydrogenated amorphous carbon (HAC) and formation of soot or fullerene will be candidates of investigation.

3.7 Literatur / References

- Allamandola, L. J., Tielens, A. G. G. M., Barker, J. R. *Polycyclic aromatic-hydrocarbons and the unidentified infrared-emission bands – auto exhaust along the milky-way*, *Astrophys. J.* **290** (1985), L25.
- Allamandola, L.J., Tielens, A.G.G.M., Barker, J.R., *Interstellar polycyclic aromatic-hydrocarbons infrared-emission bands, the excitation emission mechanism, and the astrophysical implications*, *Astrophys. J. Suppl. Series*, **71** (1989), 733.
- Baboul, A. G., Curtiss, L. A., Redfern, P. C., Raghavachari, K., *Gaussian-3 theory using density functional geometries and zero-point energies*, *J. Chem Phys.*, **110** (1999), 7650.
- Bakes, E. L. O., Tielens, A. G. G. M. *The photoelectric heating mechanism for very small graphitic grains and polycyclic aromatic-hydrocarbons*. *Astrophys. J.* **427** (1994), 822.
- Barthel, R.: *Theoretische Untersuchung zur Bildung von Kohlenwasserstoffen unter astrophysikalischen Bedingungen*, Master Thesis, Technische Universität, (2003).
- Barthel, R.: *Computational study of interstellar hydrocarbon formation*, Ph.D. Thesis, Technische Universität, (2007), under preparation.
- Barthel, R., Scholz, R., Seifert, G.: *Growth mechanisms of interstellar polycyclic hydrocarbons: reactions with methylidene*, *Astron. Astrophys.* (2007a), under preparation.
- Barthel, R., Heine, T., Joblin, C., Seifert, G.: *Photoinduced dissociation of hydrocarbons: coronene, corannulene and isomers*, (2007b), under preparation.
- Barthel, R., Seifert, G.: *Growth mechanism of interstellar polycyclic hydrocarbons: reactions with di- and trivalent polyatomic molecules*, *Astron. Astrophys.* (2007c), under preparation.
- Brechignac, P., Schmidt, M., Masson, A., Pino, T., Parneix, P., Brechignac, C., *Photoinduced products from cold coronene clusters a route to hydrocarbonated nanograins?* *Astron. Astrophys.* **442** (2005), 239.
- Curtiss, L. A., Raghavachari, K., Redfern, P. C., Rassolov, V., Pople, J. A., *Gaussian-3 (G3) theory for molecules containing first and second-row atoms*, *J. Chem. Phys.* **109** (1998), 7764.
- Duley, W. W., Williams, D. A., *The infrared-spectrum of interstellar dust surface functional-groups on carbon.*, *Mon. Not. Roy. Astron. Soc.* **196** (1981), 269.
- Fischer, G., Barthel, R., Seifert, G. *Molecular dynamics study of the reaction $C_3+H_3^+$* , *Eur. Phys. J. D* **35** (2005), 479.
- Frisch, M.J., et al., *Gaussian 03, Rev. C.02*, Gaussian, Inc., Wallingford CT, USA,
- Habart, E., Verstraete, L., Boulanger, F., des Forets, G. P., Le Peintre, F., Bernard, J. P., *Photoelectric effect on dust grains across the L1721 cloud in the rho Ophiuchi molecular complex*, *Astron. Astrophys.* **373** (2001), 702.

- Harris, J. *Simplified method for calculating the energy of weakly interacting fragments*, Phys. Rev. B **31** (1985), 1770.
- Henkelman, G., Jonsson, H. *Improved tangent estimate in the nudged elastic band method for finding minimum energy paths and saddle points*. J. Chem. Phys. **113** (2000), 9978.
- Henkelman, G., Uberuaga, B. P., Jonsson, H. *A climbing image nudged elastic band method for finding saddle points and minimum energy paths*. J. Chem. Phys. **113** (2000a), 9901.
- Jones, A. P., Tielens, A. G. G. M., Hollenbach, D. J. *Grain shattering in shocks: The interstellar grain size distribution*, Astrophys. J. **469** (1996), 740.
- Köster A.M., et al., *deMon 2003, Ver. 1.1.0*, The National Research Council, Ottawa, Canada (2004).
- Leger, A., Dhendecourt, L., Defourneau, D. *Physics of ir emission by interstellar pah molecules*, Astron. Astrophys **216** (1989), 148.
- Leger, A., Puget, J. L. *Identification of the unidentified ir emission features of interstellar dust*, Astron. Astrophys **137** (1984), L5.
- Millar, T. J., Farquhar, P. R. A., Willacy, K.: *The UMIST database for astrochemistry 1995*, Astron. Astrophys. Suppl. Series **121** (1997), 139.
- Perez, N., Heine, T., Barthel, R., Seifert, G., Vela, A., Mendez-Rojas, M., Merino, G., *Planar tetracoordinate carbons in cyclic hydrocarbons*, Org. Lett. **7**, (2005) 1509.
- Porezag, D., Frauenheim, T., Kohler, T., Seifert, G., Kaschner, R. *Construction of tight-binding-like potentials on the basis of density-functional theory application to carbon*. Phys. Rev. B **51** (1995), 12947.
- Sasada, H., Amano, T., Jarman, C., Bernath, C.P., *A new triplet band system of C₃: The $b^3\Pi_g - a^3\Pi_u$ transition*, J. Chem. Phys. **94** (1991), 2401.
- Schulte, J., Seifert, G. *DFT-LDA molecular-dynamics of molecular collision processes*. Chem. Phys. Lett. **221** (1994), 230.
- Seifert, G., Schmidt, R. *Fusion and deep inelastic-scattering in c-60-c-60 collisions*, Int. J. Mod. Phys. B **6** (1992), 3845.
- Seifert, G., Porezag, D., Frauenheim, T. *Calculations of molecules, clusters, and solids with a simplified LCAO-DFT-LDA scheme*. Int. J. Quant. Chem. **58** (1996), 185.
- Slanina, Z., Kobayashi, K., Nagase, S. *Temperature development in a set of C₆₀H₃₆ isomers*. Chem. Phys. Lett. **382** (2003), 211.
- Smith, D. *The ion chemistry of interstellar clouds*, Chem. Rev. **92** (1992), 1473.
- Terentyev, A., Scholz, R., Schreiber, M., Seifert, G.: *Theoretical investigation of excited states of C₃*, J. Chem. Phys **121** (2004), 5767.
- Tokaryk, D.W., Civiš, S., *Infrared emission spectra of C₃: the Renner effect in the $a^3\Pi_u$ and $b^3\Pi_g$ electronic states*, J. Chem. Phys. **103** (1995), 3928.

3.1 Bericht Teilprojekt 2

3.1.1 Titel / Title

Theoretische Untersuchungen der spektroskopischen Eigenschaften von Silizium-Nanoteilchen

Theoretical investigations of the spectroscopic properties of silicon nanocrystals

3.1.2 Berichtszeitraum / reported period

01.07.2003 - 30.11.2006

3.1.3 Projektleiter / principle investigator

Scholz, Reinhard, Dr., Oberassistent
Technische Universität Chemnitz (bis Dezember 2006)
Technische Universität München (seit März 2006)

Schreiber, Michael, Prof. Dr.
Technische Universität Chemnitz

3.2 Zusammenfassung / Abstract

3.2.1 Wortlaut des Antrags / abstract of the proposal

Verschiedene Ansätze zur theoretischen Behandlung der optischen Eigenschaften von interstellaren Staubeilchen sollen in diesem Teilprojekt am Beispiel von Silizium-Nanokristallen entwickelt werden. Von der Anwendung empirischer Tight-Binding-Verfahren (ETB) und Dichtefunktional-basierter Tight-Binding-Methoden (DFTB) erwarten wir ein mikroskopisches Verständnis der spektroskopischen Eigenschaften dieser Nanoteilchen. Dafür ist die Berechnung der relaxierten Geometrien der Nanokristalle mit bzw. ohne Passivierung der Oberfläche mit Wasserstoff oder Sauerstoff vonnöten. Die optischen Anregungen sollen mit zeitabhängiger Dichtefunktionaltheorie (TD-DFT) und empirischem Tight-Binding untersucht werden. Eine von einer umgebenden Oxidschicht hervorgerufene Verspannung des Si-Kerns eines solchen Nanoteilchens soll

mit DFT-Verfahren berechnet werden. Die für die entsprechende Geometrie auftretenden Anregungsenergien sollen mit gemessenen Absorptions- und Photolumineszenz-Spektren verglichen werden. Für unvollständig passivierte Teilchen soll die Entstehung von Zuständen innerhalb der Bandlücke durch dangling bonds und Zustände an der Grenzfläche Silizium-Siliziumoxid sowie deren Einfluss auf die Photolumineszenz untersucht werden. Die dafür benötigten Veränderungen der Bindungsgeometrie im relaxierten angeregten Zustand sollen mit einer Verallgemeinerung des DFTB-Verfahrens auf elektronisch angeregte Zustände berechnet werden.

Different theoretical approaches for the investigation of the optical properties of interstellar dust shall be developed in the present project for the model system of nanocrystalline silicon. We want to obtain a microscopic understanding of the spectroscopic properties of these nanoparticles by applying empirical tight-binding (ETB) and density functional tight-binding (DFTB) techniques. This requires the computation of the relaxed geometries of the nanocrystals with and without hydrogen or oxygen passivation of the surface, and of the optical excitations with time-dependent density functional theory (TD-DFT) and empirical tight-binding. The strain induced by a surrounding silicon oxide layer on the crystalline core of the nanoparticle shall be computed on an atomistic level. The excitation energies calculated for the corresponding geometry shall be compared with the measured absorption and photoluminescence spectra. For incompletely passivated particles, the appearance of mid-gap states due to dangling bonds and to trap states at the interface between silicon and its oxide and their influence on the photoluminescence spectra shall be investigated. Changes of the bond geometry in the relaxed excited state of the nanoparticle shall be computed with extensions of the DFTB approach to optically excited electronic configurations.

3.2.2 Zusammenfassung des Berichts / abstract of the report

Durch die indirekte Bandstruktur von Silizium erfordert die impulserhaltende Photolumineszenz (PL) im Bulkmaterial die Absorption oder Emission eines Phonons. Weil die Quantisierung der elektronischen Zustände in passivierten Nanokristallen einer Ausschmierung der Wellenfunktion über einen größeren Bereich der Brillouin-Zone entspricht, ist die erforderliche Impulserhaltung in solchen Strukturen ohne Assistenz eines Phonons möglich. Die erhöhte PL-Effizienz und die Ähnlichkeit der PL-Spektren mit den breiten Emissionsbanden aus dem interstellaren Raum (Extended Red Emission, ERE) hat zu dem Vorschlag geführt, dass

nanokristallines Silizium der Träger der ERE sein könnte. Aus einem numerischen Blickwinkel sind solche Nanostrukturen mit mehreren Hundert Atomen sehr anspruchsvoll, so dass verschiedene komplementäre Methoden verfolgt worden sind, um ihre Geometrie und ihre spektroskopischen Eigenschaften zu untersuchen.

Eine der größten Herausforderungen ist die Bereitstellung von relaxierten Strukturmodellen für Siliziumkristalle, die an der Oberfläche oxidiert sind. Beim Start von einfachen Modellgeometrien, in denen ein Silizium-Nanokristall in eine Schale aus Siliziumoxid eingebettet ist, verhindert die thermische Stabilität aller Oxidphasen die Anwendung von simulierter thermischer Behandlung. Als Resultat solcher Molekulardynamik-Simulationen bei erhöhter Temperatur ergibt sich ein geschmolzener Siliziumkern in einer kaum modifizierten Oxidhülle, wobei dieser Kern bei anschließender Abkühlung amorph bleibt. Als Alternative wurde die Kollision von schnellen Sauerstoffatomen mit der Oberfläche eines kalten Siliziumkristalls untersucht. Im Prinzip ist dieses Verfahren vielversprechend, aber es kann nicht ausgeschlossen werden, dass die Endgeometrien von den kleinen Basisätzen im Dichtefunktional-Tight-Binding (DFTB) und von den statistischen Eigenschaften der Anfangsgeometrien und Kollisionsenergien beeinflusst werden.

Um einen Einfluss der Geometrieoptimierung auf die spektroskopischen Eigenschaften zu vermeiden, wurden letztere für wohldefinierte Modellcluster untersucht: wasserstoffpassivierte Siliziumkristalle mit tetraedrischer Symmetrie. Für wesentlich kleinere Systeme bis zu $\text{Si}_{99}\text{H}_{100}$ (Durchmesser $d \leq 1.5$ nm), die alle um ein zentrales Siliziumatom herum angeordnet sind, wurde die Geometrie des Grundzustands mit Dichtefunktionaltheorie (DFT) optimiert, die Geometrie im angeregten Zustand mit zeitabhängiger Dichtefunktionaltheorie (time-dependent density functional theory, TD-DFT).

Elektronische Anregungen bewirken eine Veränderung der Besetzungszahlen der beteiligten Orbitale und somit eine anisotrope Veränderung der elektronischen Ladungsdichte. Diese anisotrope Ladungsdichte verursacht eine verringerte Symmetrie der relaxierten angeregten Zustände im Vergleich zur Punktgruppe T_d im elektronischen Grundzustand. In der resultierenden tetragonalen Symmetrie ist die Entartung des höchsten besetzten Orbitals (HOMO) aufgehoben. Diese mit der Symmetrierniedrigung einhergehende Aufspaltung ist als Jahn-Teller-Effekt bekannt und erfolgt im wesentlichen proportional zur Abweichung von der tetraedrischen Geometrie des Grundzustands. Die Projektion der Deformation im relaxierten angeregten Zustand auf die verschiedenen Symmetrien erlaubt

die Zuordnung der entsprechenden Beiträge zur Stokes-Verschiebung. Für einige der untersuchten Systeme ist der Beitrag der Symmetrierniedrigung zur Rotverschiebung der PL größer als der Einfluss symmetriehaltender Deformationen.

Due to its indirect band structure, photoluminescence (PL) from bulk silicon requires phonon-assisted emission processes. In Si nanostructures like oxidized nanocrystals, the quantization of the electronic states corresponds to a spreading of the electronic states over a large range of wave vectors, resulting in momentum conservation in PL without phonon emission. The improved PL efficiency and the similarity of the PL spectra of size-selected samples with the extended red emission (ERE) from interstellar space has led to the proposition that nanosized oxidized silicon particles might be a possible carrier of the ERE. From a computational point of view, such particles containing several hundred atoms are very demanding, suggesting a combination of complementary approaches for the investigation of the geometry in the electronic ground state and spectroscopic aspects.

One of the major challenges is the definition of suitable atomistic model geometries for crystalline silicon embedded in an oxide matrix without large strain. Starting from simple model geometries consisting of a crystalline Si grain inserted into a shell of silicon oxide, the thermal stability of the various oxide phases inhibits the use of simple schemes for simulated thermal annealing. The result of such molecular dynamics (MD) simulations at elevated temperatures is a molten Si core embedded into an oxide shell which is hardly modified, and after lowering the simulation temperature, the core remains amorphous. As an alternative, we have investigated the collisions of fast oxygen atoms colliding with crystalline Si grains held at a temperature below the melting point. In principle, this route was found to be more promising, with the drawback that even in approximate schemes like DFTB, the computation of well-passivated Si clusters becomes rather tedious. Moreover, the results are likely to be influenced by the properties of the non-converged basis sets used, and by assumptions related to the ensemble of starting configurations and collision energies.

In order to circumvent any uncontrolled influence of a partly relaxed geometry on the spectroscopic properties, we have started to investigate the latter for well-defined model clusters: Nearly spherical approximants of tetrahedral Si crystals, with all surface dangling bonds passivated by hydrogen. For much smaller systems up to $\text{Si}_{99}\text{H}_{100}$ (diameter d

≤ 1.5 nm), model clusters centered around a silicon atom at the origin were optimized with DFT, and for the excited state with TD-DFT.

Optical excitation produces a change of the occupation numbers of the frontier orbitals, corresponding therefore to an anisotropic modification of the total charge density. In turn, this anisotropy defines a relaxed excited state geometry of lower symmetry with respect to the tetrahedral point group T_d of the electronic ground state. In the resulting tetragonal symmetry, the degeneracy of the HOMO is lifted. The splitting is proportional to the tetragonal deformation, a phenomenon which can be understood as a pronounced Jahn-Teller effect. The projection of the deformations at the minima of the excited state potential surface onto the different symmetries allows for a discrimination of the respective contributions to the total Stokes shift. For selected systems, the influence of the Jahn-Teller effect on the Stokes shift can exceed the red shift related to a symmetry-conserving deformation in the relaxed excited state.

3.3 Ausgangsfragen, neuester Stand der Forschung / Initial goals, current status of the field

After the observation of intense red PL from porous silicon (Canham 1990), various experimental investigations have focused on a reproducible generation of size-selected silicon nanoparticles with different preparation techniques, ranging from gas phase synthesis (Schuppler 1995, Ehbrecht 1997) over growth in nanosize surfactant aggregates (Wilcoxon 1999) and annealing of non-stoichiometric silicon oxide (Takeoka 2000) to selective electrochemical etching (Belomoin 2002). From the dependence of the PL spectra on size, there is clear evidence for quantum confinement effects and a high PL efficiency (Ledoux 2002), features which however require a surface passivation with oxygen or hydrogen (Ledoux 2001).

Even 16 years after the discovery of PL from silicon nanostructures, we did not find any publication where a PL lineshape of a silicon nanocrystal was calculated from the geometries of its relaxed ground and excited states. Instead, several groups have investigated the vertical transition energies in the ground state geometry absorption of such systems with TD-DFT, but the deformation in the relaxed excited state and the resulting Stokes shift did not receive a lot of attention. Our investigation (Scholz 2006) extends previous calculations of the optical properties of H-passivated Si nanoparticles (Puzder 2003, Mitas 2001, Rao 2004, Tsolakidis 2005) towards a detailed analysis of the influence of different

kinds of deformations on the Stokes shift. Contrary to previous studies of the Stokes shift for H-passivated Si₂₉ (Sundholm 2004) and excited state relaxations in larger tetrahedral systems (Franceschetti 2003), deformations conserving the initial symmetry and deformations towards a lower symmetry are determined separately.

3.4 Angewandte Methoden / Applied methods

In order to reconcile a high precision with an affordable effort, we use the mixed functional B3LYP and a double- ζ basis throughout. All calculations are performed with the *turbomole 5.7* program package. The silicon clusters are constructed from nearly spherical approximants to the tetrahedral bulk lattice. The ground state of each cluster is optimized in the full tetrahedral point group T_d , whereas the T_d -symmetric deformation of the optically excited state and a symmetry lowering towards the subgroup D_{2d} are treated separately. At the present stage of the project, the deformations in the relaxed excited state have been determined for H-passivated Si clusters of a diameter of $d \leq 1.5$ nm, and the next step will be to project these deformations onto the vibrational eigenvectors of the ground state potential energy surface, resulting eventually in calculated PL lineshapes including the vibronic subbands.

In collaboration with TP 11, similar calculations have been applied to the vibronic bands observed in gas phase absorption spectra obtained on benzofluorene, see below.

3.5 Ergebnisse und ihre Bedeutung / Results and their importance

3.5.1 Silicon nanoparticles

In all nonlinear closed shell molecules, optical excitation results in a spontaneous symmetry breaking with respect to the geometry of the ground state, a phenomenon known as the Jahn-Teller effect (Jahn 1937). Therefore, for a quantitative interpretation of absorption and PL, it is of utmost importance to determine the reduced symmetry at the minima of the excited state potential energy surface (PES).

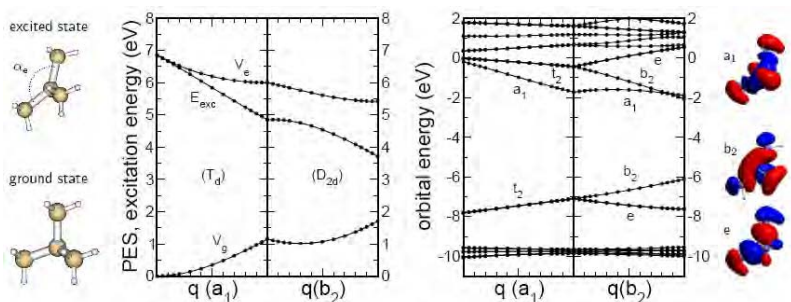


Fig. 1: Results of B3LYP/double- ζ calculations obtained for Si_5H_{12} . From left to right: Geometries in the D_{2d} -symmetric relaxed excited state (top) and in the T_d -symmetric electronic ground state (bottom); transition energies E_{exc} and potential energy surfaces of ground (V_g) and excited states (V_e) for the part $q(a_1)$ of the deformation in the relaxed excited state conserving the tetrahedral symmetry of the electronic ground state and for the subsequent tetragonal deformation $q(b_2)$ from T_d into a geometry with reduced D_{2d} symmetry; orbital energies for the deformation $q(a_1)$, and splitting of orbitals along the deformation $q(b_2)$; frontier orbitals in the relaxed excited state: a_1 (LUMO), b_2 (HOMO), and e (HOMO-1).

For the spherical approximants to a tetrahedral bulk lattice centered around a silicon atom investigated in the following, all dangling bonds at the surface are passivated with hydrogen atoms. For silane (SiH_4) and the molecules Si_5H_{12} and $\text{Si}_{17}\text{H}_{36}$, the terminal Si atoms have more than two hydrogen neighbours. As these systems are still too small to form closed six-membered Si rings, the dendrimer-like bond geometries remain rather flexible. In the electronic ground state of these systems, the t_2 -symmetric HOMO is occupied by 6 electrons, resulting in an A_1 -symmetric electronic configuration. After a dipole-allowed excitation to the a_1 -symmetric LUMO, the symmetry of the electronic configuration is reduced to $(t_2)^5 a_1 = T_2$, inducing a distortion of the molecular geometry

to tetragonal symmetry. Both the deformations conserving the tetrahedral point group T_d and subsequent D_{2d} -symmetric distortions give large reductions of the excitation energy, compare Figs. 1 and 2. The relaxed excited geometries of Si_5H_{12} and $\text{Si}_{17}\text{H}_{36}$ reveal strong deviations of the bond angle α_e around the central atom from a regular tetrahedron. This lowering of the symmetry results in a splitting of the threefold degenerate highest t_2 orbital into a HOMO transforming according to the b_2 representation in the subgroup $D_{2d} \subset T_d$ and a double degenerate orbital of e symmetry.

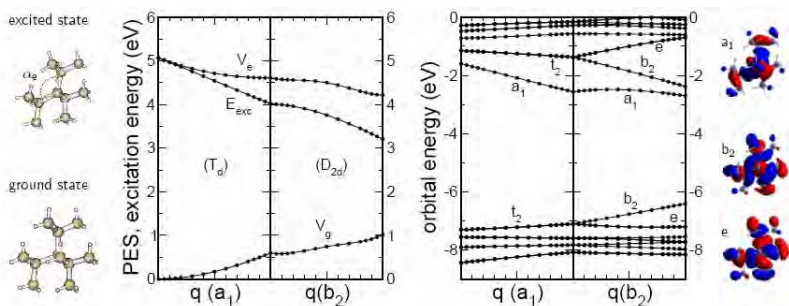


Fig. 2: As Fig. 1, but for $\text{Si}_{17}\text{H}_{36}$.

As the deformation responsible for the symmetry lowering consists mainly in a distortion of the bond angles between adjacent bonds around the central atom, only orbitals with a large contribution at this site are strongly influenced. More specifically, the highest occupied orbitals of t_2 symmetry are based on p orbitals on the central atom, splitting into a higher b_2 orbital with a node plane normal to the direction of the tetragonal compression of the tetrahedron, and a lower pair of e orbitals where the tetragonal axis is included in the node plane. The t_2 states above the LUMO consist mainly of p orbitals on the central atom, but in this case superimposed in an anti-bonding fashion with contributions localized around peripheral atoms. The a_1 -symmetric LUMO is based on an s -symmetric orbital on the central site, surrounded by p -symmetric contributions from the peripheral Si atoms. It has a non-monotonous dependence on the deformation $q(b_2)$ in D_{2d} , so that the PES of the excited state results in a saddle point for $q(b_2) \rightarrow 0$. The curvature of the excited state potential along this direction is an immediate consequence of this specific dependence of the energy of the a_1 orbital on the tetragonal deformation.

In Fig. 3 and Table I, we compare the influence of the tetrahedral and tetragonal parts of the deformation in the relaxed excited geometries

of Si-H clusters on their respective excitation energies. Beyond $\text{Si}_{17}\text{H}_{36}$, all clusters have surface Si atoms bound into six-membered silicon rings, with the exception of $\text{Si}_{71}\text{H}_{84}$ where the surface is terminated by $-\text{SiH}_3$ end groups.

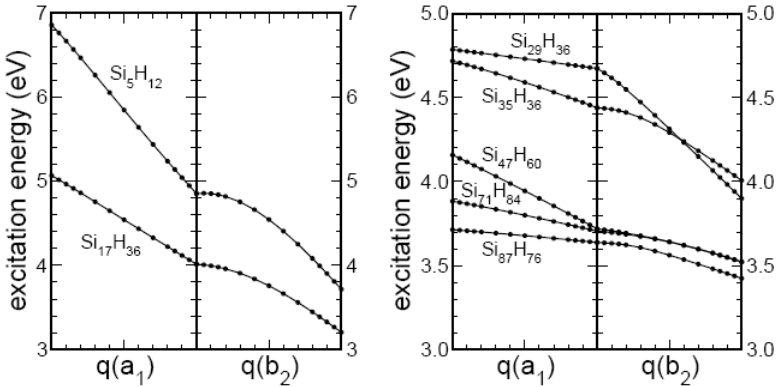


Fig. 3: Excitation energies of H-passivated silicon nanocrystals as a function of the tetrahedral part $q(a_1)$ and the tetragonal part $q(b_2)$ of the deformation in the relaxed excited state. Left: Si_5H_{12} and $\text{Si}_{17}\text{H}_{36}$, as annotated; right: $\text{Si}_{29}\text{H}_{36}$, $\text{Si}_{35}\text{H}_{36}$, $\text{Si}_{47}\text{H}_{60}$, $\text{Si}_{71}\text{H}_{84}$, and $\text{Si}_{87}\text{H}_{76}$.

For the small dendrimer-like molecules Si_5H_{12} and $\text{Si}_{17}\text{H}_{36}$, the tetrahedral $q(a_1)$ deformation induces a significant stretching of the bonds surrounding the central site, resulting in turn in a large Stokes shift exceeding 1 eV. The tetragonal $q(b_2)$ deformation, on the other hand, has a much smaller influence on the bond length, modifying merely the angles between these bonds. The corresponding Jahn-Teller contribution to the Stokes shift is 1.1 eV (Si_5H_{12}) and 0.8 eV ($\text{Si}_{17}\text{H}_{36}$), remaining below the influence of the tetrahedral deformation for both molecules. In silane, the Stokes shift is even larger: 2.5 eV for the tetrahedral deformation $q(a_1)$, and 1.5 eV for the tetragonal distortion $q(b_2)$. Even though the larger Si nanocrystals are expected to be more rigid, they still experience a large red shift of the PL. Moreover, in $\text{Si}_{29}\text{H}_{36}$, $\text{Si}_{35}\text{H}_{36}$, $\text{Si}_{71}\text{H}_{84}$ and $\text{Si}_{87}\text{H}_{76}$, the Jahn-Teller contribution to the Stokes shift exceeds the influence of the tetrahedral deformation, whereas only in $\text{Si}_{47}\text{H}_{60}$, the tetrahedral deformation is dominant.

TABLE I: Geometric parameters of the optimized geometry of H-passivated Si clusters, calculated transition energies, and Stokes shift. d_g , d_e : bond length (Å) around the central atom in the electronic ground and excited states, respectively; α_e : angle (degrees) between bonds around central atom in the relaxed excited state. Where available, the calculated absorption energy E_{abs} is compared to experimental data, and the calculated values for the tetrahedral and tetragonal contributions to the Stokes shift ΔE are reported separately.

	SiH ₄	Si ₅ H ₁₂	Si ₁₇ H ₃₆	Si ₂₉ H ₃₆	Si ₃₅ H ₃₆	Si ₄₇ H ₆₀	Si ₇₁ H ₈₄	Si ₈₇ H ₇₆
$d_g(T_d)$	1.49	2.38	2.45	2.40	2.40	2.47	2.42	2.40
$d_e(T_d)$	1.73	2.70	2.68	2.40	2.43	2.59	2.46	2.43
$d_e(D_{2d})$	1.69	2.64	2.63	2.41	2.41	2.59	2.45	2.41
α_e	148.2	140.3	128.2	112.7	111.7	113.5	112.2	111.4
E_{abs}	10.44 (8.8 ^a)	6.85 (6.5 ^b)	5.07	4.79	4.72	4.16	3.88	3.71
$\Delta E(T_d)$	-2.54	-2.00	-1.05	-0.11	-0.28	-0.44	-0.18	-0.08
$\Delta E(D_{2d})$	-1.57	-1.14	-0.81	-0.77	-0.43	-0.20	-0.18	-0.21

a (Itoh 1986), *b* (Delley 1993)

3.5.2 Absorption spectra of benzofluorene

In collaboration with TP 11, we have investigated the lowest excitation of benzofluorene, $S_1 \leftarrow S_0$. Similar to previous DFT calculations based on the BLYP functional (Banisaukas 2004), our TD-DFT calculations based on B3LYP gave an inversion of the lowest two excitations: The strong $S_2 \leftarrow S_0$ transition measured at about $E_{00}=32030 \text{ cm}^{-1}$ (Banisaukas 2004) was found *below* the weak $S_1 \leftarrow S_0$ transition observed at $E_{00}=29894 \text{ cm}^{-1}$ (compare TP 11). For basis sets up to double- ζ , the lowest two excited state PES crossed between the ground state geometry and the relaxed excited geometry of the PES in the electronic configuration S_1 . Only a rather large triple- ζ basis gave PES of S_1 and S_2 which did not cross between the geometries of interest, compare Fig. 4.

Both excited PES have a modified curvature with respect to the ground state. This can be interpreted as a modification of the mechanical properties of the chemical bonds resulting from the excitation of an electron from an occupied bonding orbital to a virtual anti-bonding orbital.

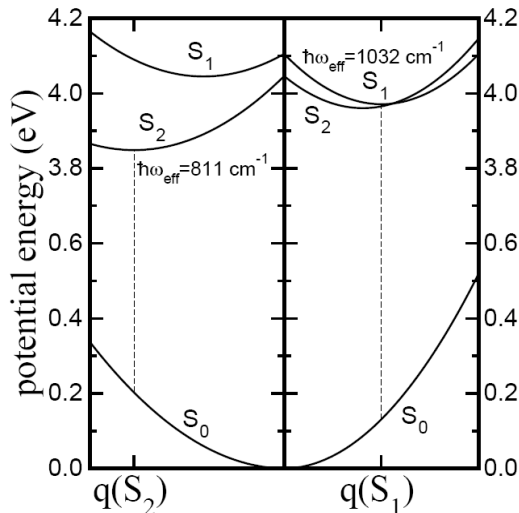


Fig. 4. Potential energy surfaces of the electronic configurations S_0 , S_1 and S_2 of benzofluorene, as obtained in a TD-DFT calculation at the B3LYP/triple- ζ level. The electronic configurations are denoted according to the energetic ordering observed in the gas phase. The curvature on the PES of the excited states is given in terms of an effective vibrational mode $\hbar\omega_{\text{eff}}$ along the deformation between the relaxed geometries of the electronic ground state and the excited electronic configurations. With respect to the measured transition energies, the calculated origin band $E_{00}(S_1)$ is overestimated by about 0.30 eV, whereas the origin band $E_{00}(S_2)$ is underestimated by about -0.12 eV. This results in an inversion of the energetic ordering of the PES corresponding to S_1 and S_2 .

TABLE II: Comparison of vibrational bands observed for the weak $S_1 \leftarrow S_0$ transition of benzofluorene with a TD-DFT calculation at the B3LYP/triple- ζ level. From left to right: observed transition energies; energies with respect to E_{00} ; observed intensities, normalized to the transition at $E_{00}+710 \text{ cm}^{-1}$; tentative assignment of the observations to vibrational modes calculated on the PES of S_0 ; ratio of mode frequencies deduced from the ratio of curvatures of the PES along the direction of the eigenvectors in the configuration S_0 ; Huang-Rhys factors obtained on the PES of S_0 , normalized with respect to the intensity of the origin band E_{00} . The modes are assigned according to their ordering of the estimated frequencies $\hbar\omega(S_1)$.

E (cm⁻¹)	$E-E_{00}$ (cm⁻¹)	intensity	$\hbar\omega(S_0)$	$\hbar\omega(S_1)/\hbar\omega(S_0)$	$S[\hbar\omega(S_0)]$
29894.00	0	>> 1			1.0
30039.35	145.35	0.084	157	1.10	0.023
30192.50	298.5	0.055	314	1.04	0.028
30236.80	342.80	0.102	359	1.03	0.005
30448.50	554.50	0.115	590	1.02	0.080
30596.19	702.19	0.104	721	1.00	0.001
30603.91	709.91	1.0	764	0.93	0.095
30658.70	764.70	0.070	800	0.97	0.007
30701.50	807.50	0.049	?		
30711.40	817.40	0.094	847		0.026
30852.00	958.00	0.053	?		
30878.00	984.00	0.264	1036	0.99	0.027
31208.00	1314.00	0.106	1344	1.03	0.011
31230.20	1336.20	0.129	1599	0.90	0.032
31265.00	1371.00	0.138	1378	1.05	0.042
31269.00	1375.00	0.725	1637	0.89	0.080
			1400	1.05	0.049
31288.00	1394.00	0.235	1503	0.99	0.028
31359.20	1465.00	0.735	1464	1.01	0.062
			1503	0.99	0.028
			1632	0.92	0.020
			1608	0.95	0.054

From the measured intensities of the various vibronic sidebands, we can deduce an effective mode energy of 1058 cm^{-1} along the deformation between the relaxed geometries of the states S_0 and S_1 , reproduced in the B3LYP/triple- ζ calculation within 3%. The projection of the deformation pattern at the minimum of the PES related to S_1 onto the vibrational eigenvectors determines the Huang-Rhys factor $S(\hbar\omega)$ of all vibrational modes of a' symmetry. These values for $S(\hbar\omega)$ give directly the ratio between the intensities of the first vibronic transition E_{01} of each mode with respect to the origin band E_{00} .

In the calculations performed till now, it turned out that the curvature of the S_1 PES along a vibrational eigenvector on the PES of S_0 can be strongly modified, compare Table II. Based on these large changes of the curvature, we suspect that the change in the electronic configuration will induce a substantial Dushinsky rotation between the two sets of vibrational eigenvectors. Therefore, the projection of the relaxed excited state deformation onto the vibrational eigenvectors on the PES of S_0 can only serve as a preliminary interpretation of the vibronic progression observed in absorption, and a more quantitative analysis would require the use of the eigenvectors on the upper PES corresponding to S_1 . Such a projection scheme allowing for different eigenvectors on the PES corresponding to S_0 and S_1 would improve the vibrational frequencies, and it would significantly modify the assignment of the Huang-Rhys factors. At the present stage, the corresponding calculation of the vibration eigenvectors on the upper PES is under way.

3.6 Zusammenfassung und Ausblick / Summary and future

Mit DFT und TD-DFT wurden die Geometrien von H-passivierten Si-Kristallen bis zu einem Durchmesser von 1.5 nm im elektronischen Grundzustand und im symmetriegebrochenen angeregten Zustand optimiert. Für alle untersuchten Modellcluster wurde der Einfluss der tetragonalen und tetraedrischen Deformation auf die Stokes-Verschiebung einzeln bestimmt, so dass ein quantitativer Vergleich des Jahn-Teller-Effekts mit symmetrieerhaltenden Verformungen möglich war. In einigen der untersuchten Fälle war der Einfluss der Symmetrierniedrigung auf die Rotverschiebung dominant.

Der nächste Schritt unserer Untersuchungen wird die Projektion der Deformationen auf die Vibrationseigenvektoren im elektronischen Grundzustands sein, so dass die vibronischen Progressionen in den PL-Spektren erstmals berechnet werden können. Von einem methodischen

Standpunkt betrachtet ist die einzige benötigte Information der Huang-Rhys-Faktor jeder Vibrationsmode. Der einzige Unterschied zu einer quantitativen Analyse der vibronischen Banden in der Absorption ist die für die Projektion verwendete Potentialfläche: Absorption muss auf der angeregten Potentialfläche analysiert werden, PL auf der Fläche des elektronischen Grundzustands.

Für Benzofluoren wurde die Deformation in den relaxierten Geometrien der zwei niedrigsten angeregten Zustände ermittelt. Die Verteilung der stark ausgelenkten Moden im elektronischen Grundzustand auf verschiedene Frequenzbereiche entspricht im wesentlichen den in TP 11 beobachteten Absorptionslinien. Der nächste Schritt wird eine Berechnung der Vibrationsmoden im elektronisch angeregten Zustand sein, so dass die Dushinsky-Rotationen quantifiziert werden können. Darüber hinaus erwarten wir von einer Projektion der Verformung auf die Vibrationsmoden im elektronisch angeregten Zustand eine bessere Übereinstimmung mit den experimentell ermittelten Modenintensitäten.

Applying DFT and TD-DFT techniques to H-passivated silicon clusters in the size range up to a diameter of 1.5 nm, we have determined their geometries in the electronic ground state and at the minima of the excited state potential energy surface. In each case, tetrahedral and tetragonal deformations in the relaxed excited state were determined separately, allowing for a quantitative assignment of the influence of the Jahn-Teller effect on the Stokes shift. In specific cases, it was demonstrated that the energetic influence of a tetragonal distortion towards D_{2d} symmetry can exceed the Stokes shift resulting from a tetrahedral deformation alone.

A straightforward extension of the present work will be the projection of the deformation in the relaxed excited state of each Si nanocrystal on the vibrational eigenvectors of the ground state potential energy surface (Pouladsaz 2007). Presumably, this will result in the first calculation of the PL spectra of Si nanoparticles including the vibrational subbands. From a methodological point of view, such a calculation is directly based on the determination of the Huang-Rhys factors. The only difference with respect to an interpretation of the absorption spectra is the PES used in the projection scheme: Absorption has to be analysed on the PES of the excited state, PL on the PES of the ground state.

Concerning benzofluorene, we have calculated the elongation of the vibrational modes obtained on the PES of the electronic ground state in the relaxed excited geometry of the S_1 configuration. The main results

were compatible with the gas phase spectra determined in TP 11, including the intensity distribution over regions with prominent modes. The next step will be a calculation of the vibrational modes in the PES of the excited state S_1 , allowing a detailed assignment of Dushinsky rotations. We expect that a projection scheme based on the vibrational modes obtained on the excited PES will lead to an improved distribution of the intensities over the vibronic sidebands.

3.7 Literatur / References

- Banisaukas, J., Szczepanski, J., Vala, M., and S. Hirata, *Vibrational and electronic absorption spectroscopy of 2,3-benzofluorene and its cation*, J. Phys. Chem. A **108** (2004) 3713.
- Belomoin G., Therrien J., Smith A., Rao S., Twesten R., Chaieb S., Nayfeh M. H., Wagner L., and Mitas L., *Observation of a magic discrete family of ultrabright Si nanoparticles*, Appl. Phys. Lett. **80** (2002) 841.
- Canham L. T., *Silicon quantum wire array fabrication by electrochemical and chemical dissolution of wafers*, Appl. Phys. Lett. **57** (1990) 1046.
- Ehbrecht M., Kohn B., Huiskens F., Laguna M. A., and Paillard V., *Photoluminescence and resonant Raman spectra of silicon films produced by size-selected cluster beam deposition*, Phys. Rev. B **56** (1997) 6958.
- Itoh U., Toyoshima Y., Onuki H., Washida N., and Ibuki T., *Vacuum ultraviolet absorption cross sections of SiH_4 , GeH_4 , Si_2H_6 , and Si_3H_8* , J. Chem. Phys. **85** (1986) 4867.
- Delley B. and Steigmeier E. F., *Quantum confinement in Si nanocrystals*, Phys. Rev. B **47** (1993) 1397.
- Jahn H. A. and Teller E., *Stability of polyatomic molecules in degenerate electronic states. I. Orbital degeneracy*, Proc. Roy. Soc. A **161** (1937) 220.
- Ledoux G., Gong J., and Huiskens F., *Effect of passivation and aging on the photoluminescence of silicon nanocrystals*, Appl. Phys. Lett. **79** (2001) 4028.
- Ledoux G., Gong J., Huiskens F., Guillois O., and Reynaud C., *Photoluminescence of size-separated silicon nanocrystals: Confirmation of quantum confinement*, Appl. Phys. Lett. **80** (2002) 4834.
- Mitas L., Therrien J., Twesten R., Belomoin G., and Nayfeh M. H., *Effect of surface reconstruction on the structural prototypes of ultrasmall ultrabright Si_{29} nanoparticles*, Appl. Phys. Lett. **78** (2001) 1918.
- Puzder A., Williamson A. J., Reboredo F. A., and Galli G., *Structural Stability and Optical Properties of Nanomaterials with Reconstructed Surfaces*, Phys. Rev. Lett. **91** (2003) 157405.
- Pouladsaz D., thesis: *Density functional studies of the spectroscopic properties of Si nanocrystals* (2007) in preparation.

- Rao S., Sutin J., Clegg R., Gratton E., Nayfeh M. H., Habbal S., Tsolakidis A., and Martin R. M., *Excited states of tetrahedral single-core Si_{29} nanoparticles*, Phys. Rev. B **69** (2004) 205319.
- Scholz R., Pouladsaz D. and Schreiber M., *Influence of the Jahn-Teller effect on absorption and photoluminescence spectra of Si nanocrystals*, phys. stat. sol. (c) **3** (2006) 3561.
- Schuppler S., Friedman S. L., Marcus M. A., Adler D. L., Xie Y.-H., Chabal Y. J., Harris T. D., Brus L. E., Brown W. L., Chaban E. E., Szajowski P. F., Christman S. B., and Citrin P. H., *Size, shape, and composition of luminescent species in oxidized Si nanocrystals and H-passivated porous Si*, Phys. Rev. B **52** (1995) 4910.
- Sundholm D., *Density functional studies of the luminescence of $Si_{29}H_{36}$* , Phys. Chem. Chem. Phys. **6** (2004) 2044.
- Tsolakidis A. and Martin R. M., *Comparison of the optical response of hydrogen-passivated germanium and silicon clusters*, Phys. Rev. B **71** (2005) 125319.
- Wilcoxon J. P., Samara G. A., and Provencio P. N., *Optical and electronic properties of Si nanoclusters synthesized in inverse micelles*, Phys. Rev. B **60** (1999) 2704.

3.1 Bericht Teilprojekt 3

3.1.1 Titel / Title

*Astrophysikalische Modellierung -- chemische Entwicklung
protoplanetarer Scheiben*

*Astrophysical Modeling -- The Chemical Evolution of Pro-
toplanetary Disks*

3.1.2 Berichtszeitraum / reported period

01.07.2003 - 31.12.2006

3.1.3 Projektleiter / principle investigator

Henning, Thomas, Prof. Dr.
Max-Planck-Institut für Astronomie, Heidelberg

3.2 Zusammenfassung / Abstract

3.2.1 Wortlaut des Antrags / abstract of the proposal

Die Modellierung der chemischen Entwicklung protoplanetarer Akkretionsscheiben zieht zunehmend die Aufmerksamkeit von Astrophysikern auf sich, da ein Verständnis dieser Entwicklung die Grundvoraussetzung für ein besseres Verständnis der Anfangsbedingungen für den Sonnennebel sowie die Entstehung extrasolarer Planetensysteme liefert. Die chemische Entwicklung wirkt in direkter Weise auf die dynamische Entwicklung zurück, wobei als Beispiel der für MHD-Simulationen ausschlaggebende Parameter Ionisationsgrad dienen kann. Aufbauend auf numerischen Modellen für die Chemie in 1+1D-Scheiben werden wir zunächst untersuchen, wie Schlüsselparameter wie die Massenakkretionsrate die Ergebnisse beeinflussen. Außerdem werden wir die Modelle hin zu größeren Radien ausdehnen, was eine vollkommen neue Behandlung der thermischen Struktur der Scheiben erfordert, weil hier die stellare Heizung wichtiger als die viskose Heizung wird. Dies erfordert die Einbeziehung eines 2D-Strahlungstransportes. Unabhängig von astrophysikalischen Anwendungen ist die Kopplung von komplizierten chemischen Re-

aktionsnetzwerken und dynamischen Systemen an der Grenzlinie zwischen Chemie und Physik auch von generellem Interesse und hat weite Anwendungen in verschiedenen Wissenschaftsfeldern, so bei Verbrennungsprozessen.

The modeling of the chemical evolution of protoplanetary disks attracts presently great attention in astrophysics because of the increasing interest in the initial conditions for the solar nebula and other planetary systems. Furthermore, chemistry interacts with the dynamical evolution of disks with the ionization degree, important for MHD calculations, as a key example. Based on our models developed for chemistry in 1+1D disks we will start an exploratory phase to understand how different networks and physical parameters such as the mass accretion rate influence chemistry. In addition, we will extend the models to larger radii where stellar radiation dominates over viscous heating in determining the disk structure and dynamics. This will require the treatment of 2D radiation transfer. The results of our calculations can be checked against observational results coming from molecular spectroscopy of circumstellar envelopes and disks. Apart from astrophysics, we want to note that the coupling of a complicated chemical reaction network with a dynamical system is a fundamental problem on the borderline between chemistry and physics, important in many different scientific areas such as combustion chemistry.

3.2.2 Zusammenfassung des Berichts / abstract of the report

Using the reduction scheme developed during the first funding period, we investigated in detail the chemistry of ionization in an accreting protoplanetary disk. From chemical perspective the disk is divided into highly ionized, mostly atomic surface, less ionized, chemically rich intermediate layer, and dark, dense and cold neutral midplane. We found that in the darkest region of the midplane accretion cannot be efficiently sustained by turbulence and thus this zone is “dead”.

Another important part of the project was the detailed chemical and line radiative transfer modeling of the (sub)-millimeter single-dish and interferometric observations of the protoplanetary disk and remnant envelope around young star AB Aur. We used a 2 D model of the disk physical structure, a gas-grain chemical network with surface reactions, and a 2 D line radiative transfer code to calculate molecular abundances and to simulate synthetic spectra and spectral maps. By varying a priori unknown parameters, these spectra were modeled and iteratively com-

pared to the observational data. The best-fit model of the AB Aur system allowed us to constrain the size, orientation, kinematics, mass, and even the age of the AB Aur disk and envelope.

Finally, we succeeded in coupling an extended chemical network that includes gas-phase processes as well as surface reactions and gas-grain interactions (accretion, desorption) with 1 D and 2D turbulent mixing models of a steady-state protoplanetary disk. A comparison between models with and without 1D and 2D mixing is made, and a puzzling observational evidence of very cold CO gas in disks is explained in framework of the full 2D mixing chemistry.

3.3 Ausgangsfragen, neuester Stand der Forschung / Initial goals, current status of the field

The understanding of disk chemistry provides unique information on disk physical structure and chemical composition (including ionization degree) at various evolutionary stages. This will become even more true when the next generation of radio interferometers like ALMA (Atacama Large Millimeter Array) and space-borne infrared satellites like Herschel will start to operate within several year and offer unprecedented spatial and spectral resolution and high sensitivity at many frequencies. The observational studies of nearby young stars enshrouded in protoplanetary disks, coupled to advanced chemical modeling, allow to reveal initial conditions for planet formation and thus are tightly related with cosmochemistry of the early Solar nebula. Since young accretion disks are highly dynamical entities, it is necessary to couple disk chemistry and dynamics. However, modeling of complex chemistry involving gas-phase and grain surface reactions as well as gas-grain interactions on top of dynamical evolution of accretion disks requires high numerical demands and thus remains a challenge for numerical astrophysics. This was the initial and ultimate goal of the funded project.

During the last two years significant progress in understanding of the disk structure was achieved both theoretically and observationally. A number of nearby dense disks that were imaged at VLA (Very Large Array, USA) at millimeter and centimeter wavelengths reveal evidence of significant grain growth (Przygodda *et al.* 2003, Rodmann *et al.* 2006). The question how dust grains do grow in such disks was addressed theoretically and a general scheme of the grain evolution in proto-planetary disks was developed (Dullemond and Dominik 2005). Initially tiny sub-micron grains that are well mixed with the gas collide and stick and form

larger aggregates. Eventually these aggregates become so big (about 10 cm) that they are not supported by gas drag forces against gravitation and slowly sediment toward the midplane, changing the entire disk structure. This is a crucial process for the disk chemistry as the UV penetration, disk density and temperature, dust-to-gas mass ratio are all changing with time. It was found that molecular column densities for most species, excluding HCO^+ and H_2D^+ , are not much affected during the initial growth phase to millimeter-sized particles but strongly affected in more evolved disks (Aikawa and Nomura 2006, Jonkheid *et al.* 2006).

A first attempt to couple chemistry with dynamics in outer disk region beyond 100 AU using a 1D vertical turbulent mixing code with gas-grain chemical network was done by Willacy *et al.* (2006). They found that vertical mixing modifies abundances and column densities of many molecules, and is in better agreement with observational results than the steady-state (non-mixing) model. Semenov *et al.* (2006) used a 2D-mixing code coupled with a complex chemistry and found that transport processes in disks are capable of sustaining a large reservoir of very cold CO in their midplane, a puzzling observational fact that cannot be understood in frame of conventional static chemical models (Dartois *et al.* 2003).

3.4 Angewandte Methoden / Applied methods

The coupling of a complex, gas-grain chemical network with surface reactions with multidimensional transport processes (turbulent mixing, global accretion flows) requires the development of a computationally efficient yet numerically stable integration scheme. We developed such a method that at present allows us to model the disk chemical evolution within 1 - 5 Myr using an extended chemical network consists of about 250 species and 2500 reactions that is coupled to a 1D or 2D turbulent mixing model. Even for the most extreme case of the 2D coupled chemodynamical model the necessary computational demands are low: the calculations usually take 1 - 2 weeks on a single CPU machine (2.8 GHz Xeon, 2 GB of RAM). This goal could not be achieved without the use of the reduction method to remove unnecessary species and reactions from a chemical network which was developed during the first half of the funding period.

3.5 Ergebnisse und ihre Bedeutung / Results and their importance

The first step in our project was to study chemistry of the ionization degree in a protoplanetary disk from inner to outer parts (Semenov *et al.* 2004). While the latter is interesting because it can be directly observed, the inner disk zone is important from dynamical point of view as viscous heating dominates over stellar heating there. For that we used the mathematically correct algorithm to reduce the number of reactions and molecules in a chemical model that was developed during the first half of the project time, adopted a disk model with a vertical temperature gradient (D'Alessio *et al.* 1999), and coupled it with a gas-grain chemistry including surface reactions, the ionization due to stellar X-rays (Glassgold *et al.* 1997), stellar and interstellar UV radiation, cosmic rays and radionuclide decay. We could isolate small sets of chemical reactions that reproduce the evolution of the ionization degree at several distinct disk zones with an accuracy of 50–100 % for the entire evolutionary span of 1 Myr. We found that in the dark midplane, where most of molecules are frozen out onto dust grain surfaces, the ionization degree is controlled by cosmic rays and radionuclides only and is very low. Since turbulence cannot be driven by the magnetorotational instability this region is a quiescent (the so-called "dead zone") from the evolutionary point of view, and accretion should be layered in protoplanetary disks (Gammie 1996).

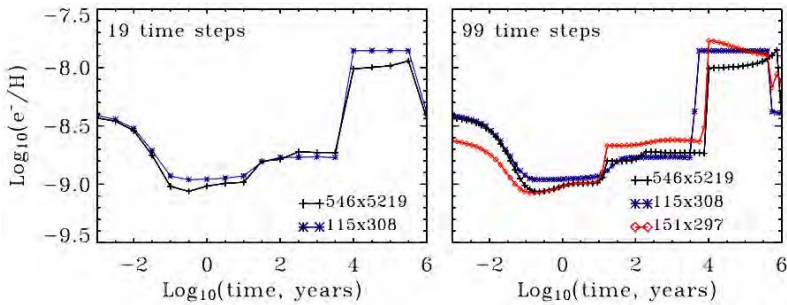


Fig. 1: (Left) Comparison of the time-dependent disk fractional ionization in the intermediate layer at 10 AU calculated with the full (546 species in 5219 reactions) and a reduced network for 19 evolutionary time moments. The overall accuracy of the reduced network made of 115 species and 308 reactions is about a factor of 2. (Right) Same as the left panel but with better time resolution (99 time steps) and the added case of the fractional ionization computed with the automatically reduced (151 \times 297) network. The manually reduced network is inaccurate by a factor of 8 in this case, while the automatically reduced one is accurate up to the factor of 2.

In contrast, in the intermediate layer the chemistry of the fractional ionization is driven by the attenuated stellar X-rays and is far more complicated as X-rays produce ionized helium and hydrogen, which initiate a quick. This region is particularly interesting for interpretation of the observed spectra because many molecular lines are excited there (van Zadelhoff *et al.* 2003). For the first time we found that surface hydrogenation of long carbon chains (e.g., HC_5N) can be of crucial importance for the evolution of the ionization degree in protoplanetary disks (see Fig.1). In the intermediate layer reduced networks contain more than a 100 species and hundreds of reactions, while in the unshielded low-density surface layer it is sufficient to keep about 20 species and reactions in reduced networks. Note that these reduced networks are different in different parts of the intermediate layer, which indicates that the chemistry of ionization is dominated by different ions. We found that C^+ is the most abundant ion in the disk, but HCO^+ is the dominant observable ion. Finally, we compared calculated column densities of key molecules to the results of other recent studies and observational data, and found a fairly good agreement between the theoretical results and observed abundances.

Since with the adopted disk chemical and physical model we reproduced the column densities of many observed species, we decided to apply it and study one particular object in detail. The main difficulty with interpretation of the spectral data obtained with a single-dish antenna or interferometer is unbiased determination of the observed quantities (temperature, density, column density). In contrast to absorption lines that are generated by absolute amount of absorbing material on the line of sight, (sub-) millimeter emission lines are typically excited in various disk regions with distinct physical conditions, kinematics, and chemical composition. Therefore, often it is not possible to extract a wealth of information from the line data without sophisticated chemical and line radiative transfer modeling.

We focused on the AB Aur system that represents a young Herbig Ae intermediate-mass star (~ 2.5 solar masses) surrounded by a compact (about 600 AU) dense disk and a more extended ($>10,000$ AU) envelope. Nowadays this object attracts a particular attention in observational astrophysics since spiral arms, a dark lane, and other inhomogeneous structures were discovered in the AB Aur disk (Fukagawa *et al.* 2004, Pietu *et al.* 2005). Nine different molecular species in a dozen rotational transitions were detected at low resolutions (10–30") using the IRAM telescope: CO, C^{18}O , CS, HCO^+ , DCO^+ , H_2CO , HCN, HNC, and SiO. In contrast, with PdBI we detected only the $\text{HCO}^+(1-0)$ emission from the AB

Aur disk at the modest 5'' resolution. The size and symmetric appearance of the $\text{HCO}^+(1-0)$ velocity map allowed us to constrain the radius of the disk ($\sim 200\text{--}500$ AU) assuming face-on orientation and its rotational profile ($V \propto r^{-0.5}$).

To account for these observational data, we used for the first time a coherent modeling of the disk and envelope physical structure, chemical evolution, and radiative transfer in molecular lines. Since many parameters of the AB Aur disk were known from other studies, we adopted a 2D flared passive disk model with vertical temperature gradient assuming Keplerian rotation (Dullemond & Dominik 2004). To represent the AB Aur envelope, we adopted the infalling isothermal spherical cloud model with a central region shadowed by the disk and two wide cones transparent to the stellar radiation. Next, for both the disk and envelope models we computed time-dependent abundances and column densities using the gas-grain chemical network supplied by dust surface reactions. After that, the calculated abundances were used to simulate the spectra of $\text{CO}(2-1)$, $\text{C}^{18}\text{O}(2-1)$, $\text{HCO}^+(1-0; 3-2)$, $\text{CS}(2-1)$, and $\text{CS}(5-4)$ transitions by mean of the 2D non-LTE line radiative transfer code (Pavlyuchenkov & Shustov 2004). Finally, these synthetic line spectra and spectral map were iteratively compared with the observational data (about 30 times) in a robust step-by-step way, constraining various parameters of the AB Aur system and their uncertainties one in a time.

Surprisingly, our best-fit disk model reproduces the intensities, widths, and profiles of the observed HCO^+ spectra on the entire interferometric map (see Fig.2). The constrained parameters of the AB Aur disk are the following. The AB Aur disk is in Keplerian rotation and inclined by 17 ± 6 deg., the disk radius is 400 ± 200 AU, and the disk mass is 1.3×10^{-2} solar masses with a factor of 7 uncertainty. The best-fit model of the AB Aur envelope successfully reproduces the intensities, widths, and profiles of the single-dish $\text{CO}(2-1)$, $\text{C}^{18}\text{O}(2-1)$, $\text{HCO}^+(1-0; 3-2)$, and $\text{CS}(2-1)$ spectra with the exception of the $\text{CS}(5-4)$ data, which can be fitted only by the clumpy. We found that the large ~ 2 km/s width of the observed $\text{CO}(2-1)$ emission cannot be explained by this model alone and is likely due to contamination by moving gas clouds along the line of sight to AB Aur. The best-fit envelope model has a mean temperature of about 35 ± 14 K, power-law density distribution $r^{-1.0 \pm 0.3}$ with the initial density of 10^{-19} g/cm³ and mass of about 6×10^{-3} solar masses. Our best-fit model predicts that the mass accretion in the AB Aur system is regulated by steady contraction of the envelope which will roughly last for another

25 Myr, which can also be true for other protoplanetary disk systems with surrounding envelopes (Semenov *et al.* 2005).

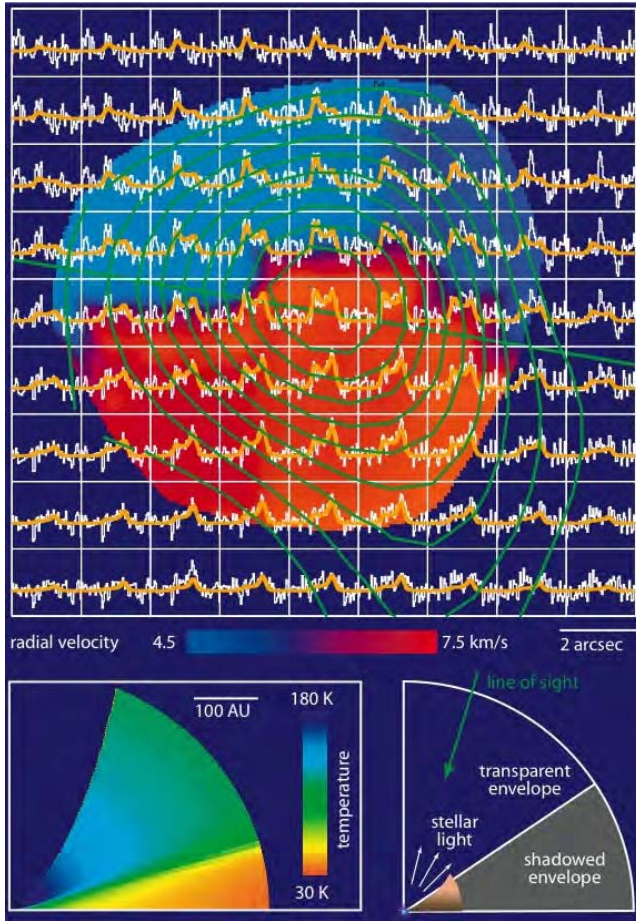


Fig. 2: The AB Aurigae system consists of a small and dense protoplanetary disk surrounded by a large diffuse envelope, which we seen nearly face-on. (Top) The gas velocities in the AB Aur disk probed with the Plateau de Bure interferometer in $\text{HCO}^+(1-0)$ (red-blue ellipse) are overplotted by the observed (white) and modeled (yellow) spectra. The "butterfly" pattern on the velocity map is characteristic of an inclined rotating configuration. (Bottom) The thermal structure of the flared disk model is shown on the right, the schematic sketch of the entire system is given on the left.

However, not all observational facts can be explained with advanced but steady-state disk model. Recently, using high angular and spectral resolution interferometric imaging of DM Tau in various CO isotopic lines with the Plateau de Bure Interferometer, followed by sophisticated χ^2 -minimization fitting, Dartois *et al.* (2003) found a reservoir of the abundant CO gas in the outer disk midplane, where the temperature is lower than 20 K. According to the results of standard static (non-dynamical) models within a few million year essentially all CO should be frozen out on dust grains as it cannot thermally desorb back into the gas phase at such a low temperature. This is a strong indication that transport processes indeed may play a role in chemical evolution of protoplanetary disks.

To address this problem quantitatively, we developed a 1D/2D turbulent mixing model for a 2D flared disk coupled to the gas-grain chemical code including surface reactions. A fast and numerically efficient implicit integration scheme was developed to allow massive computations. To further speed up the chemical simulations, we utilized our mathematically-proved reduction technique and isolated a network that is accurate for key observational molecules in the entire disk. We also realized that reduced chemical networks must be used with care in studies of mixing in protoplanetary disks as they may produce spurious results for some molecules.

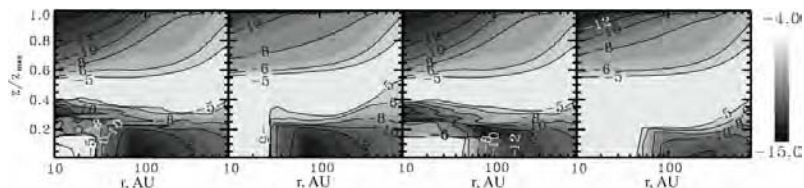


Fig. 3: Logarithm of relative gas-phase CO abundances (with respect to the total number of hydrogen nuclei) in the DM Tau disk at 5 Myr calculated with four chemical models. (From left to right): Static (non-mixing) chemistry, chemistry with vertical mixing only, chemistry with radial mixing only, and chemistry with full 2D mixing.

With this approach, we simulated the chemical evolution of the DM Tau disk within 5 Myr using static (non-mixing), vertical mixing, radial mixing, and full 2D mixing chemical models (Fig.3, see also Semenov *et al.* 2006). It was found that the gas-phase CO concentration in the outer, cold disk regions can be significantly enhanced due to the combined effect of vertical and radial mixing, which thus acts as efficient non-thermal desorption mechanism. The frozen CO together with grains

is eventually transported from the disk midplane to the warm intermediate layer and evaporates into the gas phase, while the CO gas sinks back toward the midplane and freezes onto the grain surfaces again. Overall, turbulent mixing tends to increase the gas-phase CO concentration by a few orders of magnitude, which is sufficient to explain the column densities of the CO gas at $T=13$ K observed by Dartois *et al.* (2003). Note that it is quite difficult to suggest other robust non-thermal mechanism of such enhancement in the outer, cold and dark disk midplane, since most of the free-floating CO molecules should stick there to the grain surfaces within a few hundred years and never come back. We ruled out a hypothesis of the substantial grain growth that could potentially decrease the efficiency of the gas-grain interactions and thus postpone the complete freeze out of the CO gas because in this case the disk midplane will likely be warmer than 10–20K, which contradicts to the observations.

3.6 Zusammenfassung und Ausblick / Summary and future

In dem Teilprojekt 3 der Forschergruppe verfolgten wir das Ziel, ein chemisches Netzwerk mit etwa 2500 Reaktionen zwischen 250 Reaktionspartnern mit einem hydrodynamischen 1+1-Modell einer protoplanetaren Akkretionsscheibe zu koppeln. Wir haben uns darauf konzentriert, den Einfluss von Reaktionsraten und Stern-Scheibe-Parametern (stellare Leuchtkraft, Akkretionsrate) auf die Resultate der Modellrechnungen zu untersuchen. Das Projekt schliesst die Entwicklung eines Ionisationsmodells für proto-planetare Akkretionsscheiben sowie von numerischen Verfahren zum Test der Empfindlichkeit der Ergebnisse bezüglich geänderter Reaktionsraten ein.

Insgesamt war das Projekt sehr erfolgreich, alle geplanten Untersuchungen konnten durchgeführt werden. In den kommenden Jahren wollen wir das chemisch-dynamische Modell ausweiten, indem wir sowohl Staubwachstum und -sedimentierung mit einbeziehen als auch das Eindringen von hochenergetischer Strahlung (UV, Röntgenstrahlen) in die Scheibe konsistent berücksichtigen. Zusätzlich ist geplant, in das Reaktionsnetzwerk auch Deuterierung aufzunehmen, neuste Modelle für Desorption zu berücksichtigen und die Chemie auf den Stauboberflächen mit einem stochastischen Ansatz zu behandeln. Nicht zuletzt sollen die berechneten Daten immer wieder mit aktuellen Beobachtungen verglichen werden.

The goal of this project was the coupling between a chemical network including about 2500 reactions between 200 species and the 1+1 D

model for a protoplanetary accretion disk. The studies have concentrated on the influence of reaction rates and stellar/disk parameters (stellar luminosity and accretion rates) on the outcome of the model. The project included the development of an ionization model for protoplanetary accretion disks and numerical tools to test the sensitivity of the results to different reactions.

This project was very successful and delivered results as planned in the proposal. During the next few years we want to extend our disk chemodynamical model by accounting for the grain growth and sedimentation, and by treating more consistently the penetration of high-energy radiation (UV, X-rays) into the disk. In addition, we plan to switch to a larger set of chemical reactions including deuteration, newly discussed desorption processes, and a feasible (stochastic) approach to simulate surface chemistry. Last but not least, the predictions made with our model will be thoroughly compared with available and forthcoming observational data.

3.7 Literatur / References

- Aikawa, Y., Nomura, H.: *Physical and Chemical Structure of Protoplanetary Disks with Grain Growth*, *Astrophys. J.* **642** (2006) 1152-1162.
- D'Alessio, P., Calvet, N., Hartmann, L., Canto, J.: *Accretion Disks around Young Objects. II. Tests of Well-mixed Models with ISM Dust*, *Astrophys. J.* **527** (1999), 893-909.
- Dartois, E., Dutrey, A., Guilloteau, S.: *Structure of the DM Tau Outer Disk: Probing the vertical kinetic temperature gradient*, *Astron. Astrophys.* **399** (2003), 773-787.
- Dullemond, C., Dominik, C.: *Dust coagulation in protoplanetary disks: A rapid depletion of small grains*, *Astron. Astrophys.* **434** (2005), 971-986.
- Fukagawa, M., Hayashi, M., Tamura, M.: *Spiral Structure in the Circumstellar Disk around AB Aurigae*, *Astrophys. J.* **605** (2004), L53-L56.
- Jonkheid, B., Dullemond, C., Hogerheijde, M., van Dishoeck, E.: *Chemistry and line emission from evolving Herbig Ae disks*, accepted by *Astron. Astrophys.* (2006), astro-ph/0611223.
- Gammie, C. F.: *Layered Accretion in T Tauri Disks*, *Astrophys. J.* **457** (1996), 355.
- Glassgold, A., Najita, J., Igea, J.: *X-Ray Ionization of Protoplanetary Disks*, *Astrophys. J.* **480** (1997), 344.
- Pavlyuchenkov, Ya., Shustov, B.: *A Method for Molecular-Line Radiative-Transfer Computations and Its Application to a Two-Dimensional Model for the Starless Core L1544*, *Astron. Reports* **48** (2004), 315-326.
- Pietu, V., Guilloteau, S., Dutrey, A.: *Sub-arcsec imaging of the AB Aur molecular disk and envelope at millimeter wavelengths: a non Keplerian disk*, *Astron. Astrophys.* **443** (2005), 945-954.
- Przygodda, F., van Boeckel, R., Abraham, P. *et al.*: *Evidence for grain growth in T Tauri disks*, *Astron. Astrophys.* **412** (2003), 43-46.
- Rodmann, J., Henning, T., Chandler, C. J. *et al.*: *Large dust particles in disks around T Tauri stars*, *Astron. Astrophys.* **446** (2006), 211-221.
- Semenov, D., Wiebe, D., Henning, T.: *Reduction of chemical networks. II. Analysis of the fractional ionisation in protoplanetary discs*, *Astron. Astrophys.* **417** (2004), 93-106.
- Semenov, D., Pavlyuchenkov, Ya., Schreyer, K. *et al.*: *Millimeter Observations and Modeling of the AB Aurigae System*, *Astrophys. J.* **621** (2005), 853-874.
- Semenov, D., Wiebe, D., Henning, T.: *Gas-Phase CO in Protoplanetary Disks: A Challenge for Turbulent Mixing*, *Astrophys. J.* **647** (2006), L57-L60.
- Van Zadelhoff, G.-J., Aikawa, J., Hogerheijde, M., van Dishoeck, E.: *Axi-symmetric models of ultraviolet radiative transfer with applications to circumstellar disk chemistry*, *Astron. Astrophys.* **397** (2003), 789-802.

3.1 Bericht Teilprojekt 4

3.1.1 Titel / Title

Infrarot- und Ferninfrarot-Spektroskopie molekularer Ionen: Vom Hydronium-Ion (H_3O^+) über Cluster bis zum Eis.

Infra-red and far infra-red spectroscopy of molecular ions: from the hydronium ion (H_3O^+) via clusters to ice.

3.1.2 Berichtszeitraum / reported period

01.07.2003 - 31.12.2006

3.1.3 Projektleiter / principle investigator

Schlemmer, Stephan, Dr., Dipl.-Phys., Universitätsprofessor
I. Physikalisches Institut, Universität zu Köln

3.2 Zusammenfassung / Abstract

3.2.1 Wortlaut des Antrags / abstract of the proposal

Die meisten Moleküle zeigen ihre charakteristischen spektralen Fingerabdrücke im infraroten und submillimeter Wellenlängenbereich. Daher konzentrieren sich zukünftige Beobachtungsmissionen wie Herschel auf diesen Spektralbereich. In diesem Projekt wird die Kombination eines 22-Pol Ionenspeichers mit abstimmbarer IR Laserstrahlung dazu benutzt, um Spektren astrophysikalisch relevanter Moleküle zu bestimmen. Die Schwingungs-Rotationsanregung des Muttermoleküls führt zu einer Änderung der Anzahl von Produktionen in ausgewählten Ionen-Molekül Reaktionen (laserinduzierte Reaktion [LIR]). Der Nachweis der Produkte dient damit als sehr empfindlicher Nachweis für die IR bzw. FIR Anregung. Das Hydronium Ion und Wasser Cluster Ionen stehen im Mittelpunkt der Untersuchungen, da Wasser eine Schlüsselrolle in vielen astrophysikalischen Umgebungen zugeschrieben wird. Strukturelle Isomere können identifiziert werden und ihre thermische bzw. nicht-thermische Zusammensetzung im Speicher mittels LIR untersucht werden. Ebenso können Prozesse innerhalb des Clusters wie Isomerisierung oder chemische Reaktionen in Heteroclustern studiert werden. Diese Untersuchungen sollen helfen, den Übergang von Molekülen zu sehr kleinen Aggregaten zu verstehen.

Most molecules show their unmistakable chemical signature at infrared and sub-millimeter wavelengths, therefore future observational missions like Herschel will focus on this spectral range. In this project, the combination of a variable temperature 22pole ion trap (TV-22PT) and tunable IR-laser radiation is used to obtain laboratory spectra of molecular ions relevant to astrophysical chemistry. The ro-vibrational excitation alters the product abundance from selected ion-molecule reactions which serves as a very sensitive detector for IR or FIR absorption of the parent ion (laser induced reaction [LIR]). The hydronium ion and water cluster ions are the prime targets of this project because water is a key ingredient in many astrophysical environments. Structural isomers can be identified and their thermal or non-thermal composition in the trap can be investigated using LIR. Also intra-cluster processes such as isomerization or chemical reactions in heterogeneous clusters can be studied and help to understand the transition from molecular species towards very small grains.

3.2.2 Zusammenfassung des Berichts / abstract of the report

The objective of this project is the determination of IR and FIR spectra of molecular ions as well as the quantitative understanding of the dynamics of ion molecule reactions at temperatures relevant to the interstellar medium. In a 22-pole ion trap apparatus the rather specific and ultra-sensitive method of laser induced reactions (LIR) is applied to obtain spectra for small hydrocarbon ions as well as other small ions of astrophysical relevance. It was the original aim to focus on the possibility to record spectra of very cold water cluster ions as model systems for water ice. Unfortunately the proposed LIR mechanisms did not work out. Due to the moves to Leiden and later to Köln a substantial reconstruction of the 22-pole apparatus was not possible. Therefore the focus of the project has been directed towards spectroscopy of C_2H_2^+ , CH_5^+ and H_2D^+ for which the main results were obtained. In all cases new vibrational modes were found and characterized. The detailed LIR studies revealed information on the break down of the separation of the motions of electrons and nuclei for the description of a molecule. For C_2H_2^+ the Renner-Teller coupling of electronic and nuclear motion was determined experimentally for the first time. For H_2D^+ the experiments show that non-Born Oppenheimer terms in the potential energy surface are relevant. For CH_5^+ first overview spectra from about 500 cm^{-1} up to 3200 cm^{-1} could be recorded. Comparison to theoretical work confirmed the structural scheme for this very floppy molecule as a CH_3 tripod to which a H_2 moiety is attached by a three centre two electron ($3c2e$) bond.

3.3 Ausgangsfragen, neuester Stand der Forschung / Initial goals, current status of the field

This project is the continuation of TP4 of the first period of funding of the FGLA but with the aim to focus the method of laser induced reactions (LIR) to specific systems of interest in the astrophysical context. Water complexes have been chosen as templates for water ice systems in particular for ice layers on interstellar grains. Although isolated water complexes are not expected to exist in space in high enough concentrations to be observed by present telescopes, it was an important aim of this project to extend the methodology to more complex systems.

In order to evaluate the results of this project it is important to recall the boundary conditions which emerged due to the move of the PI and the apparatus from Chemnitz to Leiden in April 2003 and further to Köln in March 2006. Thanks to the generosity of Dieter Gerlich in supporting the move of the 22-pole ion trap apparatus it was possible to continue the work begun in Chemnitz. Funding of one graduate student (Edouard Hugo, hired in 2004) by DFG allowed to obtain part of the results presented here. In Leiden the group had access to two solid state ice experiments which were also used to record IR spectra of interstellar ice analogues and also to obtain temperature programmed desorption (TPD) spectra of these ices. This work was mostly funded by the Dutch science foundation (NWO). Nevertheless this work is also strongly related to the astrophysical questions of this project. After about one year in Leiden the PI was offered a C3 position in Köln in the astrophysics institute, which was accepted and started in late 2004. In Köln the group has access to a number of new experiments which focus on the high-resolution spectroscopy of molecules of astrophysical interest. In the meantime the 22-pole apparatus was bought from Chemnitz using startup money. In 2005/2006 a new all solid state spectrometer in the 2-3 mm wavelength range (100 GHz) has been build. In addition the OROTRON instrument, the most sensitive 100 GHz spectrometer available worldwide, has been used to obtain spectra of water dimers. As a result of these substantial changes the main direction of the project changed significantly.

In Leiden the main aim was to obtain a first funding of the laboratory group. In order to be successful in the highly competitive dutch system it was mandatory to make use of the free electron laser FELIX in Rijnhuizen/Utrecht as soon as possible. Our beamtime application was successful and the first beamtime was granted in January 2004. At that time we repeated LIR measurements of the C-H stretching vibration of C_2H_2^+ , see below. Most importantly we obtained the first spectra of the ν_5

cis bending vibration of C_2H_2^+ . This was a first low bending vibration spectrum taken with LIR.

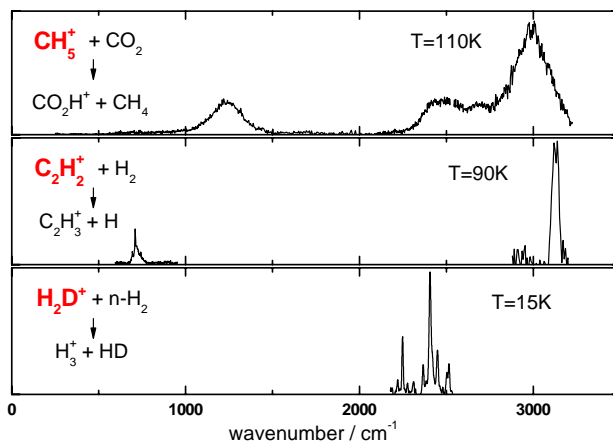


Fig. 1: Summary of the LIR spectra obtained during the funding period. Many details of the spectra are not observable in these broad, low resolution spectra. However the wide spectral range covered by combination of LIR and FELIX is demonstrated in this overview.

In 2003 we proposed two major routes for the application of LIR in order to obtain spectra of water cluster ions. The first route was to find favorable reactions to exchange e.g. a hydrogen for a deuterium in a water cluster ion in order to use isotopic labeling as a detection method. First experiments along these lines have been carried out already in Chemnitz in 2003. Since the reaction of H_3O^+ ($m=19$ u) with HD to form $\text{H}_2\text{DO}^+ + \text{H}_2$ did not proceed ($k < 10^{-15} \text{ cm}^3/\text{s}$) at the low temperatures aimed for, this route had to be discarded. The second route involved the formation of water cluster ions in an external source. A corona discharge nozzle for this approach was available from earlier cluster experiments in the Gerlich group. However, due to the lack of initial funding in Leiden it was impossible to set up a differential pumping stage including a turbo molecular pump with pumping speeds larger than 1000 l/s. Therefore this route could not be followed. Instead, as the LIR experiments with other astrophysically interesting molecules were successful, we decided to continue LIR of those molecules, as was also suggested by the astronomers in Leiden, Köln and by the reviewers of our initial proposal.

As a result of these developments and the successes of LIR we focused on IR spectra of other astrophysically important ions like C_2H_2^+ , CH_5^+ and H_2D^+ . Fig. 1 shows an overview of all the spectra we obtained in the last three years relevant for this report. This project has been imported to the SFB494 in Köln and was positively evaluated. Therefore LIR spectroscopy and dynamics is also funded after the end of the FGLA.

3.4 Angewandte Methoden / Applied methods

Various methods have been used in the project. Storage of ions at variable temperatures in a 22-pole ion trap as described in detail before (e.g., Gerlich 1995) in combination with laser induced reactions (LIR) was the main experimental tool in this project. Further details can be found in earlier work (Schlemmer *et al.* 1999, 2002, 2005b).

Experimental: trapping

Traps have been used for many years to store ions and to study ion-molecule collisions in great detail. Thanks to the invention of higher order multipole traps, mainly developed in the group of Dieter Gerlich (1992), it became possible to study these collisions at energies comparable to those of cold environments in space, in particular dense molecular clouds. In recent years we combined the trapping technique with IR and FIR radiation sources (Schlemmer *et al.* 2002, Asvany *et al.* 2005a, 2005b). As it turns out many reactions of astrophysical interest are substantially enhanced due to internal excitation of the ion. This fact is used in the method of laser induced reactions to obtain (i) spectra of molecular ions and (ii) state specific knowledge of the ion molecule reaction. The method is so sensitive that only ~1000 parent ions are necessary.

Basic concept: LIR

The LIR technique has been developed in the group of Dieter Gerlich. First experiments have been conducted already in Freiburg. In Chemnitz the method was first used in the IR wavelength range. During this project the technique has been extended into the mid-IR and FIR wavelength range, especially thanks to the available of the free electron laser FELIX at FOM Rijnhuizen/Utrecht, which can be tuned from 40 cm^{-1} up to 3200 cm^{-1} .

In short, ions are generated and collected in a storage ion source, mass selected in a quadrupole mass filter and then pulsed into the 22-pole ion trap. On entrance the ions are cooled down to the ambient cryogenic temperature by a short intense helium pulse. During the storage period of several seconds, the ions are subject to reactant gases and tunable laser

light entering one end of the apparatus through the axially transparent setup. The result of this interaction is measured by extracting the stored ion cloud into another mass filter and counting the reaction products in the detector. With this setup, a LIR spectrum of the ions is recorded by counting the products of a suitable ion-molecule reaction as a function of the laser frequency. Some results concerning spectroscopy have been summarized in the book of abstracts of the FGLA meeting in Pillnitz 2005 and have been published recently (Asvany *et al.* 2005a, 2005b, and Schlemmer *et al.* 2006, 2005a, 2005b).

UHV surface science apparatus: CRYOPAD

Thanks to the move to Leiden one UHV apparatus for studies of interstellar ice analogues was available. This machine has been reconstructed and finished during the PI's appointment and became operational in 2004. First results of this experiment have been published recently (van Broekhuizen *et al.* 2006, Öberg *et al.* 2006, Fuchs *et al.* 2006 and Bisschop *et al.* 2006) and will only be described briefly below.

Millimeter – wave spectrometers

In the Köln laboratory spectroscopy group a millimetre-wave intracavity spectrometer (OROTRON) is available for the investigation of pure rotational transitions and internal motions of weakly bound complexes. In this instrument a beam of molecules is intersected with the cavity of a backward wave oscillator (BWO). Due to the intracavity absorption the sensitivity of the instrument is exceptional and allows for the detection of extremely weak or forbidden lines. As a result, very detailed information on the intermolecular potential is available from this experiment.

Also very high-resolution THz spectrometers are used in collaboration with Frank Lewen to investigate low lying vibrations of complex molecules. With the OROTRON instrument particular tunnelling motions of the water dimer are accessible with very high sensitivity. Using some start up money a new all solid state millimetre spectrometer has been built.

3.5 Ergebnisse und ihre Bedeutung / Results and their importance

LIR of small molecules

Based on the successful experiments on C_2H_2^+ another beamtime was granted for January 2005. During this beamtime the most visible success of this project could be achieved, taking a global IR spectrum of pro-

tonated methane, CH_5^+ . The spectrum is shown in Fig. 3. In addition to the high frequency wing of the C-H-stretching motion at 3000 cm^{-1} which has been observed previously by White *et al.* (1999), two lower frequency features extending down to 2300 cm^{-1} have been detected. Furthermore, there is a broad H-C-H bending band centering around 1200 cm^{-1} .

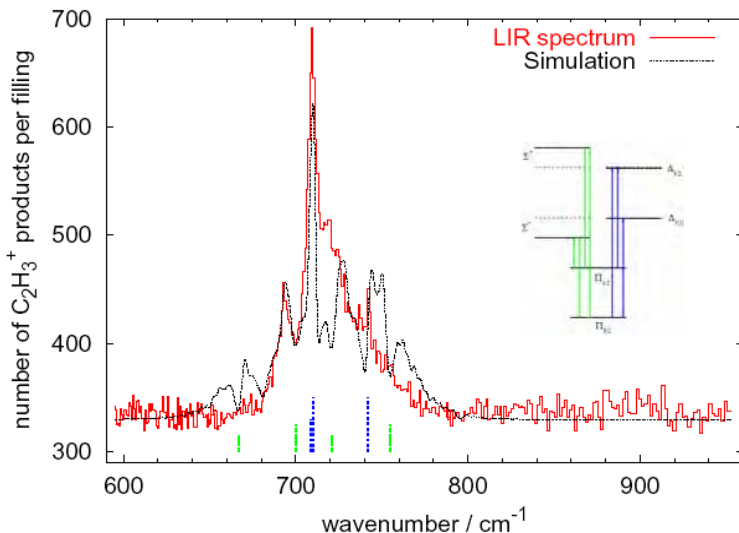


Fig. 2: Spectrum of the ν_5 cis bending vibration of C_2H_2^+

As mentioned above, FELIX has been used for recording the ν_5 cis bending vibration of C_2H_2^+ (Asvany *et al.* 2005a). The recorded spectrum of the number of C_2H_3^+ product ions is displayed in Fig. 2. Both electronic transitions Δ - Π and Σ - Π with their corresponding spin-orbit and Renner-Teller substructure have been observed and have been partly resolved. Using a perturbative analysis, the vibrational frequency and the Renner-Teller parameter have been determined to be $\omega_5=710\text{ cm}^{-1}$ and $\epsilon_5=0.032$. This year a new REMPI work with full rotational resolution on C_2H_2^+ was published by Yang & Mo (2006). They determined $\omega_5=704.1\text{ cm}^{-1}$ and $\epsilon_5=0.019$ which is in good agreement with our results. This example demonstrates that LIR is a competitive technique to REMPI for the study of primary ions provided a high-resolution IR source is available. In contrast REMPI does not work for secondary ions, which can only be formed in a sequence of ionization and reaction. Here LIR is a very sensitive tool for spectroscopy.

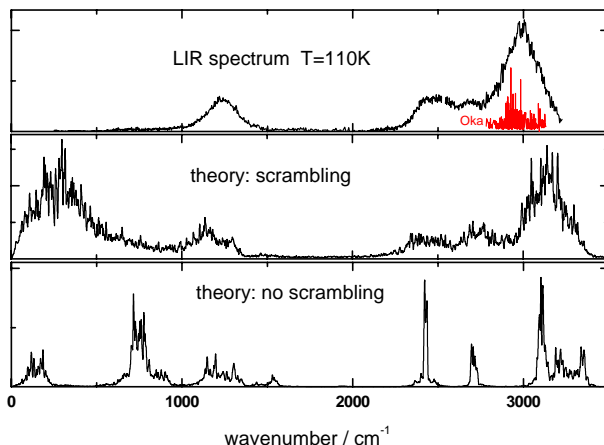


Fig. 3: *Upper panel:* Experimental LIR spectrum of CH_5^+ . The endothermic proton transfer to CO_2 , i.e. detection of HCO_2^+ , is used to monitor the excitation of the CH_5^+ parent molecule. In red the high-resolution study of the Oka group in the C-H stretching region is reproduced for comparison. *Middle and lower panel:* theoretical spectrum calculated at different temperatures, simulating a scrambling and non-scrambling situation in CH_5^+ .

By measuring the dependence of the LIR signal on the neutral number density (here H_2), lifetimes of the excited state have been determined. Fluorescence into the vibrational ground state can be a competitive channel compared to reaction when the radiative lifetime is of the same order of magnitude as the time between collisions. Careful analysis of the complex kinetics reveals the radiative lifetimes for the C-H stretching vibration, $\tau_3 = (3 \pm 1)$ ms, and for the ν_5 cis bending vibration of C_2H_2^+ $\tau_5 = (200 \pm 50)$ ms. Moreover, it turns out that excitation of the stretching vibration is about ten times as efficient to drive hydrogen abstraction as compared to the bending vibration. More details of this study are discussed in Schlemmer *et al.* (2005a). This example shows another time that LIR not only serves as a spectroscopic method, but also reveals characteristic times and rate coefficients of a given collision system. A summary of the current status of the experimental tool of LIR has been described recently (Schlemmer and Asvany 2005b).

Based on the successful experiments on C_2H_2^+ , another beamtime was granted for January 2005. During this beamtime the most visible success of this project could be achieved, taking a global IR spectrum of pro-

tonated methane, CH_5^+ . The spectrum is shown in Fig. 3. In addition to the high-frequency wing of the C-H-stretching motion at 3000 cm^{-1} which has been observed previously by White *et al.* (1999), two lower frequency features extending down to 2300 cm^{-1} have been detected. Furthermore, there is a broad H-C-H bending band centering around 1200 cm^{-1} .

The measurements were complemented by calculations of the IR spectrum at finite temperatures from the Fourier transform of the classical time-autocorrelation function of the total dipole moment. The underlying trajectories were generated by microcanonical *ab initio* molecular dynamics relying on a density functional treatment. As a result of this combined theoretical and experimental effort, CH_5^+ can be considered as a H_2 moiety attached to a CH_3 tripod.



These subunits give rise to different CH-stretching fingerprints. The broad feature around 3000 cm^{-1} is due to stretching within the tripod, while its two low-frequency ‘bumps’ are attributed to stretching involving the H_2 moiety. The broad H-C-H bending feature is predicted by the simulations and confirmed by the LIR measurements. The observed single broad peaks are indicative for the hydrogen scrambling of CH_5^+ . This fluxionality is caused by a low-lying C_{2v} transition state for the scrambling motion, as well as the ease of rotation of the H_2 moiety. A more detailed description of the work in collaboration with the group of Prof. Marx (Bochum) can be found in Asvany *et al.* (2005b). First spectra of deuterated versions of CH_5^+ have been recorded. This study is not completed since during these experiments in January 2006 there was a fire at FELIX, which destroyed part of the free electron laser. Also our trap experiment was affected. Due to the fall out of smoke as a consequence of the fire all electronic devices needed to be cleaned which damaged a considerable fraction of the equipment. In practice it took three months to reconstruct the apparatus such that first experiments with a cold trap could be achieved in June 2006, when the FGLA finished. Despite these difficulties we are very grateful to the brave FELIX team which had to face a much bigger loss. Thanks to their enthusiasm FELIX came into operation

again later this year. Our plans are to continue recording IR spectra of some of the deuterated versions of CH_5^+ , see below.

A third example for IR spectroscopy deals with the astrophysically important H_2D^+ ion. Also during our 2005 beamtime at FELIX first spectra of the fundamental vibrations ν_2 and ν_3 have been recorded (see Fig. 1 lower panel). The endothermic reaction $\text{H}_2\text{D}^+ + \text{H}_2 \Rightarrow \text{H}_3^+ + \text{HD}$ could be substantially enhanced by the ro-vibrational excitation of the H_2D^+ parent ion. In order to record a spectrum the number of H_3^+ ions has been detected as a function of excitation wavelength. While for the fundamental frequencies high-resolution data are available, higher overtone transitions are sparse. The first overtone of ν_2 and combination bands have been studied recently by Farnik *et al.* (2002). In this work, diode lasers covering the range between $6200\text{--}7200\text{ cm}^{-1}$ have been used to record 19 transitions in H_2D^+ and several more transitions in D_2H^+ . Thanks to the very high quality predictions of the transition frequencies by the Tennyson group in London, it was possible to find the transitions.

As has been described earlier (Farnik *et al.* 2002) several levels of H_2D^+ and D_2H^+ can be strongly perturbed by Coriolis and Fermi interactions. Therefore it is practically impossible to predict the line frequencies from effective Hamiltonian models. The *ab initio* methods of Tennyson and co-workers treat the problem more rigorously and therefore any interaction is treated implicitly. In addition the theory includes non-Born-Oppenheimer corrections of the potential energy surface. As a result theoretical predictions are accurate below the 1 cm^{-1} level, i.e. spectroscopic accuracy is achieved. The spectroscopic accuracy of our experiments is below the 0.01 cm^{-1} level and serves therefore as a critical test for theoretical predictions.

Fig. 4 shows a comparison between experiment and theory. In all cases two quanta of the ν_2 bending vibration have been excited. In addition one quantum of each vibration (ν_1 symmetric stretch, ν_2 bending, ν_3 asymmetric stretch) are excited in these modes. Apparently the discrepancy between theory and experiment is largest for the bending vibration. This finding is not unexpected since the current state of the non-BO treatment is based on a diatomic model which comes much closer to a stretching vibration in a polyatomic molecule than a bending vibration. This example shows, that more extensive models have to be developed in order to achieve a better agreement between theory and experiment. While this is certainly possible the question is whether such a calculation would be valuable for any potential application, in particular in an astrophysical environment. Indeed, the calculation of highly excited molecular

species is strongly needed in order to understand the emission curves of stars like our sun which can carry substantial atmospheres and which have surface temperatures which can vary a lot, e.g. due to sun spots (3000 K on the sun) where the temperature of the gas is substantially lower than for the rest of the surface (6000 K). Spectra of such objects are strongly determined by the spectra of highly excited species like H_3^+ , water, methane etc. Because of this situation it is very valuable to test theory which predicts all these lines up to the dissociation level and above.

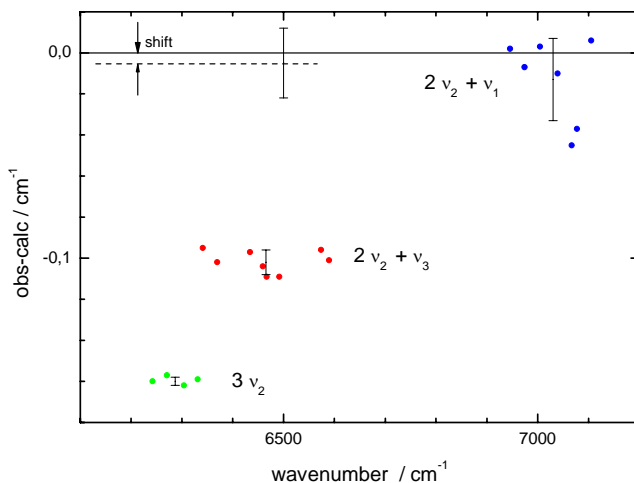


Fig. 4: Comparison of the observed to the calculated transition frequencies of second overtone vibrations for H_2D^+ . Discrepancies between theory and experiment are below 0.15 cm^{-1} , which is exceptional for a polyatomic species. Significant differences are found with respect to the different vibrational motions. The observed tendency hints at limitations of the present day non-Born Oppenheimer treatment (see text).

It is gratifying to see that present day theory compares rather well with experiment. Including more sophisticated non-BO treatments for such light systems as mentioned above will help to reach similar accuracies for even higher levels of excitation. A joint publication with J. Tenynson is in preparation.

From an experimental point of view the LIR intensities from the H_2D^+ experiments can be used to determine the rotational state distribu-

tion of the cold H_2D^+ . It will be described in section 3.6 how such measurements can be used to understand the deuterium fractionation in the most fundamental reaction: $\text{H}_3^+ + \text{HD} \Rightarrow \text{H}_2\text{D}^+ + \text{H}_2$. This work is continued within SFB494 project E4.

The role of deuterium fractionation of small molecular ions has been studied in this project without the use of laser excitation. Measurements on the temperature dependence of the proton transfer reaction $\text{CH}_5^+ + \text{CO}_2 \Rightarrow \text{HCO}_2^+ + \text{CH}_4$ have been carried out. Fig. 5 shows one example of a trap experiment at 294 K. From this measurement a rate coefficient of some $6 \times 10^{-11} \text{ cm}^3/\text{s}$ has been derived. This small value drops for lower temperatures in an Arrhenius type behaviour. From the slope of the Arrhenius curve an activation energy of $(542 \pm 30) \text{ cm}^{-1}$, corresponding to $(6.5 \pm 0.4) \text{ kJ/mol}$, has been determined. This value is more than a factor of two larger than the difference in proton affinities of methane (540.5 kJ/mol) and CO_2 (543.5 kJ/mol) as recommended by the NIST chemistry webbook.

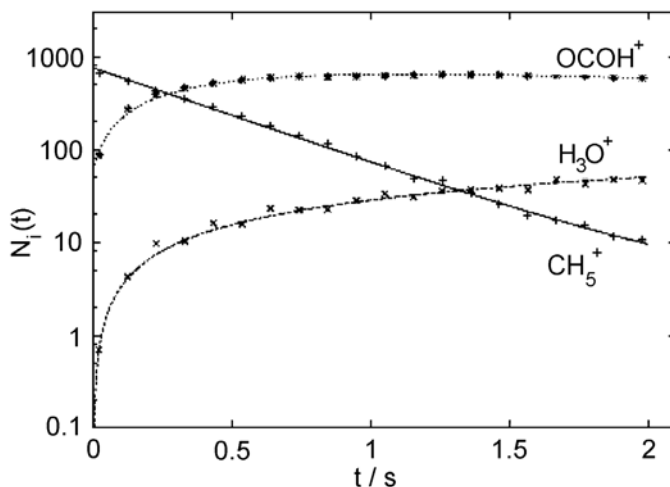


Fig. 5: Number of various ions, N_i as a function of storage time t at $T = 294 \text{ K}$. Determination of the rate coefficient for proton transfer from The injected CH_5^+ react with CO_2 . In the simulation (solid lines) the exothermic proton transfer to the H_2O background is accounted for.

In Chemnitz the equilibrium rate coefficient has been determined rather carefully in a trap experiment where an equilibrium between CH_5^+ and HCO_2^+ has been established. Also these experiments have been carried out as a function of temperature. From the temperature dependence

of the equilibrium rate coefficient the difference in proton affinity has been determined to be (7.1 ± 0.5) kJ/mol. This value is in much better agreement with our value for the activation barrier than with the literature value for the PA difference. Therefore it might be safe to assume that the proton transfer reaction is endothermic but without an additional barrier.

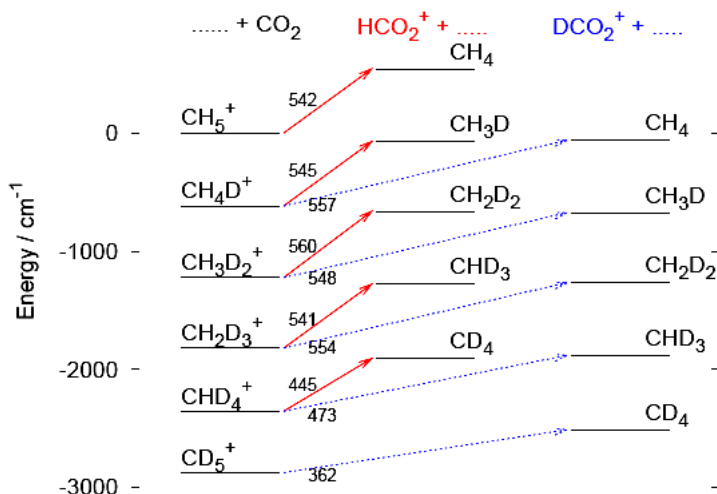


Fig. 6: Energetics for the proton / deuteron transfer from methane to CO_2 for different isotopologues. The activation energy for the fully hydrogenated case has been adopted from this work, 542 cm^{-1} . All ZPE differences are taken from spectroscopic data (methane in all isotopic forms) and theoretical predictions (HCO_2^+ , DCO_2^+ and CH_5^+ in all isotopic forms).

More activation energies have been determined for the proton transfer reaction of CH_5^+ , CD_4H^+ and CD_5^+ in collision with CO_2 . Proton transfer becomes less endothermic for the deuterated versions of CH_5^+ . According to the picture of a barrierless but endothermic reaction this behavior is due to the differences in zero point vibrational energies of the corresponding reactants and products (ZPE). Since the ZPE is rather well known for methane and its isotopologues the observed differences can be related to the differences in ZPE of protonated methane and protonated CO_2 . Calculated values for the ZPEs are available for all species. The combined experimental (difference in PA) and theoretical (ZPEs) energetics of the reactions considered are displayed in Fig. 6. Differences between measured and calculated activation energies are found for the deuterated proton transfer reactions. Lower experimental values hint at smaller ZPE differences in CH_5^+ , CD_4H^+ and CD_5^+ than predicted. As a

result trap experiments can serve as a quantitative test for state-of-the-art theory predicting potential energy surfaces (PES) and ZPEs. A joint publication between the Chemnitz group (D. Gerlich, A. Luca, and H.-J. Deyerl) and the Köln group (O. Asvany, E. Hugo and S. Schlemmer) is in preparation.

Interstellar ices

In Leiden the focus of the laboratory work lies on experimental investigations of interstellar ices. A wide variety of IR spectra of ices of mixed and layered ices are available as a database (<http://www.strw.leidenuniv.nl/~lab/databases/>). The focus of these data lies on the main molecular species in interstellar ices.

In recent years the “match and mix” approach to reproduce the observed spectra from ISO and presently from the Spitzer satellite telescope is changed for more fundamental experiments, trying to understand the underlying mechanisms. For this purpose two surface science apparatus operating at UHV conditions have been built over the last six years. CRYOPAD, the CRYOgenic Photoproduct Analysis Device, became operational in 2004. The first work concentrated on the quantitative determination of binding energies of molecules in ice in order to understand the freeze out of important constituents like CO and N₂. In many astronomical sources CO has been observed to be frozen out while N₂, which is traced by N₂H⁺, is not (e.g. Bergin & Langer 1997). Fig. 7 shows the possible scenarios of ice compositions. As molecules freeze out at different temperatures, layered ices are expected to play an important role. However, heating processes can lead to mixed ices. Both situations are associated with different desorption behaviors which have been studied in great detail in the last two years in the Leiden laboratory. Desorption rates and sticking coefficients for CO and N₂ interstellar ices have been determined by Öberg *et al.* (2005) and later in even greater detail by Bisschop *et al.* (2006). The relative difference between the CO and N₂ binding energies as derived from these experiments is significantly less than that currently adopted in astrochemical models. Detailed infrared spectroscopy studies of solid CO-CO₂ mixtures and layers have been carried out by van Broekhuizen *et al.* (2006).

These studies of interstellar ice analogues are continued by the new head of the laboratory group in Leiden, Harold Linnartz. The ultimate goal is to understand the formation mechanisms of more complex molecules which cannot be formed in gas phase processes in large enough quantities to explain observations. One chemical route concerns hydrogenation of CO which is believed to be the main route to the formation of

interstellar methanol. Due to the new Spitzer telescope, ices are studied via their main IR bands. Very detailed measurements reveal nowadays maps of solid ices. The Leiden observatory group lead by Ewine van Dishoeck is pushing the frontiers toward this direction, see for example: *Origin and evolution of ices in star forming regions: A VLT-ISAAC 3-5 micron spectroscopic survey* (van Dishoeck *et al.* 2003). Like for the gas phase molecules maps of the ices show the physical and chemical structure of star forming regions. The Köln spectroscopy group will also in the future concentrate on the detection of gas phase molecules, irrespective whether formed in gas phase processes, or on grains, or in icy mantles and desorbing, or even undergoing gas phase reactions after desorption from grains.

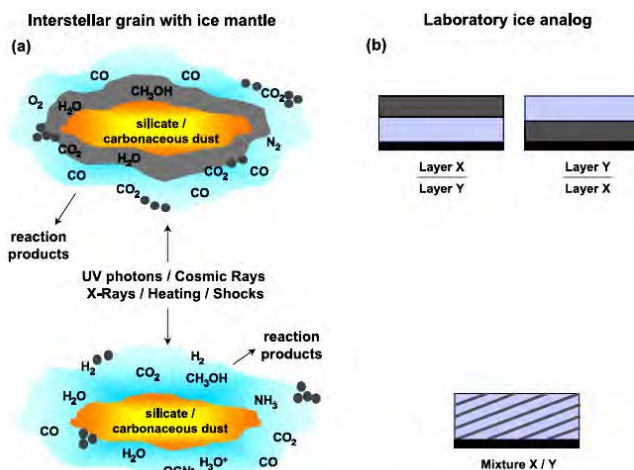


Fig. 7: (a) Two schematic models of the structure of an interstellar ice mantle, (top) formed due to the condensation of gases, thermal distillation or via surface reactions, and (bottom) formed as a result of thermally induced diffusion and chemical reactions induced in the bulk of the ice mantle. Reaction products that may desorb in the process of formation, or due to thermal warming of the ice are indicated. (b) Two schematics of a simulated interstellar ice mantle under laboratory conditions showing a layered (top) and a mixed (bottom) ice analogue composed of molecules X and Y. They are used as models for more complex situations potentially found in space.

3.6 Zusammenfassung und Ausblick / Summary and future

Zusammenfassung / Summary

Thanks to the funding within the FGLA it was possible to develop LIR into a mature technique for IR and FIR spectroscopy of molecular ions. C_2H_2^+ , CH_5^+ and H_2D^+ have been explored quite intensively. In all three cases new spectral features or new ro-vibrational lines have been detected. Comparison to theoretical work on these important examples helped to improve our understanding on the molecular structure (CH_5^+) the intramolecular potential (H_2D^+) and couplings between the electronic and vibrational motion of a molecule (C_2H_2^+). Applying LIR to water cluster ions was unsuccessful. Alternative routes of LIR, e.g. unimolecular decomposition, have not yet been tried because of the lack of a differential pumping stage.

Ausblick / future

Based on the present LIR work several new directions are a natural extension of this interesting method:

- Combination of LIR with millimetre and submillimetre radiation should make it possible to record pure rotational spectra of molecular ions. Direct rotational excitation of H_2D^+ has been tested with the help of FELIX, which can be tuned from 40 cm^{-1} up to 3200 cm^{-1} . 100 cm^{-1} of extra rotational energy should be sufficient to drive the hydrogenation reaction in collisions with H_2 . However, first tests at FELIX did not yield any LIR signal. This might be due to efficient rotationally inelastic collisions. Unfortunately these studies were interrupted by the fire at FELIX early in 2006. Another route towards this direction is to diminish the LIR signal of a particular IR transition by rotational pumping of the ground state. This method should work very well at low temperatures when only few states are populated. Therefore H_2D^+ is a very good candidate for this method. It is planned to use higher overtone transitions from a $1.4\text{ }\mu\text{m}$ laser for the probing and FELIX for a pure rotational excitation. High resolution sources in the THz range are available in Köln and could open this very interesting field. For H_2D^+ the rotational spectrum is rather well known. However, for the interesting CH_2D^+ molecule this is not the case. For a complex molecule like CH_5^+ such a scheme is probably much more difficult to apply due to the more crowded spectrum. Nevertheless this method appears as one of the promising methods to unravel the structure of CH_5^+ in greater detail.

- H_5^+ is the important intermediate molecule in collisions of H_3^+ with H_2 . Understanding the structure of this molecule and in particular of its isotopologues poses a very critical test to state-of-the-art theory. Recently this system has attracted great attention by a number of theoretical groups (Bowman and McCoy, see e.g. Xie *et al.* 2005). Experiments along these lines are still missing except for the early low resolution study by Okumura *et al.* (1988). H_5^+ has to be formed in a high pressure discharge source as was missing for the current project. An alternative is to produce the cluster in the trap prior to LIR experiments. This approach would call for a non-destructive, *in-situ* mass separation. Several techniques can be considered. Mass selective excitation like in ICR apparatus is one option. Another method concerns the superposition of a quadrupolar field of a mass selector with the high order multipole field of a low temperature trap. A third choice is a split trap consisting of a mass selective and a trapping part which could be accessed alternatively by applying appropriate DC potentials. Much engineering development has to be put in the design of an operating trap.
- Other molecules of astrophysical interest can be explored using LIR. Among these belongs C_3H^+ .
- LIR is an important method to reveal information on the efficiency of inelastic and reactive collisions as well as radiative processes. In order to exploit this in a more quantitative way, the LIR signal has to be analysed very carefully. For this it is essential that the LIR signals are reproducible to rather high levels of accuracy. This requires not only stable trapping conditions but also stable laser sources for the excitation. Current experiments with H_2D^+ show that reliable relative Einstein B-coefficients can be determined when LIR starts from the same ground state level. A full simulation of the LIR experiments finally allows the determination of reliable rotational state populations. In case of H_2D^+ the ratio of ortho to para hydrogen plays a crucial role for the rotational population. At laser powers above several mW many transitions can be saturated. As a consequence depletion sets in for the limited number of parent ions. This can be seen when comparing measurements to full simulations. As a result rate coefficients for inelastic processes (rotation, fine structure, hyperfine structure and nuclear spin) can be derived. First results for H_2D^+ show that rotationally inelastic processes in the vibrational ground state are much less efficient than anticipated. Very systematic studies along these lines will reveal a detailed insight into the possible fates of ion-molecule collisions.

Several of the discussed options for LIR are currently developed in the existing 22-pole trap apparatus in order to form the basis for new scientific aims.

3.7 Literatur / References

- Asvany, O., Giesen, T., Redlich, B. and Schlemmer, S., *Laser Induced Reaction: the antisymmetric bending vibration of $C_2H_2^+$* , Physical Review Letters, **94** (2005a), 073001.
- Asvany, O., Kumar, P., Hegemann, I., Redlich, B., Schlemmer, S., and Marx, D., *Understanding the LIR Infrared Spectrum of Bare CH_5^+* , SCIENCE **309**, (2005b) 1219-1222.
- Bergin, E. A., & Langer, W. D., *Chemical evolution in preprotostellar and protostellar cores*, ApJ, **486**, (1997) 316
- Bisschop, S.E., Fraser, H.J., Öberg, K. I., van Dishoeck, E., and Schlemmer, S., *Desorption Rates and Sticking Coefficients for CO and N2 Interstellar Ices* Astronomy & Astrophysics, **449**, (2006) 1297-1309.
- Endres, E., Müller, H.S.P., Brünken, S., Paveliev, D.G., Giesen, T., Schlemmer, S. and Lewen, F., *High resolution rotation-inversion spectroscopy on doubly deuterated ammonia, ND_2H up to 2.6THz*, Journal of Molecular Structure, **795**, (2006) 244-252.
- Farnik, M., Davis, S., Kostin, M.A., Polyansky, O.L., Tennyson, J. and Nesbitt, D., *Beyond the Born-Oppenheimer approximation: High-resolution overtone spectroscopy of H_2D^+ and D_2H^+* J. Chem. Phys., **116** (2002) 6146–6158.
- Gerlich, D.: *Inhomogeneous Electrical Radio Frequency Fields: A Versatile Tool for the Study of Processes with Slow Ions*. Adv. in Chem. Phys., **LXXXII**, (1992) 1 - 176.
- Gerlich, D., *Ion-Neutral Collisions in a 22-pole trap at very low energies*, Physica Scripta, **T59** (1995) 256 - 263.
- Gerlich, D., Herbst, E., Roueff, E., *Low-temperature laboratory measurements and interstellar implications* Planetary and Space Science, **50** (2002) 1275.
- Jacox, M. E., *Infrared spectra of $HOCO^+$ and of the complex of H-2 with CO_2 -trapped in solid neon* JCP **119** (2003) 10824.
- Jacox, M.E., *vibrational and electronic energy levels of polyatomic transient molecules* J. Phys. Chem. Ref. Data, Monograph No.3, (1994)
- Jin, Z., Braams, B.J., and Bowman, J.M., *Dissociated potential energy surface of CH_5^+* J.Phys. Chem. A **110** (2006) 1569.
- Kreckel, H., J. Mikosch, R. Wester, J. Glosik, R. Plasil, M. Motsch, D. Gerlich, D. Schwalm, D. Zajfman and A. Wolf: *Towards state selective measurements of the H_3^+ dissociative recombination rate coefficient*, Journal of Physics: Conference Series **4** (2005a) 126 - 133.
- Lee, T. J. and Schaefer, H. F., J. Chem. Phys. **85** (1986) 3437, Lee, T. J., Rice, J.E., and Schaefer, H. F., *ibid.* **86** (1987) 3051.
- Mikosch, J., Kreckel, H., Plasil, R., Gerlich, D., Glosik, J., Schwalm, D., Wolf, A.: *Action spectroscopy and temperature diagnostics of H_3^+ by chemical probing*, J. Chem. Phys., **121** (2004) 11030 - 11037.

- Öberg, K. I., van Broekhuizen, F., Fraser, H., Bisschop, S. E., van Dishoeck, E., and Schlemmer, S., *Competition between CO and N₂ Desorption from Interstellar Ices*, The Astrophysical Journal, **621** (2005) L33-L36.
- Okumura, M., Yeh, L.I., Lee, Y.T., *Infrared spectroscopy of the cluster ions H₃⁺.(H₂)_n* J.Chem.Phys. **83** (1988) 79-91.
- Schlemmer, S., Kuhn, T., Lescop, E., Gerlich, D., *Laser excited N₂⁺ in a 22-Pole trap, Experimental Studies of Rotational Relaxation processes* Int. J. Mass Spectrom., **185** (1999) 589.
- Schlemmer, S., Lescop, E., v. Richthofen, J., Gerlich, D. and Smith, M.A., *Laser Induced Reactions in a 22-Pole Ion Trap: C₂H₂⁺ + hv₃ + H₂ → C₂H₃⁺ + H*, J. Chem. Phys., **117** (2002) 2068.
- Schlemmer, S., Asvany, O., and Giesen, T., *Comparison of the cis-bending and C-H stretching vibration on the reaction of C₂H₂⁺ with H₂ using laser induced reactions*, Phys. Chem. Chem. Phys. **7** (2005a) 1592-1600.
- Schlemmer, S., and Asvany, O., *Laser induced Reactions in a 22-pole ion trap*, Journal of Physics: Conf. Ser. **4** (2005b) 134-141.
- Schlemmer, S., Asvany, O., Hugo, E. and Gerlich, D., *Deuterium Fractionation and Ion-Molecule Reactions at low Temperatures*, in Proceedings of the 231st IAU Symposium, D.Lis, G.A. Blake, and E. Herbst (eds.), Cambridge University Press, 2006.
- Surin, L.A., Potapov, A.V., Müller, H.S.P., Panfilov, V.A., Dumesh, B.S., Giesen, T.F. and Schlemmer, S., *Millimeter-wave study of the CO-N₂ van der Waals complex: new measurements of CO-orthoN₂ and assignments of new states of CO-paraN₂*, Journal of Molecular Structure, **795** (2006) 198-208.
- van Broekhuizen, F., Groot, I.M.N., Fraser, H.J., van Dishoeck, E. and Schlemmer, S., *Infrared spectroscopy of solid CO-CO₂ mixtures and layers*, Astronomy & Astrophysics, **451** (2006) 723-731.
- Xie, Z., Braams, B.J., Bowman, J., *Ab initio global potential-energy surface for H₃⁺ → H₃⁺ + H₂* J. Chem. Phys. **122** (2005) 224307.

3.1 Bericht Teilprojekt 5

3.1.1 Titel / Title

*Reaktionen von gespeicherten kalten Ionen mit H Atomen
und interstellar relevanten Molekülen*

*Reactions of stored cold ions with H atoms and molecules of
interstellar relevance*

3.1.2 Berichtszeitraum / reported period

01.07.2003 - 31.12.2006

3.1.3 Projektleiter / principle investigator

Gerlich, Dieter, Prof. Dr., Dipl.-Phys., Universitätsprofessor
Institut für Physik, Technische Universität, 09107 Chemnitz

Luca, Alfonz, Dr., wiss. Assistent
Institut für Physik, Technische Universität, 09107 Chemnitz

3.2 Zusammenfassung / Abstract

3.2.1 Wortlaut des Antrags / abstract of the proposal

Für viele **Gasphasenreaktionen** zwischen Ionen und Neutralen ist nach wie vor unbekannt, ob und wie schnell sie **bei tiefen Temperaturen** ablaufen, vor allem wenn es sich einerseits um Radikale wie z.B. das H-Atom oder andererseits um astrochemisch wichtige Moleküle wie CO, CO₂ oder H₂O handelt. Um die Wechselwirkung solcher Reaktanten mit gespeicherten Ionen zu untersuchen, wird in diesem Projekt die Multipol-speicherapparatur AB-22PT eingesetzt, die alternativ mit einem Atom- oder einem Düsenstrahl kombiniert werden kann. Typische Stoßpartner für die H-Atome werden Ionen von CH⁺ bis C_nH_m⁺ sein. Es soll auch untersucht werden, unter welchen Bedingungen das H-Atom einfach "stecken" bleibt, d.h. die Lebensdauer des Stoßkomplexes so lang ist, dass er sich durch Emission von Strahlung stabilisiert. Im Rahmen solcher Messungen wird auch nach Molekülen XY⁺ gesucht, die über eine sequentiell-

le Absorption von zwei H-Atomen **katalytisch H_2** produzieren. Eine wichtige, experimentell unbekannte Reaktionsklasse, die ebenfalls untersucht werden soll, ist die ein- bzw. mehrfache **Isotopenanreicherung** bei Stößen von Ionen wie H_3^+ , C_nH_m^+ oder NH_n^+ mit D-Atomen. Ein weiterer Schwerpunkt der Experimente wird die **Strahlungsassoziation** von Ionen mit kondensierbaren Gasen sein. Von diesem Prozeß nimmt man an, dass er eine dominante Rolle bei der Bildung größerer Moleküle in dichten interstellaren Wolken spielt. Dazu wurden erste Ergebnisse mit der AB-22PT Apparatur erhalten. Die Bildung von protoniertem Methanol beim Stoß von CH_3^+ mit H_2O ist deutlich unwahrscheinlicher als bisher in den chemischen Modellen angenommen. Weitere Untersuchungen zur Wechselwirkung von CH_3^+ mit CO, HCN und CH_3OH oder von H_3O^+ mit C_2H_2 und H_2O sind geplant.

For many **gas phase reactions** between ions and neutrals it is still unknown whether at all and how fast they proceed **at low temperatures**, especially when the targets are radicals such as H-atoms or astrochemically important molecules such as CO, CO_2 or H_2O . In order to study the interaction of such reactants with stored ions, a 22-pole ion trap apparatus (AB-22PT) is used in this project, which can be combined with an effusive beam of slow atoms or a supersonic beam of molecules. Typical collision partners for the H-atoms are hydrocarbon ions ranging from CH^+ to larger C_nH_m^+ . One (still) unsolved question is under which conditions an H-atom just "sticks", i.e., when the lifetime of the collision complex is so long that emission of radiation leads to its stabilization. In this context also molecules XY^+ are searched for, which may produce **H_2** in a **catalytic cycle** via sequential absorption of two H-atoms. An important experimentally unknown class of reactions, which also will be studied, is single or multiple **isotope enrichment** in collisions of ions such as H_3^+ , C_nH_m^+ or NH_n^+ with D-atoms. Another subject of the project is **radiative association** of ions with condensable molecules. This process is assumed to be of significance for the formation of larger molecules in dense interstellar clouds. Results for the formation of protonated methanol in collisions of CH_3^+ with H_2O have been obtained and the rate coefficient is significantly smaller than assumed until now. Further systems include the interaction of CH_3^+ with CO, HCN and CH_3OH or reactions of H_3O^+ with C_2H_2 and H_2O .

3.2.2 Zusammenfassung des Berichts / abstract of the report

One of the aims of the *FGLA* was to simulate in the laboratory astrochemical gas phase processes occurring under inter or circumstellar conditions. In TP 5 a rather complicated ultrahigh vacuum apparatus has been developed and characterized which allows to study collisions between cold ions confined in a trap and a neutral beam of atoms, molecules or radicals traversing the trapped ion cloud with a controllable velocity distribution. Special attention has been given to the interaction of H and D atoms with simple molecular ions at temperatures down to 10 K; however, also first experiments with condensable targets have been started.

This report describes briefly the present status of the complex molecular beam - ion trap machine with emphasis on the progress made with the integration of the hydrogen atom beam. This new instrument has been used for measuring rate coefficients for a variety of ions colliding with H- or D-atoms. A general observation is that, in the case of hydrocarbons, collisions with H₂ generally lead to hydrogenation while collisions with H atoms often cause dehydrogenation. Recent models of cold clouds have revealed the importance of deuteration of molecules. Therefore more weight than originally planned has been put onto H - D exchange reactions using deuterium in the discharge source.

Initially it was planned to reach a technical level which allows to operate the machine as a flexible user facility. This goal included not only two traps for gas phase and nanoparticle work, but also several beams of neutral radicals and molecules. Such a universal experimental setup would have allowed to study many different systems, especially with the help and initiatives from guest researchers. In several test arrangements, the potential of the combination of individual modules has been demonstrated. For example, a pulsed supersonic H₂O beam was successfully used for producing protonated methanol from CH₃⁺ via association. However, the last years have shown that much more engineering work and another scientific environment would have been necessary for getting the required technical reliability of achieving the aims of the ambitious research plan. In order to continue all the initiatives started in the *FGLA*, several new collaborative projects have been started. They are mentioned in the outlook. In Tucson, for example, the construction of the next generation of trapping apparatus for astrochemical applications is under construction, supported by an NSF grant.

3.3 Ausgangsfragen, neuester Stand der Forschung / Initial goals, current status of the field

Hydrogen is the most abundant baryonic species in the universe. Therefore, many astrophysical and -chemical processes involve H and H₂. For improving our quantitative understanding of gas phase and surface mediated processes with H radicals, the initial proposal of TP 5 contained an ambitious experimental program. Since both gas phase processes and grain surfaces play a central role in the chemistry of cold clouds, it was planned to construct a versatile atomic or molecular beam machine and to utilize alternatively two modules, a temperature variable 22pole trap and a quadrupole trap for charged nanoparticles.

The research program was quite ambitious as well. One class of astrochemically relevant reactions involves just three atoms in total, e.g., AH⁺ + H or AB⁺ + H. Such systems are simple enough that theoretical methods are capable, at least in principle, to predict reactive cross sections from first principles including all degrees of freedom. The very basic collision system H₂⁺ + H has not yet been studied because of parasitic reactions with the H₂ background. Another class of reactions refers to polyatomic systems such as CH₅⁺ + H, C₂H₃⁺ + H, C₃H₂⁺ + H. Basic questions included the role of small barriers in low temperature ion molecule reactions, radiative and ternary association, cyclic and linear isomers, etc. A specific project was the search for complex molecular ions, XY⁺, which allow for an efficient catalytic production of H₂ molecules via two sequential association processes, i.e., XY⁺ + H → XYH⁺ + H → XY⁺ + H₂. Finally, deuterium fractionation via collisions with D atoms became an additional weight in the research program. The importance of deuterium enrichment in hydrogen bearing molecules has been discussed for example by Gerlich *et al.* (2002). So far interesting results have been obtained for XH⁺ + D → XD⁺ + H with X=C and CH₄.

As already outlined in the original proposal, there have been very few experiments studying the interaction between ions and H or D atoms under conditions relevant for astrochemistry. The early ICR studies and those using the SIFT technique have been operated at 300 K or at higher effective temperatures. In gas phase studies, the overall situation has not changed in the last years, while there have been many theoretical and experimental activities aiming at understanding interactions of H atoms with surfaces and ice layers. To our knowledge, there is, besides ours, no low temperatures ion chemistry experiment involving hydrogen atoms. One gas phase result, the interaction of C_n⁻ or C_nH⁻ anions with H, has been reported from the Boulder ion group (Barckholtz *et al.* 2001). Another

related activity are beam experiments with H atoms, excited to Rydberg states. A joint study has on the state-to-state dynamics of high- n Rydberg H-atom scattering with D₂ has been published recently (Dai *et al.* 2005, Song *et al.* 2005).

Originally it was thought, that a special quadrupole trap for confining and monitoring single nanoparticles could be used in the TP 5 beam machine in exchange with the 22PT. The initial progress (Schlemmer *et al.* 2001, Gerlich 2003) made in our laboratory with the development of the *ultra high precision nanoparticle mass spectrometry* method has stimulated this optimistic planning. Unfortunately the technical and personal reality forced us to cancel this part of TP 5. Nonetheless it is certain (Schlemmer *et al.* 2004) that this experimental method is well-suited for measuring adsorption and desorption of hydrogen atoms on nano-surfaces or to study catalytic formation of H₂ molecules on interstellar grain analogues. An other innovative application is described in the report of TP 7. Some aspects of the state of the art of the nanoparticle trapping method is described in a few recent publications dealing with (i) the determination of light induced forces on isolated micron-size dust particles confined in an electrodynamic trap (Krau and Wurm 2004), (ii) photoelectric emission measurements on the analogs of individual cosmic dust grains (Abbas *et al.* 2006), and (iii) the observation of charging mechanisms of trapped nanoparticles which have been exposed to soft X-rays (Grimm *et al.* 2006).

3.4 Angewandte Methoden / Applied methods

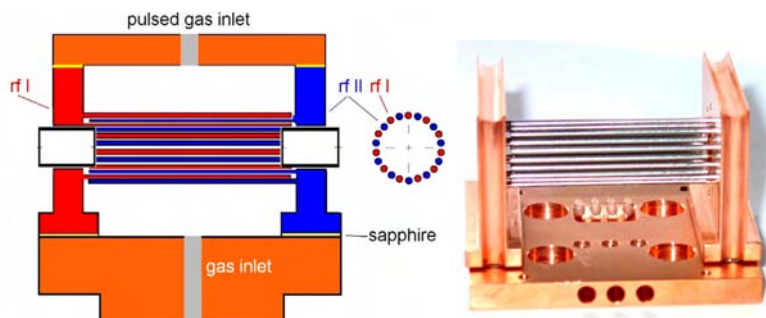


Fig. 1: The 22pole trap shown here has been first described in (Gerlich 1995). Today it is used worldwide in at least eight machines for buffer gas cooling of molecular ions for spectroscopy and reaction dynamics.

Most experiments, performed in TP 4, TP 5 and TP 7 use innovative tools which are based on radio frequency ion guides and traps (Gerlich 1992). The very sensitive instruments allow not only to perform unique fundamental studies of ion-molecule reactions with an unprecedented sensitivity but have also important applications in mass spectroscopy (Gerlich 2003a), chemical analysis (Gerlich 2004), ion spectroscopy (Dzhonson *et al.* 2006, see also TP 4) and nanoparticle research (Grimm *et al.* 2006). One very important module, the 22pole trap, is shown in Fig. 1. Further details of the method, references and its applications in laboratory astrochemistry have been summarized recently (Gerlich and Smith 2006a).

3.4.1 The AB-22PT machine

The Atomic Beam 22-Pole Trap Apparatus (AB-22PT) developed in this project, combines various modules for producing primary ions and neutral reactants with the components from a standard 22pole trapping machine (Gerlich 1995). One version is shown schematically in Fig. 2. A progress report on some technical details and its applications has been presented recently (Luca *et al.* 2005). Since 22PT based machines have been described thoroughly in the literature (see also TP 4) and since many details of the final version will be given in a separate publication (Luca *et al.* 2007) only a few remarks characterizing of the H-atom beam are made here.

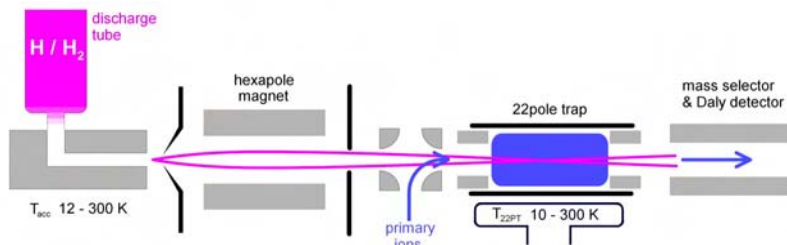


Fig. 2: Schematic view of the combination of a temperature variable (10 - 300 K) 22pole trap with an H-atom beam, focused by an hexapole magnet. Primary ions which are created and mass selected in a part of the machine not shown in the figure, are injected into the trap via an electrostatic quadrupole bender. After a variable storage time in the trap all ions are extracted for mass analysis and detection.

During the thesis work of G. Borodi (2007a) a lot of important additions, modifications and improvements have been made on the

AB-22PT machine. More recent progress is due to the graduate student C. Mogo. One of the central technical activities of the last years was the construction of a modular and flexible H atom source and its characterization. The requirements included large flux of atoms, high degree of dissociation, low H_2 background, and slow velocities.

There are many publications describing the creation of H-atoms by dissociation of H_2 molecules using either sufficiently hot filaments or discharges (radio-frequency, microwave). In the present work a standard rf driven plasma source is used. The literature also contains several recipes and tricks for getting dissociation degrees up to 95%. In addition to specific procedures to prepare the surface of the discharge tube and suitable localization of the rf power close to the exit, small amounts of oxygen or water have been added successfully to the purified hydrogen or deuterium. During our tests, G. Borodi has developed a very efficient method to decrease the H-H recombination rate on the walls by coating them with a well-defined amount of water (Borodi 2007a). First results have been presented in 2005 during the Pillnitz meeting, a summary is included in (Luca *et al.* 2007). It is planned to study the specific surface effects which are also of astrophysical interest, in more detail in a specific test arrangement (Borodi, private communication).

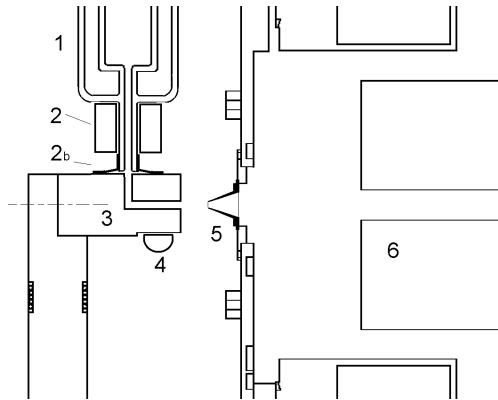


Fig. 3: H-atom source with discharge tube (1), precooling to 100 K (2) and temperature gap (2b). The accommodator (3) cools the atoms to the final temperature determined with a Si temperature sensor (4). A 2 mm \varnothing skimmer (5) separates first chamber (pumping speed for deuterium 2800 l/s) from the second one containing the first hexapole magnet (6).

For slowing down the H atoms emerging from the hot discharge to velocities which are representative for the low temperatures prevailing in

the ISM, cryogenic cooling has been used. As indicated in Fig. 3, the hydrogen atoms pass first through a glass tube surrounded by a precooling (2) followed by a copper piece (3) the temperature of which can be set at values between $T_{acc} = 12$ K - 300 K. For avoiding recombination it is important that the temperature changes in a very narrow gap (2b) from the 100 K of the precooling to the final temperature of the copper piece. The optimum geometry is still searched for.

The effusive beam is skimmed and passes another aperture. All three regions are pumped rather efficiently; nonetheless, the background density of H_2 in the trap is still comparable to that of H. A beam catcher and additional cryo-pumping could reduce this problem. Two hexapole magnets (6) are used for confining those atoms which are in weak field searching states.

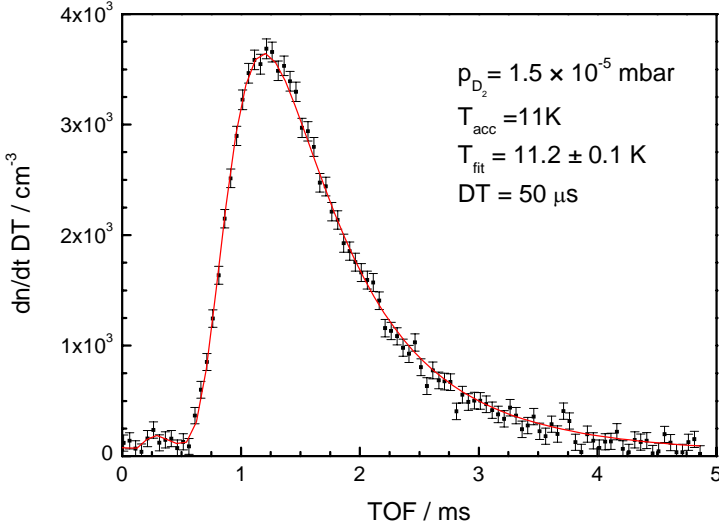


Fig. 4: Measured and simulated TOF distribution of an effusive D_2 beam coming from a $T_{acc} = 11$ K cold accommodator. P_{D_2} is the deuterium pressure in the first chamber, the pressure in the source (3) is several hundred times larger. The red line is a M-B distribution calculated for $T_{fit} = 11.2$ K.

The number density of H atoms and the H_2 background in the interaction region has been determined by replacing the 22PT with a calibrated universal detector which is based on electron bombardment ionization followed by mass selection and ion counting. At $T_{acc} = 100$ K, typical H and H_2 densities are some 10^8 cm^{-3} if one operates the discharge at

typically 0.03 mbar. Insertion of the hexapole magnets enhances the atomic signal by a factor 25 at 60 K.

At the lowest temperature, $T_{acc} = 12$ K, the H atom density drops to $2 \times 10^8 \text{ cm}^{-3}$. Due to the sensitivity of the trapping method, this is sufficient to measure rate coefficients down to $10^{-12} \text{ cm}^3 \text{ s}^{-1}$. One advantage to operate the 22PT at 10 K is that condensation of H_2 on the walls reduces the H_2 background to a much lower value, $5 \times 10^7 \text{ cm}^{-3}$.

In order to test the efficiency of the accommodator, velocity distributions have been measured using the universal detector in combination with a chopper wheel. The example shown in Fig. 4. has been taken at $T_{acc} = 11$ K for D_2 molecules (discharge switched off). The comparison of the data with a Maxwell–Boltzmann distribution, calculated for an effusive beam with $T_{fit} = 11.2$ K, reveals that there are enough wall collisions in the channel (1.2 mm diameter and 22 mm length) to thermalize the molecules.

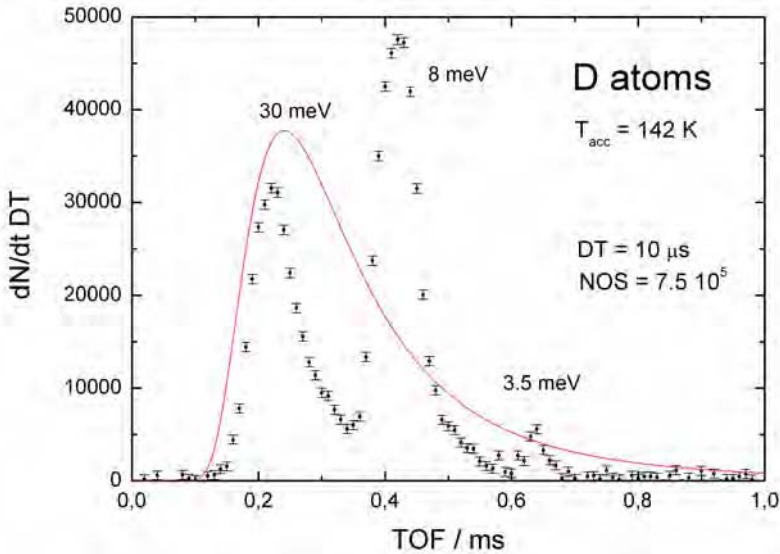


Fig. 5: TOF distributions of D atoms measured for $T_{acc} = 142$ K. The focusing properties of the two hexapole magnets favor some velocity groups and suppresses other parts. The red curve is a M-B distribution for 142 K.

For the atomic beam, the velocity distribution are structured as can be seen from Fig. 5. This is due to focusing of the effusive neutral beam in the harmonic guiding field of the magnets. For the boundary conditions

imposed by the present geometry (see Luca *et al.* (2007)) the energies indicated in the figure are transmitted efficiently. The 8 meV peak can be explained by one half wave in the first magnet and a quarter wave in the second one, leading to a parallel beam. Cooling the accommodator to 12 K leads to a beam in which the 3.5 meV part dominates with an half width smaller than 1 meV.

In summary the development of the H-atom beam and its integration into the AB-22PT machine has been very successful (Borodi 2007a). It allows now to study ion-neutral reactions at low ion temperatures and for defined velocity distributions of the H atom beam. Supersonic or effusive beams add to the versatility of the instrument.

3.4.2 Project organization, challenges and problems

During the first funding period it was tried in the group *Gasentladungs- und Ionenphysik* to operate three separate machines devoted to a variety of specific projects both in gas phase and grain chemistry. All projects were based on innovative ion guiding and trapping techniques which, in 1994, have been transferred from Freiburg to Chemnitz. The aim was to improve the machines in a cooperative way, to increase their sensitivity and to utilize or develop together additional tools and new detection schemes. Various ion guides and traps already have been combined in our group successfully with molecular beams, laser based analysis or preparation of selected ions using photons. A number of specific ion sources have been implemented into our machines ranging from standard ionizers via storage sources to a corona discharge source for clusters. Also first steps to integrate a commercial electrospray source have been made. The experimental challenges of our contributions to the FGLA were to measure reactions with H atoms, the integration of a carbon beam, the study of properties of interstellar dust equivalents and the combination with new laser based methods both for spectroscopy and state specific reactivity.

For a variety of reasons the resulting technical demands were to high. One problem was the missing technical support from a technician or a permanent engineer in the laboratory. The mechanical and electrical shops did not have much experience in the sophisticated technical demands of our machines. Moreover the know-how of the group itself decayed after the first generation of graduate students left the TUC. More and more time has been wasted with technical trivialities. As a consequence, it became necessary to reorganize the group in the second fund-

ing period. The total number of projects and machines has been reduced in the group. For example the Guided Ion Beam apparatus has been switched off although also this instrument has made significant contributions to astrochemistry as demonstrated with the last publication dealing with ion-molecule reactions of relevance for Titans atmosphere (Nicolas *et al.* 2003).

Other changes were dictated by fluctuations in the personal. The project leader of TP 4 moved with the original 22PT machine to Leiden and later to Köln. There have been significant problems in TP 7 (see report). In 2002, the molecular beam based apparatus and TP 5 was transferred - from a collective of three leaders - to a new assistant (A. Luca). He became responsible, with one graduate student, exclusively for this machine and for its application in the gas phase part of TP 5. These changes finally lead to results which are unique and recognized world-wide.

3.5 Ergebnisse und ihre Bedeutung / Results and their importance

The AB-22PT machine has been used in several developments stages for measuring reactions between a variety of stored ions and the H- or D-atom beam (Borodi *et al.* 2007a) First results have been reported in Luca *et al.* (2005). Since there are no other experiment at all that allow to study the interactions between cold ions and a slow H-atom beam, it was necessary to perform a lot of consistency checks. There are standard reactions, e.g. with CH_4^+ or CO_2^+ , which have been used at room temperature for tests and calibration purposes. Other measurements gave new insight into the new field of ultracold chemistry. Many unexpected results have been obtained. For example hydrogen abstraction in $\text{CH}_5^+ + \text{H}$ collisions occurs at low temperatures, in contradiction to predictions using the proton affinity of methane. In order to query such an "established" value, it became necessary to better characterize the energy distribution of the H atom beam.

$\text{CH}_4^+ + \text{H}$

Typical features of the AB-22PT apparatus are demonstrated with results measured for the 2.7 eV exothermic reaction (Luca *et al.* 2007).

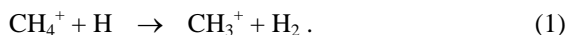


Fig. 6 shows the exponential decay of the injected CH_4^+ ions. They have been thermalized to the trap temperature of 80 K via collisions with ambient He buffer gas. The temperature of the H atom source has been set to

$T_{acc} = 100$ K. Although the H-atom density is lower than the H_2 background (see figure caption), formation of CH_3^+ via reaction (1) prevails. In addition a few CH_5^+ are formed via the hydrogen abstraction reaction

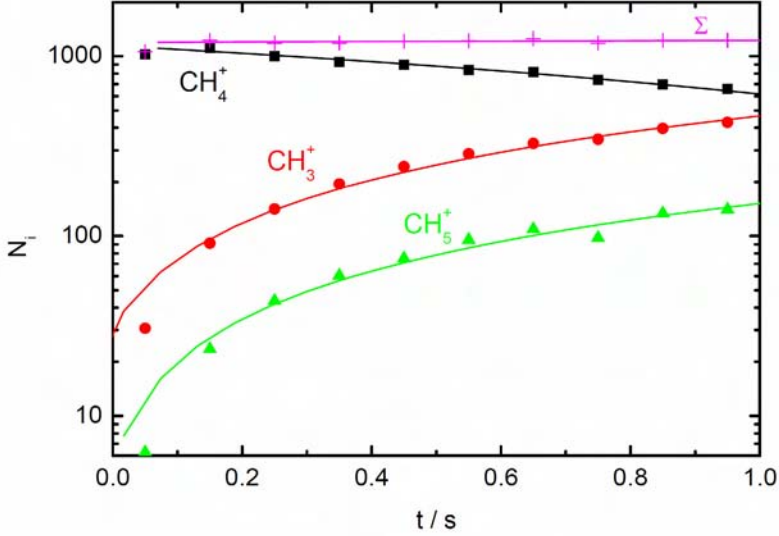
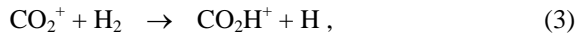


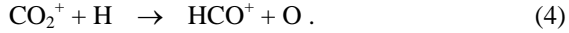
Fig. 6: Reactions of CH_4^+ with hydrogen atoms ($0.9 \times 10^9 \text{ cm}^{-3}$, $T_{acc} = 100$ K) and hydrogen molecules ($1.4 \times 10^9 \text{ cm}^{-3}$) at $T_{22PT} = 80$ K. Plotted is the averaged number of ions per filling, N_i , as a function of the storage time t . The ions are thermalized via collisions with He ($3.7 \times 10^{12} \text{ cm}^{-3}$).

This reaction is rather slow at 80 K, $k = (1.1 \pm 0.2) \times 10^{-10} \text{ cm}^3 \text{ s}^{-1}$, in accordance with recently published 22PT results (Asvany *et al.* 2004a). The rate coefficient for reaction (1) has been determined to be $k(80 \text{ K}) = (5 \pm 1) \times 10^{-10} \text{ cm}^3 \text{ s}^{-1}$.

$CO_2^+ + H/H_2$

Another reaction which is of importance for characterizing the machine, has been studied some time ago by Tosi *et al.* (1984) in a drift tube at energies between 60 and 140 meV. These measurements have shown that CO_2^+ ions react both with atomic and molecular hydrogen with a rather large rate coefficients. Fortunately, the reactions lead to different products,





Therefore this reaction can be used as an *in situ* calibration standard for the effective H and H₂ number density prevailing in the ion trap (Luca *et al.* 2007).

In addition, the two reactions (3) and (4) and the deuterated variants have been studied at temperatures between 20 K and 300 K. Although exothermic, reaction (3) increases significantly with decreasing temperature,

$$k_{\text{H}_2} = 1.0 \times 10^{-9} \text{ cm}^3 \text{ s}^{-1} (T / 300 \text{ K})^{-0.23} ,$$

$$k_{\text{D}_2} = 0.5 \times 10^{-9} \text{ cm}^3 \text{ s}^{-1} (T / 300 \text{ K})^{-0.38} ,$$

while reaction (4) is independent both on the ion temperature and the H atom energy,

$$k_{\text{H}} = 4.4 \times 10^{-10} \text{ cm}^3 \text{ s}^{-1} ,$$

$$k_{\text{D}} = 2.3 \times 10^{-10} \text{ cm}^3 \text{ s}^{-1} .$$

A publication of these interesting results is in preparation (Borodi *et al.* 2007b).

CH⁺ + H

CH⁺, the simplest hydrocarbon ion, was the first charged molecule discovered in the interstellar medium. Whereas early simple gas-phase models predicted the observed neutral CH abundances quite well, this was not the case for ionic CH⁺. The pathways of its synthesis are still subject of discussions. Given the ubiquity of H atoms, the reaction



represents an important destruction mechanism of CH⁺. Until recently the rate coefficient for reaction (5) has been predicted just by using phase space theory (Gerlich *et al.* 1987). Our first measurements which have been reported by Luca *et al.* (2005), are depicted in Fig. 6. The temperature dependence is in accord with the trend predicted by the high temperature SIFDT data.

While phase space theory is in reasonable agreement with the measured data, the RIOSA-NIP calculations underestimate the measured values significantly. It is obvious that more theoretical developments are needed in order to understand this fundamental triatomic hydrocarbon collision system from first principles. For stimulating theoreticians, additional experimental results at different trap temperatures (i.e. for different rotational populations of CH⁺), for various energies of the H-atom beam, and for deuterated variants (see below) will be reported soon (Borodi *et al.* 2007c).

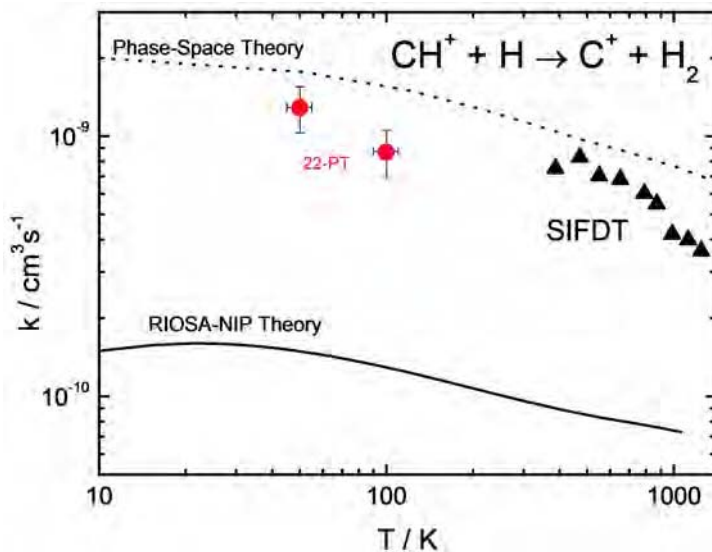


Fig. 6: Temperature dependence of the rate coefficient for hydrogen abstraction in $\text{CH}^+ + \text{H}$ collisions (Luca *et al.* 2005). The results of phase space theory are slightly larger while calculations using the RIOSA-NIP method (Stoecklin and Halvick 2005) are one order of magnitude too small.

$\text{CH}_5^+ + \text{H}$

The CH_5^+ ion has attracted a lot of interest in recent years (see TP 4 and Gerlich 2005). As discussed briefly by Luca *et al.* (2005) a rather surprising result has been obtained for the reaction



Based on accepted thermodynamical data the thermal rate coefficient for this reaction should become negligible at temperatures below 80 K (see dotted line in Fig. 7). Nonetheless a significant CH_4^+ production rate has been observed at the coldest conditions $T_{22PT} = 10$ K and $T_{acc} = 12$ K. Our standard analysis results in a rate coefficient of $10^{-11} \text{ cm}^3 \text{ s}^{-1}$. However, as discussed above, the hydrogen beam has a mean kinetic energy of 3.5 meV under these conditions. In order to predict the effective rate coefficient as a function of the kinetic energy of the H atoms, a more detailed analysis is necessary. Corresponding work including the separate determination of the proton affinity of methane, is in progress and will be published soon (Borodi *et al.* 2007c).

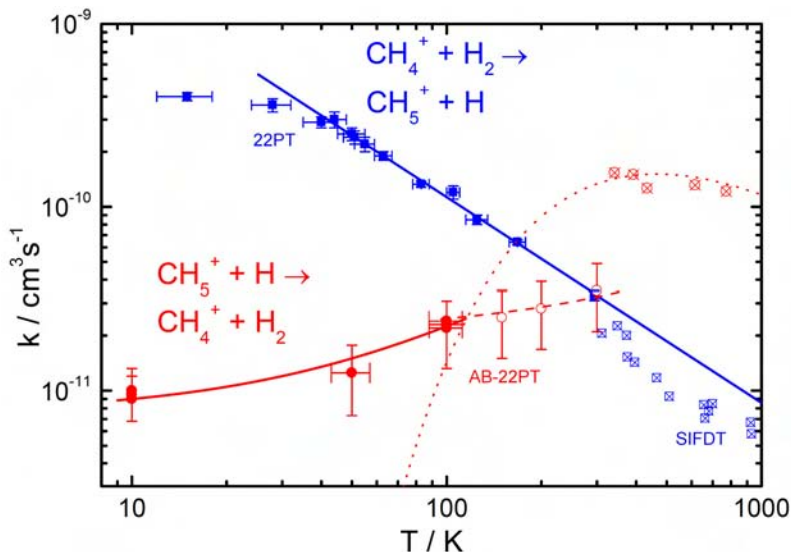


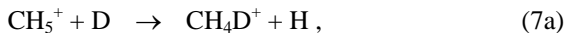
Fig. 7: Temperature dependent rate coefficients for the reaction $\text{CH}_4^+ + \text{H}_2 \rightarrow \text{CH}_5^+ + \text{H}$ (Asvany *et al.* 2004a) and its backward reactions (Luca *et al.* 2005). The high temperature data have been obtained with a SIFDT apparatus while low temperature data have been measured in two different 22pole traps. The solid red circles have been measured for $T = T_{\text{acc}} = T_{22\text{PT}}$, the open ones for $T_{\text{acc}} = 100 \text{ K}$ and $T = T_{22\text{PT}}$.

Low temperature deuterium fractionation

During the 6 years of our FGLA activities, observation of singly and multiply deuterated molecules became quite popular, requiring new reaction rates for understanding the astrophysical process of deuterium fractionation. Some aspects have been discussed for example by Roberts *et al.* 2004. Closely correlated to these activities, we have started dedicated laboratory studies (Gerlich *et al.* 2002a, Gerlich and Schlemmer 2002b, Asvany *et al.* 2004b, Schlemmer *et al.* 2006). The work has concentrated first on reactions with HD. Later D_2 has been used, too (Gerlich *et al.* 2006b) since this molecule may be quite abundant in cold interstellar clouds. In addition we have started in TP 5, to put some emphasis on H-D exchange reactions in collisions of hydrogenated ions with D atoms.

One important result was the experimental verification, that CH_5^+ ions cannot be deuterated in collisions with HD. The rate coefficient is

smaller than $4 \times 10^{-17} \text{ cm}^3 \text{ s}^{-1}$ (Asvany *et al.* 2004a). Since it was speculated that deuteration of protonated methane could be achieved by the simple exchange



we have studied this reaction; however, also in this case the rate coefficient is too small, $k = 1.3 \times 10^{-12} \text{ cm}^3 \text{ s}^{-1}$, that reaction (7a) could play a role in astrochemistry. In addition it competes with HD formation via



The rate coefficient for reaction (7b) has been determined to be $k = 5.5 \times 10^{-13} \text{ cm}^3 \text{ s}^{-1}$. No formation of CH_3D^+ could be detected above the background. Comparison with the results shown in Fig. 7 reveals that there is a strong isotope effect: hydrogen abstraction in reaction (7b) is 40 times slower than in reaction (6).

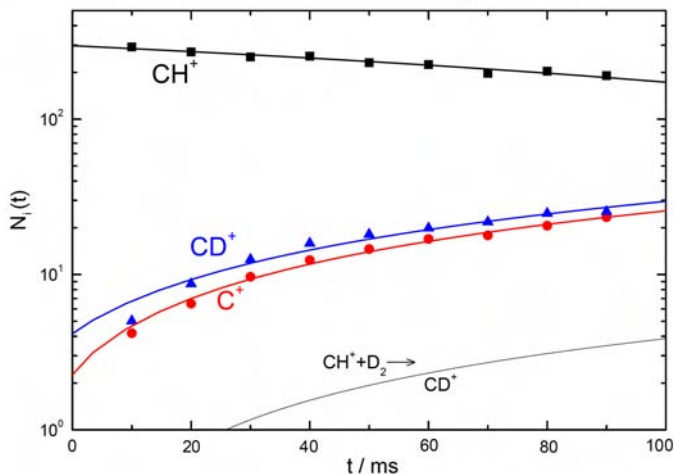


Fig. 8: Reaction of CH^+ with D ($8 \times 10^8 \text{ cm}^{-3}$) and D_2 ($3 \times 10^9 \text{ cm}^{-3}$) at $T_{22PT} = 80 \text{ K}$ and for $T_{acc} = 36 \text{ K}$. As indicated by the simulation in the lower part, contributions to CD^+ via reactions with D_2 are negligible.

A similar competition between H-D exchange and hydrogen abstraction occurs in



As can be seen from Fig. 8, both channels react very fast ($k = 1.2 \times 10^{-9} \text{ cm}^3 \text{ s}^{-1}$) while reactions with the 3 times more abundant D_2 is negligible.

There are some speculations that pre-protostellar cores can become so cold that all heavy elements vanish from the gas phase and become integrated into ice layers coating dust grains. In such a situation the hydrogen chemistry gets an enormous weight as illustrated by the simulations carried out by Walmsley *et al.* (2004). Inspection of the table of reactions they use in their model reveals that many of the rate coefficients are based on pure speculations. This statement also holds for the important class of low temperature collisions with H or D atoms.

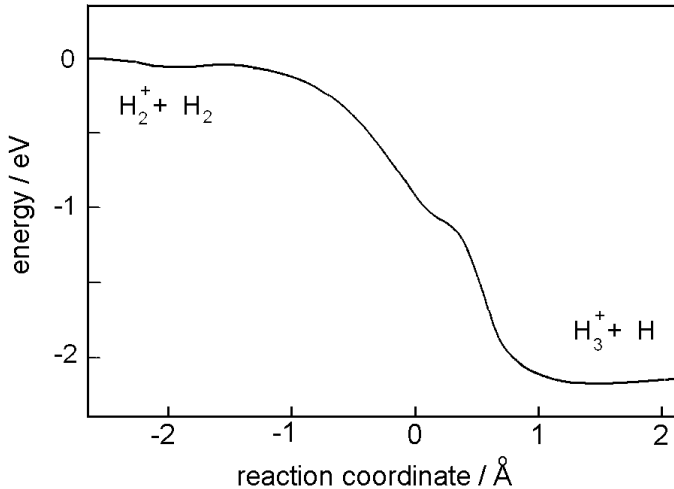


Fig. 9: Schematic illustration of the H_4^+ interaction potential along the reaction coordinate. Low temperature collisions are significantly influenced by the long range attractive van der Waals interaction (not to scale).

The overall status of our present knowledge about H_mD_n^+ collision systems has been reviewed recently for $m+n \leq 5$ (Gerlich *et al.* 2006b) ranging from the simple 3 protons 2 electrons system $\text{H}^+ + \text{H}_2$ to the complex five center reaction system H_5^+ . An intermediate case is the four center system H_4^+ . Relevant for the work of this project and important for astrochemical applications is the scrambling reaction



which is exothermic by 860.1 cm^{-1} (598 K). So far there are no measurements available with cold ions; however, it is planned that they will be a part of C. Mogo's thesis. As can be seen from Fig. 9, this process occurs on a very weakly interacting potential energy surface which is presently calculated with modern methods (J. Bowman, private communication 2006). A special interesting aspect of H - D interaction is the role of nuclear spin or, with other words, the fact that there are mainly fermions in reaction (9) while bosons dominate in the $\text{D}_3^+ + \text{H}$ collision system.

Reactions with other radicals and condensable gases

It was planned to use the AB-22PT arrangement in addition for studying collisions between cold ions and condensable gases using molecular beams. With a pulsed beam first results have been obtained for association of CH_3^+ with H_2O at low temperatures (Luca *et al.* 2002). In principle it is no problem to replace the complicated atomic beam with a beam of a molecule of astrochemical importance such as CO, H_2O , HCN, NH_3 , C_2H_2 , CH_4 , CH_3OH , or CH_3CN . Because of condensation reactions with these targets cannot be studied in the standard 22PT. As explained in Section 3.4 this goal could not be reached, exclusively because of lack on suitable men power.

3.6 Zusammenfassung und Ausblick / Summary and future

Zusammenfassung / Summary

In the center of the activities of TP 5 was hydrogen, especially in its atomic form. Although this atom is the simplest one - just one electron and one proton - and although it is several orders of magnitude more abundant in the universe than any other element, there have been almost no studies of specific reactions which may be, for example, of basic importance for star formation in very cold gas clouds.

The central engineering challenge was the development of the *Atomic Beam 22-Pole Trap Apparatus* (AB-22PT), a complex ultrahigh vacuum machine in which several innovative modules had to be combined and tested. The central element is our 22pole ion trap, a very sensitive instrument which not only allows to perform unique fundamental studies of ion-molecule reactions with unprecedented sensitivity but also has important applications in mass spectroscopy, chemical analysis, and ion spectroscopy. In this device the temperature and pressure can be lowered so far that one can simulate conditions prevailing in "dense" preprotostellar discs. Another technical problem was the construction of a modular and flexible H- or D-atom source and its characterization. Most requirements such as sufficiently large flux, high degree of dissociation, low H₂ background, and slow velocities have been fulfilled. The new machine - it is still a prototype - allows now to study collisions between cold ions confined in the trap and a neutral beam of atoms, molecules or radicals traversing the trapped ion cloud with a controllable velocity distribution.

During the various stages of development, the instrument has been used for studying reactions between ions of astrochemical importance and cold hydrogen atoms. Since there exist worldwide no other experiment at all that allows to study these class of processes, it was necessary to perform specific consistency checks. Standard reactions, e.g. with CH₄⁺ or CO₂⁺, have been used at room temperature for tests and calibration. Several unexpected results have been obtained with the innovative instrument. For example hydrogen abstraction in CH₅⁺ + H collisions is not in accord with the proton affinity of methane. In order to query such an "established" value, it became necessary to characterize the energy distribution of the H atom beam. Another important class of reactions, we have started to explore is **isotope enrichment** in collisions of ions with D-atoms. In cold H and D containing chemical reactions, the nuclear spin plays a central role, or with other words, H and D are not really chemi-

cally equivalent at very low temperatures. In addition to differences in zero point energies, caused by the different masses of the isotopes, exchange processes are influenced by the fermionic and bosonic properties of H and D, respectively.

Ausblick / future

This project has made unique contributions to low temperature astrochemistry and opened up new fields of research. Unfortunately A. Luca has decided - very recently - to leave the university this year; however, there are various plans how the new instrument itself could be used in the future after C. Mogo has finished the experimental work for his thesis.

Our FGLA activities have stimulated several other groups to use low temperature multipole traps or nanoparticle traps for new applications. In order to continue some of the initiatives started in the FGLA, we have contributed to the planning and development of several new projects in Heidelberg, Basel, Prag and especially Tucson. In the Max-Planck-Institute für Kernphysik in Heidelberg, a 22PT ion source has been developed with our help for determining state selective rate coefficient for dissociative recombination in low-energy $\text{H}_3^+ + \text{e}^-$ collisions (Krekel *et al.* 2005a, 2005b). First evidence for nuclear spin effects has been obtained recently (Wolf *et al.* 2006). Our method of laser induced reactions has been used successfully for characterizing the stored H_3^+ ion cloud (Mikosch *et al.* 2004). It is planned to continue - together with S. Schlemmer (TP 4) and J. Glosik (Prague) - the fruitful cooperation in order to gain more information on the H_mD_n^+ collision system (Gerlich *et al.* 2006b). In Basel a new apparatus has been developed in collaboration of John Maier with us with the aim of measuring the electronic spectra of large ions at low vibrational and rotational temperatures, as of relevance to astronomical observations (Dzhonson *et al.* 2006).

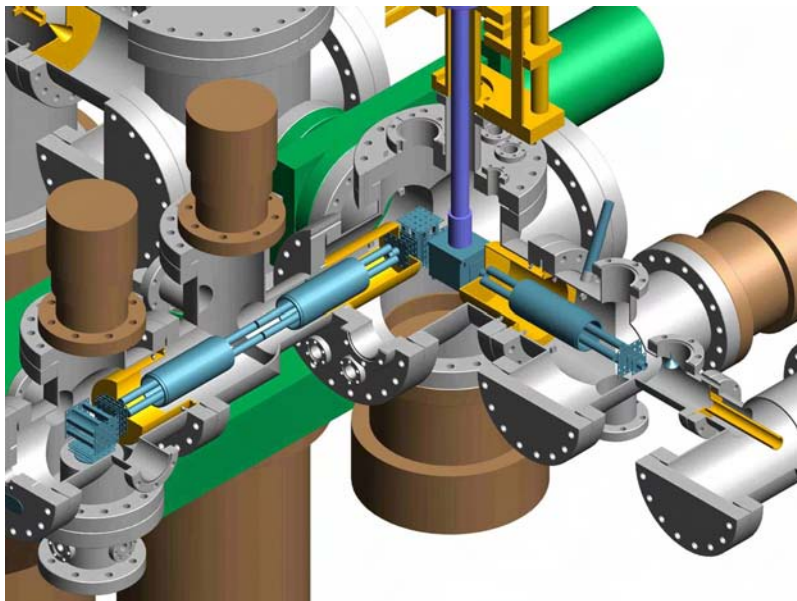


Fig. 10: Next generation trapping machine for astrochemical applications (PI: M. Smith, University of Arizona). Ions which are prepared in the lower left part interact in a multipole trap (in the center) with a beam of radicals coming from the upper left part. The detector is on the right side. The temperature can be varied over a wide range (4-700 K) using liquid He cooling or heating.

A new large project which is very closely related to the activities of TP 5, has been started recently in Tucson. In the center is the construction of a machine similar to ours (see Fig. 10). It is supported by an NSF grant (PI: Mark A. Smith, University of Arizona) and an NSF CRIF-Instrument Development grant (Co-Investigator D. Gerlich). It can be foreseen that several of the ambitious experiments of astrochemical importance which could not be performed in the last 6 years in Chemnitz may be performed in this new machine. The scientific environment in Tucson ranging from world class astrophysics to laboratory astrochemistry certainly will stimulate a lot of new ideas and projects.

3.7 Literatur / References

- Abbas, M. M., Tankosic, D., Craven, P. D., Spann, J. F., LeClair, A., West, E. A., Weingartner, J. C., Tielens, A., Nuth, J. A., Camata, R. P., and Gerakines, P. A.: *Photoelectric emission measurements on the analogs of individual cosmic dust grains*, Ap. J. **645** (2006) 324 - 336.
- Asvany, O., Savic, I., Schlemmer, S., and Gerlich, D.: *Variable temperature ion trap studies of $\text{CH}_4^+ + \text{H}_2$, HD and D_2 : negative temperature dependence and significant isotope effect*, Chem. Phys. **298** (2004a) 97 - 105.
- Asvany, O., Schlemmer, S., and Gerlich, D.: *Deuteration of CH_n^+ ($n=3-5$) in collisions with HD measured in a low temperature ion trap*, Astrophys. J., **617** (2004b) 685 - 692.
- Barckholtz, C., Snow, T. P., Bierbaum, V. M.: *Reactions of C_n^- and C_nH^- with atomic and molecular Hydrogen*, Ap. J **547** (2001) L171 - L174.
- Borodi, G.: PhD-thesis, TU Chemnitz, (2007a) to be finished soon.
- Borodi, G., Luca, A., Gerlich, D.: *Reactions of $\text{CO}_2^+ + \text{H} / \text{H}_2$ and deuterated analogues*, in preparation (2007b)
- Borodi, G., Geppert, W.D., Luca, A., Mogo, C., Gerlich, D.: *Formation and destruction of CH^+ in interstellar space*, in preparation (2007c)
- Borodi, G., Luca, A., Gerlich, D.: *Collisions of cold trapped CH_5^+ ions with a slow H atom beam*, in preparation (2007d)
- Dai, D., Wang, C. C., Wu, G., Harich, S. A., Song, H., Hayes, M., Skodjes, R. T., Wang, X., Gerlich, D., Yang, X.: *State -to-State Dynamics of High- n Rydberg H-Atom Scattering with D_2* , Phys. Rev. Lett. **95**, (2005) 13201-1 - 4.
- Dzhonson, A., Gerlich, D., Bieske E. J., and Maier, J. P.: *Apparatus for the study of electronic spectra of collisionally cooled cations: para-dichlorobenzene*, J. Mol. Struct. **795** (2006) 93 - 97.
- Gerlich, D., Disch R., and Scherbarth S.: *$\text{C}^+ + \text{H}_2(j) \rightarrow \text{CH}^+ + \text{H}$. The effect of reagent rotation on the integral cross section in the threshold region*, J. Chem. Phys., **87** (1987) 350 - 359.
- Gerlich, D.: *Inhomogeneous Electrical Radio Frequency Fields: A Versatile Tool for the Study of Processes with Slow Ions*. Adv. in Chem. Phys., **LXXXII**, (1992) 1 - 176.
- Gerlich, D.: *Ion-Neutral Collisions in a 22-pole trap at very low energies* Physica Scripta, **T59**, (1995) 256 - 263.
- Gerlich, D., Herbst, E. & Roueff, E.: *$\text{H}_3^+ + \text{HD} \rightarrow \text{H}_2\text{D}^+ + \text{H}_2$: Low-temperature laboratory measurements and interstellar implications*, Plan. Sp. Sci. **50**, (2002a) 1275 - 1285.
- Gerlich, D., Schlemmer, S.: *Deuterium fractionation in gas phase reactions measured in the laboratory*, Plan. Sp. Sci. **50**, (2002b) 1287 - 1297.
- Gerlich, D.: *Molecular ions and nanoparticles in RF and AC traps*, Hyperfine Interactions, **146/147** (2003) 293 - 306.

- Gerlich, D.: *Rf Ion Guides*, in "The Encyclopedia of Mass Spectrometry", Vol 1, Ed. by P. B. Armentrout, Elsevier Ltd., (2003a) 182 - 194.
- Gerlich, D.: *Applications of rf fields and collision dynamics in atomic mass spectrometry*, J. Anal. At. Spectrom., **19** (2004) 581 - 590.
- Gerlich, D.: *Probing the structure of CH_5^+ ions and deuterated variants via collisions*, Phys. Chem. Chem. Phys. **7** (2005) 1583 - 1591.
- Gerlich, D., Smith, M.: *Laboratory astrochemistry: studying molecules under inter- and circumstellar conditions*, Phys. Scr. **73** (2006a) C25 - C31.
- Gerlich, D., Windisch, F., Hlavenka, P., Plašil, R., Glosik, J.: *Dynamical constraints and nuclear spin caused restrictions in H_mD_n^+ collision systems and deuterated variants*, Phil. Trans. R. Soc. Lond. **A 364** (2006b) 3007 - 3034.
- Grimm, M., Langer, B., Schlemmer, S., Lischke, T., Becker, U., Widdra, W., Gerlich, D., Flesch, R., Rühl, E.: *Charging mechanisms of trapped element-selectively excited nanoparticles exposed to soft X-rays*, Phys. Rev. Lett. **96** (2006) 066801 - 066805.
- Krauß, O., and Wurm, G.: *Radiation pressure forces on individual micron-size dust particles: a new experimental approach*, JQSRT, **89** (2004) 179 - 189.
- Kreckel, H., Motsch, M., Mikosch, J., Glosik, J., Plasil, R., Altevogt, S., Andrianarijaona, V., Buhr, H., Hoffmann, J., Lammich, L., Lestinsky, M., Nevo, I., Novotny, S., Orlov, D. A., Pedersen, H. B., Sprenger, F., Terekhov, A. S., Toker, J., Wester, R., Gerlich, D., Schwalm, D., Wolf, A., and Zajfman D.: *High-Resolution Dissociative Recombination of Cold H_3^+ and First Evidence for Nuclear Spin Effects*, Phys. Rev. Lett. **95** (2005b) 263201.
- Kreckel, H., Mikosch, J., Wester, R., Glosik, J., Plasil, R., Motsch, M., Gerlich, D., Schwalm, D., Zajfman, D. and Wolf, A.: *Towards state selective measurements of the H_3^+ dissociative recombination rate coefficient*, Journal of Physics: Conference Series **4** (2005a) 126 - 133.
- Luca, A., Voulot, D., and Gerlich, D.: *Low temperature reactions between stored ions and condensable gases: formation of protonated methanol via radiative association*, WDS'02 Proceedings of Contributed Papers, PART II, ed. Safrankova, (2002) 294 - 300.
- Luca, A., Borodi, G., Gerlich, D.: *Interactions of ions with Hydrogen atoms*, Progress report in XXIV ICPEAC 2005, Rosario, Argentina, July 20-26, 2005, Edited by F.D.Colavecchia, P.D.Fainstein, J.Fiol, M.A.P.Lima, J.E.Miraglia, E.C.Montenegro, and R.D.Rivarola
- Luca, A., Borodi, G., Mogo, C., Smith, M., Gerlich, D.: *On the combination of a temperature variable H/D atom beam with a multipole ion trap*, to be submitted to Rev. Sci. Instr. (2007)
- Mikosch, J., Kreckel, H., Plasil, R., Gerlich, D., Glosik, J., Schwalm, D., Wolf, A.: *Action spectroscopy and temperature diagnostics of H_3^+ by chemical probing*, J. Chem. Phys., **121** (2004) 11030 - 11037.

- Nicolas, C., Torrents, R., and Gerlich, D.: *Integral and differential cross section measurements at low collision energies for the $N_2^+ + CH_4 / CD_4$ reactions*, J. Chem. Phys. **118** (2003) 2723 - 2730.
- Roberts, H., Herbst, E. & Millar, T. J.: *The chemistry of multiply deuterated species in cold, dense interstellar cores*, Astron. & Astroph. **424** (2004) 905-917.
- Schlemmer, S., Illelmann, J., Wellert, S. and Gerlich, D.: *Non-destructive high resolution and absolute mass determination of single, charged particles in a 3D quadrupole trap*", J. Appl. Phys. **90** (2001) 5410 - 5418.
- Schlemmer, S., Wellert, S., Windisch, F., Grimm, M., Barth S., and Gerlich, D.: *Interactions of electrons and molecules with a single trapped nanoparticle*, Appl. Phys. A, **78** (2004) 629 - 636.
- Schlemmer, S., Asvany, O., Hugo E., and Gerlich, D.: *Deuterium fractionation and ion-molecule reactions at low temperatures*, Proceedings of the International Astronomical Union, Symposium, Cambridge University Press, **S231** (2006) 125 - 134.
- Song, H., Dai, D., Wu, G., Wang, C.C., Harich, S. A., Hayes, M. Y., Wang, X., Gerlich, D., Yang, X., Skodje, R. T.: *Chemical reaction dynamics of Rydberg atoms with neutral molecules: A comparison of molecular-beam and classical trajectory results for the $H(n)+D_2 \rightarrow HD+D(n')$ reaction*, Journal of Chem. Phys. **123** (2005) 074314-1 - 10.
- Stoecklin, T., Halvick, Ph.: *Low temperature quantum rate coefficient of the $H + CH^+$ reaction*, Phys. Chem. Chem. Phys. **7** (2005) 2446 - 2452.
- Tosi, P., Iannotta, S., Bassi, D., Villinger, H., Dobler, W., Lindinger, W.: *The reaction of CO_2^+ with atomic hydrogen*, J. Chem. Phys. **80** (1984) 1905 - 1906.
- Walmsley, C. M., Flower, D. R., Pineau des Forets, G.: *Complete depletion in prestellar cores*, Astron. & Astroph. **418** (2004) 1035-1043.
- Wolf, A., Kreckel, H., Lammich, L., Strasser, D., Mikosch, J., Glosík, J., Plašil, R., Altevogt, S., Andrianarijaona, Buhr, H., Hoffmann, J., Lestinsky, M., Nevo, I., Novotny, S., Orlov, D. A., Pedersen, H. B., Terekhov, A. S., Toker, J., Wester, R., Gerlich, D., Schwalm, D., and Zajfman, D.: *Effects of molecular rotation in low-energy electron collisions of H_3^+* , Phil. Trans. R. Soc. Lond. **A 364** (2006) 2981–2997.
- Tosi, P., Iannotta, S., Bassi, D., Villinger, H., Dobler, W., Lindinger, W.: *The reaction of CO_2^+ with atomic hydrogen*, J. Chem. Phys. **80** (1984) 1905 - 1906.

3.1 Bericht Teilprojekt 6

3.1.1 Titel / Title

Photophysik und Photochemie an Grenzflächen von Silizium Nanoteilchen

Photophysics and photochemistry at interfaces of silicon nanoparticles

3.1.2 Berichtszeitraum / reported period

01.07.2003 - 31.12.2006

3.1.3 Projektleiter / principle investigator

Cichos, Frank, Prof. Dr. rer. nat.
Institut für Physik der Technischen Universität Chemnitz

von Borczyskowski, Christian, Prof. Dr. rer. nat.
Institut für Physik der Technischen Universität Chemnitz

3.2 Zusammenfassung / Abstract

3.2.1 Wortlaut des Antrags / abstract of the proposal

Während der ersten Antragsperiode wurde demonstriert, dass eine Untersuchung auch einzelner Silizium Nanokristalle möglich ist. Bei optischer Anregung zeigen größenselektierte Partikel-Ensembles zeitabhängige spektrale Verschiebungen und Intensitätsveränderungen. Einzelne Nanokristalle zeigen Blinken in der Emissionsintensität. Diese Effekte werden auf den Einfluss der Nanokristallhülle bzw. auf die direkte Umgebung der Nanokristalle zurückgeführt. Die Mikrostruktur und chemische Zusammensetzung dieses Grenzflächenbereiches erzeugt Pfade auf denen photochemische Reaktionen, wie z.B. Ladungstransfer stattfinden können. Innerhalb dieses Projektes sollen die Experimente aus der ersten Antragsperiode auf eine systematische Untersuchung dieser Grenzflächeneffekte auch in Abhängigkeit einer durch AFM –Methoden bestimmten Größe erweitert werden. Dabei sollen die Grenzflächeneigenschaften mit

Blick auf einfache astrophysikalisch Modellsysteme (Einbettung in molekulares Eis, PAH dotiertes Eis) gezielt variiert werden, um so Informationen über photophysikalisch-photochemische Prozesse an der Partikelgrenzfläche zu erhalten. Der enge Bezug zu astrophysikalischen Bedingungen schließt die Variation der Temperatur ein, die für viele Prozesse ein entscheidender Parameter ist.

During the last period the feasibility to investigate the spectroscopic properties of (single) silicon nanoparticles was demonstrated. Upon optical excitation size selected particle ensembles show spectral shifts and intensity changes. Single nanoparticles exhibit blinking behavior. These effects are thought to be closely related to properties at the interface of the particle with the environment. The microstructure and chemical composition of this interface create funnels via which photochemical reactions such as charge transfer may proceed. In this project we will extend the experiments of the first application period towards a systematic variation of the interface properties of the particles as a function of size determined via AFM methods with a close relation to simple astrophysical model environments. Such environments are mainly pure molecular ice and doped (polycyclic aromatic hydrocarbons) ice environments. Since temperature plays a key role for many astrophysical processes and can largely change between different interstellar regions, all experiments will be related to temperature variation.

3.2.2 Zusammenfassung des Berichts / abstract of the report

Since in the first period of the research work experiments have revealed that the photoluminescence (PL) dynamics were subject to a variety of photoinduced processes we concentrated on the investigation of the nature these processes. They depend strongly on the presence of the SiO_2 interface since in the absence of such an interface no PL is observed at all. We therefore investigated in the second period (i) porous silicon nanocrystals (prepared via electro-chemical etching followed by ultrasonic treatment) and (ii) silicon nanocrystals prepared in the gas phase via laser pyrolysis (Prof. Huysken, Jena).

Spectroscopic and dynamic information is more subtle in case of single particle detection. For this reason we concentrated during the second research period mainly on single particle investigations. Although it finally turned out that single particle detection was only feasible for a limited range of PL energies (corresponding to crystal diameters between 2 nm and 3 nm), comparison of the overall dynamics (blinking and bleach-

ing) shows that at least photoinduced dynamics are comparable over the total PL range of silicon nanoparticles, independently whether they have been determined from ensemble or single particle experiments.

However, spectroscopy on single silicon particles in the energy range from 1.9 eV to 2.45 eV revealed that as compared to ensemble experiments reported in the literature, the PL of small silicon particles is strongly influenced by electron-phon coupling to vibrations in the oxide shell. Additionally, the exciton becomes probably localized at energies above 1.9 eV. We can provide strong evidence, that electron and hole are independently localized at different crystalline sizes, thus settling an unsolved question frequently posed in literature.

3.3 Ausgangsfragen, neuester Stand der Forschung / Initial goals, current status of the field

The goal of the proposed project within the first period was the study of photophysical properties of silicon nanocrystals and relating these findings to the interstellar extended red emission (ERE) (Witt 1998, Smith 2002, Ledoux 2001). At that time the radiative pathways of the indirect silicon band gap emission were not understood. Especially the interrelation of silicon core and (SiO₂) capping shell were completely open.

For this reason the second period has been focused on the investigation of phenomena related to interface properties.

During the last three years the investigation of interface phenomena in nanocrystals has been intensively investigated for II/VI colloidal nanocrystals. Recent experiments and models (Issac 2005, Tang 2005) have provided strong evidence that photoejected electrons are trapped in the dielectric environment even outside the capping layers.

Additionally to the literature already cited in the previous report, new single particle experiments on silicon nanoparticles have been reported (Sychugow 2005). Independent of the existing possibility of the relevance of silicon photoluminescence for the ERE emission (Witt 2005) the clarification of photoinduced interface dynamics is still an open question not only with respect to astrophysics.

Concerning optical properties of silicon nanocrystals several papers related to exciton localisation (Garrido 2004, Heitmann 2004) and electron phonon coupling (Sa`ar 2005) have been published and have been considered to be a general base for our own detailed single particle investigations.

3.4 Angewandte Methoden / Experimental methods

One of the goals of the project was to apply single particle microscopy methods to study the photophysics of silicon nanocrystals. The reasons to apply these methods lie mainly in the strong inhomogeneous broadening of nanoparticle ensemble spectra due to the strong size dependence of single particle transition energies. Furthermore single particle emission shows an intermittency due to the existence of so called dark states, where the particle cannot emit. The use of single particle optical microscopy allows direct access to these dark periods and will therefore provide detailed information about the physical processes connected with the dark periods, which are indicative for photoinduced physico-chemical processes. Such processes are also expected in interstellar matter.

3.5 Ergebnisse und ihre Bedeutung / Results and their importance

In the previous report we could show that silicon nanocrystals either prepared from gas phase (in cooperation with Prof. Huisken, Jena (TP10)) or porous silicon particles exhibit photoluminescence (PL) properties which could be related to the ERE emission. Additionally, we reported PL dynamics which are subject to (reversible) photobleaching of the ensemble emission and PL intermittency (blinking) of porous nanoparticles. At that time we were not able to perform experiments on (more uniquely characterized) single particles prepared from gas phase.

Since the advantage of the single particle approach lies in the removal of the inhomogeneous broadening of the emission bands, we extended our efforts to make the detection of single gas phase prepared nanocrystals feasible. Finally we succeeded and concentrated both on the spectral characterisation of single silicon nanoparticles and the comparison of PL dynamics from differently prepared samples.

3.5.1 Photoluminescence dynamics

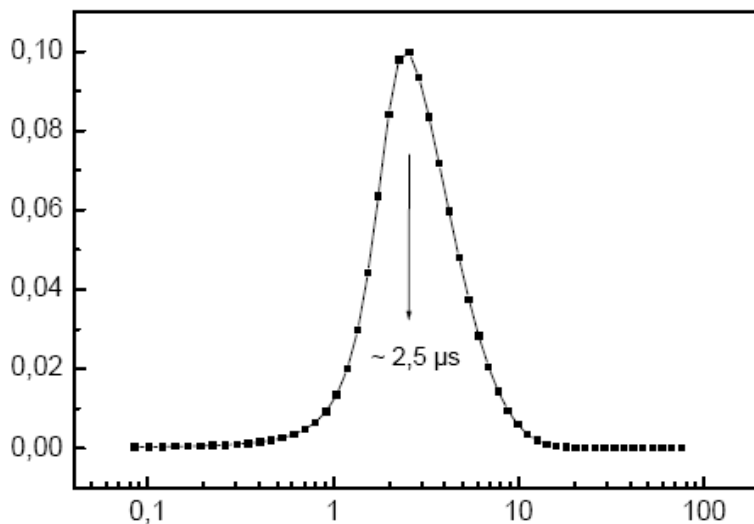


Fig. 1: Lifetime distribution of a non-size selected sample of gas-phase prepared silicon nanocrystals

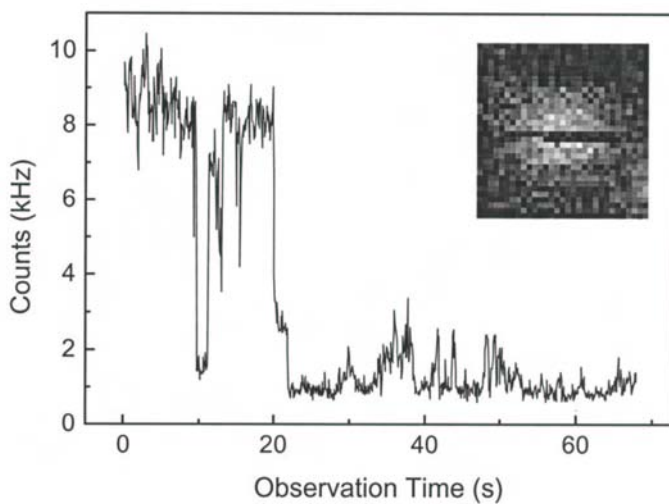


Fig. 2: PL blinking of a single porous silicon nanocrystal. The insert shows a confocal image of PL with black strips (off-times).

Ensemble PL of all type of silicon nanocrystals shows strong non-exponential decay dynamics as is shown in Fig. 1. This is usually attributed to the remaining size distribution relating each size to an individual decay rate. It is assumed that the main reason for this inhomogeneity is related to the (forbidden) indirect band gap transition of silicon which becomes modified by the size dependent quantum confinement. Whether this is indeed the only reason for the experimentally observed rate distribution is a not yet definitely answered question since experiments on other types of semiconductor nanocrystals such as CdSe (Fischer 2004) have shown that even for single nanocrystals the PL decay rate varies during the experimental observation time. Related phenomena are charging processes of the nanocrystals. For this reason we continued our experiments on photoinduced dynamics, which are also relevant in the astrophysical context, on silicon nanocrystals both on the single particle as on the ensemble level.

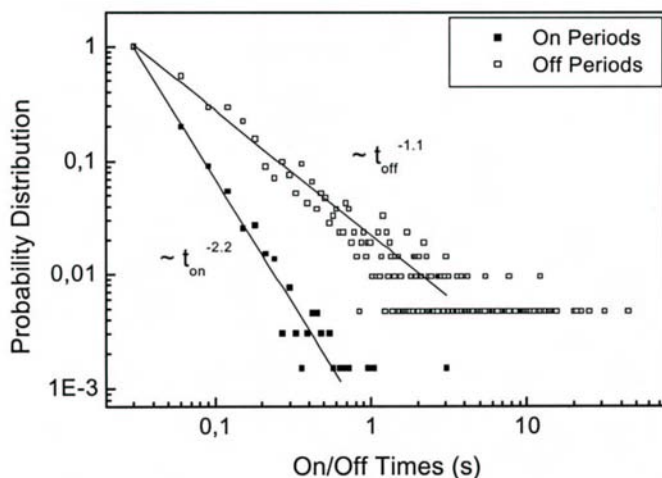


Fig. 3: Probability distribution of on- and off-times for one single porous silicon nanocrystal. The fits show a power law distribution.

Photoluminescence intermittency

As has already been reported in the previous report PL of single silicon nanocrystals turns “on” and “off” on time scales of ms and shorter (which is, however, not detectable due to our time resolution of about 10 ms and longer). A typical example is shown in Fig. 2 for a single nanocrystal from porous silicon. The figure shows PL intensity fluctua-

tions which are also seen as “dark” or “bright” stripes during a confocal scan across the image of a nanocrystal. Counting dark (off) and bright (on) periods in a statistical manor results in probability distributions as is shown in Fig. 3 for a single nanocrystal and in Fig. 4 for 100 different nanocrystals. In both cases the statistics follow a power law $P \sim t^{-\alpha}$ behaviour with $\alpha \approx 2.2$ for the “on”-times and $\alpha \approx 1.2$ for the “off”-times. However, Fig. 5 shows while following the statics for single particles separately that there is broad distribution for α . Figs. 3 and 4 also reveal that time scales may definitely reach times of less than 100 μs . From this we conclude that these blinking dynamics might be also part of the decay dynamics collected in Fig. 1.

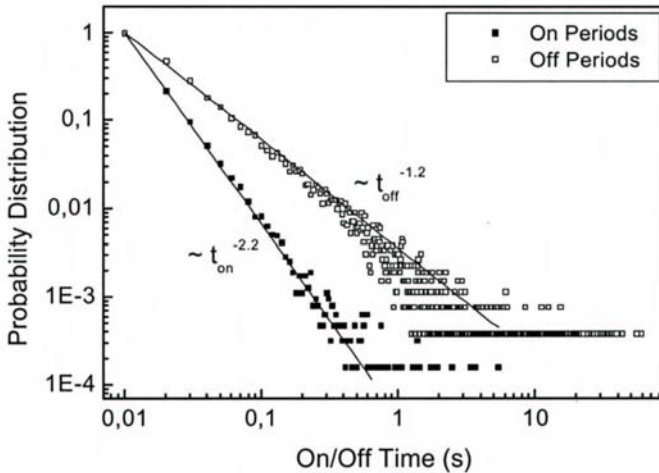


Fig. 4: Probability distribution of on- and off-times for 100 single porous silicon nanocrystals. The fits show a power law distribution.

Blinking dynamics have also been observed for other quantum systems such as colloidal semiconductors (Issac 2005) or organic molecules (Schuster 2005) with power law exponents α between 1 and 2. During the last years strong evidence has been provided (Issac 2005, Schuster 2005) that the reason for blinking dynamics is the charging of the quantum systems which is accompanied by a photoejection of the electron of the exciton, followed by a long-lived electron self-trapped in the dielectric environment. In the recently reported systems, this self-trapping depends on the dielectric constant of the embedding matrix. Contrary to the experiments on those systems, we did not observe a dependence of α on the dielectric properties of the environment, which we varied from quartz to

PMMA. This might be related to the fact that the diameter of the SiO_2 shell is much larger than 1 nm which is at least the case for most of the porous nanoparticles (see Fig. 6). TEM reveals that the particle size is on average larger than 20 nm, while the experimentally observed PL is related to Si-core diameters smaller than $d = 10$ nm. From this we conclude that electron trapping occurs in the (amorphous) SiO_2 shell or at the Si/ SiO_2 interface.

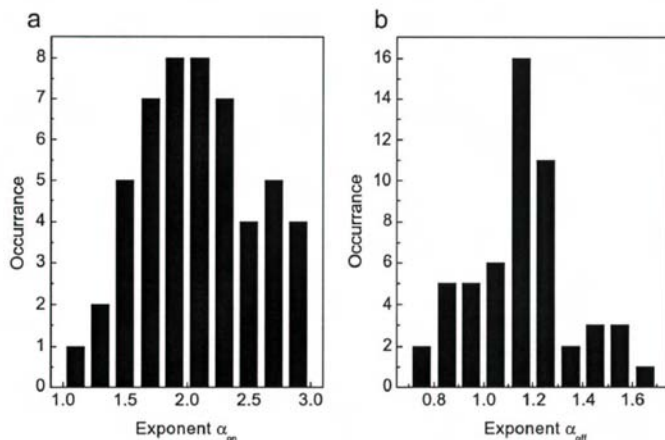


Fig. 5: Probability histogram finding a certain power law exponent for the on-times (a) and the off-times (b).

Comparing the power law exponents reveals that $\alpha_{\text{on}} > \alpha_{\text{off}}$ which is similar to the blinking behaviour of molecules (Schuster 2005) but different from CdSe/ZnS where we observed nearly independent of the crystalline size that $\alpha_{\text{on}} \leq \alpha_{\text{off}}$ (Issac 2005).

A comparison of the results of different model calculations with experiments suggests that more than one process is involved in the formation of the dark state. Details of this comparison can be found in Ref. (Cichos 2004a).

Photoluminescence bleaching and recovery

A consequence of the blinking experiments on single nanocrystals with $\alpha_{\text{off}} < 1.5$ is, that with increasing observation times the “off” periods increase continuously. This corresponds to a so called “statistical aging”. It should also be manifested in ensemble experiments. As we have already mentioned in the previous report, PL spectra decay in time scales of

seconds and PL is shifted to the red upon continuous photoexcitation. However, blinking experiments suggest, that this might not be a permanent photobleaching but that at least part of the PL intensity is recovered after sufficient long waiting periods while keeping the sample in the dark.

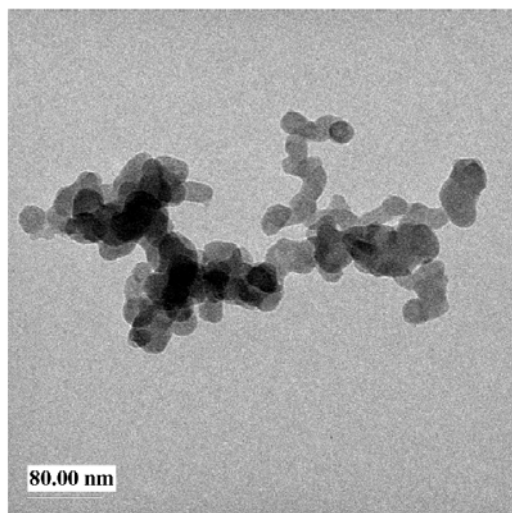


Fig. 6: TEM of porous silicon with silicon oxide shells. (Electron Microscopy Laboratory, Prof. Hietschold, TU Chemnitz)

In fact, this can be experimentally observed as is shown in Fig. 7. After switching the exciting laser on, the PL intensity of a silicon ensemble decreases on time scales of seconds. After waiting in the dark the intensity is recovered. We have performed Monte Carlo simulations (for details see Ref. (Cichos 2004b) for the bleaching and recovery for different power law distributions (see Fig. 8) and compared it to the experimental data in Fig. 7. We were able to predict the bleaching and emission recovery of nanocrystal ensembles from the blinking statistics of single crystals and vice versa. This provides an additional tool to study nanocrystal blinking behaviour especially at long times, where it is difficult to obtain sufficiently good statistics. Our results indicate that while waiting in the dark at least 80 % of the bleached PL can be recovered. The close relationship between bleaching and PL intermittency is also demonstrated in Fig. 9 where the decay (bleaching) is compared with the sum of individual blinking traces normalized to the same initial intensity.

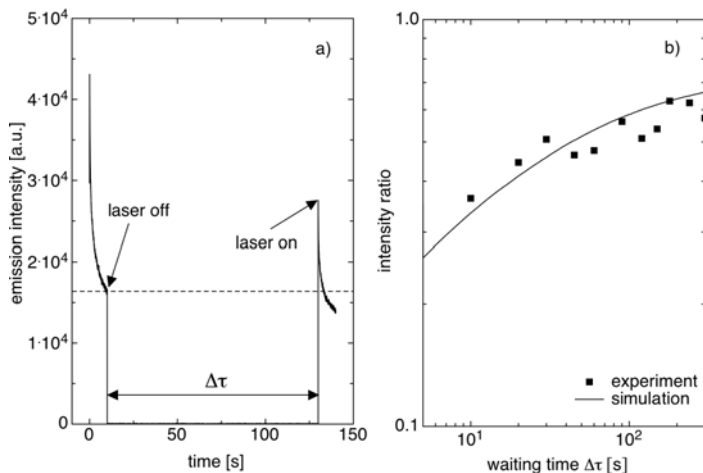


Fig. 7: (a) PL intensity as a function of laser irradiation time. (b) Ratio of PL intensity after switching the laser on to the intensity before switching off as a function of waiting time in the dark. The line shows a simulation with $\alpha = 1.7$ (see Fig 8).

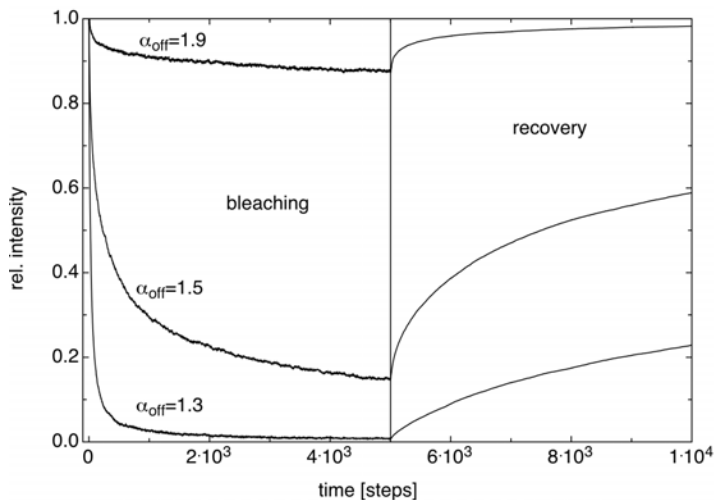


Fig. 8: Simulated bleaching and recovery curves for an ensemble of nanocrystals with different power law distributions for the off times.

These qualitative results are also of astrophysical relevance, since occurrently happening photobleaching will not destroy PL for long times but will result in a PL recovery after sufficient long waiting times.

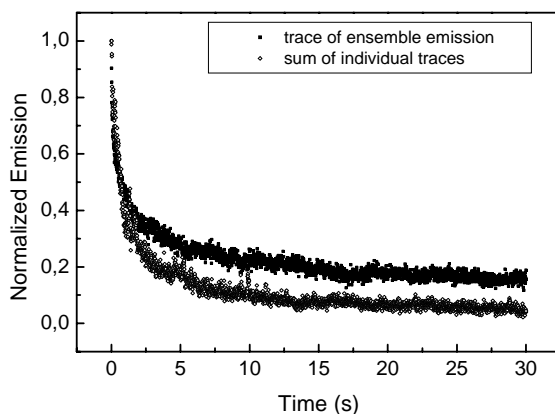


Fig. 9: Comparison between bleaching behaviour of an ensemble of gas-phase produced silicon crystals and the sum of 100 emission traces of single porous particles.

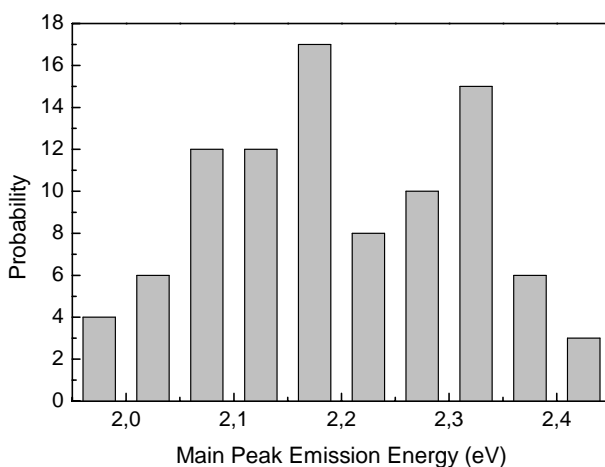


Fig. 10: Experimental probability to detect a single silicon nanocrystal as prepared from gas-phase with laser excitation at 2.54 eV.

3.5.2 Spectroscopy on single silicon nanocrystals

Already in the previous report we have shown the feasibility to obtain PL spectra of at that time single porous silicon nanocrystals. We have extended these experiments and were now able to perform also spectroscopy on single crystals prepared in the gas phase.

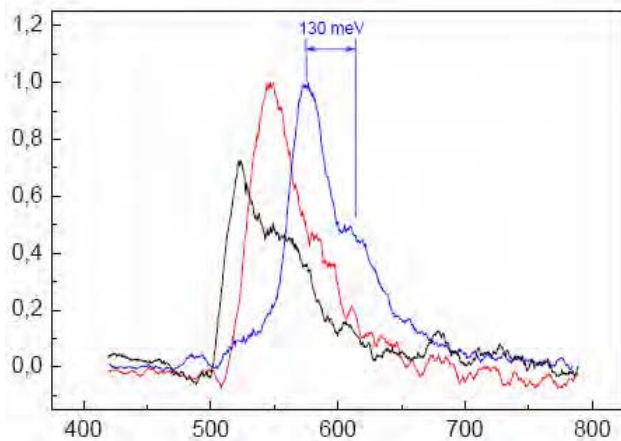


Fig. 11: Wavelength (in nm) PL spectra of 3 single porous silicon nanoparticles on a quartz substrate.

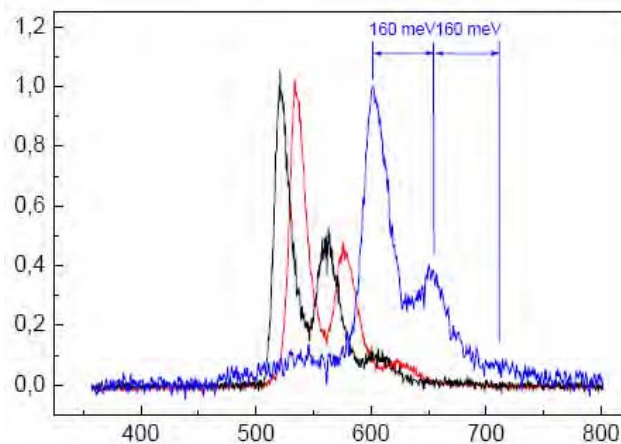


Fig. 12: Wavelength (in nm) PL spectra of 3 single porous silicon nanoparticles embedded in a PMMA matrix on a quartz substrate.

However, as Fig. 10 reveals, the spectral range in which we were able to detect silicon nanocrystals is limited to an energy range between about 1.9 and 2.45 eV. While the upper bound might be explained by a combination of the decreasing number of very small particles and the fixed excitation energy of 2.54 eV, the lower bound contradicts the range of PL observed in ensemble experiments. Presently this discrepancy is not completely understood but may be related to the increasing (radiative) decay rate (Huiskens 2002) while decreasing the size of the nanocrystals.

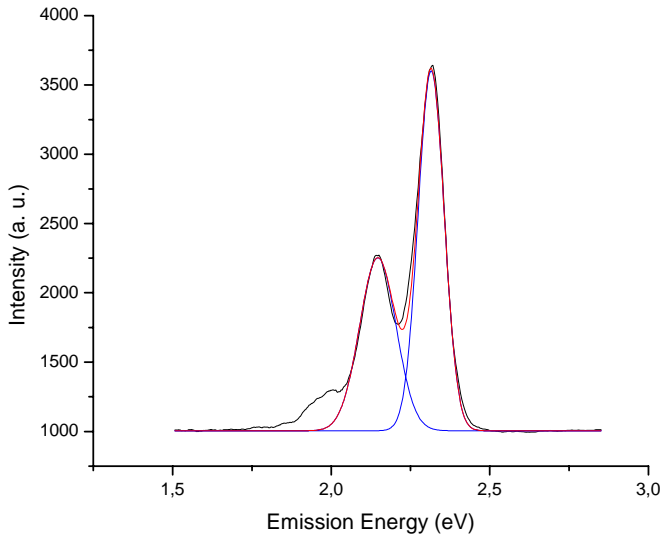


Fig. 13: PL energy of 1 single gas-phase prepared silicon nanoparticle on a quartz substrate. The zero phonon line and the phonon side band have been fitted by two Gaussian lines.

Figs. 11 – 13 show a selection of PL spectra under various conditions. They all have in common, that besides a (zero phonon) band at high PL energies additional bands are observed at lower energies, which are separated from the first band by energies corresponding to about 130 – 160 meV or multiples of these values. Since these splittings are too large to be related to Si phonons we assign them to SiO₂ vibrations of the SiO₂ shell. Corresponding TO- and LO-vibrations have been determined to be close to these values (Sa`ar 2005). However, a comparison of many spectra of single crystals reveals that these frequencies vary from crystal to

crystal and seem also to depend on the crystal preparation or embedding matrix. Even crystals of - according to the PL energy - same size have different dynamic and static properties.

We like to make the point again that we could observe single crystal spectra only over a limited PL range, which – according to quantum confinement models- belongs to Si core diameters between 2 nm and 3 nm. This corresponds to the small diameter range of the size distribution, where we might expect an increased leaking of the excited wave function into the SiO₂ shell. We therefore have investigated the corresponding electron-phonon coupling following concepts adapted from solid state spectroscopy.

3.5.3 Electron-phonon-coupling

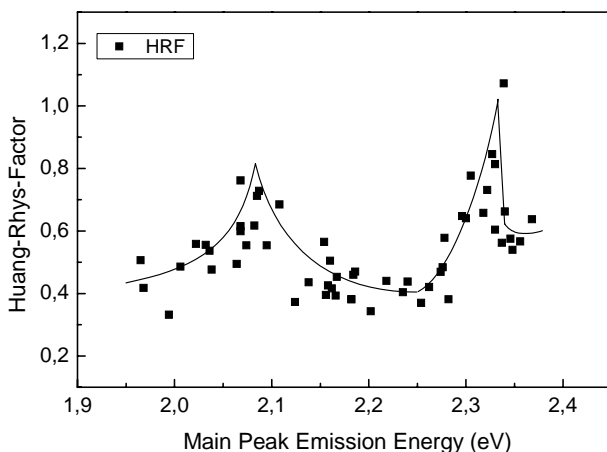


Fig. 14: Huang-Rhys Factor S as a function of PL energy of the zero phonon transition of gas-phase prepared single silicon nanoparticles.

For a series of spectra of gas phase prepared single crystals we have determined the electron-phonon coupling as a function of PL energy. A common way to parameterize the coupling is to determine the Huang-Rhys factor S , which corresponds to the intensity ratio of the first phonon band to the zero phonon band. The results are shown in Fig. 14. Surprisingly, the Huang-Rhys factor S shows two peaks, which are clearly above

the experimental error and close to the maxima of the distribution of particles which has been presented in Fig. 10. Presently we do not have a unique interpretation of the results. But strong evidence is provided that the observed phenomena are related to the localisation of the exciton from the initially excited silicon core into surface or trap states. Related observations have been recently reported (Wolkin 2002, Garrido 2004). Moreover, the similar structure observed in the distribution of PL energies (Fig. 10) and in the distribution of S (Fig. 14) as a function of PL energy indicate that this localisation might occur stepwise, that is via an independent localisation of electron and hole at different PL energies (crystal sizes).

3.5.4 Comparison of various silicon nanocrystals

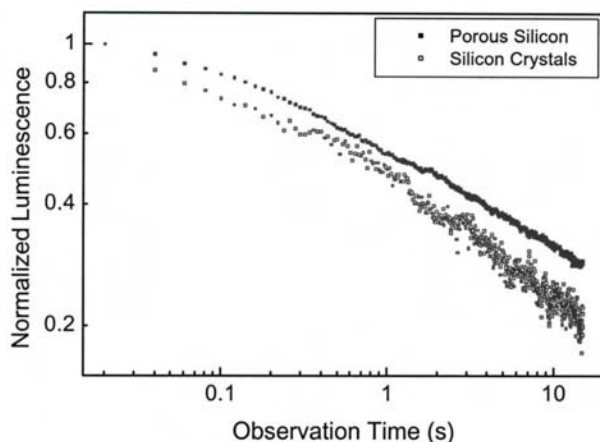


Fig. 15: PL intensity as a function of laser irradiation time of a silicon porous layer (top) and silicon from gas-phase preparation (bottom).

Our experiments have shown that independent of the preparation technique silicon nanocrystals exhibit comparable behaviour both with respect to spectral (see 3.5.2) and dynamic (see 3.5.1) properties.

Despite the differences in core/shell relations both types are obviously subject to very similar photodynamics which are (as can be also seen from Fig. 15) quite similar. Despite the fact that the preparation of porous silicon is a not very well defined chemical procedure and has often risen doubts about features reported for such type of materials our results demonstrate that porous silicon crystals are suitable model compounds to describe silicon nanocrystals.

3.6 Zusammenfassung und Ausblick / Summary and future

In the last period we have collected and modelled photoluminescence dynamics and PL spectra for two types of differently prepared silicon nanocrystals. A comparison shows that there are no principal differences among these two systems. Over a limited range of PL energies silicon nanoparticles could be detected on the single particle level. Comparison of the photodynamics of single particles (blinking) and ensemble (bleaching) showed that with respect to dynamics both ensemble and single particle are subject to generally the same photoinduced processes. These processes are probably also present in interstellar space and might explain the persistence and spectral distribution of ERE emission, since in silicon nanoparticles photoinduced PL quenching is a reversible process being more effective at short PL wavelengths (small particles).

With respect to the spectroscopic behaviour we could only investigate silicon particles above PL energies of 1.9 eV, where we could detect an energy (size) dependent electron-phon coupling to interface vibrations, which is probably accompanied by a step-wise localisation of the exciton.

To investigate the processes at the interface in more detail, we suggest to continue experiments at low temperatures in order to increase spectral resolution. Although intended in the present period we were not able to address this question, since the determination of the electron-phonon coupling turned out to be quite time consuming. Furthermore, a detailed investigation of PL lifetimes on the single particle level will provide more insight into the relation of radiative/non-radiative decay channels.

With respect to astrophysical relevance of silicon nanoparticles we suggest excitation wavelength dependent bleaching experiment at various temperatures in order to provide insight into the PL wavelength dependence of ERE with respect to the spatial proximity of various stellar radiation sources.

3.7 Literatur / References

- Cichos, F., Martin, J., von Borczyskowski, C.: *Characterizing the non-stationary blinking of silicon nanocrystals*, J. Luminesc. **107** (2004a) 160-165.
- Cichos, F., Martin, J., von Borczyskowski, C.: *Emission intermittency in silicon nanocrystals*, Phys. Rev. B **70** (2004b) 1153141- 11543149.
- Fischer, B.R., Eisler, H.-J., Stott, V.E., Bawendi, M.G.: *Emission intensity dependence and single-exponential behaviour in single colloidal quantum dot fluorescence lifetimes*, J. Phys. Chem. B **108** (2004) 143-148.
- Garrido, B.; López, M.; Pérez-Rodríguez, A.; García, C.; Pellegrino, P.; Ferré, R. Moreno, J. A.; Morante, J. R.; Bonafos, C.; Carrada, M.; Claverie, A.; de la Torre, J.; Souif, A. *Optical and electrical properties of Si-nanocrystals ion beam synthesized in SiO₂*, Nucl. Instr. Meth. B. **216** (2004) 213-221.
- Heitmann, J., Müller, F., Yi, L., Zacharias, M. Kovalev, D., Eichhorn, F.: *Excitons in Si nanocrystals: Confinement and migration effects*, Phys. Rev. B **69** (2004) 1953091-7.
- Huisken, F., Ledoux, G., Guillois, O., Reynaud, L.: *Light-emitting silicon nanocrystals from laser pyrolysis*, Adv. Mater. **14** (2002) 1861-1865.
- Issac, A., Cichos, F., von Borczyskowski, C.: *Correlation between photoluminescence intermittency of CdSe quantum dots and self-trapped states in dielectric media*, Phys. Rev. B **71** (2005) 1613021-1613024 (R).
- Ledoux, G., Guillois, O., Huisken, F., Kohn, B., Porterat, D., Reynaud, C.: *Crystalline silicon nanoparticles as carriers for the Extended Red Emission*, Astron. Astro. Phys. **377** (2001) 707.
- Martin, J., Cichos, F., Chan, I. Y., Huisken, F., von Borczyskowski, C.: *Photoinduced processes in silicon nanoparticles*, Isr. Journ. Chem. **44** (2004) 341-351
- Martin, J., Cichos, F., von Borczyskowski, C.: *Spectroscopy of single silicon nanoparticles*, J. Luminesc. **108** (2004) 347-350.
- Martin, J., Cichos, F., von Borczyskowski, C.: *Confocal microscopy of electrostatic properties of Si-quantum dots and silica surfaces by charge sensitive dye molecules*, Opt. Spectr. **99** (2005) 281- 288 and **99** (2005) 297-303.
- Petrov, E.P., Cichos, F., Zenkevich, E.I., Starukhin, D., von Borczyskowski, C.: *Time resolved photoluminescence anisotropy of CdSe/ZnS nanoparticles in toluene at room temperature*, Chem. Phys. Lett. **402** (2005) 233–238.
- Petrov, E.P., Cichos, F., Spange, S., von Borczyskowski, C.: *Investigation of the etherable distilbazolium compounds as fluorescent probes in nanostructured silica sol-gel materials*, Photochem. Photobiol. **81** (2005) 898-907.
- Petrov, E.P., Cichos, F., von Borczyskowski, C.: *Intrinsic photophysics of semiconductor nanocrystals in dielectric media: formation of surface states*, J. Luminesc. **119-120** (2006) 412-417.

- Sa'ar, A.; Reichmann, Y.; Dovrat, M.; Krapf, D.; Jedrzejewski, J.; Balberg, I.: *Resonant coupling between surface vibrations and electronic states in silicon nanocrystals at the strong confinement regime*, Nan. Lett, **5** (2005) 2443-2447.
- Schuster, J., Cichos, F., von Borczyskowski, C.: *Blinking of single dye molecules in various environments*, Opt. Spectr. **98** (2005) 712-717.
- Schuster, J., Cichos, F., von Borczyskowski, C.: *Influence of self-trapped states and photoproducts on the intermittency of single molecules*, Appl. Phys. Lett. **87** (2005) 5195.
- Schuster, J., Cichos, F., von Borczyskowski, C.: *Variation of power-law dynamics caused dark state recovery of single molecule fluorescence intermittency*, SPIE **6358** (2006) 6258041-8.
- Schuster, J., Brabandt, J., von Borczyskowski, C.: *Discrimination of Photoblinking and Photobleaching on the Single Molecule Level*, J. Luminescence 2007, in print.
- Shamirzaev, T.S., Gilinsky, A.M., Bakarov, A.K., Toropov, A.I., Tenne, D.A., Zhuravlev, K.S., von Borczyskowski, C., Zahn, D.R.T.: *Millisecond photoluminescence kinetics in a system of direct-bandgap InAs quantum dots in an AlAs matrix*, JETP Letters **77** (2003) 459-463.
- Shamirzaev, T.S., Gilinsky, A.M., Toropov, A.I., Bakarov, A.K., Tenne, D.A., Zhuravlev, K.S., von Borczyskowski, C., Zahn, D.R.T.: *Model of Photoluminescence of InAs quantum dots embedded in dielectric band gap AlGaAs matrices*, Material Science (2004) 157- 1160.
- Shamirzaev, T.S., Gilinsky, A.M., Toropov, A.I., Bakarov, A.K., Tenne, D.A., Zhuravlev, K.S., von Borczyskowski, C., Zahn, D.R.T.: *Millisecond fluorescence in InAs quantum dots embedded in AlAs*, Physica E **20** (2004) 282-285.
- Smith, Tracy L., Witt Adolf N.: *The photophysics of the carrier of extend red emission*, Astrophys. J. **565** (2002) 304-318.
- Sychugov, I., Juhasz, R., Linnros, J., Valenta, J.: *Luminescence blinking of a Si quantum dot in a SiO₂ shell*, Phys. Rev. B **71** (2005) 113331-5.
- Tang, J., Macus, R.A.: *Diffusion-controlled electron transfer processes and power law statistics of fluorescence intermittency of nanoparticles*, Phys. Rev. Lett. **95** (2005) 107401.
- von Borczyskowski, C., Cichos, F., Martin, J., Schuster, J., Isaac, A. Brabandt, J.: *Common luminescence fluctuations of single particles and single molecules*, Europ. Phys. Journ. in print.
- Witt, A. N., Gordon, K. D., and Furton D. G.: *Silicon nanoparticles as a source of extended red emission*, Astrophys. J. **501** (1998) L111-L115.
- Witt, A.: *Observations of neutral and ionized PAM's in the red rectangle*, Symp. On Interstellar Reactions, Pillnitz (2005).

- Wolkin, M. V., Jorne, J., Fauchet, P. M., Allan, G., Delerue, C.: *Electronic states and luminescence in porous silocon quantum dots: The role of oxygen*, Phys. Rev. Lett. **82** (1999) 197-200.
- Zenkevich, E.I., Shulga, A.M., Petrov, E.P., Cichos, F., von Borczyskowski, C.: *Key-Hole principles and photochemistry of porphyrin self-organization on semiconductor quantum dots*, J. Porphyrins and Phthalocyanines **8** (2004) 4583.
- Zenkevich, E.I., Shulga, A., Cichos, F., Petrov, E., Blaudeck, T., von Borczyskowski, C.: *Nanoassemblies designed from quantum dots and molecular arrays*, J. Phys. Chem. B **109** (2005) 8679-8692.
- Zenkevich, E.I., von Borczyskowski, C.: *Structure and excited state relaxation dynamics in nanoscale self-assembled arrays: Multiporphyrin Complexes, Porphyrin-Quantum Dot Composites.*, SPIE **5849** (2005) 29-40.
- Zenkevich, E.I., Shulga, A.M., Blaudeck, T., Cichos, F., von Borczyskowski, C.: *Competition in the formation of nanosize multiporphyrin complexes and porphyrin-quantum dot heterocomposites*, In: "Physics, Chemistry and Applications of Nanostructures. Reviews and Short Notes to Nanomeeting-2005" (V.I. Borisenko, S. V. Gaponenko, V. S. Gurin, Eds.), World Scientific Publishing Co., New Jersey, London, Singapore, Beijing, Shanghai, Hong-Kong, Taipei, Chennai. 367-370 (2005).
- Zenkevich, E.I., von Borczyskowski, C.: *Photoinduced electron transfer and relaxation in selforganized multipohyrin nanoassemblies* , In: "Fundamental Photoprocesses and Inhomogeneous Broadening of Electronic Spectra of Organic Molecules in Solution", Ed. V.I. Tomin, Slupsk (2006).
- Zenkevich, E.I., Blaudeck, T., Shulga, A.M., Cichos, F., von Borczyskowski, C.: *Identification and assignment of porphyrin-CdSe hetero-nanoassemblies*, J. Luminesc. **122-123** (2007) 784-788.
- Zenkevich, E.I., Shulga, A., Blaudeck, T., von Borczyskowski, C.: *Fabrication and primary photoevents in self-assembled nanocomposites on semiconductor quantum dots and tetrapyrrole Chromophores*, SPIE, in print.
- Zenkevich, E.I. , Blaudeck, T., Abdel-Mottaleb, M., Cichos, F., Shulga, A.M., von Borczyskowski, C.: *Photophysical properties of self-aggregated porphyrin-semiconductor nanoassemblies*, Int. Journ. Photoenergy, in print.

3.1 Bericht Teilprojekt 7

3.1.1 Titel / Title

Wachstum und Zerstörung von kohlenstoffreichen Molekülen und Clustern unter inter- und zirkumstellaren Bedingungen

Growth and destruction of carbon-rich molecules and clusters under inter- and circumstellar conditions

3.1.2 Berichtszeitraum / reported period

01.07.2003 - 31.12.2006

3.1.3 Projektleiter / principle investigator

Gerlich, Dieter, Prof. Dr., Dipl.-Phys., Universitätsprofessor
Institut für Physik, Technische Universität, 09107 Chemnitz

3.2 Zusammenfassung / Abstract

3.2.1 Wortlaut des Antrags / abstract of the proposal

Die Kombination von Speichern und verschiedenen Nachweismethoden mit einem Kohlenstoffstrahl erlaubt es uns, chemische und optische Eigenschaften von Kohlenwasserstoffen $C_nH_m^+$ zu bestimmen ($n < 10000$ and $m \geq 0$). Erste Ergebnisse wurden erhalten für die astrochemisch wichtige Wechselwirkung von H_3^+ mit C_3 . Weiterhin wurden Reaktionen von CH_4^+ , C_3^+ und C_3H^+ mit H_2 und HD untersucht. Für diese kleinen Systeme werden z. Zt. in Zusammenarbeit mit TP 4 und TP 5 die systematischen Untersuchungen bis zu $n = 4$ ausgedehnt. In der kommenden Bewilligungsperiode wird sich dieses Projekt ganz darauf konzentrieren, einzelne Cluster ($n > 50$) bzw. Nanoteilchen in einem Vierpol (4PT, NPMS Technik) zu speichern, mit *in-situ* Nachweismethoden zu untersuchen und physikalisch oder chemisch zu modifizieren. In einem ersten Experiment wird der Nachweis des gespeicherten Objektes auf der Beobachtung von laserinduzierter Schwarzkörperstrahlung beruhen. Die spektrale Zerlegung des bei verschiedenen Temperaturen emittierten Lichts erlaubt es, optische Konstanten und ihre Abhängigkeit von Größe und

Struktur zu bestimmen. Weitere Untersuchungen basieren auf der Veränderung des isolierten, gespeicherten Teilchens durch Anlagerung von weiteren Kohlenstoffatomen, thermischer Relaxation, Heizen bis zum Massenverlust oder chemische Modifikation wie Oxydation, vor allem aber die *in situ* Anlagerung von Wasserstoff. Perspektivisch sollen Methoden entwickelt werden, die die Beobachtung von Photolumineszenz und über Massenverlust die Aufnahme von IR Absorptionsspektren erlauben.

The combination of ion or particle traps and various detection schemes with a carbon beam, allows us to study chemical and optical properties of hydrocarbons $C_nH_m^+$ ($n < 10000$ and $m \geq 0$). Recently, results have been obtained for the astrochemically important interaction of H_3^+ with C_3 . In addition various products have been detected from the reactions of CH_4^+ , C_3^+ and C_3H^+ with H_2 and HD. For these small systems, the studies are presently extended to $n = 4$ in cooperation with TP 4 and TP 5. In the next funding period the main aim of this project is to concentrate on *in-situ* characterization and modification of clusters or nanoparticles stored in a quadrupole trap (4PT, NPMS technique). In a first approach, detection shall be based on observation of laser induced black body radiation. Spectral analysis of this emission for various temperatures will provide information on the optical constants and their dependence on the particle size and structure. Future experiments shall be based on modifying trapped objects by adding or removing C atoms, thermal annealing, or on other chemical modifications changes such as oxidation or hydrogenation. There are plans, to observe photoluminescence and to develop techniques for recording IR absorption spectra, based on mass loss of physisorbed atoms or molecules.

3.2.2 Zusammenfassung des Berichts / abstract of the report

The aim of TP 7 was to study the formation and destruction of carbonaceous material under inter- and circumstellar conditions, including simple hydrocarbon ions, a neutral carbon beam and carbon nanoparticles. For this purpose, four different rf devices have been used, a ring electrode trap, a 22pole trap, a guided ion beam arrangement, and, in ongoing experiments, a new quadrupole trap. One of the challenges was to provide an intense carbon beam. For this purpose, a graphite sublimation source has been combined successfully with the other modules. For the first time, it became possible to study collisions between stored ions and small neutral carbon molecules C_n ($n = 1-3$). Results for $D_3^+ + C_3$ revealed that D^+ transfer dominates over all other exothermic product channels. Formation of C_3D^+ is almost twice as slow as assumed in astrophysical models.

In order to extend our knowledge about ion chemistry involving three carbon atoms, reactions of C_3^+ , C_3H^+ and $C_3H_3^+$ with H_2 and HD have been studied between room temperature and 15 K. A large set of data which is important for understanding the hydrocarbon astrochemistry, has been summarized in the PhD thesis of Igor Savić (2004) and in several publications. Many unexpected results have been obtained. For example, the low temperature reactivity of C_3^+ indicates that C_3^+ is floppy. One explanation is a low energy pseudorotation of a cyclic structure. This idea has been corroborated by very recent *ab initio* calculations (Rosmus 2006). For $C_3H^+ + HD$ collisions, a huge isotope effect has been discovered: formation of C_3HD^+ is over one hundred times faster than of $C_3H_2^+$.

During this funding period, a significant step forward has been made with the optical detection of stored nanoparticles, one of the main aims of TP 7. Combining an octopole with an efficient optical system, we succeeded to record *in situ* the black body radiation from a cloud of C_{60}^+ molecules which have been heated to temperatures above 3000 K with a pulsed laser. The correlation of the decay via C_2 loss and radiative cooling with the temperature is discussed. These experiments which are continued, open up new methods to study chemistry at very high temperatures. Presently, a quadrupole trap and a CW laser is implemented in order to reach stationary conditions. In parallel to the activities in Chemnitz, co-operations with several groups have been started in order to contribute to the initial goals of TP 7.

3.3 Ausgangsfragen, neuester Stand der Forschung / Initial goals, current status of the field

In the first proposal of TP 7, many different experimental activities have been proposed to study carbonaceous material under inter- and circumstellar conditions. The goals included gas phase collisions with neutral carbon atoms, chemistry of carbon anions, singly and multiply charged C_{60} ions and nanometer-sized carbon particles. The ambitious research plan was based on the combination of the experiences accumulated in the group *Gasentladungs- und Ionenphysik* with those of an assistant, who joined the group in 1999. Several problems (see below) forced us in the second funding period, to reorganize our FGLA projects. As described also in its final report, we decided that TP 5 should concentrate on gas phase reactions, mainly with H atoms, while TP 7 should focus on optical detection of stored nanoparticles.

Despite the large effort undertaken in many laboratories (we just mention here just Joblin *et al.* 2006), investigations of the structure and reactivity of large hydrocarbon molecules at inter- and circumstellar temperatures remain sparse. Concerning gas phase reactions, the current status of the field has been summarized in our recent publications (Savić *et al.* 2005a-c, 2006a,b). The wealth of our new data leads to the conclusions that the description of hydrocarbon reactions under interstellar conditions has to be revised and that more low temperature studies are needed to provide reliable data for astrochemical databases. Stimulated by this and other activities (see TP 5) a new project has been started recently in collaboration with the university of Arizona. In the center is the construction of a new machine similar to ours (see Fig. 10 in the report of TP 5). It is supported by an NSF grant (PI: Mark A. Smith, University of Arizona) and an NSF CRIF-Instrument Development grant (Co-Investigator D. Gerlich).

Another motivation at the beginning of TP 7 was to learn more about optical properties of carbon molecules and carbon containing compounds. They are certainly responsible for many absorption and emission features of the interstellar medium, e.g. the diffuse interstellar bands (DIBs), the interstellar extinction hump at 217 nm, or emission bands in the infrared. In the past three years a new apparatus has been developed in Basel in the group of John Maier in collaboration of with us (Dzhonson *et al.* 2006). The primary aim of this experiment is to measure electronic spectra of large ions at low vibrational and rotational temperatures, as of relevance to astronomical observations. One special example of mutual interest is to record an optical spectrum of stored C_{60}^+ ions which has been observed so far only in a matrix (Maier 1994).

A third field of interest is to study the interaction of charged hydrocarbons with UV and FUV light. In this context we mention here briefly a proposal by M. Tulej (2006) who intends to create, modify and detect large nanosized singly and doubly charged hydrocarbons by combining synchrotron radiation, ion spectroscopy, and the ion trapping and cooling technology, developed in our laboratory. The main task of this project is the preparation and subsequent analysis of large charged hydrocarbon compounds involving 20 to 200 carbon atoms including hydrocarbon chains and polycyclic aromatic molecules (PAHs) by using of tunable VUV radiation.

In summary one can say that our initial goals have been reached only in part; however, they have stimulated many new initiatives in the field of carbonaceous astrochemistry.

3.4 Angewandte Methoden / Applied methods

3.4.1 RF and AC trapping

TP 7 has utilized a variety of rf and ac traps and ion guides for studying carbonaceous material under inter and circumstellar conditions - ranging from simple hydrocarbon ions to nanostructures (Gerlich 2004). Making use of the modular design, specific ion and particle sources have been combined with neutral beams and rf devices. Fig. 1 shows the arrangement of a carbon sublimation source and a ring electrode trap. Technical details and many fundamental results have been described by Savić *et al.* (2005a). The trap has been operated between 80 K and room temperature; however, it also can be heated to higher temperature (up to 800 K) in order to simulate conditions of circumstellar discs.

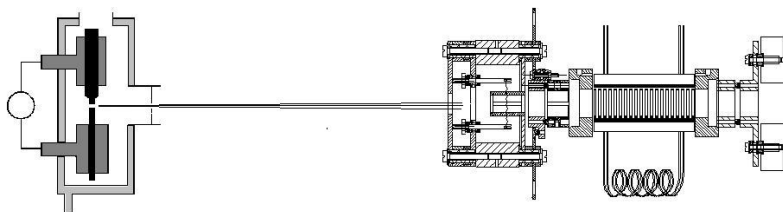


Fig. 1: Schematic diagram of the combination of a carbon evaporator and an ionizer with a ring electrode trap. For analysis, the trapped ions are extracted, mass selected and detected with a Daly type detector (to the right, only the entrance of the QPMS is indicated). The parts are at scale with exception of the distance between the carbon rods and the trap which is 40 cm (the inner diameter of the trap is 1 cm). In the trapping volume C_3 number densities up to $2 \times 10^8 \text{ cm}^{-3}$ have been reached.

Another series of experiments (Savić *et al.* 2005b,c and 2006a,b) has been performed in the temperature variable 22PT which has been described thoroughly in the literature (see Gerlich 1995 and related references in TP 4 and TP 5).

The Guided Ion Beam arrangement

In order to gain more experience with monitoring hot carbon nanoparticles via photo emission, we have used the well-tested Guided Ion Beam arrangement (GIB) shown in Fig. 2. Via a window and an large optical system (see Fig. 3), light emitted from confined ions can be detected quite efficiently. Originally such an arrangement has been used for monitoring chemiluminescent ion-molecule reactions or photons induced

by a laser (Gerlich 1992). In the present experiment we follow the black body radiation emitted from laser heated particles.

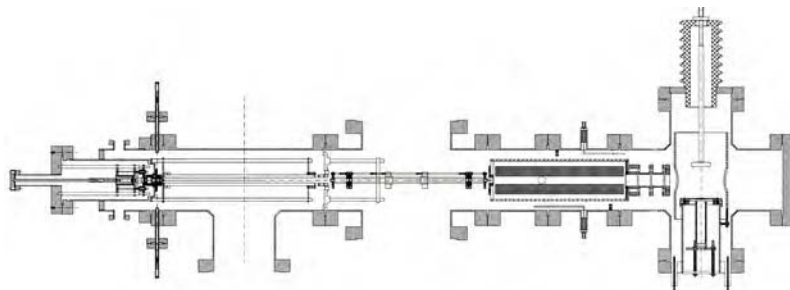


Fig. 2: An octopole ion guide is used in the center of the arrangement for optimizing the optical detection system which has been constructed for monitoring laser heated carbon structures via black body emission.



Fig. 3: The optical detection system uses a photomultiplier (R1527P) for single photon detection. The quantum efficiency is 10 %, the visible trapping volume is also about 10% of total storage volume, and the collection efficiency for photons is 2% (through the octopole rods).

The tests which have been performed with C_{60}^+ ions created from gaseous C_{60} in a sublimation oven via electron impact ionization, are described below.

The SRE-4PT

The ultimate goal of this experiment is to monitor, characterize, and modify for long time just one single carbonaceous nanoparticle which is localized in a quadrupolar field. A technical development which is well-suited for this purpose is the high-resolution nanoparticle mass spectrometer (HR-NPMS) developed in our laboratory. It is based on long time trapping of one charged object in a three-dimensional quadrupole field and on non-destructive optical detection (Schlemmer *et al.* 2004,

Gerlich 2004, Grimm *et al.* 2006). The charge to mass is derived from observing and evaluating the oscillatory motion in the trap. This allows one to record very precisely changes of the charge and gain or loss of mass.

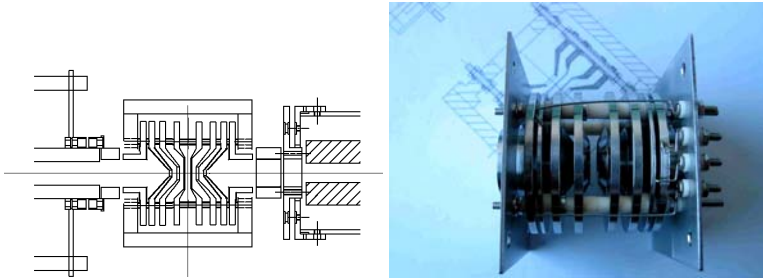


Fig. 4: There are various electrode arrangements to approximate the Paul trap, i.e. the ideal boundary conditions of a quadrupolar field. The depicted design (Decker 2007) which is rotationally symmetric, has many advantages in comparison to electrode arrangement used previously (Ille-
mann 2000).

The innovative technique, however, still needs a lot of investment and effort. Many attempts have been made to improve the geometry (see Fig. 4). Presently we favor arrangement which is rotationally symmetric and where the central electrode (the ring electrode in the quadrupole) is approximated by two rings. So far, the particle has been illuminated by a visible laser and detected via the scattered light. Due to the size dependence of the scattering cross section, this detection scheme is limited to particles larger than 50 nm. In the present project, thermal emission at high temperatures is used for monitoring the trapped object. More details are given below.

The HR-NPMS technique can be used in material science, in aerosol analysis or "just as a scale" in fg-mass spectrometry. In the present project it is used especially for studying astrophysical dust analogous. The special benefit of this techniques lies in the isolation of the particle with respect to disturbing surfaces and gases, i.e., UHV- and low temperature conditions, and in a very good localization of the particle (in principle better than 1 μm). This makes it perfectly suited to sensitive optical detection (scattering, fluorescence, absorption, non linear processes).

Carbon source

An important experimental progress made in this TP was the integration of a graphite sublimation source (see Fig. 1) into a trapping machine. The early version of the arrangement has been described by Čermák *et al.* (2002). There are various standard methods to form a carbon beam, based on laser ablation of carbon rods, sublimation of graphite, or evaporation of suitable carbon containing compounds. The carbon source used in this project has been described in detail by Decker (2003), Savić (2004), and Savić (2005a). It was developed originally in Krätschmer's group in Heidelberg for spectroscopic studies on matrix-isolated carbon molecules (Čermák *et al.* 1998). Only minor changes have been made on the basic design while the control of the source parameters has been improved leading to a better longtime stability.

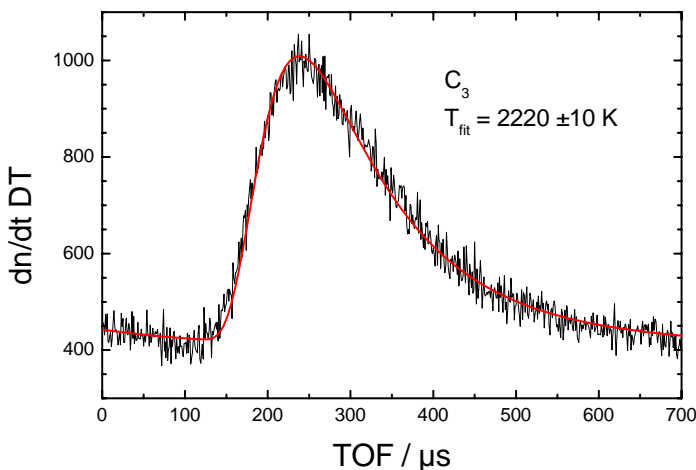


Fig. 5: Measured TOF distribution of C_3 emerging from the resistively heated carbon rod. The red line is a fit with $T = 2220$ K. This value is in accordance with the surface temperature measured with a calibrated pyrometer.

Recently an universal detector has been used to determine the composition and velocity distribution of the carbon cluster beam. The results, $80 \pm 8\%$ C_3 , $8 \pm 2\%$ C_2 , and $12 \pm 6\%$ C , are in good accordance with the distribution determined in the trap using proton transfer from H_3^+ (chemical probing). In the ion trap (= interaction region, see Fig. 1) which is 40 cm away from the carbon rods, one obtains a number density of some 10^8 cm^{-3} .

There are various physical properties which have been used for characterizing the operating conditions of this carbon source. One of them is the rod resistance which is measured via a four-point scheme. There are other parameters such as surface temperature, total flux, cluster composition or velocity distribution. A not expected observation was that the material is ejected in intense quasiperiodic pulses with a few Hz (Decker 2003).

The TOF distributions measured recently (see Fig. 5) have revealed that the translational temperature of the beam is 2220 K. This is in accordance with the surface temperature measured with a pyrometer. This and the pulsed nature is a hint that the emitted carbon flow does not sublimate directly from the surface area of the rods. Whether the quasiperiodic eruptions are due to high pressure carbon gas in small cavities or liquid bubbles produced inside of the rods, is still uncertain. More studies are in progress in collaboration with I. Savić and W. Krätschmer.

3.4.2 Project organization, challenges and problems

As discussed in more detail in the report of TP 5 (Section 3.4) we have tried during the first funding period to operate, in a cooperative way, three separate machines devoted to a variety of specific research projects. For several reasons, ranging from lack of technical support to loss of know-how in the group, the resulting expectations were too high, especially since TP 7 intended to cover a wide field reaching from molecular to solid state physics, and including anorganic and organic chemistry.

Looking back it seems to be obvious that our group of researchers was too small for making the progress which has been promised seven years ago. A key problem in TP 7, however, was caused by the fact that Dr. I. Čermák, who has joint the TUC in 1999 and who has stimulated the ambitious carbon proposal, became sick in summer 2002. Unfortunately, he could not come back to work until his contract as assistant ended in February 2005. He did not contribute at all to put together the report in 2003 and to the proposal for the second funding period. Nonetheless the graduate student, I. Savić, finished his PhD successfully, in part with work performed on a different apparatus (Savić 2004). The remarkable progress made on the carbon trapping machine in the last years is mainly due to the graduate student S. Decker who started with his PhD work in 2004.

3.5 Ergebnisse und ihre Bedeutung / Results and their importance

The astrophysical motivation for the experiments of this project is to contribute to our understanding of growth and destruction or chemical modification of carbonaceous structures. The experiments we have performed are relevant as well for the chemistry of cold interstellar molecular clouds as well for processes occurring in hot and dense circumstellar environments (see Fig. 6 for illustration).

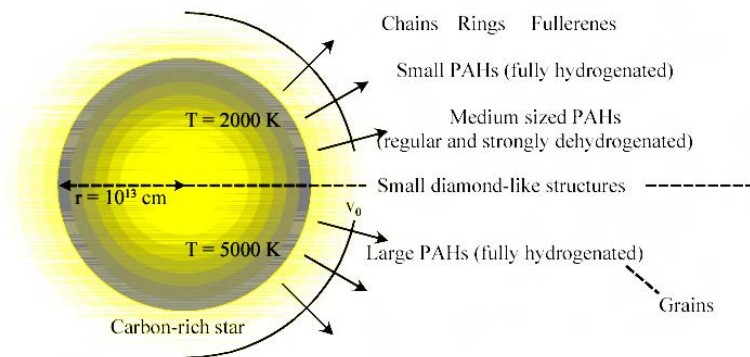


Fig. 6: Summary of typical carbon molecules and clusters formed in the outer atmosphere of a carbon-rich star (Pascoli and Polleux 2000). Many molecules are formed in stellar outflows, where the emitted material cools from 5000 K or higher down to 50 K and where the number density goes from about 10^{12} cm^{-3} to 10^6 cm^{-3} . Some more details are discussed in the thesis from Savić (2004).

Reactions with C_n

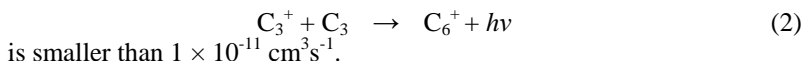
Exchange or association reactions with neutral carbon atoms and molecules play an essential role in the chemistry of interstellar clouds and of circumstellar discs; however, performing related laboratory work is an experimental challenge. During the FGLA, an experimental set-up has been developed for the first time which allows us to study collisions between trapped ions and carbon molecules C_n ($n = 1-3$) and . The machine which uses a ring-electrode trap (RET) is shown schematically in Fig. 1. Concerning description of experimental details we refer to Savić (2004) and Savić *et al.* (2005a). Specific test measurements have been summarized recently by Savić *et al.* (2006a).

Results for two classes of reaction systems have been included in Savić *et al.* (2005a): reactions with D_3^+ and with carbon ions. An impor-

tant observation is that, in collisions of D_3^+ with C_n , deuteron transfer dominates over all other exothermic product channels, i.e.,



Despite this preference, the absolute rate coefficients for forming C_nD^+ are a factor two smaller than the values used in astrophysical models. The collision systems $C_m^+ + C_n$ are important for the growth of pure carbon chains or rings, also via radiative association. First results indicate that, also in this case, the rate coefficients are much slower than generally assumed. Due to the weak signal, only upper limits could be determined. Accounting for the sensitivity of the apparatus we concluded that the association rate coefficient for

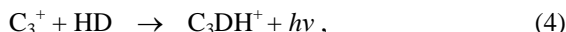


Reactions of $C_mH_n^\pm$

One of the motivations to study in more detail reactions involving three carbon atoms, was the large abundance of the C_3H_2 molecule and its deuterated variants observed in dark interstellar clouds. In order to improve the input data of astrochemical models, a large table with results for reactions of $C_3H_n^+$ with H_2 and HD has been published by Savić and Gerlich (2005b). Many results have been unexpected, e.g. the reaction



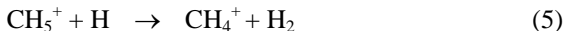
is 6 times faster ($k = 9.3 \times 10^{-10} \text{ cm}^3 \text{ s}^{-1}$) than previously assumed. For the first time a radiative association process,



has been observed in a small reaction system with a competing exothermic channel ($k_r = 6 \times 10^{-11} \text{ cm}^3 \text{ s}^{-1}$). The reaction system $C_3H^+ + H_2$ shows a strong temperature dependence. In $C_3H^+ + HD$ collisions an incredible isotope effect has been discovered favoring deuteration. Some additional aspects on the various routes in forming hydrocarbon ions with three carbon atoms and deuterated variants under interstellar conditions have been summarized recently (Savić and Gerlich 2006b). One of the general conclusions from all the new results is that, in contrast to the general opinion that such systems have been well studied, more systematic studies of carbon clusters are needed, especially over a wide range of temperatures.

Although it is very important to go to larger systems ($m > 3$) there are still open questions for $m = 1$ and $m = 2$. Some of them have been

mentioned in the reports of TP 4 and TP 5. Reactions of $C_2H_3^+$ or $C_3H_2^+$ with H are still pending. A special role plays protonated methane, CH_5^+ . Of astrochemical importance is its formation via radiative association of CH_3^+ with H_2 (Gerlich and Horning 1992) and its destruction via



which is discussed in TP 5 (Borodi *et al.* 2007). Very interesting, from a fundamental point of view, is also the reactivity and the structure of this hypercoordinated carbocation, characterized by a two electron – three center configuration. A summary of collision experiments which provide information on the structure of CH_5^+ ions and deuterated variants has been published recently (Gerlich 2005a). A big step forward was the first global IR spectrum mentioned in TP 4. Also these results can be found in the literature together with new calculations (Asvany *et al.* 2005).

Carbon at high temperatures

As illustrated in Fig. 6 carbonaceous material can grow in stellar environments to large structures including fullerenes, PAHs, HACs, or graphite like particles. In addition to the gas phase work described above, it was the aim of TP 7 to study growth, destruction and chemical modification of large carbonaceous structures ($1 \text{ nm} < d < 100 \text{ nm}$) at high temperatures. For this purpose two experimental arrangements described above (Section 3.4) have been constructed. The experimental strategy is based on the combination of destructive (QPMS) or non-destructive (NPMS) mass spectrometry with optical detection, i.e. monitoring and characterizing the hot trapped particles via blackbody radiation. The spectral distribution of the light allows directly to get a measure for the mean excitation energy (\sim temperature) of the trapped ions or nanoparticles.

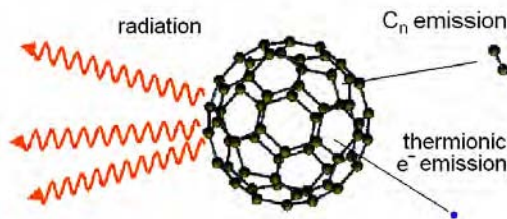


Fig. 7: Laser heated carbonaceous structures are studied in an octopole trap by measuring a correlation between the black body radiation and mass or charge loss. Under the conditions of our experiments, thermionic emission is negligible.

For testing the experimental setup, C_{60}^+ ions have been produced by electron bombardment of C_{60} in the sublimation source shown in Fig. 2. After mass selection, the ions are trapped in the linear rf octopole using suitable potentials on two ring electrodes. For heating the stored ensemble a pulsed Nd:YAG laser has been used (Continuum Powerlite 9030, wavelength $\lambda=1064$ nm, pulse width 10 ns, repetition rate 30 Hz, beam diameter of 2 mm). The laser beam passes nearly parallel through the machine in axial direction. Intensities up to 10^8 W/cm² have been used.

The octopole trap has been filled 30 times a second with some thousand ions per cm³ each time. After a trapping time of 5 ms, the laser has been fired; however, only every second time for background subtraction. Following the excitation with an IR pulse (energy 10 - 30 mJ), the hot ions are stored for another 5 ms. During this time the emitted photons are detected with a multi-channel scaler in the two wavelength regions, 380 nm - 460 nm and 455 nm - 700 nm,. Based on a dielectric model and accounting for the geometry, detection efficiencies etc., temperatures have been determined by simulating the emission in the two different spectral ranges. A typical result is shown in Fig. 8.

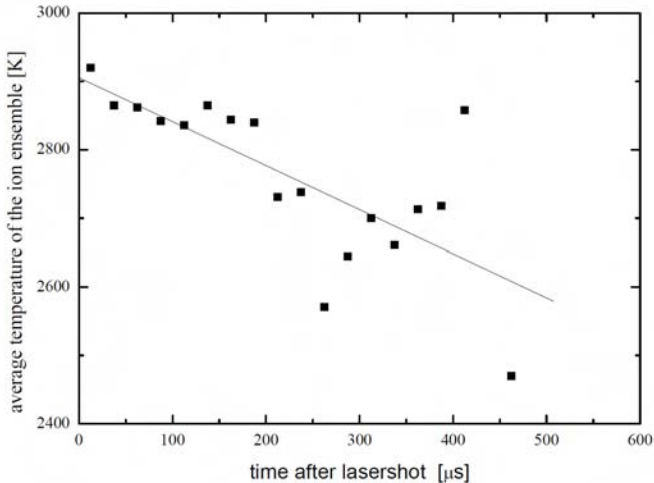
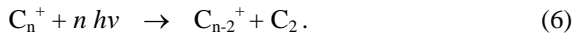


Fig. 8: Temperature drop of C_{60}^+ ions heated with a 10 ns IR laser pulse. The temperature has been derived from thermal emission recorded in two wavelength ranges. The straight line is the result from a model calculation explained in the text.

The highest temperatures observed with the time resolution used ($>10 \mu s$) was always below 3000 K although the energy content of the ions certainly gets higher during the laser pulse. The reason is efficient cooling of the hot ions via sequential emission of C_2 molecules,



Mass analysis of the stored ions corroborates this. As an example, Fig. 9 shows the number of various C_n^+ fragments after heating the stored ensemble with single laser pulses with energies between 10 mJ and 30 mJ.

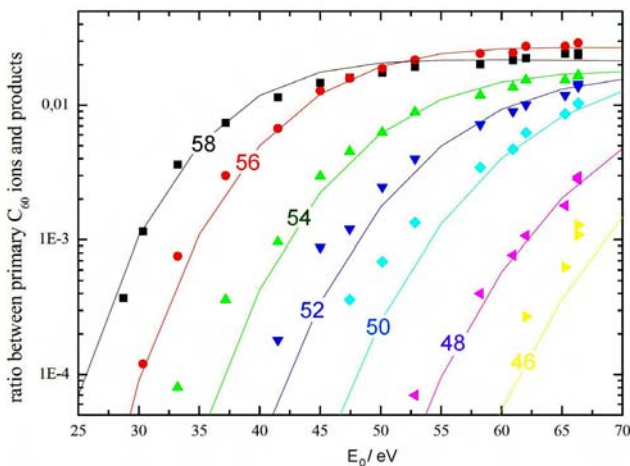


Fig. 9: Number of C_n^+ fragments ($n = 58, 56 \dots$) measured relative to the injected number of C_{60}^+ as a function of the internal energy E_0 , calculated from the mean laser energy per pulse (see Eq. 7). The solid lines indicate that the experimental data can be nicely simulated with a kinetic model which is based on sequential C_2 emission.

From an experimental point of view it is important that there is quantitative agreement between the loss of C_{60}^+ and the sum of fragments. This indicates that the trapping potential was high enough to confine also the fragments accelerated by the laser induced fragmentation process. In some measurements Helium buffer gas up to 10^{-5} mbar has been used; however, no significant additional cooling or relaxation has been observed. Emission of a second electron from C_{60}^+ can be neglected at the conditions of our experiment.

Hot fullerene neutrals, cations and also anions have been investigated rather often in the last decade using sophisticated experimental

methods (Mitzner and Campbell 1995, Wörgötter *et al.* 1996, Concina *et al.* (2005), Hertel *et al.* (2005), Bekkerman *et al.* (2006)). From the point of view of the technology the Aarhus storage ring experiment is somewhat related to our approach (Tomita *et al.* 2001, Andersen *et al.* 2001). The observations are usually analyzed using more or less complex simulations. They account, often in a simplified way, for the heating processes, the evolution of the internal energy, cooling via blackbody radiation, and ejection of particles. A critical inspection of the publications and the reported parameters reveals that the model calculations always have enough free parameters to obtain satisfying agreement between observations and simulation. Also our data can be nicely approximated as can be seen from Fig. 8 and Fig. 9. In our simulations, the simple linear relationship between the mean energy of the laser pulse, E_{hv} , and the obtained internal excitation E_0 is used,

$$E_0 / \text{eV} = 2.7 \times E_{hv} / \text{mJ} + 18 . \quad (7)$$

As common in the literature, photon emission is described with a simple dielectric model while C_2 loss is calculated with the Arrhenius like expression

$$k = A \exp(-E_b/kT) . \quad (8)$$

For A and E_b we have used the parameters published by Concina *et al.* (2005), e.g. $A = 1.2 \times 10^{21} \text{ s}^{-1}$ and $E_b = 10.7 \text{ eV}$ for C_{60}^+ . Earlier experiments have used $A = 2 \times 10^{19} \text{ s}^{-1}$, lowering the dissociation energy by 0.8 eV. The rather large uncertainties in the pre-exponential factors and the binding energies may be caused by non-equilibrium conditions in various experiments. As illustrated by the model calculation shown in Fig. 10, a special problem is the very fast sequential decay of highly excited ions.

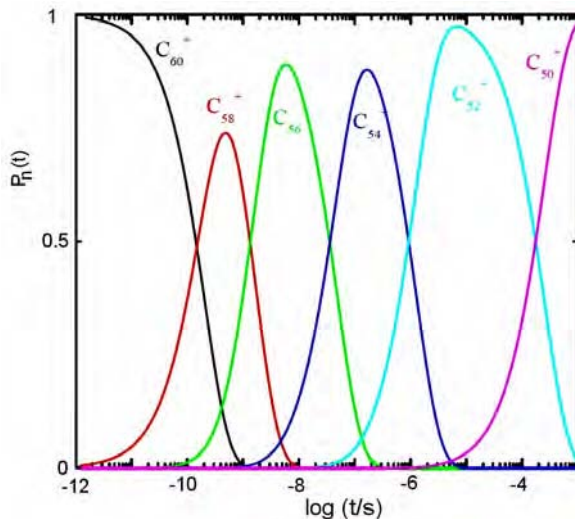


Fig. 10: Simulation of the sequential decay of a C_{60}^+ ion starting at $t = 0$ s with an internal energy of $E_0 = 65$ eV. The calculation is based on reaction (6), Eq. 8, and the assumption, that emission of a C_2 reduces the total energy just by its binding energy.

The main conclusion from our experiment (and also from others) is that better strategies are needed in order to understand the high temperature chemistry of carbonaceous material. Heating an ensemble of molecules by a pulsed laser or by particle bombardment often leads to uncertain or even ill-defined initial conditions. A better approach is to confine the particles in a trap for long times and to heat them using a continuous laser beam.

Recently the 8PT in the machine shown in Fig. 2 has been replaced by the quadrupole trap described above. This allows for very good localization of the C_{60}^+ ensemble. Estimates indicate that a continuous CO_2 laser beam with up to 20 W, focused to 100 μm , is sufficient to maintain a stationary equilibrium at temperatures up to of 3000 K. The wide range of storage times and the sensitivity of the trapping technique will allow us to record decay rates between $0.001 s^{-1}$ and $1000 s^{-1}$. Presupposing that Eq. 8 and the parameters reported by Concina *et al.* (2005) are correct, this corresponds to temperatures between 2237 K and 3061 K, respectively. Such experiments are well suited to determine reliable thermochemical values. A fundamental question is whether the concept of a temperature is ade-

quate at all for describing an ensemble of non-interacting C_{60}^+ ions or a single isolated carbon nano-particle stored in a laser beam.

There are many other interesting applications of the new instrument. Maintaining a stationary state at low decay rates will allow for recording precisely the emission spectrum of nanoparticles and provide optical constants for astrophysical models of hot regions. Inert buffer gas will introduce another weak cooling mechanism which can be studied in detail. The use of molecular gases such as methane or acetylene leads not only to collisional cooling but also to dissociation and chemical reactions. It is planned to determine the deposition rate of carbon at high temperatures. Finally, the combination of the carbon source with the trap will allow us to investigate in temperature depended growing rates, a process of huge importance for the chemistry of carbon rich stars.

3.6 Zusammenfassung und Ausblick / Summary and future

Durch seine chemische Vielfalt ist Kohlenstoff ein faszinierendes Atom. Da es außerdem das häufigste nichtflüchtige Element im Universum ist, spielt es eine wichtige Rolle in der Astrochemie. Das Hauptziel des TP 7 war es, die Bildung und Zerstörung von einfachen Kohlenstoffketten, Kohlenwasserstoffen und Nanoteilchen im Labor unter inter- und zirkumstellaren Bedingungen zu verfolgen. Dies wurde durch den Einsatz von verschiedenen innovativen Speichertechniken ermöglicht, einem Ringelektrodenspeicher, einem 8-Pol und einem 22-Pol, und einer neuen Vierpolfalle. Eine besondere Herausforderung war der Aufbau eines Kohlenstoffstrahls und seine Integration in eine Ionenspeicher-Apparatur. Damit konnten erstmals Ratenkoeffizienten für Reaktionen zwischen Ionen und neutralem Kohlenstoff C_n ($n = 1-3$) unter zirkumstellaren Bedingungen gemessen werden, z.B. für den Protonentransfer in $H_3^+ + C_3$ Stößen. Um unser Verständnis der Bildung von einfachen Kohlenwasserstoffen mit drei C-Atomen zu vertiefen, wurden umfangreiche Untersuchungen zu Reaktionen von C_3^+ , C_3H^+ und $C_3H_3^+$ mit H_2 and HD durchgeführt. Viele der gemessenen Ergebnisse waren überraschend. Es zeigte sich z. B., dass selbst einfache Fragen noch nicht geklärt sind, wie z.B. die Struktur von C_3^+ , ganz zu schweigen von einem Spektrum unter interstellaren Bedingungen. Ein anderes Beispiel betrifft einen extremen Isotopeneffekt: Die Bildung von C_3HD^+ in $C_3H^+ + HD$ Stößen ist über 100 mal wahrscheinlicher als die von $C_3H_2^+$. In der Astrochemie sind H und D auf keinen Fall chemisch äquivalent!

Neben einfachen Gasphasenexperimenten wurde damit begonnen, nanometergroße Kohlenstoffteilchen in einer Falle zu speichern. Der Nachweis basiert auf dem Heizen mit einem infraroten Laser und der Beobachtung der resultierenden Schwarzkörperstrahlung. Die spektrale Zerlegung des bei verschiedenen Anregungsenergien emittierten Lichts erlaubt es, die Temperatur, optische Konstanten und ihre Abhängigkeit von Größe und Struktur zu bestimmen. Erste erfolgreiche Testmessungen wurden an einem Ensemble von C_{60}^+ Ionen durchgeführt, die in einem Achtpolspeicher mit einem gepulsten Laser auf bis zu 5000 K geheizt wurden. Eine detaillierte Analyse des emittierten Lichtes und des Abdampfens von C_2 zeigte, dass derartige Experimente im stationären Strahlungsgleichgewicht durchgeführt werden müssen. Daran wird gegenwärtig gearbeitet. Neben der Bestimmung von astrochemisch wichtigen Daten soll dabei auch in Zukunft der grundsätzlichen Frage nachgegangen werden, ob die Temperatur eines einzelnen gespeicherten Nanoteilchens überhaupt sinnvoll definierbar ist.

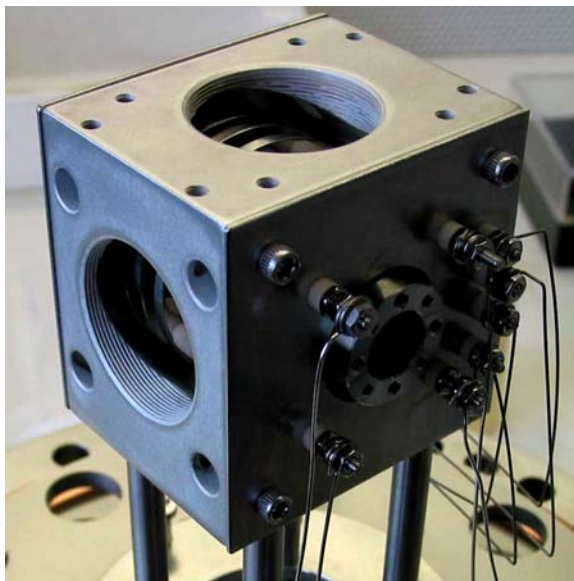


Fig. 11: The new quadrupole trap which is described in Section 3.4 and shown in Fig. 4 is nearly ready. It is especially designed for optical applications.

Future

There are many other questions which can be answered using the experiences gained in TP 7. With the high sensitivity of the trapping technique one can proof whether cyclic carbon cluster ions are really non-reactive in dense clouds. Important for astrochemical applications is a systematic study of adding low velocity H atoms to cold $C_mH_n^+$ ions via radiative association (see TP 5). An even more complex project is the *in situ* synthesis of branched carbon structures by adding carbon atoms to cold trapped ions. First tests performed into this direction indicate the feasibility of such experiments. Very interesting from a dynamical point of view is C_3 elimination, observed for C_6^+ and $C_8^+ + D_2$. Such and many more interesting projects are in the focus of the new instrument which is, with our contribution, under construction in Tucson (see Fig. 10 of TP 7)

One of the most innovative technique which has been developed in our group is the combination of quadrupole trapping and optical detection. In TP 7 a significant step forward has been made by replacing the optical detection scheme, which was based exclusively on light scattering by *in situ* observation of the dust analogue via laser heating and black body radiation. A new trap which is especially suited for optical experiments has been finished (Fig. 11). It can be foreseen that this instrument will provide new insight into the role of hot carbon particles.

3.7 Literatur / References

- Andersen, J. U., Gottrup, C., Hansen, K., Hvelplund, P., Larsson, M. O.: *Radiative cooling of fullerene anions in a storage ring*, Eur. Phys. J. **17** (2001) 189-204.
- Asvany, O., Kumar, P., Hegemann, I., Redlich, B., Schlemmer, S., and Marx, D., *Understanding the LIR Infrared Spectrum of Bare CH_5^+* , SCIENCE **309**, (2005) 1219-1222.
- Bekkerman, A., Kolodney, E., von Helden, G., Sartakov, B., van Heijnsbergen, D. Meijer, G.: *Infrared multiphoton ionization of superhot C_{60} : Experiment and model calculations*, J. Chem. Phys. **124**, (2006) 184312.
- Borodi, G., Luca, A., Gerlich, D.: Collisions of cold trapped CH_5^+ ions with a slow H atom beam, in preparation (2007).
- Čermák, I., Förderer, M., Čermáková, I., Kalhofer, S., Stopka-Ebeler, H., Monninger, G., Krätschmer, W.: *Laser-induced emission spectroscopy of matrix-isolated carbon molecules: Experimental setup and new results on C_3* , J. Chem. Phys. **108** (1998) 10129.
- Čermák, I., Savić, I., and Gerlich, D.: *Ion-trapping apparatus for studies on reactions between ions and neutral carbon species*", WDS'02 Proceedings of Contributed Papers, Part II, Safrankova (ed), Matfyzpress, (2002) 281-287.
- Concina, B., Gluch, K., Matt-Leubner, S., Echt, O., Scheier, P., Märk, T.D.: *Metastable fractions and dissociation energies for fullerene ions C_n^+ $42 < n < 70$* , Chem. Phys. Lett. **407** (2005) 464 - 470
- Decker, S.: *Temperaturbestimmung von elektrisch- und lasergeheizten Kohlenstoff-Teilchen*, Diplomarbeit TU Chemnitz (2003).
- Decker, S.: *Glühender Kohlenstoff: von C_{60}^+ über Russ bis Stäben*, PhD Thesis, TU Chemnitz (planned for 2007)
- Dzhonson, A., Gerlich, D., Bieske E.J., and Maier, J.P.: Apparatus for the study of electronic spectra of collisionally cooled cations: para-dichlorobenzene, J. Mol. Struct. **795** (2006) 93 - 97.
- Gerlich, D.: *Inhomogeneous Electrical Radio Frequency Fields: A Versatile Tool for the Study of Processes with Slow Ions*. Adv. in Chem. Phys., **LXXXII**, (1992) 1-176.
- Gerlich, D. and Horning, S.: *Experimental Investigations of Radiative Association Processes as Related to Interstellar Chemistry* Chem. Rev. **92** (1992) 1509-1539.
- Gerlich, D., Luca, A., and Schlemmer, S.: *Interaction of trapped ions and nanoparticles with atomic and molecular beams*, in: XIX International Symposium on Molecular Beams, Book of Abstracts, ed. A. Giardini Guidoni, Universita di Roma, (2001) 9-12.
- Gerlich, D.: *Molecular ions and nanoparticles in RF and AC traps*, Hyperfine Interactions, **146/147** (2003) 293-306.

- Gerlich, D.: *Applications of rf fields and collision dynamics in atomic mass spectrometry*, J. Anal. At. Spectrom., **19** (2004) 581-590.
- Gerlich, D.: *Probing the structure of CH_5^+ ions and deuterated variants via collisions*, Phys. Chem. Chem. Phys. **7** (2005) 1583- 1591.
- Gerlich, D., Smith, M.: *Laboratory astrochemistry: studying molecules under inter- and circumstellar conditions*, Phys. Scr. **73** (2006a) C25-C31.
- Grimm, M., Langer, B., Schlemmer, S., Lischke, T., Becker, U., Widdra, W., Gerlich, D., Flesch, R., Rühl, E.: *Charging mechanisms of trapped element-selectively excited nanoparticles exposed to soft X-rays*, Phys. Rev. Lett. **96** (2006) 066801-066805.
- Hertel, I.V., Laarmann, T., Schulz, C.P.: *Ultrafast excitation, ionization and fragmentation of C_{60}* , Adv. At. Mol. Opt. Phys. **50** (2005) 219.
- Illema, J.: *Präzisionsmassebestimmung einzelner Partikel im Femtogramm-bereich und Anwendungen in der Oberflächenphysik*, PhD thesis TU Chemnitz (2000) <http://archiv.tu-chemnitz.de/pub/2000/0067>.
- Joblin, C., Simon, A., Bruneleau, N., Toubanc, D., Armengaud, M., Frabel, P., Nogues, L.: 17th International Mass Spectrometry Conference, Prague, 2006.
- Maier, J.P.: *Interstellar detection of C_{60}^+* , Nature **370** (1994) 423-424.
- Mitzner, R.: Campbell, E.E.B.: *Optical emission studies of laser desorbed C_{60}* , J. Chem. Phys. **103** (1995) 2445 - 2453.
- Pascoli, G. and Polleux, A.: *Condensation and growth of hydrogenated carbon clusters in carbon-rich stars*, Astronomy & Astrophys. **359** (2000) 799-810.
- Rosmus, P.: *The structure of C_3^+* , private communication (2006)
- Savić, I.: *Formation of Small Hydrocarbon Ions Under Inter- and Circumstellar Conditions: Experiments in Ion Traps*, PhD Thesis, TU Chemnitz (2004) <http://archiv.tu-chemnitz.de/pub/2004/0132>.
- Savić, I., Čermák, I., Gerlich, D.: *Reactions of C_n ($n=1-3$) with ions stored in a temperature-variable radio frequency trap*, Int. J. Mass Spectrom., **240** (2005a) 139 - 147.
- Savić, I., Gerlich, D.: *Temperature variable ion trap studies of C_3H_n^+ with H_2 and HD* , Phys. Chem. Chem. Phys. **7** (2005b) 1026 – 1035.
- Savić, I., Schlemmer, S., Gerlich, D.: *Low-temperature laboratory measurements of forming deuterated C_3H_3^+* , Ap. J. **621** (2005c) 1163-1170.
- Savić, I., Lukic, S.R., Guth, I., Gerlich, D.: *Test measurement on ion-molecule reactions in a ring electrode ion trap*, Astr. Obs. Belgrade **80** (2006a) 207-210.
- Savić, I., and Gerlich, D.: *Some routes in forming C_3H_n^+ ions and deuterated variants under interstellar conditions* AIP Conference Proceedings **876** (2006b) 415-422.

- Schlemmer, S., Illemann, J., Wellert, S. and Gerlich, D.: *Non-destructive high resolution and absolute mass determination of single, charged particles in a 3D quadrupole trap*", J. Appl. Phys. **90** (2001) 5410-5418.
- Schlemmer, S., Wellert, S., Windisch, F., Grimm, M., Barth S., and Gerlich, D.: *Interactions of electrons and molecules with a single trapped nanoparticle*, Appl. Phys. A, **78** (2004) 629-636.
- Tomita, S., Andersen, J. U., Gottrup, C., Hvelplund, P., Pedersen, U.V.: *Dissociation Energy for C2 Loss from Fullerene Cations in a Storage Ring*, Phys. Rev. Lett. **87** (2001) 073401.
- Tulej, M., *Formation and detection of large nano-size singly and doubly charged hydrocarbons by trapped ion spectroscopy and synchrotron radiation*, Paul Scherer Institute, EURYI proposal, 2006.
- Wörgötter, R., Dünser, B., Scheier, P., Märk, T. D., Foltin, M., Klots, C. E., Laskin, J., Lifshitz, C.: *Self-consistent determination of fullerene binding energies BE (C_n⁺-C₂), n=58 . . . 44*, J. Chem. Phys. **104** (1996) 1225-1231.

3.1 Bericht Teilprojekt 8

3.1.1 Titel / Title

*Gasphasen-Kondensation von Kohlenstoff-Nanopartikeln
und ihre strukturelle Charakterisierung*

*Gas phase condensation of carbon nanoparticles and their
structural characterization*

3.1.2 Berichtszeitraum / reported period

01.07.2003 - 30.06.2006

3.1.3 Projektleiter / principle investigator

Mutschke, Harald, Dr. rer. nat.,
Friedrich-Schiller-Universität Jena

3.2 Zusammenfassung / Abstract

3.2.1 Wortlaut des Antrags / abstract of the proposal

In der Fortsetzung dieses Projektes werden wir uns zum ersten weiter mit den Auswirkungen des Einbaus von Heteroatomen in Kohlenstoff-Nanopartikel befassen. Zweitens soll der Einfluss von Nukleations-Keimen auf die Kondensationsprozesse untersucht werden. Zum dritten ist geplant, die Möglichkeiten zur Nukleation von Nanodiamanten in den verfügbaren Syntheseprozessen zu studieren. Die Kondensationsprozesse sowie die resultierende Mikrostruktur und optische Eigenschaften der Partikel sollen detailliert untersucht werden, um das Verständnis für die Eigenschaften analoger kosmischer Nanoteilchen zu verbessern.

The continuation of this project is aimed in the investigation of (1) the effect of hetero-atom incorporation into carbon nanoparticles, (2) the influence of nucleation seeds on carbon condensation, and (3) the possibilities for nucleation of nano-diamond structures. The condensation processes and the resulting microstructure as well as the optical properties of the particles will be studied in detail in order to improve our understanding of analogous cosmic nanoparticles.

3.2.2 Zusammenfassung des Berichts / abstract of the report

In this project, we have investigated the formation of carbonaceous nanoparticles by means of condensation experiments in connection with electron microscopic and spectroscopic techniques. This comprises investigation of (1) the incorporation of hydrogen in order to set constraints for the carrier of the interstellar 3.4 μm band, (2) the influence of carbide nucleation seeds on the condensation process, and (3) the influence of an aromatic precursor molecule on the properties of the condensate. Products from a variety of processes such as laser pyrolysis with pulsed and continuous-wave lasers, laser ablation in reaction gas atmospheres, and combustion at variable C/O ratio have been applied. Analytical techniques included spectroscopic measurements from the infrared to the far-ultraviolet wavelength range. In the former, measurements have been carried out in-situ to avoid contamination with atmospheric hydrocarbons. In the latter, special emphasis was given to the separation of scattering and absorption losses.

The most pronounced differences in the structure and the spectroscopic properties of the condensates have been found to be related to variations in the reaction temperature. Pulsed processes such as laser ablation and pulsed-laser pyrolysis involved high temperatures and fullerene-like condensates are produced. The influence of nucleation seeds has been found to be minor, the one of an aromatic precursor was significant but did not change the structures dramatic. In contrast, cw laser pyrolysis and combustion at low C/O ratio produce different structures and a large amount of volatile components under certain conditions. The structures have been explored in detail by high-resolution electron microscopy and conclusions for the nucleation processes at high temperatures have been drawn. The infrared and UV spectra measured on the condensates have been compared to astronomical spectra mainly of evolved objects. Condensates rich in volatiles possess spectral features partly in common with condensates in such astrophysical environments shedding light on the relation of amorphous carbon grains and aromatic molecules in space. The strong UV resonance of such materials is similar to the interstellar UV hump but at a slightly different position.

During the project, a close connection to TP 11 has been developed. Carbonaceous materials produced in low-temperature pyrolysis and combustion processes are interesting sources of aromatic molecules for spectroscopic studies. Extraction of the aromatics and analysis by mass spectrometry and gas chromatography has revealed their molecular composition.

3.3 Ausgangsfragen, neuester Stand der Forschung / Initial goals, current status of the field

Carbonaceous nanoparticles are an abundant and important component of the interstellar medium and of circumstellar disks and outflows. Spectral signatures of these dust particles and of related species such as large aromatic molecules are found in the interstellar extinction as well as in emission from young stellar objects and from galaxies. However, the assignment of these features to corresponding carbon structures is difficult, since carbon modifications and structures are extremely variable and the available experimental data on the relation of optical and structural properties of carbon structures are not sufficient yet. For instance, it is not clear whether the interstellar particles producing the interstellar 3.4 μm absorption band and identified as consisting of a hydrocarbon material poor in oxygen and nitrogen and containing both aromatic and aliphatic carbon forms (Pendleton and Allamandola 2002) are also related to the 217.5 nm UV interstellar extinction feature, which may represent a π -electron transition band of aromatic carbon structures.

Moreover, the carriers of the “aromatic infrared emission bands”, which are ubiquitous in interstellar and circumstellar galactic and extragalactic environments (e.g. Kwok *et al.* 2001, Peeters *et al.* 2002), have not yet been firmly identified, although it is clear that they have to be small aromatic structures with the size of nanoparticles or large molecules. In principle, these characteristics are similar to those required for the carrier of the UV extinction feature (Duley and Seahra 1999) and evidence for spectral features similar to the interstellar band is available (e.g. Duley and Lazarev 2004), however, currently the idea of onion-like graphitic grains is more popular (Chhowalla *et al.* 2003, Iglesias-Groth 2004, Tomita 2004). In a few objects in space, preferentially the environments of young stars, diamond grains have been identified by assignment of C-H stretching bands observed at 3.43 and 3.53 μm (Van Kerckhoven *et al.* 2002).

To improve our understanding of carbonaceous nanoparticles in space therefore means, on the one hand, to establish firm relations between carbon structures and spectroscopic signatures and, on the other hand to study the relation of molecular and solid species in formation processes. Unfortunately, the chemical networks determining the formation routes of nanoparticles from the gas phase are quite complex, even in “well-defined” laboratory systems. Therefore, our current knowledge about the condensation and modification of carbonaceous nanoparticles is

still limited. A scenario for graphite grain condensation within the O-rich CO core of Type II supernovae has been proposed by Clayton *et al.* (2001). The authors claimed the formation of C_n linear chains which can be transformed into ringed isomers, the building blocks of bigger carbon structures. The most probable places for the formation of PAHs are the circumstellar envelopes of carbon-rich late type stars (Allain *et al.* 1997). The formation process of interstellar PAHs has not been clarified so far. One possibility is that PAHs are precursors, intermediate steps or side products in the carbon nanoparticle condensation in different astronomical environments and therefore their composition should be closely related to the condensation process. From laboratory soot condensation experiments it is quite evident that soluble components are formed in addition to soot during the condensation process (Keller *et al.* 2000). Better laboratory data on these processes as well as on the spectroscopic properties of the resulting materials are urgently needed for the interpretation of the observations (Reynaud *et al.* 2001).

3.4 Angewandte Methoden / Experimental methods

3.4.1 Laser ablation

The laser ablation experiment uses a pulsed laser Nd:YAG laser working at 532 nm (pulse length 5ns, pulse energy 230mJ) for evaporation of solid carbon material. The condensation of carbon particles is caused by collisions between the generated C-clusters (Witanachchi *et al.* 2000) and cooling gas atoms. We have applied helium, hydrogen, water vapor and mixtures of those as reactive and cooling gases. In order to influence *the size* of the originally condensed particles and the amount of *hydrogen* that can be incorporated into the carbon structure, the pressure in the reaction chamber was varied between 1 and 10 Torr and the laser power densities in the focused laser beam was varied between 2×10^8 and 9×10^9 W/cm². In most experiments graphite targets have been used. In two other experimental series the *co-condensation* of graphite / titanium carbide and graphite / silicon carbide targets has been studied.

The laser ablation source has been combined with a molecular beam technique in order to deposit the soot particles onto an optical window, transparent for different spectral ranges (FUV/UV/VIS and NIR/MIR), and to measure their infrared spectral properties *in situ*. In the second project phase, the setup for laser ablation has been extended with a substrate mount that can be *heated* to temperatures of up to 600K which allowed studying the influence of adsorption of organic gas-phase mole-

cules on the reactive surface of nano-sized carbon grains. The physical adsorption of such molecules could be observed by in-situ measurements of the $3.4\mu\text{m}$ C-H stretching band strength. The adsorbed molecules were easily desorbed from the particle surfaces by heating the condensed material up to 273K.

3.4.2 Laser-induced gas pyrolysis

In this term of the project the laser pyrolysis technique capabilities have been further developed. The incorporation of an URENCO-TEA- CO_2 laser (Modell ML104 produced by Uranit) with a maximum output energy of 6 J and a working frequency between 10 and 50 Hz into the pyrolysis setup has provided the necessary tool for studying the properties of the pyrolysis products in dependence on the *laser power*. The use of ethylene and benzene precursor gases has allowed us to investigate the influence of higher hydrogen content than with the previously used acetylene and of an *aromatic precursor* structure on the pyrolysis products. In addition, thermal *annealing* of some of the samples has been performed in order to understand the incorporation of volatile species into the grains during the condensation processes.

3.4.3 Combustion (CAST)

The Combustion Aerosol Standard generator (CAST, Jing-CAST Technologies) is a device used for generation of “standard” soot particles with controllable properties. For this purpose it uses condensation in a co-flow diffusion flame of propane and air at variable flow rates. The combustion products are extracted from the flame and quenched by a strong flow of cool N_2 intersecting at a certain flame height. The quenching prevents the soot particles from further oxidation, thermal processing, deposition and agglomeration. The main parameter determining the soot condensation is the *C/O atomic ratio in the flame* which is inversely correlated with the flame temperature. We have used C/O ratios between 0.29 and 0.61. The condensates have been deposited to CaF_2 optical windows, TEM grids and aluminum foil by means of an impactor with rotating stages (Hauke, model LPI ROT 25/0.018/2.0), the stage numbers corresponding to increasing aerodynamic diameter cutoffs (between 0.0180 and $16.0\mu\text{m}$ for stages 1 to 11, respectively).

From the particles deposited on the aluminum foils, the deposited masses at the different stages have been determined by vaporiza-

tion/combustion and subsequent CO₂ detection. In this analysis, the components released by vaporization at T<350°C (OC1) and T<650°C (OC2, “organic carbon”) could be measured separately from the remaining “elemental carbon” (EC) component. Samples deposited by the first stage of the impactor, i.e. the smallest-size component, tended to possess the highest amount of OC. Thermal treatment up to 650°C has also been performed on the samples deposited to optical windows for separation of the absorption contribution of the volatile components. These experiments have been performed in collaboration with Dr. M. Schnaiter from the Institut für Meteorologie und Klimaforschung Karlsruhe.

3.4.4 Spectroscopic and TEM analysis

The analysis of the samples includes spectroscopy in a wide wavenumber range from the mid-infrared (MIR) to the far-ultraviolet (FUV). In this project period, the UV measurements have been extended by using an integrating sphere accessory to the Perkin Elmer Lambda 19 spectrometer and by angle-resolved light-scattering measurements with the FUV spectrometer. This allowed separate measurements of the scattering and absorption contributions to the extinction spectra, which provides very important information in order to correctly characterize the deposited products. For comparison, absorption and scattering curves have been calculated from published optical constants of carbonaceous materials (Zubko *et al.* 1996 and Schnaiter *et al.* 1998) for single and aggregated particles.

Particle sizes and structures of the condensed carbon grains have been determined by means of transmission electron microscopy at both low (TEM) and high resolution (HRTEM, 300 keV). The HRTEM is equipped by an energy dispersive X-ray analysis system (EDX) for quantitative analysis of the chemical composition. The vapor-phase condensed particles were mostly directly deposited on Lacey carbon supported TEM grids. HRTEM provides a direct view inside the medium-size order of the carbon structures by imaging the edge-on aromatic layers. In carbon nanoparticles, graphene layers can curl within the particles but they still appear as fringes. For derivation of quantitative information about the carbon structures we performed image analyses similar to Palotas *et al.* (1996) and Galvez *et al.* (2002). Moreover, we constituted a new possibility to get structural information on very disordered systems. The HRTEM bright field micrographs were Fourier transformed to see 'periodicity' in the structure and to derive main distances between the observed graphene

layers. The corresponding FT images show rather broad arcs with a distribution of different radii. We have used the intensity profiles of the computer-generated diffractograms to measure the mean distances d_{002} between the graphene layers for the chosen sample area. The mean L_a sizes of these graphene layers were determined by selecting an adequate sample area of a diameter of 15 nm for all evaluated HRTEM images. These image parts were skeletonized by filtering the images using ring-shaped masks, which were evaluated to eliminate the majority of periodicities without physical sense. An inverse FT from the filtered image was used to generate the skeletonized image which was employed to measure the sizes of the graphene layers. To avoid artifacts the filtered images were carefully compared to the raw images of the sample area. The quantitative analyses using FT of the digital images and measurements of graphene layer lengths and distances were performed by applying the Digital Micrograph 3.9.0 software. The image analyses have been employed to condensed carbon from laser pyrolysis and laser ablation.

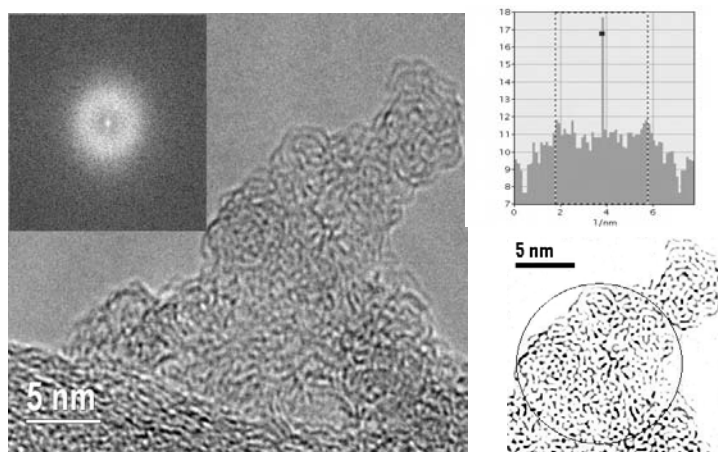


Fig. 1: Bright field HRTEM image of gas-phase condensed soot grains. The insert shows the Fourier transformed image. The right upper panel shows the intensity profile of the FFT image whereas the right lower panel represents a skeletonized image of the left micrograph.

3.5 Ergebnisse und ihre Bedeutung / Results and their importance

3.5.1 Hydrogen incorporation by laser ablation in reactive atmosphere

In our study of gas-phase condensation of carbon grains we have focused on the relation between the internal structure of the condensed carbon grains and its effect on the spectral properties of the grains. For the spectroscopy the main activities were concentrated on the optimization of hydrogen incorporation into the soot structure and its influence on the spectral properties from FUV to the IR range. The incorporation of hydrogen into carbon structures can take place in two different ways. Firstly, it could be bonded to aromatic sp^2 or to saturated sp^3 hybridized carbon atoms. In both cases hydrogen strongly affects the structure and spectroscopic properties of the generated soot particles. For an efficient integration of these atoms we have varied the temperature in the condensation zone and used new reactive gas mixtures such as He/H₂O for quenching and condensation of carbon nanoparticles. The sizes, the morphological appearance and the internal structure of soot grains produced in the laser ablation experiments using a pulsed laser did not show strong variations as shown in Fig. 2. In both cases very small fullerene-like carbon grains are visible. The left panel shows carbon grains containing a low H/C ratio of 0.14 and the carbon grains in the right panel are typical for materials with high H/C ratio of 0.5. The grain sizes and the strongly bent graphene layers are comparable. The difference is the lower order of the grain structures in the right image.

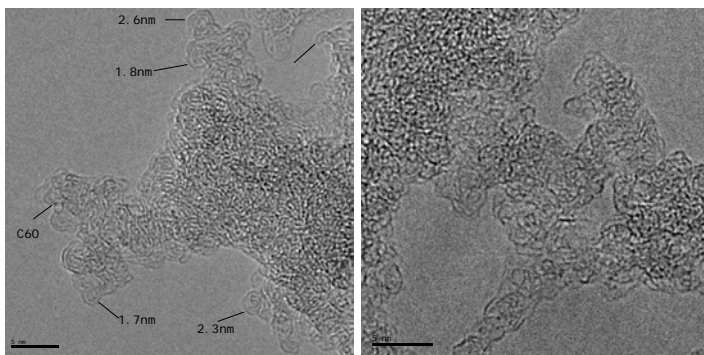


Fig. 2:. HRTEM bright field images of carbon grains with low (left panel) and high hydrogen content (right panel). In both images very small seed-like particles with fullerene structures are visible.

Table 1 shows an overview on the compositional and structural properties of the carbon grains produced in He/H₂ atmospheres at different pressures. There are strong variations in the hydrogen content but much smaller differences in the mean graphene layer sizes and distances between the graphene layers. The content of sp² hybridized carbon was found to be 57% in a low-hydrogen containing sample (H/C=0.16) and 48% in a sample with a H/C ratio of 0.5. The content of sp² hybridized carbon was measured using EEL spectroscopy of free-standing grains. However, despite only small structural varieties occurred, strong differences were found in the spectral properties of the condensed carbon matter. Fig. 3 contains the IR and FUV spectra of the carbon material presented in Table 1.

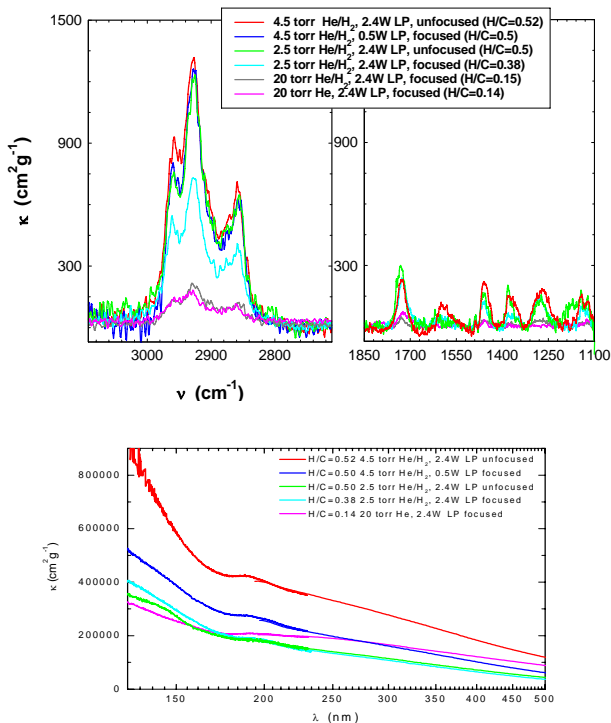


Fig. 3: IR and FUV/UV/VIS spectra of condensed soot grains containing different H/C ratios. The samples are the same as reported in Tab 1.

The incorporated hydrogen is mainly bonded to sp^3 hybridized carbon atoms forming up methyl ($-CH_3$) and ethyl ($-CH_2$) groups showing strong absorption bands in the $3.4 \mu m$ ($2800-3000 \text{ cm}^{-1}$) range of the IR spectrum due to stretching vibrations. Maximum mass extinction coefficients of $1500 \text{ cm}^2 \text{ g}^{-1}$ at $3.4 \mu m$ for the laser ablated materials could be measured. These saturated, aliphatic functional groups are bonded to the aromatic islands or connect the strongly bent graphene layers in the particles. The mean sizes L_a of the aromatic graphene layers are rather small in the fullerene-like grains comprising no more than 3 condensed rings in the L_a extension. The insertion of hydrogen in the condensing grains is highest for samples produced with low laser power or unfocused laser beam. An explanation for this specific result could be found in the condensation mechanism and rate coefficients of the chemical equilibrium between hydrogen abstraction and C-H bond formation.

LP (W)	P (Torr)	Gas	Mean seed size (nm)	Mean L_a size (nm)	Mean d_{002} value (nm)	H/C
2.4f	20	He	1.56	0.53-0.6	0.43	0.14
2.4f	20	He/H ₂ 2:1	1.42	0.488	0.51	0.16
2.4f	2.5	He/H ₂ 2:1	1.2	0.45	0.54	0.39
0.5f	4.5	He/H ₂ 2:1		0.42	0.59	0.5
2.4uf	4.5	He/H ₂ 2:1	1.43	0.42	0.57	0.52

Table 1: Structural parameters of soot grains containing different H/C ratios.

The complete IR spectrum shows the same bands that can be observed in the spectrum of carbon particles condensed in He/H₂O atmospheres. The incorporation of hydrogen in condensing carbon grains using He/H₂O atmospheres was however much more efficient compared to the samples produced in He/H₂ atmospheres. The mass extinction coefficients at $3.4 \mu m$ vary between 300 and $1500 \text{ cm}^2 \text{ g}^{-1}$. We produced a carbon sample with the highest H/C ratio of 0.54 in a He atmosphere with a partial pressure of 0.09 Torr H₂O. Typical for all IR spectra of the laser ablation soot samples is the occurrence of vibrational bands at 3300 and 2100 cm^{-1} caused by C-H and C-C groups of sp hybridized carbon atoms. These bands disappear when the samples are exposed to air. The observed instability of the IR bands due to triply bonded carbon is typical for polyynes (Bogana *et al.* 2005). A much more detailed description of the re-

sults of the laser ablation experiments can be found in Jäger *et al.* (2007b).

The FUV/UV/VIS spectra of all samples (see lower panel in Fig. 3) did not show distinct UV bumps but a strong rise of the mass absorption coefficient up to the expected electronic σ - σ^* transition at wavelengths less than 100 nm. The very small peak at about 190 nm is not caused by π - π^* transitions but by electronic transitions in C=O groups which can also be found in such carbon structures. The very broad distribution of the electronic π - π^* transitions that are partially masked by the strong absorption in the FUV are due to the strongly varying curvatures of the graphene layers in the fullerene-like nano-sized carbon grains.

The absorption properties of soot particles containing an H/C ratio of 0.5 reproduce the intensity as well as the spectral profile of the interstellar 3.4 μ m absorption band (see Fig. 4). However, the 80 ppm interstellar carbon available to form solid grains is completely consumed in order to reproduce the high intensity of the interstellar band.

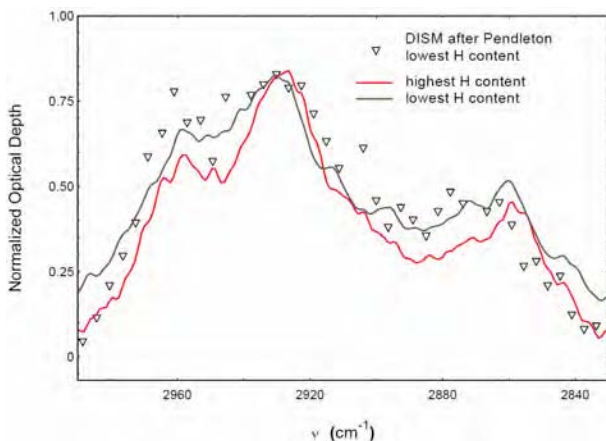


Fig. 4: Interstellar absorption 3.4 μ m absorption profile compared to a lab materials with high H content and a $\kappa(2950\text{cm}^{-1})=1400\text{cm}^2\text{g}^{-1}$ (corresponding H/C ratio of 0.5) and low H content (H/C=0.14). In order to fit the intensity of the DISM profile one needs about all the left carbon (80 ppm).

The effect of physically adsorbed organic molecules has also been investigated by in-situ IR spectroscopy. We found a very efficient adsorption of molecules from the gas phase within seconds in air, and within a few hours (2-3) in vacuum (10^{-6} mbar). The increase of the mass extinc-

tion coefficient of the C-H stretching vibrations was especially strong for the small fullerene-like carbon grains due to their large surface. The enhancement of the C-H bands is coupled with an increase of the C=O band at about 1720 cm^{-1} . A certain amount of the increase results from the reaction of the soot surface with water molecules leading to the formation of C-H bonds on the surfaces. Heating of the sample to 500 K results in the abstraction of the physically bonded alkyl groups. After hydrogen abstraction the original mass extinction coefficient is obtained. The results of the adsorption experiments demonstrate that for carbon samples containing small and strongly disordered particles only in-situ IR measurements provide real mass extinction coefficients in the region of the stretching vibrations of alkyl groups at $3.4\text{ }\mu\text{m}$.

3.5.2 Co-condensation of graphite and carbide grains

We have studied the influence of carbides on the nucleation process of carbon grains. The experiments were performed by laser ablation of mixed targets (graphite/carbide mixtures) in different quenching gas atmospheres. The precondensed carbide can serve as nucleation seeds for further condensation of carbon materials. Such nucleation seeds of titanium carbide could be identified in meteoritic graphite grains by Stadermann et al (2005). Their sizes range from 15 to 500 nm. Lodders and Fegley (1999) have calculated condensation sequences of dust grains in N-type stars ($\text{C/O} > 1$) and found that TiC is the first condensate in the shells of such stars. SiC usually condenses after graphite but there are exceptions caused by temperature differences between gas and grains (Chigai and Yamamoto 2003).

Under such conditions SiC grains can either precede the graphite condensation or can be formed simultaneously with graphite grains. Therefore, we were interested in the study of the influence of titanium carbide and silicon carbide on the gas-phase nucleation process of carbon grains. The analytical characterization of the generated carbon nanopowders was mainly based on high-resolution electron microscopy combined with EDX analyses. The optical properties of the generated carbon samples were studied by means of FUV, UV/VIS and IR spectroscopy.

The result of these studies can be summarized as following. The influence of titanium carbide and silicon carbide on the structure of the condensing carbon grains is negligible. In the case of TiC we were able to identify cubic TiC crystals up to sizes up to 25 nm but also small amounts of titanium oxide and metallic titanium.. This result was based on the

EDX analysis of the individual grains. The TiC crystal structure was identified by measuring the distances between the lattice fringes which were visible in the HRTEM images. These grains are covered by a small amorphous carbon layer. However, the majority of the condensates show the same very small fullerene-like carbon grains as already observed in the pure graphite samples. Hence, the effect of the spectral properties of the grains is rather low. The hydrogen insertion into the carbon structures is comparable to the samples prepared with the pure graphite target under the same conditions. The maximum mass extinction coefficients for the 3.4 μm stretching region are nearly similar. The spectral properties in the FUV/UV/VIS region are caused by carbon structures which are completely comparable to structures produced with pure graphite.

A difference in the condensation was found for samples produced by laser ablation of mixed graphite/SiC targets. HRTEM images did not show distinct SiC particles but also the fullerene-like particles very small carbon seeds. However, EDX analyses have shown that at least up to 4% SiC was incorporated in the carbon structure (see Fig. 5). The structural properties of the condensed carbon seeds is again the same like in the laser ablation of pure graphite targets.

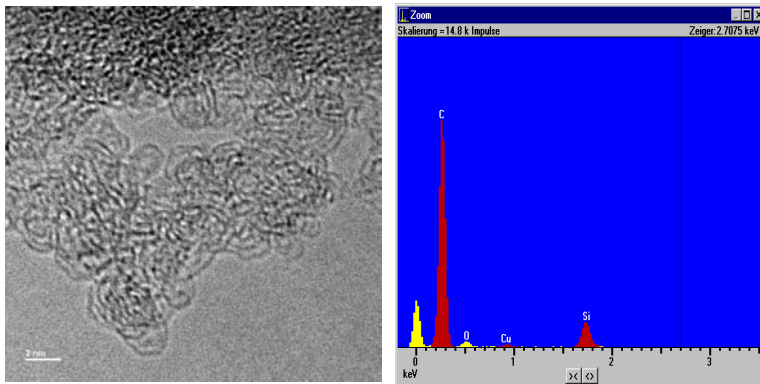


Fig. 5: HRTEM image of carbon grains produced by co-condensation of graphite and SiC. The very small seed-like grains show fullerene-like structures. The right panel displays the EDX analysis of a representative area of the sample. An amount of 6 % Si is contained in the carbon material.

The spectral behaviour of these SiC containing samples is again affected by the fullerene-like structures of the small-sized condensed soot grains. The fullerene-like structures with strongly bent graphene layers

and very disordered structure show the same IR spectral properties and typical FUV/UV/VIS behaviour all the soot samples produced by our laser ablation experiments.

3.5.3 Influence of precursor gas and laser power on laser pyrolysis products

In our study of particle condensation by laser induced pyrolysis of hydrocarbon gases, the use of precursors with different bonding nature (aromatic/aliphatic), such as benzene, acetylene and ethylene has provided important information about the incorporation of aromatic molecules into the grains as well as about the influence of the precursor gas on the morphology and internal structure of the particles. The incorporation of hydrogen into the grains has been studied by using ethylene as precursor instead of acetylene. Systematic studies concerning the effect of the different experimental parameters on the final properties of the products have been also extended. In previous studies, the influence of the catalyst/precursor ratio was investigated in detail (Llamas Jansa 2002, Llamas Jansa *et al.* 2003), but no investigations of the laser power effect were possible at that time.

a) Size, morphology and internal structure

TEM and HRTEM images show that the pyrolysis particles are rather spherical in shape and that they easily form aggregates containing hundreds to thousands of particles. The size of the particles ranges from 3 to 14 nm and shows a dependence on the nature of the precursor, with larger particles seen in the benzene-based samples. An inverse correlation between the laser power and the size of the particles is observed. The internal structure of the particles is made of coagulation seeds with sizes between 3 and 5 nm that are probably the beginning of further graphitization of the grains into more onion-like structures. The amount of these seeds is related to the precursor gas, with a higher density of seeds in the benzene-based samples. The internal structure of the seeds is made of BSUs (Robertson and O'Reilly 1987) that can be formed of more or less extended graphene layers. No correlation between the size of the graphene layers and the precursor or the laser power is found. Particles made of an organic component similar to that observed in the CAST samples (see 3.5.4.) and different from the more refractory ones have been observed in some of the benzene-based samples. The organic component has been further studied by means of thermal treatments.

b) Spectroscopy

The results of the infrared spectroscopy show that the incorporation of aromatic groups is highly effective for the benzene precursor compared to the processes based on aliphatic precursors (Fig. 6). This fact is seen by the appearance of a strong “solo” aromatic C-H out-of-plane bending band at $\sim 885\text{ cm}^{-1}$, which is not present in the acetylene and ethylene samples. The presence of the solo band together with the other aromatic deformation bands at wavenumbers between 885 and 755 cm^{-1} is similar to the observed profile in the combustion CAST samples. A further incorporation of hydrogen atoms due to the use of ethylene instead of acetylene for the pyrolysis is not seen in the IR results. This observation indicates that, although the condensation mechanism may have been changed with ethylene, the hydrogen has been likely released in the form of H_2 molecules during the process and is not incorporated into the grains.

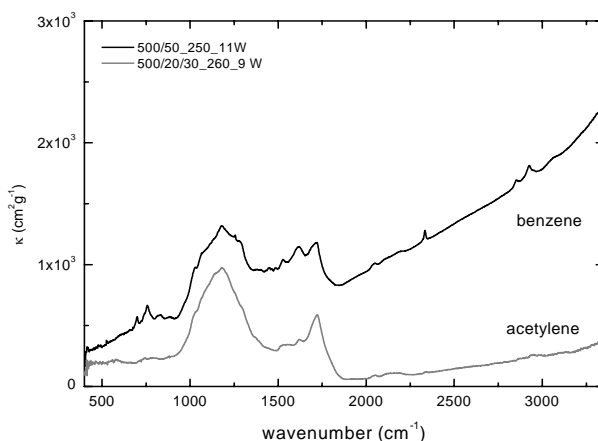


Fig. 6: Infrared spectral curves corresponding to pyrolysis samples produced with different precursors. The legend indicates the experimental parameters: gas flow ratio, pressure and laser power, respectively.

Systematic studies of the spectral properties in the wide wavenumber range from the near infrared (NIR) to the far ultraviolet (FUV) have been carried out for all the series of samples produced. The results show that no correlation between the laser power and the optical behaviour of the samples can be drawn but that the nature of the precursor gas strongly influences the spectral properties (Fig. 7). The curves have been charac-

terized using deconvolution into Gaussians (parameters peak position, width and area) and by the gap energy (E_g) parameter derived from the Tauc's relation. A shift of the main absorption peak towards smaller wavenumbers and a decrease of the E_g value have been observed for the samples produced with benzene compared to the aliphatic-based samples.

For this analysis it has been important to separate the scattering contribution, especially at the small wavenumbers close to the optical gap. The experimental investigation of the scattering coefficient showed that the benzene-based samples present considerably higher scattering in the $\sim 1\text{--}4\ \mu\text{m}^{-1}$ range with values between 51 and 56% at $4\ \mu\text{m}^{-1}$ and between 65 and 79% at $2\ \mu\text{m}^{-1}$ than the acetylene samples with 27 and 47% at $4\ \mu\text{m}^{-1}$ and between 11 and 38% at $2\ \mu\text{m}^{-1}$. This fact is likely related to the smaller particles observed for the latter samples.

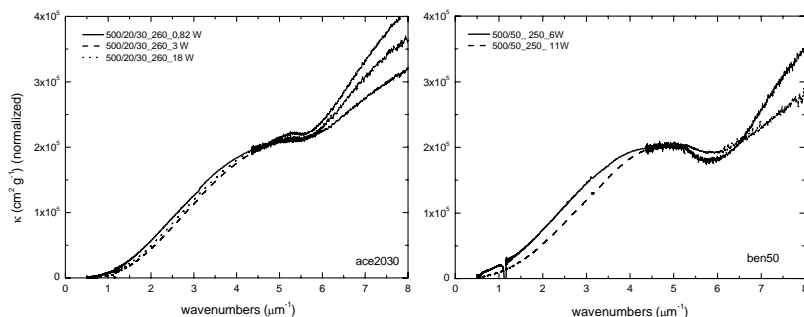


Fig. 7: UV/VIS spectral extinction curves for samples produced with acetylene (left panel) and benzene (right panel).

Scattering measurements carried out in the FUV range demonstrate that the strong rise of the FUV extinction towards higher wavenumbers seen in the spectral behaviour of the pyrolysis samples is not a scattering feature but a characteristic of the absorption. Simulated curves obtained using optical constants of carbonaceous materials from the literature (Zubko *et al.* 1998 and Schnaiter *et al.* 1998) do fit the measurements to a certain extent when considering particle aggregates. The simulations show that for $\lambda^{-1} > 4\ \mu\text{m}^{-1}$ the scattering curve is generally structured and nonlinear, but does not strongly increase. To our knowledge these are the first scattering measurements on soot particles at far UV wavelengths.

c) Thermal annealing

Thermal annealing experiments of some of the pyrolysis samples have been carried out in the 350-450°C range in vacuum in order to collect more information about the presence of volatile components in the pyrolysis samples (see also 3.5.4). The results show that the 5.1 μm^{-1} feature present in the UV spectra of some of the samples disappears after the thermal treatment. Second, a shift of the main absorption peak occurs with increasing annealing temperature. Additional information provided by IR spectroscopy concerns the loss of oxygen-based components (C=O bands) and a decrease of the content of aromatic groups in the benzene-based samples. These observations indicate that the 5.1 μm^{-1} feature is likely related to the presence of oxygen on the particles probably incorporated during the condensation processes. The fact that the aromatic groups are diminished at these temperatures also indicates that they are caused by some kind of PAHs representing part of the volatile component of the grains.

3.5.4 Spectroscopic properties of soot rich in volatiles

a) Combustion (CAST) products

Whereas the pulsed-laser induced processes used in our laboratory generally produce amorphous-carbon condensates through processes which strongly limit the formation of a volatile, i.e. molecular component, we have obtained condensates rich in such molecules through collaborations. In the NILPRP Bucharest (collaboration with I. Voicu), cw-laser-induced gas pyrolysis has been applied to produce carbonaceous condensates containing up to 30% of aromatic molecules. These products could be obtained in large amounts allowing the chemical analysis of the molecular component. In the IMK Karlsruhe (with M. Schnaiter), standard (CAST) soots have been produced by combustion of propane at C/O atomic ratios between 0.29 and 0.61, which have been investigated mainly by spectroscopic and electron microscopic techniques. The amount of volatiles (the „organic component, OC“) has been measured by a heating experiment and correlates with the C/O ratio (see 3.4.2.).

For the infrared (IR) spectroscopic investigation, material originally deposited on aluminum foils has been embedded into KBr pellets. The spectra of samples produced at high C/O ratios differ from those produced at low C/O ratios first by a much lower IR continuum absorptivity (a factor of six for C/O=0.5 compared to C/O=0.29) and second by the

presence of strong aromatic C-H bands such as the stretching band at about 2950 cm^{-1} and the out-of-plane bending vibration bands in the $700\text{--}900\text{ cm}^{-1}$ range (see Fig. 8). These bands are absent in the condensate produced at $\text{C/O}=0.29$. The out-of-plane bending vibrations at the lowest wavenumbers indicate highly hydrogenated aromatic rings, which are greatly diminished after heating to 350°C . This leads to the conclusion that the volatile component is dominated by relatively small polyaromatic molecules which form an abundant component of the condensates (OC content up to 65%).

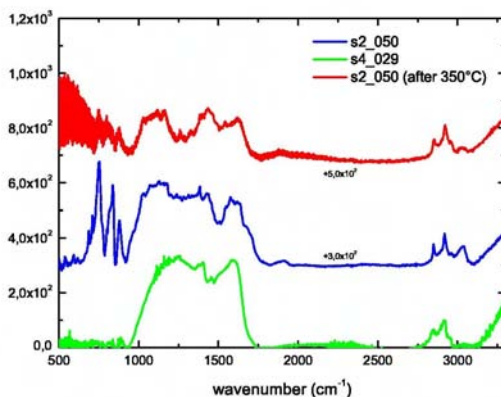


Fig. 8: Infrared absorption spectra (continuum subtracted) for CAST soot produced at $\text{C/O}=0.29$ (lower curve) and $\text{C/O}=0.50$ (middle) as well as the $\text{C/O}=0.50$ material after annealing at 350°C . Note the varying strength of the aromatic C-H bands at wavenumbers $<1000\text{ cm}^{-1}$ and $>3000\text{ cm}^{-1}$.

Correspondingly, electron microscopy revealed that condensates obtained at high C/O ratio do not consist of well isolated soot particles with graphitic structure (such as those produced at low C/O), but appear covered with or even consist of a structureless amorphous material which may be dominated by aggregated molecules. At intermediate C/O the graphitic soot particles and the structureless molecular component are even seen as separate populations, the latter forming rather large spherical particles (see Fig. 9). The correlation between the presence of this structureless component and the strength of the aromatic C-H bands indicates that the polyaromatic molecules formed in the combustion tend to condense either as a separate population of particles or, at the highest C/O ratios and lowest temperatures, dominate the condensed material as a whole.

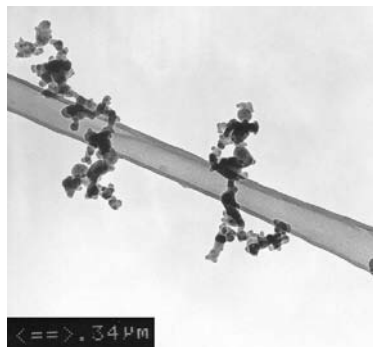


Fig. 9: TEM image of a CAST soot produced at C/O=0.4 showing larger spherical particles of a condensed molecular component attached to aggregates of smaller refractory particles.

These changes of the chemical and structural properties of the condensates are reflected by the UV spectra of the samples. The dependence on the C/O ratio is especially pronounced for the smallest size fraction deposited with the impactor on CaF_2 substrates (Fig. 10a). At low OC content the π -electron transition band of the material is peaking at about $3.5 \mu\text{m}^{-1}$ and extends down to $0 \mu\text{m}^{-1}$. For C/O=0.5 it narrows considerably and shifts its peak to about $4.8 \mu\text{m}^{-1}$. The optical gap energy determined from the slope of the absorption at visible wavelengths increases to values of about 1.7 eV. The absorption in the visible lowers by about one order of magnitude and obtains much steeper wavelength dependence (Schnaiter *et al.* 2006). At near infrared wavelengths scattering becomes dominant over absorption and gains also a higher importance in the ultraviolet (albedo up to 0.4, Fig. 10b) because of the influence of the larger particle size (I. Llamas Jansa, PhD thesis 2006).

The spectroscopic and TEM investigation after thermal treatment at 450°C supports these findings on the influence of molecular aggregates. The loss of the OC component leads to distinctive changes in strength, width and peak position of the π -electron band (Fig. 10c), which can be interpreted as the evaporation of part of the volatiles plus a carbonization of another part, which is clearly indicated by an increase of the absorption at wavenumbers between 0.5 and $2.5 \mu\text{m}^{-1}$. The spectra of CAST soots produced at C/O=0.29 lack these annealing effects. With the measurements in the FUV it was possible for the first time to explain the reasons for the OC dependence of the albedo and the visible absorption in terms of the changes of the π -electron transition band profile.

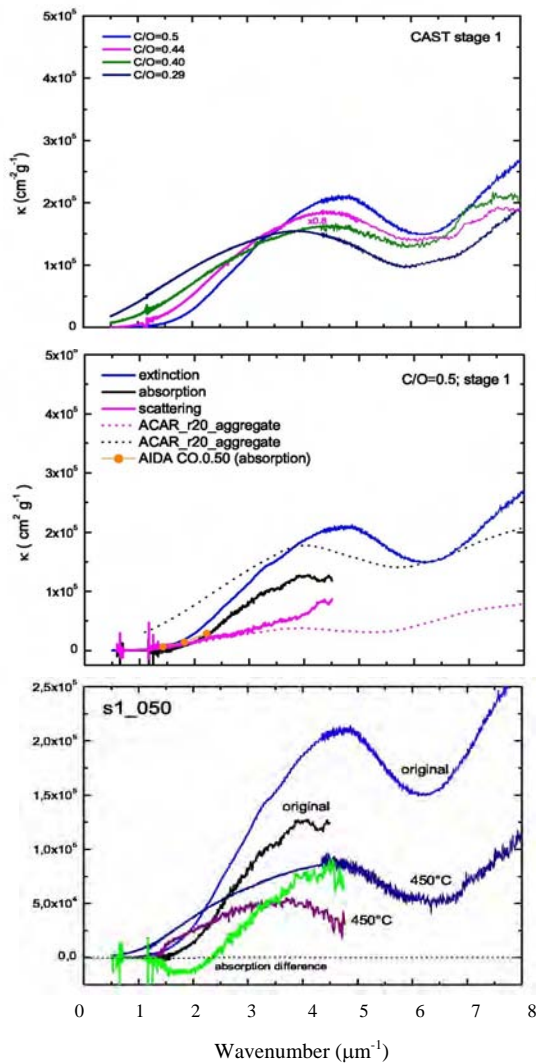


Fig. 10: UV spectra of CAST soots produced at different C/O ratios (top, a), contributions of absorption and scattering to the extinction for C/O=0.5 (middle, b, dotted line is a simulation) and change in extinction and absorption after annealing at 450°C (bottom, c, green curve is the difference of the absorption spectra).

The experimental UV profile of the volatile-rich material has been demonstrated to reproduce the shape and position of an astronomical extinction feature observed in a carbon-rich post-AGB object (HD 44179, “Red Rectangle”, data by Vijh *et al.* 2005). This is true down to wavelengths of about 180nm whereas the steep extinction rise at shorter wavelengths cannot be explained (Fig. 11). Especially, this rise is not likely to be due to scattering from grains, which according to our results is non-monotonous and always weaker than absorption in this spectral range (I. Llamas Jansa, PhD thesis 2006). Vijh *et al.* (2005) attribute the FUV rise to the ionization edge of aromatic molecules.

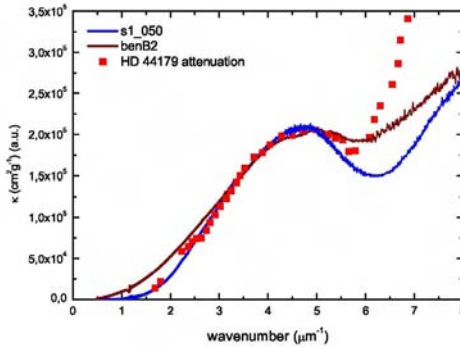


Fig. 11: Comparison of the UV extinction spectrum of the post-AGB object HD 44179 (“Red Rectangle”) with those of the CAST soot produced at C/O=0.5 and with a pyrolysis product based on benzene precursor.

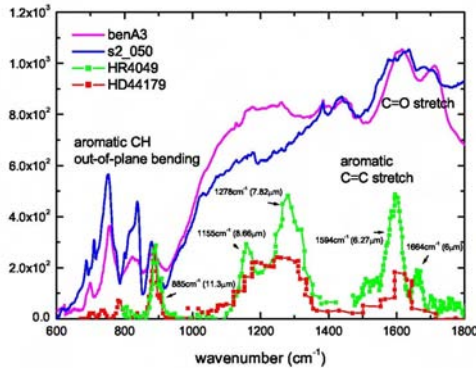


Fig. 12: Comparison of the IR emission spectra of the post-AGB objects HD 44179 (“Red Rectangle”) and HR 4049 with those of the CAST soot produced at C/O=0.5 and with a pyrolysis product based on benzene precursor.

The infrared spectrum of our material unfortunately does not well reproduce the emission spectrum of the Red Rectangle which is entirely dominated by aromatic C-H and C=C bands. Although some of these bands are present in the experimental spectrum as well, our material is clearly stronger hydrogenated and possesses aliphatic components as well (Fig. 12). The same is true for pulsed-laser pyrolysis condensates from benzene. Note that the emission from HD 44179 originates from a different location within this object than the UV absorption spectrum, so that this does not contradict the possible presence of a material like our product in part of the object.

b) Products from cw laser pyrolysis

The carbon nanopowder samples were prepared by laser pyrolysis in collaboration with I. Voicu at the National Institute for Lasers, Plasma and Radiation Physics in Bucharest, Romania. The production of the PAH containing soot is described in detail in Jäger et al 2006. The addition of benzene to a precursor gas mixture of acetylene and ethylene increased the formation efficiency of PAHs in the soot materials considerably. In order to remove the soluble components from the soot sample quantitatively we used an extraction method such as soxleth extraction with toluene as the elution solvent. The toluene was removed by distillation. The extracts as well as the soot were characterized by different spectroscopic methods such as IR, UV/VIS and a combination of gas chromatographic and mass spectrometric (GC/MS) analyses.

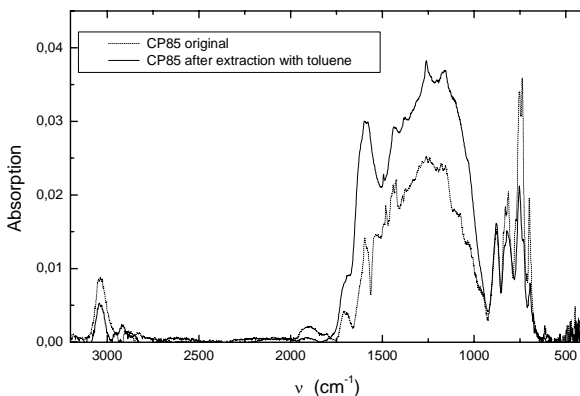


Fig. 13: Baseline corrected IR spectra of the soot sample before and after extraction of the PAH compounds.

The content of soluble components in the soot was determined to account for about 32% of the total soot mass. Interestingly, The PAHs can also be completely removed by heating the soot up to 350 °C in vacuum (10^{-5} mbar). The IR spectrum of the carbon nanopowder before and after extraction is shown in Fig. 15. The comparison of the spectra shows a partly disappearance or weakening of bands. First the intensity of the weak aromatic stretching vibration at 3050 cm^{-1} decreases by about 1/3. The intensity of the C=O band does not change in the extracted soot sample but disappears in annealed soot. The band at about 1600 cm^{-1} caused by C=C stretching vibrations becomes broader and stronger. However, the intensities and band profiles of the C-H out of plane vibrations between 700 and 900 cm^{-1} alter considerably. The first band at 879 cm^{-1} does not decrease its intensity, demonstrating that this band is completely originating in the soot structure. The two other features weaken extensively. Interestingly, the fourth band at 700 cm^{-1} is reduced by the half. This band is caused by 5 adjacent H atoms in an aromatic ring typical for compounds like biphenyl, triphenyl or triphenylbenzene.

The IR spectrum of the soluble soot component itself shows the presence of a variety of functional groups (Fig. 14). Bands between 3300 and 2800 cm^{-1} are caused by -C-H stretching vibrations of differently hybridized carbon. There are various aromatic =C-H bands between 3000 and 3100 cm^{-1} . These bands can originate from either a mixture of polycyclic aromatic compounds or the existence of substituents at the aromatic rings, which can influence the position of adjacent =C-H vibrational bands.

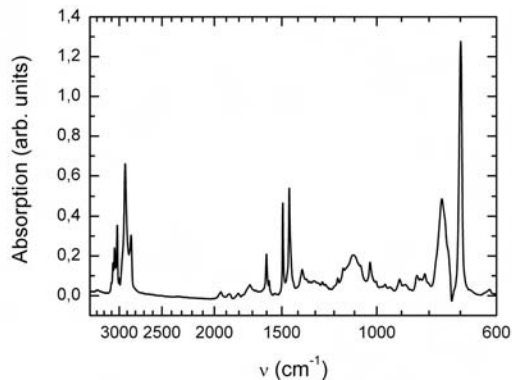


Fig. 14: IR absorption spectrum of the toluene extract measured as a film on a KBr substrate

The saturated -C-H stretching vibrations cause 2 strong bands at 2923 and 2853 cm^{-1} assigned to asymmetric and symmetric stretching vibrations of $-\text{CH}_2$ groups. Two weak shoulders at the short wavelength tail of these two bands can be attributed to the asymmetric and symmetric stretching vibrations of saturated $-\text{CH}_3$ groups. Since the oscillator strength of the aromatic $=\text{C}-\text{H}$ stretching vibration is about 5 times less than the oscillator strength of saturated $-\text{C}-\text{H}$, an overabundance of aromatic $=\text{C}-\text{H}$ can be deduced. The strong dominance of saturated CH_2 compared to CH_3 groups is interesting. The dominance of the CH_2 groups results from the formation of dihydro-groups in the aromatic rings resulting in the destruction of the aromatic character of that ring and in the formation of compounds such as dihydro-cyclopentapyrene, dihydro-benzo-pyrene.

The features between 700 and 900 cm^{-1} due to out of plane vibrations of aromatic $=\text{C}-\text{H}$ show the strongest IR band at 700 cm^{-1} which is already present in the soot spectrum before extraction ($=\text{C}-\text{H}$ out of plane, 5 adjacent H atoms). There are two other strong bands at 731 and 756 cm^{-1} typical for 4 and 3 adjacent H atoms. Two weak bands between 800 and 850 cm^{-1} show a minor presence of 3 and 2 H in the aromatic ring.

M/z	PAHs
152,154	biphenyl, ethylnaphthalene and biphenylene
178	phenanthrene, anthracene and methylene-fluorene.
202	pyrene,fluoranthene
204	anthrocyclobutene, dicyclobutabiphenylene
226	cyclopentapyrene
228	naphthacene, chrysene, triphenylene: coronene
230	dimethyl-, ethyl-fluoranthene, dihydrocyclopenta-pyrene
252	benz-ace-phenanthrylene, phenylanthracene, perylene, benzopyrene
254	binaphthalene, phenylanthracene, dihydrobenzopyrene, dihydrobenzo-fluoranthene
276	dibenzochrysene, indenopyrene
278	benzochrysene, dihydrobenzoperylene
300	coronene
302	dibenzonaphthacene, naphthochrysene

Table 2 List of PAHs detected by GC/MS with mass number.

The GC/MS analyses show a distribution of PAH masses m/z ranging from 152 to 530. A zoo of different PAH molecules could be identified with the corresponding mass spectra (see Table 2). The extracted PAH compounds were used for further spectroscopic measurements in the UV/VIS and IR region. A more detailed description of the measurements and results is given in Jäger *et al.* (2006 and 2007a).

We found that the optical properties of the soot can be influenced by the adsorbed PAHs but we have also observed the opposite effect. The position of the IR bands of PAHs can be affected by the soot which was proven by IR measurements of phenanthrene molecules adsorbed on soot particles measured at room temperature (Fig. 15). The two strong bands of phenanthrene due to b_1 vibrations (818.8 and 732.9 cm^{-1}) were found to be at nearly the same position like phenanthrene molecules at 10 K (812.8 and 735.0 cm^{-1}) (Hudgins and Sandford 1998). However, according to these authors the difference of the temperatures should cause a shift by -3 cm^{-1} which cannot be observed. The expected band shift is obviously compensated by an equal shift to larger wavenumbers which is caused by an electronic interaction of the p electron system of the PAH molecules with the rather electron-poor p bonds in bent graphene layers on the surface of the soot nanoparticles.

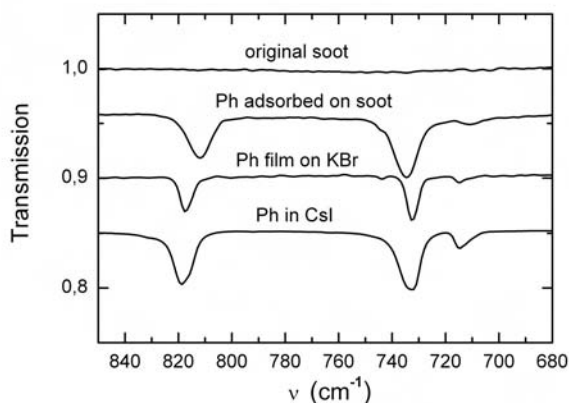


Fig. 15: IR spectrum of phenanthrene (Ph) adsorbed on carbon soot particles in comparison with spectra obtained from a phenanthrene film on KBr and from phenanthrene powder embedded in CsI.

3.5.5. Investigation of the carbon grain formation process in gas-phase condensation

The high power densities of 2×10^8 - 9×10^9 W/cm² due to the use of a pulsed laser in the laser ablation condensation experiments lead to high temperatures in the reaction and condensation zone and the formation of fullerene-like soot. By using the particle beam extraction in the hot and dense condensation zone we were able to quench the first carbon seed particles in the original condensation state and to avoid further processing like coalescence of the seeds to larger structures.

The HRTEM images of the soot samples show a number of fullerene-like particles with sizes between 1-3 nm. The observed particles consist of more or less disturbed or elongated carbon cage structures. Fig. 16 shows some small grains which are built by differently sized carbon cages. Especially interesting is the finding of parts of cage structures which are not closed completely. Such structures can be observed in Fig. 18. The right panel of this figure shows a bowl-like structure.

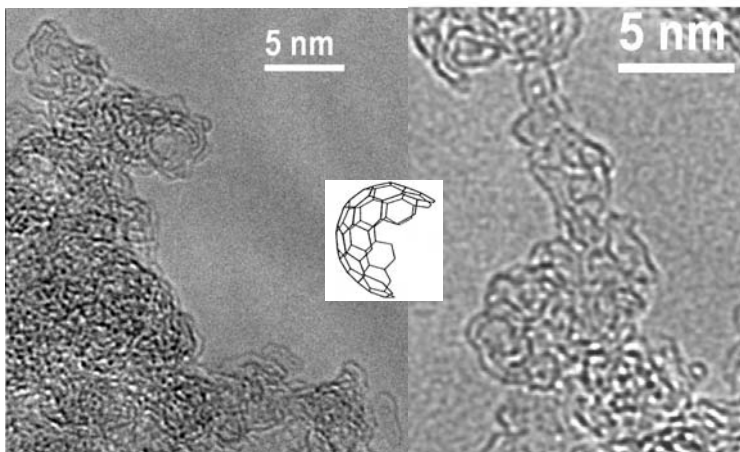


Fig. 16 HRTEM bright field images of small fullerene-like grains showing elongated fullerene structures and carbon cages. In the right panel one can observe an example of an incomplete cage structure (upper left corner).

The detection of these structures and the additional occurrence of $\equiv\text{C-H}$ bands of sp-hybridized carbon point to a particle formation process starting with C polyynes chains. These chains form finally saucer-shaped carbon structures which can combine to fullerene-like particles. This soot formation process is similar to a fullerene condensation process proposed by Kroto and McCay (1988). The side product or soluble components in these condensates are fullerenes. Laser pyrolysis of gas-phase hydrocarbons has been often used as an effective method to produce extractable components such as PAHs and fullerenes in condensed soots. Pope (1996) has calculated that the fullerene yield is at most for high temperatures and low pressures between 1800 and 2500 K. At temperatures lower than 1800 K, the side products are mainly PAHs, whereas at temperatures higher than 2500 K the pyrolysis products are composed of polyyne-based compounds.

Pulsed CO_2 laser pyrolysis of acetylene, ethylene and mixtures of both gases produces the same kind of very small fullerene-like carbon condensates (see Table 3). The power densities in the reaction zone which could be realized with the pulsed laser are between 10^7 - 10^9 W/cm^2 still preferring a high-temperature condensation process.

Precursor	Buffer gas	LP (W)	Laser	Power density W/cm^2	Side products
C_2H_2 , C_2H_4 , SF_6	He	1-20	pulsed	5×10^7 - 1×10^9	fullerene-like soot
C_2H_4 , C_6H_6	Ar	600	cw	5200	soot + PAHs (33wt%)
	Ar	850	cw	6500	soot + PAHs (17wt%)
C_6H_6 , SF_6	Ar	60	cw	900	100% PAHs (no soot)

Table 3 Laser pyrolysis experiments used to condense carbon soot with different structures and soluble components.

The application of a cw laser with much less power density between 5200 and 6500 W/cm^2 provides a completely different condensate.

The soot grains are rather large showing longer and less disturbed grapheme layers. The produced soot materials contain a remarkable amount of soluble components which turned out to consist of a mixture of plane PAH molecules (see next section). Here, the soot formation process is different compared to the high energy condensations. The lower the power density the higher is the content of PAHs. The decrease of the power density in the reaction zone reduces the amount of insoluble carbon soot grains. For a 60 W cw-CO₂ laser corresponding to a power density of 900 W/cm² only a soluble condensate was produced consisting of a mixture of PAHs. The soot condensation process is driven by a combination of small molecules, C₂ addition, formation of plane PAHs and subsequent condensation and growth of carbon grains, a formation scheme described by Richter and Howard (2000).

3.6 Zusammenfassung und Ausblick / Summary and future

We have investigated the structural and spectroscopic properties of carbonaceous condensates from various processes in a comprehensive way including co-condensation of carbides, different precursors, temperatures and reactive atmospheres. The results obtained allowed to draw conclusions about the incorporation of hydrogen and the condensation processes at high and low temperatures. The spectra measured agree partly with astronomical spectra of circumstellar carbon condensates. A strong UV resonance has been found with material rich in volatiles, the position of which, however, is different from the one of the interstellar UV hump. Furthermore, our investigation of the UV spectral properties of nanodiamonds from primitive meteorites (Mutschke *et al.* 2004) has led to a collaboration on the UV extinction in Active Galactic Nuclei (Binette *et al.* 2005, 2006)

We will continue this research in two directions. First, we intend to investigate the influence of UV irradiation on carbon structures and their UV spectra. According to Mennella *et al.* (1998) this has a crucial influence on the UV properties, but only a single experimental study is available for this so far. Second, we plan to intensify the investigation of volatile components from soot including a separation of the molecular species and their spectroscopic measurement.

3.7 Literatur / References

- Allain, T., Sedlmayr, E., Leach, S., PAHs in circumstellar envelopes I. Processes affecting PAH formation and growth, *Astron. Astrophys.*, **323** (1997), p. 163
- Binette, L., Magris C., G., Krongold, Y., Morisset, C., Haro-Corzo, S., Antonio de Diego, J., Mutschke, H., Andersen, A.C.: *Nanodiamond dust and the far-ultraviolet quasar break*, *Astrophys. J.*, **631** (2005) 661.
- Binette, L., Andersen, A.C., Mutschke, H., Haro-Corzo, S.: *Nanodiamond dust and the energy distribution of quasars*, *Astron. Nachr.* **327** (2006) 151.
- Bogana, M., Ravagnan, L., Casari, C.S., *et al.*: *Leaving the fullerene road: presence and stability of sp chains in sp² carbon clusters and cluster-assembled solids*, *New Journal of Physics* **7** (2005) 81
- Chhowalla, M., Wang, H., Sano, N., *et al.*: *Carbon Onions: Carriers of the 217.5nm Interstellar Absorption Feature*, *Phys. Rev. Lett.* **90** (2003) 155504.
- Chigai, T., Yamamoto, T.: *Condensation sequence of SiC and graphite grains around carbon stars*, *Geochim. Cosmochim. Acta* **67** (2003) Suppl. 1, A64.
- Clayton, D.D., Deneault, E.A.N. and Meyer, B.S.: *Condensation of carbon in radioactive supernova gas*, *Astrophys. J.* **562** (2001) 480.
- Duley, W.W., and Seahra, S.S.: *2175 Å and 3.4 Micron Absorption Bands and Carbon Depletion in the Diffuse Interstellar Medium*, *Astrophys. J.* **522** (1999), L129
- Duley, W.W. and Lazarev, S.: *Ultraviolet absorption in amorphous carbons: PAHs and the 2175 Å extinction feature*, *Astrophys. J.* **612** (2004), L33.
- Galvez, A., Herlin-Boime, N., Reynaud, C., Clinard, C., Rouzaud, J.N. : *Carbon nanoparticles from laser pyrolysis*, *Carbon* **40** (2002) 2775.
- Hudgins, D., Sandford, S., *J. Phys. Chem. A* **102** (1998) 329
- Iglesias-Groth, S.: *Fullerenes and buckyonions in the interstellar medium*, *Astrophys. J.* **608** (2004), L37.
- Jäger, C., Krasnokutski, S., Staicu, A., Huiskens, F., Mutschke, H., Henning, Th., Poppitz, W., Voicu, I.: *Identification and spectral properties of PAHs in carbonaceous soot produced by laser pyrolysis*, *Astrophys. J. Suppl. Ser.* **166** (2006) 557 .
- Jäger, C., Mutschke, H., Huiskens, F., Henning, Th., Voicu, I., Poppitz, W.: *Spectral characterization of soot by-products obtained by CO₂ laser pyrolysis of benzene/hydrocarbon vapors*, *Phys. Chem. Chem. Phys.* (2007a) in preparation
- Jäger, C., Mutschke, H., Henning, Th., *Spectral and structural properties of carbon nanoparticles produced by laser ablation*, *Astrophys. J.*, (2007b), in preparation.

- Keller, A., Kovacs, R. and Homann, K.-H.: *Large molecules, ions, radicals and small soot particles in fuel-rich hydrocarbon flames*, Phys. Chem. Chem. Phys. **2** (2000) 1667.
- Kwok, S., Volk, K., and Bernath, P.: *On the origin of infrared plateau features in proto-planetary nebulae*, Astrophys. J. **554** (2001), L87
- Kroto, H.W., McKay K.: *The formation of quasi-icosahedral spiral shell carbon particles*, Nature **331** (1988) 328.
- Llmas Jansa, I., Jäger, C., Mutschke, H., Henning, Th.: *Far-ultraviolet to near-infrared optical properties of carbon nanoparticles produced by pulsed-laser pyrolysis of hydrocarbons and their relation with structural variations*, Carbon, (2007), submitted
- Llmas Jansa, I.: *Experimental study on the optical and structural properties of carbon nanoparticles*. Ph. D. Thesis, Friedrich Schiller Universität Jena, (2006)
- Llmas Jansa, I.: *Spectroscopy and Structural Characterization of Carbon Nanoparticles Produced by Laser Pyrolysis of Acetylene*, Master Thesis (2002), Friedrich-Schiller-Universität Jena
- Llmas Jansa, I., Mutschke, H., Clément D., Jäger, C., Henning, Th.: *IR spectroscopy of carbon nanoparticles from laser-induced gas pyrolysis*, In: Exploring the ISO Data Archive-Infrared Astronomy in the Internet Age, ed. C. Gry *et al.*, ESA SP-511 (2003) 69.
- Lodders, K., Fegley Jr., B.: *Condensation chemistry of circumstellar grains*, In: Asymptotic Giant Branch Stars, ed. T. Le Bertre *et al.*, IAU Symp. **191** (1999) 279.
- Mennella, V., Colangeli, L., Bussoletti, E., Palumbo, P., Rotundi, A.: *A new approach to the puzzle of the ultraviolet interstellar extinction bump*, Astrophys. J. **507** (1998) L177.
- Mutschke, H., Andersen, A.C., Jäger, C., Henning, Th., Braatz, A.: *Optical data of meteoritic nano-diamonds from far-ultraviolet to far-infrared wavelengths*, Astron. Astrophys. **423** (2004) 983.
- Palotas, A.B., Rainey, L.C., Feldermann, C.J., Sarofim, A.F., Vander Sande, J.B.: *Soot morphology: An application of image analysis in high-resolution transmission electron microscopy*. Microscopy Research and Technique **33** (1996) 266.
- Peters, E., Hony, S., Van Kerckhoven, C., *et al.*: *The rich 6 to 9 μm features of interstellar PAHs*, Astron. Astrophys. **390** (2002), 1089
- Pendleton, Y.J. and Allamandola, L.J.: *The organic refractory material in the diffuse interstellar medium: Mid-infrared spectroscopic constraints*, Astrophys. J. Suppl. Ser. **138** (2002) 75.
- Pope, C.J., Howard, J.B.: *Thermodynamic limitations for fullerene formation in flames*, Tetrahedron **52** (1996) 5161.

- Reynaud, C., Guillois, O., Herlin-Boime, N., *et al.*: *Optical properties of synthetic carbon nanoparticles as model of cosmic dust*, Spectrochim. Acta Part A **57** (2001), 797
- Robertson, J. and O'Reilly, E.P., *Electronic and atomic structure of amorphous carbon*, Physical Review **B 35** (1987), 2946
- Schnaiter, M., Mutschke, H., Dorschner, J., Henning, Th., and Salama, F.: *Matrix-isolated nano-sized carbon grains as analog for the 217.5 nanometer feature carrier*, ApJ, Vol. 498 (1998), p. 486
- Schnaiter, M., Gimmmler, M., Linke, C., Jäger, C., Llamas Jansa, I., and Mutschke, H.: *Strong spectral dependence of light absorption by organic particles formed by propane combustion*, Atmospheric Chemistry and Physics Discussions, **6** (2006) 1841.
- Stadermann, F.J., Croat, T.K., Bernatowicz, T.J., Amari, S., Messenger, S., Walker, R.M., Zinner, E.: *Supernova graphite in the NanoSIMS: Carbon, oxygen and titanium isotopic compositions of a spherule and its TiC sub-components*, Geochimica et Cosmochimica Acta, **69** (2005) 177.
- Tomita, S., Fujii, M., Hayashi, S.: *Detective carbon onions in interstellar space as the origin of the optical extinction bump at 217.5 nm*, Astrophys. J. **609** (2004) 220.
- Van Kerckhoven, C., Tielens, A.G.G.M. and Waelkens, C.: *Nanodiamonds around HD 97048 and Elias 1*, Astron. Astrophys. **384** (2002) 568.
- Vijh, U.P., Witt, A.N. and Gordon, K.D.: *Blue Luminescence and the Presence of Small Polycyclic Aromatic Hydrocarbons in the Interstellar Medium*, Astrophys. J. **619** (2005) 368.
- Witanachchi, S., Miyawa, A.M. and Mukherjee, P.: *Highly ionized carbon plasma generation by dual-laser ablation for diamond-like carbon film growth*, Mat. Res. Soc. Symp. **617** (2000) J3.6.1
- Zubko, V.G., Mennella, V., Colangeli, L., and Bussoletti, E.: *Optical constants of cosmic carbon analogue grains-I. Simulation of clustering by a modified continuous distribution of ellipsoids*, Mon. Not. R. Astron. Soc. **282** (1996) 1321.

3.1 Bericht Teilprojekt 9

3.1.1 Titel / Title

Infrarot-Spektroskopie und -Lichtstreuung von Teilchenagglomeraten

Infrared spectroscopy and light scattering of dust agglomerates

3.1.2 Berichtszeitraum / reported period

01.07.2003 - 30.06.2006

3.1.3 Projektleiter / principle investigator

Mutschke, Harald, Dr. rer. nat.,
Friedrich-Schiller- Universität Jena

Blum, Jürgen, Prof. Dr. habil,
Technische Universität Braunschweig

3.1 Zusammenfassung / Abstract

3.2.1 Wortlaut des Antrags / abstract of the proposal

Dieses Projekt setzt einerseits die Arbeiten in TP 9 fort, indem die Infrarot-Extinktion durch Teilchen und Teilchen-Agglomerate in den Schwingungsbanden des Materials gemessen werden soll. Dabei soll der in der vergangenen Projektphase entwickelte experimentelle Aufbau benutzt werden. Andererseits sollen in diesem Projekt mit der Messung der Streukoeffizienten der Teilchen Aspekte von TP 10 weiter verfolgt werden, dies soll jedoch jetzt ebenfalls im infraroten Spektralbereich geschehen. Beide Messungen sollen an den gleichen Ensembles frei fliegender Teilchen in einer Niederdruck-Gasumgebung geschehen. Die Kombination von Streu- und Extinktionsmessungen soll eine umfassende Untersuchung von Form- und Agglomerationseffekten auf die optischen Eigenschaften der Teilchen ermöglichen.

This project is aimed to continue TP 9 in measuring infrared extinction by particles and particle agglomerates in vibrational bands with the experimental setup developed in the preceding project phase. In addition, we intend to continue part of the work previously done in TP 10 by measuring the particles' scattering coefficients, but now in the infrared spectral range. Both types of measurements will be done on the same ensembles of free-flying particles in a low-pressure gas environment. The combination of these measurements will allow us to study in a comprehensive way the effect of particle shape and agglomeration on the optical properties of solid particles.

3.2.2 Zusammenfassung des Berichts / abstract of the report

In this project, we have measured for the first time the infrared absorption spectra of *free-flying* silicate and oxide particles, i.e. of particles dispersed as an *aerosol*. We have obtained spectra in the wavelength range from 5 to 30 μm for amorphous and crystalline silicates of different compositions as well as for aluminum/magnesium and titanium oxides. Unlike previous approaches, this experiment allows a direct comparison of laboratory-measured infrared data of small particles with astronomical spectra of “dusty” environments such as AGB star atmospheres, accretion disks and planetary systems. Such comparisons have been carried out for a few objects so far and the differences to data obtained with classical spectroscopic methods have been quantified (Tamanai et al. 2006a).

Second, using this method we were able to investigate correlations between the spectral band profiles and the shape and agglomerate structure of the particles as seen by electron microscopic imaging. In this course we have investigated the spectra of powders with different grain shapes and identical composition and we have studied the influence of agglomeration on the spectra of spherical SiO_2 particles. Using theoretical light-scattering models, we have simulated the effects of agglomeration and of grain shape distributions and have compared the results with our measured band profiles (Tamanai et al. 2006b). This allows to interpret the measured spectra and to calibrate the geometrical parameters of the light-scattering models (Mutschke et al. 2006 and paper in preparation).

The infrared *scattering* measurements proposed in the project proposal could not be carried out because of (1) an accident during the setting up of the absorption spectroscopy experiment which damaged the setup and delayed the experimental activities, (2) the wide range of appli-

cations which the successful absorption spectroscopy experiment opened after it was working and (3) the necessary extensive theoretical simulation work, including a check of the applicability of light-scattering models in strong infrared bands (Andersen et al. 2006), which was carried out before the experimental work started.

3.3 Ausgangsfragen, neuster Stand der Forschung / Initial goals, current status of the field

Absorption spectra of solid particles small compared to the wavelength show pronounced bands due to the excitation of lattice vibrations. These bands are characteristic for the compound and its crystal structure and are of high analytical value. Apart from the dependence on the material, however, they depend also on the grain size, shape and the environment of the particle (e.g. Fabian et al. 2001). Classical infrared spectroscopic methods such as the measurement of absorption spectra from powders embedded in a KBr or polyethylene pellet result in changes of the band profile compared to the spectral characteristics of free particles such as cosmic dust grains (Tamanai et al. 2006a). On the other hand, the calculation of absorption band profiles is difficult for realistic grain shapes because exact methods such as the discrete dipole approximation tend to have large errors in regions of strong absorption (Andersen et al. 2006). Statistical methods using a parametrization of the average geometrical properties of an ensemble of particles require calibrating the free parameters for the particle geometry (Min et al. 2006). Measured spectroscopic data in the presence of information about the grain geometry, however, are rare, especially if the state of the particle agglomeration is considered.

On the other hand, there is a growing number of observations in the infrared wavelength region which aim at the investigation of dust properties in the interstellar medium including other galaxies, evolved stars, and especially young stars with accretion disks and planetary systems. Observations from the ground (e.g. Honda et al. 2003, Przygodda et al. 2003, van Boekel et al. 2004, 2005, Schütz et al. 2005a,b) and from space using the Infrared Space Observatory (e.g. Meeus et al. 2001) and nowadays the Spitzer Space Observatory (e.g. Kessler-Silacci et al. 2006, Furlan et al. 2006) have investigated emission band profiles of dusty circumstellar disks and outflows and have begun to extract from these band profiles information about dust mineralogy and grain size. The reason is that the dust properties trace physical conditions such as thermal struc-

ture, density and transport mechanisms in these environments (Bouwman et al. 2001).

Consequently, there is an expanding need for understanding the details of the infrared spectra of silicate and oxide particles. With this project we have provided an important contribution to the current progress in this field.

3.4 Angewandte Methoden / Experimental methods

3.4.1 Aerosol generation and spectroscopy

In this project we have built up a system for aerosol generation and spectroscopy, consisting of (1) a spectroscopy chamber connected to an FTIR spectrometer (Bruker 113v) and equipped with mirrors for multiple reflection of the infrared spectrometer beam and a pyroelectric detector and (2) an aerosol generator with a rotating-brush disperser (Palas RGB 1000) and a self-constructed impactor (see Fig.1).

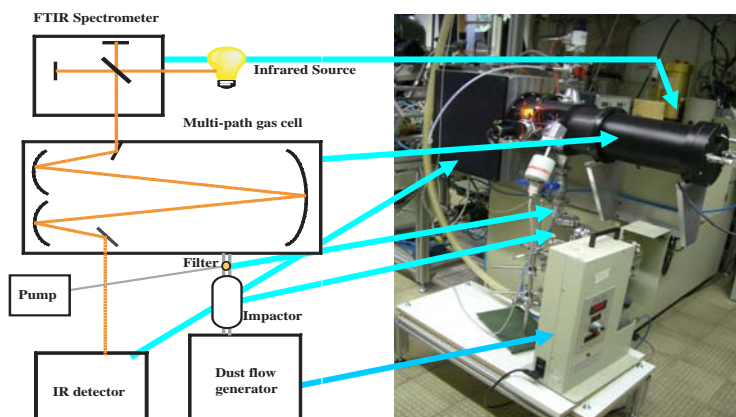


Fig. 1: Schematic setup and photo of the aerosol spectroscopy experiment.

During operation the rotating-brush disperser transports particles having grain sizes between 0.1 and 5 μm from a powder storage into a gas flow (N_2), which then carries the particles through the gas cell. The impactor is able to retain larger clumps of particles and, on the other hand, densifies the aerosol by removing some of the carrier gas. A filter can be inserted into the gas flow in order to sample particles for scanning electron microscopy (SEM). Typical electron micrographs of the aerosol

particles are shown in Fig.2. With this aerosol the spectroscopy chamber is partly filled, while additional continuous gas flows from the side protect the mirrors from contamination with particles. The aerosol density in the chamber is 10^5 - 10^6 cm⁻³ allowing for high signal-to-noise spectroscopic measurements in absorption bands with 32 passes of the infrared beam through the aerosol chamber.

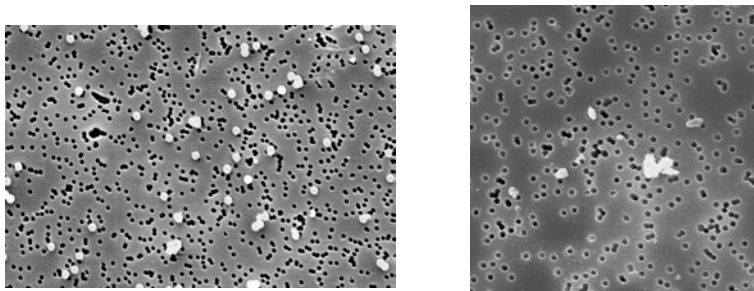


Fig. 2: SEM images of spherical SiO₂ particles of 1 μ m diameter (left) and Mg₂SiO₄ (forsterite) particles (right) sampled from the aerosol. The filter pores (dark spots) are 0.4 μ m in size

3.4.2 Pellet spectroscopy

For comparison and for additional information we have applied the conventional pellet technique, where a small amount of sample material is mixed with IR transparent KBr or polyethylene powder at a mass ratio of e.g. 1:1000 and is pressed to a pellet of 0.2 g mass. The pellet is placed in the spectrometer beam for extinction measurements. The measurements with this widely used method are important to investigate differences in the measured band profiles between free-flying and embedded grains (see Sect. 3.5.1). Moreover, they provide quantitative information in terms of the mass extinction coefficient which can be used for calibration of the aerosol measurements and they give an independently measured result which can be compared to calculations (Sect. 3.5.3).

3.4.3 Computation of extinction spectra

For the spherical SiO_2 particles we have used exact light scattering theory in order to investigate the effect of particle agglomeration on the extinction spectra. In this course, a T-matrix code (Mackowski 1994) and the Discrete Dipole Approach (DDSCAT, Draine 1988) have been applied. Although we have shown that these methods may fail to converge in strong absorption bands (Andersen et al. 2006), for the optical constants of SiO_2 they give sufficiently accurate results (see Sect.3.5.2).

In case of all other samples, we have compared with calculations of extinction spectra based on a statistical approach. This model takes a continuous distribution of particle shapes (shape factor distribution - SFD) into account (Min et al. 2006). We have determined the SFDs from the measured band profiles for a number of our samples (see Sect. 3.5.3).

3.5 Ergebnisse und ihre Bedeutung / Results and their importance

3.5.1 Comparison of aerosol and pellet spectra

Up to now, 15 different silicate and oxide materials have been measured using both the aerosol and pellet techniques. Among them are the crystalline silicate minerals forsterite (Mg_2SiO_4) and enstatite (MgSiO_3) and their amorphous counterparts as well as amorphous and crystalline SiO_2 . These compounds are the most abundant solids in space.

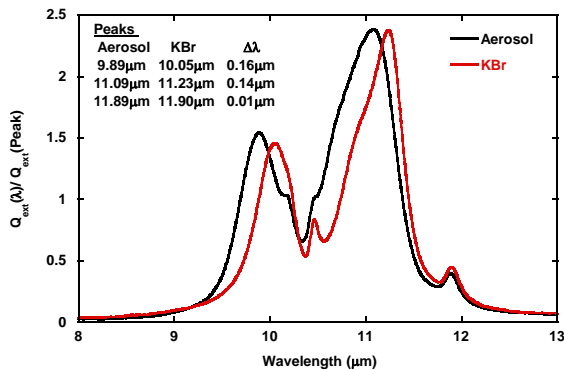


Fig. 3: Normalized extinction cross section for forsterite particles (commercial material from Alpha Johnson) measured for free (aerosol) and embedded (KBr) particles.

Their spectral signatures are observed in most dusty environments in space and are analyzed for variations in the chemical composition, crystallinity, and size of the dust grains. Accurate information on the shape of the band profiles is therefore extremely important, especially for the spectral range of the Si-O stretching vibrations (8-13 μm) which can be observed from ground and are therefore most widely investigated.

Fig.3 shows our results obtained in this spectral range with the aerosol and the pellet methods for a synthetic forsterite powder. The Figure demonstrates the significant difference between the band profiles measured using these two different techniques. The positions of the strong peaks in the band are generally at shorter wavelengths for free particles. Small peaks do not shift but can change to shoulders by merging with the strong bands.

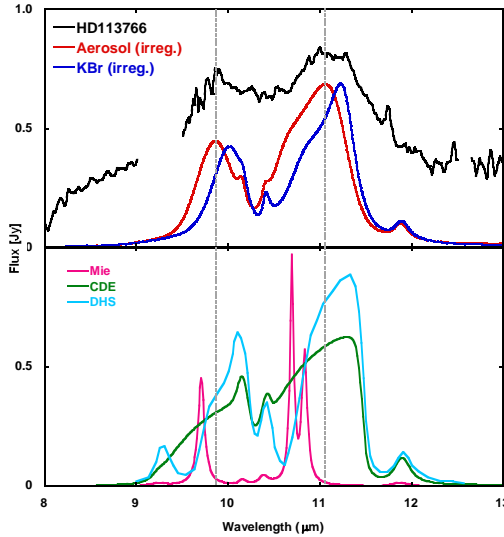


Fig. 4: Comparison of the measured spectra from Fig.3 with the observed spectrum of the main sequence object HD 113766 and with simulated forsterite spectra obtained using different light-scattering theories. The vertical lines indicate the positions of the main peaks in the aerosol spectrum.

Whereas the aerosol spectrum can directly be used for a comparison with an astronomical spectrum, the pellet result would give wrong results. This is demonstrated in Fig.4 by comparing with the observed spectrum of a

main sequence star with dusty disk and with several simulated spectra. The spectrum of the free forsterite particles coincides with a peak at 11.1 μm in the observed spectrum but not with the maximum at 11.3 μm , which would match to the spectrum of the embedded grains. Furthermore, the calculated spectra using the Mie theory, the classical Continuous Distribution of Ellipsoidal shapes (CDE, Bohren and Huffman 1983), or the more advanced Distribution of Hollow Spheres (DHS, Min et al. 2005) do not reproduce the measured band profiles (Tamanai et al. 2006a). This underlines the importance of our results and of a mandatory improvement of the theoretical approaches.

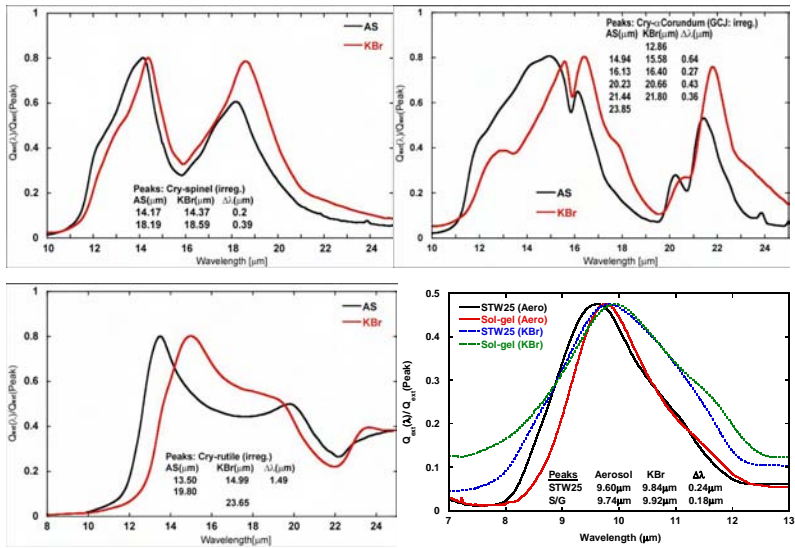


Fig. 5: Comparison of aerosol (AS) and pellet (KBr) spectra for various oxides (corundum – Al_2O_3 , spinel – MgAl_2O_4 , rutile – TiO_2) and two amorphous silicates of approximate composition MgSiO_3 (STW25 is a melting/ quenching, S/G is a sol-gel process product – Dorschner et al. 1995, Jäger et al. 2003).

Even more pronounced is the influence of the embedding medium on band profiles for some oxide materials such as Al_2O_3 , TiO_2 , and MgAl_2O_4 (see Fig.5, upper and left panels). These compounds are high-temperature condensates in oxygen-rich environments and are considered to dominate the emission from some lower-mass-loss AGB stars (Posch et al. 1999, 2003). The difference in the position of absorption peaks between embedded and free-flying particles can amount to about 1.5 μm in these cases.

Even for amorphous silicates which represent the most abundant dust material in space the effect of an embedding medium is not negligible (Fig.5, lower right panel). Although this effect is in principle known and can be approximately calculated for simple grain geometries, this is the first time that it had been quantified by measurements for a number of important and real dust materials.

3.5.2 Effect of agglomeration

In contrast to the pellet method, the aerosol technique bears the capability of studying the influence of grain growth by agglomeration on spectroscopic features experimentally. In a first approach, we have investigated the effect of larger aggregates on the spectrum by varying the abundance of clumps left from imperfect de-agglomeration in the disperser. By removing the impactor from the aerosol line, we allowed larger clumps to reach the spectroscopy chamber. There, the biggest and more compact ones settle down quickly, but smaller and more open aggregates are easily carried by the gas in addition to the well-dispersed particle fraction. Fig.6 shows an SEM image of such larger clumps together with the IR band profiles measured for SiO_2 aerosols which have been produced with and without use of the impactor (compare Fig. 2).

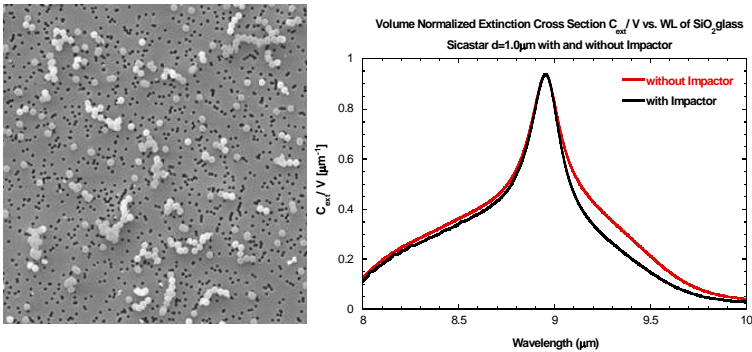


Fig. 6: SEM image and band profile obtained for SiO_2 particles without use of the impactor .

The effect of the aggregates is obviously the strengthening of a wing at the long-wavelength side of the band profile. This is supported by calculations using exact light scattering theory for aggregates of spherical SiO_2 particles (see Fig. 7). Apart from a slight mismatch of the peak position,

which may be caused by a deviation in the particle's optical constants from the bulk SiO_2 properties, these calculations demonstrate that aggregation leads preferentially to an increase of the extinction in the long-wavelength wing of the band (Tamanai et al. 2006b).

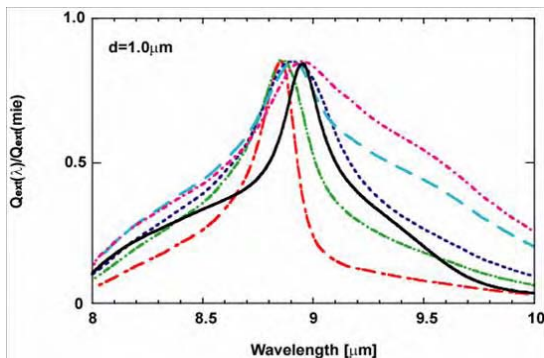


Fig. 7: Comparison of the measured band profile of SiO_2 particles ($d=1.0 \mu\text{m}$, black) with calculations for various cluster geometries using the DDSCAT code. The simulated spectra are for a single sphere (red), two touching spheres (green), a tetrahedral aggregate of four spheres (blue) and two irregular clusters of 16 spheres (light blue and magenta).

In a theoretical study, which has been performed in collaboration with colleagues in Copenhagen, Vienna, and Amsterdam, we have investigated the applicability of the DDA and T-matrix approaches for calculation of infrared band profiles for agglomerate particles composed of other materials (Andersen et al. 2006). We have demonstrated that, for resonances in which the real part of the refractive index becomes close to zero (as is the case, e.g. in the IR band of SiC) neither of these exact light-scattering calculations reaches a convergence even with very high dipole densities in the DDA or very high multipole numbers in the T-matrix calculations. Fortunately, for SiO_2 the resonance strength is moderate enough to allow at least approximate results which are shown above.

3.5.3 Shape effects and shape factor distribution

For nonspherical particles, even if they can be considered to be small compared to the wavelength, statistical light-scattering approaches are needed to reproduce or predict band profiles. However, as has been demonstrated in Fig.4, models assuming simple distributions of shape factors

such as the CDE or DHS do not reproduce measured band profiles in all detail. For a better fit, they need to be calibrated, i.e. shape factor distributions for certain particle shapes need to be determined.

The spectra measured in aerosol and in KBr provide valuable information for this purpose. Moreover, for some of the materials studied in this project, we were able to investigate particles with different shapes. Fig.8 shows spectra of forsterite powders obtained from two different sources (Marusu and Alpha Johnson, respectively) of which the former particles have a roundish shape whereas the latter have a sharp-edged, irregular shape (see the TEM images in Fig.8). Likewise, in Fig.9 we show the spectra of two Al_2O_3 powders with different particle shapes.

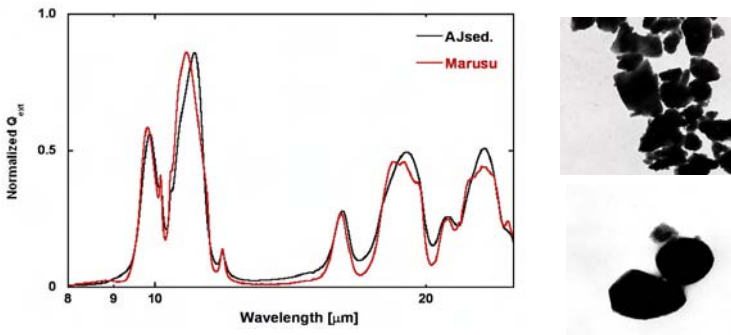


Fig. 8: Influence of particle shape on the forsterite (Mg_2SiO_4) band profiles. Grains of sample AJsed (Alpha Johnson after sedimentation, upper TEM image) have a sharp-edged shape whereas grains of sample Marusu (lower image) are round.

For both minerals, the measured spectra demonstrate a strong influence of the particle shape on the measured band profiles. Generally, for roundish (or ellipsoidal) grains the peaks of the bands are located at shorter wavelengths compared to those of the irregular grains. This is not only true for the aerosol-measured spectra but also for the pellet spectra (see Fig.10, right panel).

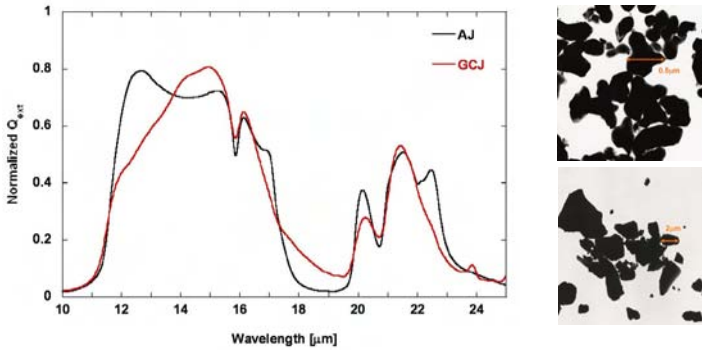


Fig. 9: Influence of particle shape on the corundum (Al_2O_3) band profiles. Sample AJ (Alpha Johnson, upper TEM image) has a roundish grain shape whereas grains of sample GCJ (Institute for Glass Chemistry Jena, lower image) are sharp-edged.

For one of the materials (forsterite), we have demonstrated that the measured spectra can be reproduced using suitable shape factor distributions (SFDs, Mutschke et al. 2006). These SFDs depend on the characteristics of the grain shape but are of course independent on the embedding medium used in the measurement. Consequently, they reproduce both the aerosol and pellet spectra at the same time (Fig.10). This is the first time that light-scattering models have been calibrated according to the influence of the grain shape for real ensembles of particles.

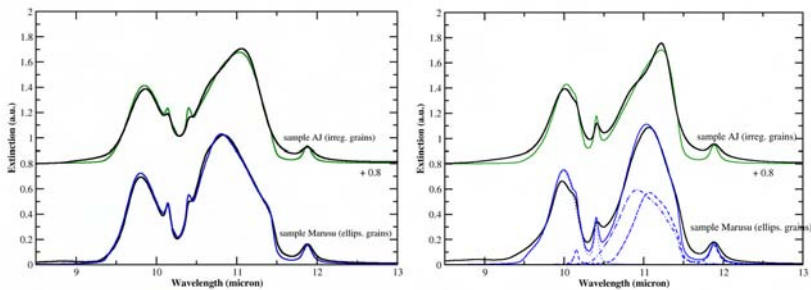


Fig. 10: Comparison of measured (black lines) and calculated spectra using special shape factor distributions for the two different forsterite powders. Left panel is for measurements in aerosol (same as in Fig.8), right is for embedded particles. Identical shape factor distributions are used for left and right. The dotted lines indicate the contributions from fields along the three forsterite crystal axes.

3.6 Zusammenfassung und Ausblick / Summary and future

The project carried out during the reported period has led to the development of a very promising experiment which in contrast to previous approaches allows (1) direct comparison of experimental and astronomical infrared spectra of solid particles, (2) the investigation of band profiles in dependence on shape and agglomeration of the particles and (3) the calibration of statistical light-scattering models for these influences.

We have recently applied for support by the DFG for a new research project which would make use of this experiment for further measurements, aiming at the development of a database of dust aerosol spectra for application to the modeling of debris disks and a continuation of the work on the calibration of light scattering models.

3.7 Literatur / References

- Andersen, A.C., Mutschke, H., Posch, Th., Min, M., Tamanai, A.: *Infrared extinction by homogeneous particle aggregates of SiC, FeO and SiO₂: Comparison of different theoretical approaches*, J. Quant. Spectr. Rad. Transfer **100** (2006) 4.
- Bouwman, J., Meeus, G., de Koter, A., Hony, S., Dominik, C., Waters, L.B.F.M.: *Processing of silicate dust grains in Herbig Ae/Be systems*, Astron. Astrophys. **375** (2001) 950
- Bohren, C.F., Huffman, D.R.: *Absorption and Scattering of Light by Small Particles*, Wiley, New York, 1983
- Dorschner, J., Begemann, B., Henning, Th., Jäger, C., Mutschke, H.: *Steps toward interstellar silicate mineralogy II. Study of Mg-Fe-silicate glasses of variable composition*, Astron. Astrophys. **300** (1995) 503.
- Draine, B.T.: *The discrete-dipole approximation and its application to interstellar graphite grains*, Astrophys. J. **333** (1988), 848.
- Fabian, D., Henning, Th., Jäger, C., Mutschke, H., Dorschner, J., Werhan, O.: *Steps toward interstellar silicate mineralogy VI. Dependence of crystalline olivine IR spectra on iron content and particle shape*, Astron. Astrophys. **378** (2001) 228.
- Furlan, E., Hartmann, L., Calvet, N., and 9 colleagues: *A survey and analysis of Spitzer Infrared Spectrograph spectra of T Tauri stars in Taurus*, Astrophys. J. Suppl. Ser. **165** (2006) 568.
- Honda, M., Kataza, H., Okamoto, Y.K., and 5 colleagues: *Detection of crystalline silicates around the T Tauri star HEN 3-600A*, Astrophys. J. **585** (2003) L59.
- Jäger, C., Dorschner, J., Mutschke, H., Posch, Th., Henning, Th.: *Steps toward interstellar silicate mineralogy VII. Spectral properties and crystallization behaviour of magnesium silicates produced by the sol-gel method*, Astron. Astrophys. **408** (2003) 193.
- Kessler-Silacci, J., Augereau, J.-C., Dullemond, C.P., and 10 colleagues: *c2d Spitzer IRS Spectra of Disks around T Tauri Stars. I. Silicate Emission and Grain Growth*, Astrophys. J. **639** (2006) 275.
- Mackowski, D.W.: *Calculation of total cross sections of multiple-sphere clusters*, J. Opt. Soc. Am. **A11** (1994) 2851.
- Meeus, G., Waters, L.B.F.M., Bouwman, J., van den Ancker, M.E., Waelkens, C., Malfait, K.: *ISO spectroscopy of circumstellar dust in 14 Herbig Ae/Be systems: Towards an understanding of dust processing*, Astron. Astrophys. **365** (2001) 476.
- Min, M., Hovenier, J.W., de Koter, A.: *Modeling optical properties of cosmic dust grains using a distribution of hollow spheres*, Astron. Astrophys. **432** (2005) 909.

- Min, M., Hovenier, J.W., Dominik, C., de Koter, A., Yurkin, M.A.: *Absorption and scattering properties of arbitrarily shaped particles in the Rayleigh domain: A rapid computational method and a theoretical foundation for the statistical approach*, J. Quant. Spectr. Rad. Transfer **97** (2006) 161.
- Mutschke, H., Tamanai, A., Min, M.: *Experimental infrared spectroscopy of dust grains in aerosol: Modeling of forsterite spectra*, Poster at the Workshop: From Dust to Planetesimals, Ringberg, Sept. 2006
- Posch, Th., Kerschbaum, F., Mutschke, H., et al.: *Infrared properties of solid titanium oxides: Exploring potential primary dust condensates*, Astrophys. J. Suppl. Ser. **149** (2003) 437
- Przygodda, F., van Boekel, R., Àbrahàm, P., Melnikov, S.Y., Waters, L.B.F.M., Leinert, Ch.: *Evidence for grain growth in T Tauri disks*, Astron. Astrophys. **412** (2003) L43
- Schütz, O., Meeus, G., Sterzik, M.F.: *Mid-IR observations of circumstellar disks. I. Pre-main sequence objects*, Astron. Astrophys. **431** (2005a) 165.
- Schütz, O., Meeus, G., Sterzik, M.F.: *Mid-IR observations of circumstellar disks. II. Vega-type stars and a post-main sequence object*, Astron. Astrophys. **431** (2005b) 175.
- Tamanai, A., Mutschke, H., Blum, J., Meeus, G.: *The 10 μm infrared band of silicate dust: A laboratory study comparing the aerosol and KBr pellet techniques*, Astrophys. J. Letters **648** (2006a) L147
- Tamanai, A., Mutschke, H., Blum, J., Neuhäuser, R.: *Experimental infrared spectroscopic measurement of light extinction for agglomerate dust grains*, J. Quant. Spectr. Rad. Transfer **100** (2006b) 373.
- van Boekel, R., Min, M., Leinert, Ch., and 20 colleagues: *The building blocks of planets within the 'terrestrial' region of protoplanetary disks*, Nature **432** (2004) 479.
- van Boekel, R., Min, M., Waters, L.B.F.M., de Koter, A., Dominik, C., van den Ancker, M.E., Bouwman, J.: *A 10 μm spectroscopic survey of Herbig Ae star disks: Grain growth and crystallization*, Astron. Astrophys. **437** (2005) 189.

3.1 Bericht Teilprojekt 11

3.1.1 Thema / Title

Spektroskopie von astrophysikalisch relevanten Molekülen in der Gasphase und in ultrakalten Helium-Tröpfchen

Spectroscopy of astrophysically relevant molecules in the gas phase and in ultracold helium droplets

3.1.2 Berichtszeitraum / Reported period

15.11.2003 – 31.12.2006

3.1.3 Projektleiter / Principal investigator

Friedrich Huisken, Prof. Dr.
Max-Planck-Institut für Astronomie, Heidelberg
und
Institut für Festkörperphysik, Universität Jena

3.2 Zusammenfassung / Abstract

3.2.1 Wortlaut des Antrags / Abstract of the proposal

Die innerhalb dieses Projekts durchgeführten Laborexperimente sollen einen Beitrag zur Identifizierung der Diffusen Interstellaren Banden (DIBs) leisten. Insbesondere soll untersucht werden, inwieweit Polyzyklische Aromatische Kohlenwasserstoffe (PAHs) und andere kohlenstoffhaltige Moleküle oder Cluster als mögliche Träger in Frage kommen. Die Experimente werden parallel und aufeinander abgestimmt an zwei verschiedenen Molekularstrahlapparaturen durchgeführt. In einer mehrstufigen Hochvakuumapparatur werden neutrale und kationische PAHs sowie Kohlenstoff-Cluster und Nanoteilchen in ultrakalte Helium-Nanotröpfchen eingebettet und mit Hilfe der sehr empfindlichen laserinduzierten Fluoreszenz sowie der massenspezifischen Depletion-Methode im Bereich zwischen 400 und 900 nm spektroskopiert. Im Gegensatz zur konventionellen Matrixspektroskopie weisen die Spektren wegen der viel geringeren Wechselwirkung nur sehr geringe Linienverschiebungen auf, so dass ein besserer Vergleich mit astrophysikalischen Beobachtungen

möglich wird. In einer zweiten Apparatur sollen die gleichen bzw. ähnliche Spezies mit einer ebenfalls sehr empfindlichen Methode, der Cavity Ring-Down Spektroskopie (CRDS), im Expansionsbereich eines Molekularstrahls untersucht werden. Diese Methode, die insbesondere zum Studium kleiner geladener PAHs geeignet ist, bietet den Vorteil einer echten Gasphasenspektroskopie an freien isolierten Spezies.

The laboratory experiments carried out within this project aim at contributing to the identification of the diffuse interstellar bands (DIBs). In particular, we will explore to what extent polycyclic aromatic hydrocarbons (PAHs) and other carbon-containing molecules or clusters can be made responsible for this observation. The experiments will be carried out in parallel in two different molecular beam machines. In the first high-vacuum apparatus, which consists of several stages, neutral and cationic PAH molecules as well as carbon clusters and nanoparticles will be incorporated into ultracold helium nanodroplets, and their spectroscopy will be studied in the spectral region between 400 and 900 nm using mass-specific depletion techniques and laser-induced fluorescence. In contrast to conventional cryogenic matrix spectroscopy, the spectra are characterized by smaller shifts, due to the significantly reduced interaction with the host. This allows for a better comparison with astrophysical observations. In another apparatus, the same or similar species will be investigated in the expansion region of a nozzle beam, employing a very sensitive method, namely cavity ring-down spectroscopy (CRDS). This method, which is particularly suited for the study of small charged PAHs, offers the advantage of genuine gas phase spectroscopy of isolated free species.

3.2.2 Zusammenfassung des Berichts / Abstract of the report

In the course of the present project, we have performed various studies on a number of PAHs either in the gas phase or in liquid helium droplets. At first, the PAH *cations* of naphthalene and anthracene were studied in the expansion of a supersonic jet employing cavity ring-down spectroscopy (CRDS). The absorption bands are rather broad which is partly due to the insufficient cooling of the vibrational degrees of freedom. The larger PAH, 2,3-benzofluorene, was studied as *neutral* species in the gas phase, *i.e.* in the expansion of a supersonic jet, and in liquid helium droplets using molecular beam depletion spectroscopy (MBDS). It turned out that, for this molecule, the matrix shift is rather small ($<5\text{ cm}^{-1}$) whereas for an argon matrix the shift is 250 cm^{-1} . Another molecule that we have studied is benzo[ghi]perylene which is composed of 6 rings. We concentrated on the weak $S_1 \leftarrow S_0$ transition and located the origin at

$25\,027\text{ cm}^{-1}$. For both neutral molecules studied (2,3-benzofluorene and benzo[ghi]perylene) no coincidence with strong DIBs was found. Finally, we have produced our own PAHs by CO_2 laser pyrolysis of hydrocarbons and by separating the molecules from the soot. High pressure liquid chromatography and mass spectrometry reveal that the extract contains various PAHs with masses up to 600 amu. First spectroscopic experiments applied to the extract (employing both CRDS in the gas phase and MBDS in liquid helium droplets) confirmed the presence of phenanthrene and anthracene as prominent constituents.

3.3 Ausgangsfragen, neuester Stand der Forschung / Initial goals, current status of the field

The Diffuse Interstellar Bands (DIBs), first discovered in 1922, represent the oldest unsolved problem in astronomical spectroscopy. Surveys with sensitive CCD detectors have shown that they consist of more than 250 absorption lines in a spectral region reaching from the blue to the IR (400 – 800 nm) (Jenniskens & Désert 1994, Herbig 1995, Galazutdinov *et al.* 2000, Tuairisg *et al.* 2000). The individual bands vary in intensity and width. In general, they are too broad to be identified as atomic lines. On the other hand, if recorded with very high resolution, some bands reveal finer details that resemble the rotational fine structure of gas phase molecules. In fact, it is now well accepted that the carriers of the DIBs must be gas phase molecules.

Compatibility with astrophysical constraints (photostability, producibility under astrophysical conditions, and abundance criteria of the elements) led to the suggestion of only a few families of molecules (Snow 1995). These are carbon chains (C_n), unsaturated hydrocarbon chains (C_nH_m), fullerenes, and polycyclic aromatic hydrocarbons (PAHs).

3.3.1 Initial Goals

In order to contribute to the clarification of the diffuse interstellar bands, we proposed to carry out electronic spectroscopy of PAH cations in supersonic jets using cavity ring-down spectroscopy (CRDS). The first species to be studied should be naphthalene⁺ (Np^+) and anthracene⁺ (An^+). At a later stage, we wanted to investigate larger cations. Besides PAH cations, it was also planned to study the absorption behavior of neutral PAHs whose absorption bands are located at shorter wavelengths than those of their cationic counterparts. Here it was the goal to go to increasingly larger species which are more difficult to prepare in the vapor phase.

At the same time and in another molecular beam apparatus, it was planned to study the same PAH molecules (neutral and cationic) in liquid helium droplets by mass spectrometer-assisted molecular beam depletion spectroscopy (MBDS). This technique has various advantages, among which the low temperature achieved for *all* degrees of freedom and the low sample concentration required are most noteworthy. On the other hand, the spectra will be affected by a small matrix effect (band shift and broadening); but, in conjunction with the gas phase spectra, very valuable information on internally *cold* molecules can be anticipated.

While the described studies are carried out with PAH samples which can be purchased from chemical suppliers or which are synthesized by cooperating organic chemists, it was also proposed to prepare our own carbonaceous samples employing CO₂ laser pyrolysis of carbon-containing gaseous precursors. These experiments should be carried out in collaboration with Dr. Ion Voicu from the National Institute for Lasers, Plasma and Radiation Physics in Bukarest/Romania who is an expert in fullerene production using this method. In contrast to purchased PAHs which are synthesized by standard wet chemical methods, it is expected that laser pyrolysis will give rise to the production of PAH species which are difficult to obtain by other means. It is hoped that the high temperature achieved during synthesis will favor the production of the most stable species which are able to survive under harsh astrophysical conditions. The molecules prepared by this technique should be studied by both CRDS in the gas phase and MBDS in helium droplets.

3.3.2 Current status of the field

In recent years, after the start of the present project, the absorption spectra of a few PAHs have been investigated under conditions relevant for astrophysics. They include neutral species such as perylene (Tan & Salama 2005a) and benzo[ghi]perylene (Tan & Salama 2005b), the cations of pyrene and acenaphthene (Biennier *et al.* 2003; Biennier *et al.* 2004), and those of 1-pyrenecarboxyaldehyde and 1-methylpyrene (Tan & Salama 2006). The main result of these studies is that the bandwidths are much larger in the electronic spectra of cations ($20 - 30 \text{ cm}^{-1}$) than in the spectra of neutral molecules. The large bandwidth is attributed to the short lifetime of the cations. Since the width of most DIBs is about $2 - 5 \text{ cm}^{-1}$, which is comparable to the bandwidths observed in the spectra of neutral PAHs, cations, as they have been characterized so far, do not seem to be good candidates for DIB carriers (Tan & Salama 2005a).

Carbon chains and derivatives have been candidates for carriers of DIBs since a long time. Such species have been extensively studied in supersonic expansions by the group of Maier in Basel. An important outcome of these investigations is that such chains and their simple derivatives cannot be associated with strong DIBs if they contain less than ten carbon atoms (Maier *et al.* 2004). Carbon rings form a new class of molecules that has come under investigation in context with DIBs. The study of band profiles in the electronic spectrum of the C_{18} ring suggests that “platelike nonpolar molecules” with sizes from C_{20} to C_{100} could possibly explain the structures observed in some DIBs (Maier *et al.* 2006).

The dissociation mechanism of PAHs following the absorption of photons has become a research topic since it is expected to occur in the interstellar medium. The dissociation of the fluorene cation under conditions similar to those encountered in the ISM has been studied by Van-Oanh *et al.* (2006a, 2006b).

Recently, it has been proposed by scientists of NASA Ames that N-substituted PAHs, so-called polycyclic aromatic nitrogen heterocycles (PANHs), could be present in molecular clouds since nitrogen is rather abundant and reactive. Therefore, such species should also be considered as possible candidates responsible for some of the DIBs. Both, experimental (Bernstein *et al.* 2005; Mattioda *et al.* 2005) and theoretical work has already been carried out to follow this idea. Recent calculations on N-substituted circumcoronene cations show that the C-C stretching frequency shifts to higher energies when the N-atom moves from a peripheral position to the center of the molecule (Mattioda 2006).

3.4 Angewandte Methoden / Experimental methods

3.4.1 CRDS in supersonic jets

Cavity ring-down spectroscopy is a very sensitive absorption technique which was developed in the 80ies of the last century (O’Keefe & Deacon 1988). It is based on the measurement of the decay or ring-down of the laser intensity coupled into a resonator of extremely high quality. The sensitivity is high enough to carry out direct absorption experiments in the low density environment of a molecular beam or supersonic jet. Preferably, the molecular beam is provided in a pulsed mode. The nozzle, into which $\sim 0.1 \text{ cm}^3$ of PAH powder is placed, can be heated up to 500°C . Thus, we achieve sufficiently high vapor pressures for many PAHs with less than 6 aromatic rings. In order to obtain

efficient rotational cooling in the expansion (~ 10 K), argon is used as carrier gas. By combining the pulsed nozzle with an electric discharge, it is possible to generate a plasma in which radicals and ions are produced (Motylewski & Linnartz 1999). For the study of neutral molecules, the discharge device was removed, in order to achieve a better cooling.

3.4.2 MBDS of helium droplets containing PAH molecules

Matrix isolation spectroscopy (MIS) has been very popular to study the spectroscopy of PAHs and other species of astrophysical interest at low temperature (Ruiterkamp *et al.* 2002). Conventional matrix materials (N_2 , Ar, and Ne), however, suffer from the fact that the spectral bands are shifted (easily by $\sim 100 \text{ cm}^{-1}$) and broadened, due to the interaction with the matrix material. An innovative and elegant means to employ helium, the least interactive rare gas, as matrix material has been pioneered by the laboratories of Scoles (Higgins *et al.* 2001) and Toennies (Toennies & Vilesov 2004). Helium is expanded at high pressure (~ 20 bar) through a small ($\sim 5 \text{ }\mu\text{m}$) nozzle cooled to temperatures below 20 K. Under such conditions, the helium atoms condense and form clusters and even nanodroplets containing up to several thousand helium atoms. If the beam of helium droplets is directed through a pick-up cell containing PAH molecules at sufficiently high pressure ($>10^{-6}$ mbar), the molecules are incorporated upon collisions into the interior of the helium droplets and carried by them to the ionizer of a quadrupole mass spectrometer. Here they are detected on the mass of the incorporated PAH since all helium atoms are evaporated following the ionization process. Spectroscopy can be performed by exciting the PAH molecules in the droplets with a tunable laser beam. The absorption can be monitored by the following laser-induced fluorescence (LIF) or the induced evaporation of helium droplets using molecular beam depletion spectroscopy (MBDS).

3.4.3 PAH synthesis by laser pyrolysis of gaseous precursors

In a cooperation with Dr. Ion Voicu, National Institute for Lasers, Plasma and Radiation Physics, Bukarest, we have employed cw CO_2 laser pyrolysis of hydrocarbons (C_2H_2 and C_2H_4) with laser powers around 650 W to produce our own PAH samples. Efficient PAH formation was achieved by adding a small amount of benzene which acts as nucleation center. It turned out that the soot produced by this method contained up to 30 weight % of PAHs. The soot was used in its original form and heated to release the PAH molecules into the vapor phase and to carry out laser

spectroscopy using both CRDS and MBDS. Helium droplet incorporation was found to be ideally suited to perform mass spectrometry and to obtain information on the PAH molecules present in the soot. In addition and in cooperation with Dr. Harald Mutschke (TP 8), the soluble part of the carbonaceous powder (which is mainly composed of PAHs) was separated from its insoluble counterpart by soxhlet extraction in toluene. Various techniques were used to obtain additional information on the composition of the extract. These included UV/visible and IR absorption spectroscopy and gas chromatography combined with mass spectrometry and, finally, high pressure liquid chromatography (HPLC).

3.5 Ergebnisse und ihre Bedeutung / Results and their importance

3.5.1 Electronic absorption spectroscopy of PAH cations

After having studied a few neutral PAH molecules such as pyrene (Rouillé *et al.* 2004; Staicu *et al.* 2004a) and anthracene (Staicu *et al.* 2004a, 2004b), we have devoted our interest to the spectral characterization of small PAH cations (positively charged ions) because, under the severe radiation conditions of the interstellar space, ionized PAH molecules should be more abundant than their neutral counterparts. Successful experiments could be carried out for the naphthalene and anthracene cations, Np^+ and An^+ , respectively (Sukhorukov *et al.* 2004). While naphthalene and its cation consists of two benzene rings, anthracene is composed of three rings in a linear configuration. Both are important PAH candidates which are expected to be present in the interstellar space.

The absorption spectra of Np^+ and An^+ corresponding to the electronic transition between the ground state, D_0 , of the cations and their D_2 states consist of single-peaked bands in the red and near infrared spectral range. Figure 1 shows the gas phase spectra of the two species as obtained in the present study using cavity ring-down spectroscopy (solid curves). They are compared with the spectra obtained earlier by other investigators using matrix isolation spectroscopy (dashed curves; Salama & Allamandola 1991 and Szczepanski *et al.* 1993). In the latter technique, the molecules are trapped (isolated) at low temperature in a matrix of frozen argon. Due to the interaction of the PAH molecules with the host matrix, their absorption spectra are significantly broadened and shifted to the red as is clearly demonstrated in the figure. The comparison further shows that, due to the pronounced shift and broadening, matrix isolation spectra

cannot be used to explain astrophysical observations. Instead, gas phase spectra obtained at low temperature and pressure are mandatory.

It should be mentioned that the absorption band of Np^+ has already been studied before in supersonic jets by Romanini *et al.* (1999) and Biennier *et al.* (2003). Our spectrum agrees very nicely with this earlier result. In contrast, the An^+ spectrum has been observed for the first time in our laboratory.

Regarding the comparison with astrophysical observations, it is interesting to note that, in a dedicated search, Krelowski *et al.* (2001) found two features which were reasonably close to the earlier laboratory observations for Np^+ . It follows that our Np^+ band is also very close. In contrast, our new An^+ band has no analogue in the broad DIB survey of Jenniskens & Désert (1994). It could be that this survey is not representative of PAH-rich regions. Therefore, a dedicated search in the spectral region around 709 nm, where we locate the An^+ absorption band, would be highly desirable.

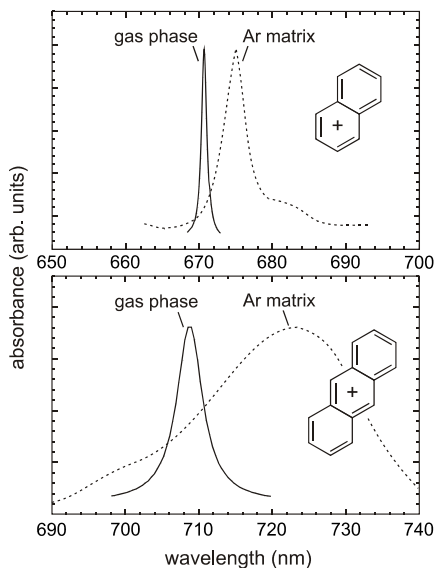


Fig. 1: Comparison of gas phase absorption spectra of Np^+ (top) and An^+ (bottom), measured by CRDS and represented by their Lorentzian fits (solid curves) with argon matrix spectra (dashed curves) (Salama & Allamandola 1991; Szczepanski *et al.* 1993).

In order to obtain information on the vibrational temperature of the PAH cations which were produced in our discharge, we investigated in detail the vibrational bands of neutral anthracene (Staicu *et al.* 2004b). Comparing the results obtained without and with discharge device mounted on the pulsed nozzle, we found that the expansion was seriously disturbed by the apertures of the discharge device. This resulted in rather high rotational (<40 K) and vibrational (~ 500 K) temperatures as could be seen by the broadening of the vibrational bands and the appearance of hot bands, respectively. The discharge itself had only a minor influence on the vibrational temperature. From this observation, we can conclude that the cation bands displayed in Fig. 1 are at least partly broadened as a result of the insufficient cooling of the vibrational degrees of freedom.

An ideal means to obtain vibrationally ultracold cations is provided by the helium droplet technique. After having studied the spectroscopy of a few neutral PAH molecules embedded in helium droplets (pyrene: Rouillé *et al.* 2004; anthracene: Krasnokutski *et al.* 2005), we tried several methods to incorporate PAH cations into helium droplets, but without success. The only method which was finally successful was to incorporate neutral PAH molecules and to ionize the helium cluster subsequently. The positive charge originally localized in the helium droplet diffuses quickly to the molecule giving rise to the formation of a PAH cation. However, due to the charge transfer, approximately 2×10^4 helium atoms are evaporated. Therefore, it is necessary to start with very large helium droplets. On the other hand, the number of helium atoms evaporated as a result of the photo-excitation of the PAH cation is at most 2.5×10^3 . This explains that, up to now, spectroscopic experiments on cations in helium droplets were not successful.

3.5.2 2,3-Benzofluorene

Another PAH molecule that we have studied in both gas phase and helium droplets is 2,3-benzofluorene ($C_{17}H_{12}$) (Staicu *et al.* 2006). Its molecular structure is composed of 1+2 benzene rings with a five-fold ring in between giving rise to a bent structure with only one symmetry element except of the identity, a plane of symmetry. Neither gas phase nor helium droplet spectra were available for this molecule. However, we could resort to argon matrix isolation studies (Banisaukas *et al.* 2004; Geigle & Hohlneicher 1999) which helped us to easily locate the origin of the $S_1 \leftarrow S_0$ transition.

Figure 2 presents the spectra that we have recorded in the wavelength range between 317 and 338 nm. The gas phase spectrum measured by cavity ring-down spectroscopy in the expansion of a supersonic jet using argon as carrier gas and a nozzle temperature of 200 °C is displayed in the bottom panel. The most intense band at 29 894.3 cm^{-1} corresponds to the origin of the $S_1 \leftarrow S_0$ transition. The other bands at higher energies belong to vibronic transitions not yet assigned. Some of

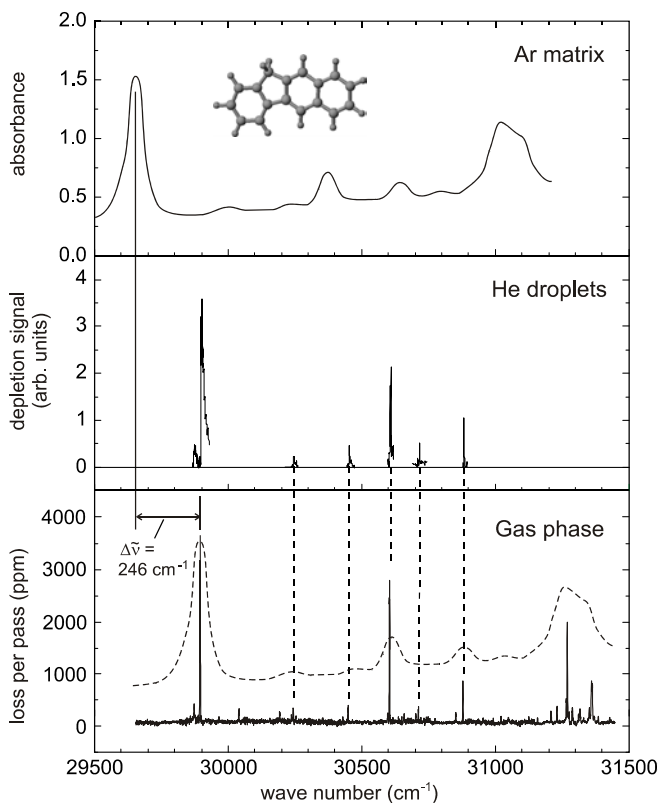


Fig. 2: $S_1 \leftarrow S_0$ absorption spectra of 2,3-benzofluorene measured in the gas phase (supersonic jet) by cavity ring-down spectroscopy (bottom panel) and in helium droplets by molecular beam depletion spectroscopy (middle panel) in comparison with the Ar matrix study of Banisaukas *et al.* (2004).

the vibronic bands including the origin band have also been measured in helium droplets employing molecular beam depletion spectroscopy with the mass spectrometer tuned to the mass of benzofluorene ($m = 216$ amu). The results are plotted in the frame above the gas phase spectrum. It is important to note that the helium droplet spectrum has not been shifted in frequency. In contrast to some other PAH molecules studied before, it appears that the frequency shifts (compared to the gas phase) are very small (blue shifts between 4.5 and 5.0 cm^{-1}). The uppermost panel shows the argon matrix spectrum measured by Banisaukas *et al.* (2004). For a better comparison, the same spectrum, but shifted by 246 cm^{-1} to higher wave numbers, is also plotted as dashed curve directly above the gas phase spectrum. This comparison nicely reveals that all the broad vibronic features of the matrix spectrum have their much narrower counterparts in the gas phase spectrum. The width of the origin band is with 71 cm^{-1} more than 40 times larger than in the gas phase (1.6 cm^{-1}). In contrast, the vibronic bands observed in helium droplets come very close to those found in the gas phase. More details of the spectroscopy of 2,3-benzofluorene will be published soon (Staicu *et al.*, in preparation). As in the case of the neutral PAHs studied earlier, we found no coincidence with astronomical observations.

3.5.3 The $S_1 \leftarrow S_0$ transition of benzo[ghi]perylene

It is only recently that spectroscopists became interested in benzo[ghi]perylene (BghiP; $\text{C}_{22}\text{H}_{12}$) under conditions relevant for astrophysics. The first study of this molecule cooled in a gas expansion was devoted to the investigation of the strong $S_2 \leftarrow S_0$ transition near 369 nm (Tan & Salama 2005b). At that time, preliminary studies of the much weaker $S_1 \leftarrow S_0$ transition by CRDS in a supersonic expansion were initiated by our group. Moreover, an absorption spectrum covering the region which includes both transitions had been recorded by argon matrix spectroscopy at 12 K. The goal was to determine whether the $S_1 \leftarrow S_0$ transition, and especially the origin band of the system, could be detected. We estimated that we would be working close to the limit of the sensitivity of our CRDS set-up.

In the meantime, the absorption spectrum of jet-cooled BghiP has been successfully recorded and investigated (Rouillé *et al.*, submitted for publication). According to HPLC measurements carried out in our group, it was found that the commercial samples contained traces of perylene (on the order of 1%). As a consequence, the upper trace in Fig. 3 shows bands of the $S_1 \leftarrow S_0$ transition of benzo[ghi]perylene and perylene as well. The

center trace shows a control spectrum of perylene, and the lower trace represents the difference between the two spectra, emphasizing the bands related to BghiP (marked by circles).

The analysis of these spectra concerning band positions and rotational contours has yielded the position of the origin band of the $S_1 \leftarrow S_0$ transition of BghiP at 399.567 nm ($25027.1 \pm 0.2 \text{ cm}^{-1}$ in vacuum). In addition, the fundamental frequencies of a dozen vibrational modes for the S_1 states of BghiP could be specified. It was important to determine the position of the origin band, in order to test the accuracy of theoretical predictions established by the means of TD-DFT-based calculations (Tan & Salama 2005b). Our conclusion is that such calculations do not perform well, especially compared to calculations based on semi-empirical models.

Incidentally, the analysis of the spectra has also yielded the position and assignment of about twenty new bands in the $S_1 \leftarrow S_0$ transition of perylene, and of a dozen bands associated with complexes of perylene with argon.

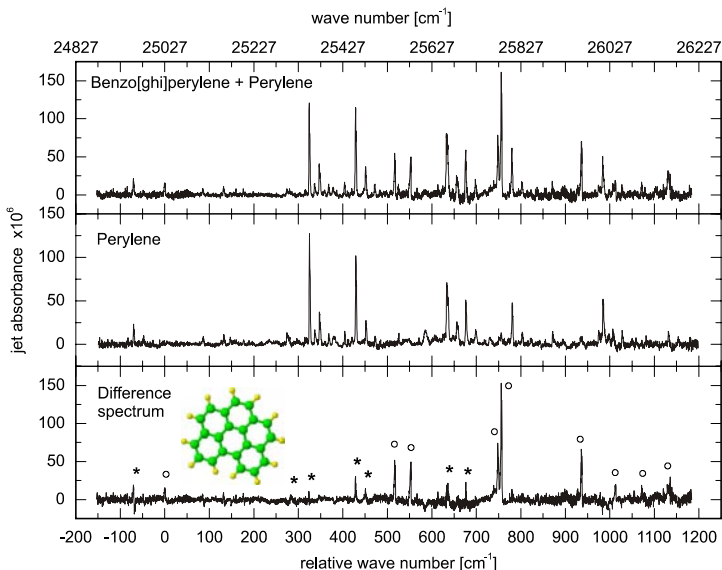


Fig. 3: CRDS spectra of benzo[ghi]perylene containing 1% of perylene (top) and pure perylene (middle), as well as the difference spectrum (bottom). The peaks designated with circles are assigned to benzo[ghi]perylene while those labelled with an asterisk are reminiscent of perylene.

Evaluating the upper trace of Fig. 3 and comparing two bands of BghiP and perylene exhibiting the same absorbance, we obtained the result that the absorption cross section related to the perylene band is about hundred times larger than the one corresponding to the BghiP band. This ratio is indicative of the very weak oscillator strength of the $S_1 \leftarrow S_0$ transition in benzo[ghi]perylene.

Finally, the comparison of the jet-cooled gas-phase spectrum with the spectrum measured in an argon matrix reveals a larger redshift for the $S_2 \leftarrow S_0$ transition than for the $S_1 \leftarrow S_0$ transition. The essential cause of redshifted electronic transition energies for PAHs in rare gas matrices is the increase of the dispersion interaction energy. In a basic model, this value depends linearly on the mean static dipole polarizability of the embedded molecule. The larger redshift of $S_2 \leftarrow S_0$ is therefore attributed to a higher polarizability of BghiP in its S_2 state than in its S_1 state.

As far as the problem of diffuse interstellar bands is concerned, the comparison of the benzo[ghi]perylene spectrum with astronomical data bases does not lead to any identification. This can be due to the fact that the first strong transition, $S_2 \leftarrow S_0$, near 369 nm, is out of the ranges covered by current DIB surveys. Yet, an interesting point is that the band contour analysis has yielded a band width of 2.7 cm^{-1} associated with a rotational temperature close to 40 K. This supports the assumption that neutral PAHs are better candidates for DIB carriers than their cations which exhibit band widths on the order of $20 - 30 \text{ cm}^{-1}$ (Tan & Salama 2005a). But in order to present electronic transitions at wavelengths longer than 400 nm, neutral PAHs have to be heavier than benzo[ghi]perylene.

3.5.4 PAHs produced by laser pyrolysis

Besides commercially available PAHs, we have also studied the carbonaceous powder that was synthesized by CO_2 laser pyrolysis of a 2:1 mixture of ethylene and benzene vapor. The resulting soot was expected to contain a large amount of PAH molecules as could also be verified by FTIR spectroscopy of the extract obtained by dissolving the soot in toluene. Moreover, UV spectra taken from the toluene extract in hexane suggested that the 3-ring PAHs phenanthrene and anthracene should be a major component (Jäger *et al.* 2006; Jäger *et al.*, in preparation). In order to corroborate this finding, we have investigated the soot as well as the extract using both spectroscopic techniques discussed before, *i.e.*, cavity ring-down and helium droplet spectroscopy. The present investigation has

been focused on the detection of phenanthrene ($C_{14}H_{10}$) as major component of the samples (Staicu *et al.* 2006; Jäger *et al.* 2006).

To calibrate the spectrometers, we have at first characterized the pure chemical substance by measuring the $S_2 \leftarrow S_0$ origin band at $35\,378.2\text{ cm}^{-1}$ (282.7 nm) and $35\,316\text{ cm}^{-1}$ (283.2 nm) in the gas phase and in helium droplets, respectively. The results of the complete study of phenanthrene evaporated from the soot and extract are presented in Fig. 3. The right panel shows the gas phase spectra obtained by cavity ring-down spectroscopy while, in the left panel, the results for helium droplets are displayed as obtained by depletion spectroscopy with the mass spectrometer tuned to the mass of phenanthrene ($m = 178\text{ amu}$). In both panels the solid curves refer to the pure substance while the dashed and dotted lines correspond to the soot and extract, respectively. The spectra clearly reveal that phenanthrene is a constituent of all samples. The smaller amplitudes of the respective peaks in the CRDS spectra (compared to the peak of the pure substance) merely reflect the fact that the phenanthrene densities are lower when the soot/extract samples are heated to $130\text{ }^\circ\text{C}$. In

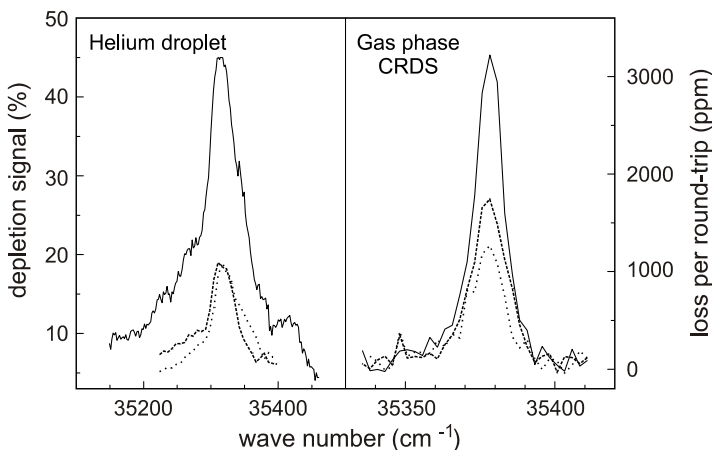


Fig. 4: Phenanthrene absorption spectra measured by cavity ring-down spectroscopy in supersonic jets (right panel) or by depletion spectroscopy in helium droplets (left panel). The solid curves refer to the pure substances of phenanthrene while the dashed and dotted lines correspond to phenanthrene spectra obtained from laser pyrolysis soot or the extract thereof. The soot and extract were heated to $100\text{ }^\circ\text{C}$ in the helium droplet experiment and to $130\text{ }^\circ\text{C}$ in the CRDS study while the pure substances were kept at $-7\text{ }^\circ\text{C}$ or $100\text{ }^\circ\text{C}$ in the respective experiments.

contrast, their smaller amplitudes in the helium droplet spectra (19 % depletion compared to 45 % for the pure substance) indicate that only 42 % of the total count rate at mass $m = 178$ amu originate from phenanthrene. The remaining 58 % are due to other molecules with the same mass (for example anthracene) or fragments of larger PAHs to this mass. Aside from the matrix shift of -62 cm^{-1} , the helium droplet spectra reveal substantial broadening. This is however difficult to quantify since the helium droplet spectra were measured at higher laser energy so that power broadening is effective.

In order to obtain quantitative information on the PAHs produced by laser pyrolysis and to separate the species from each other, high pressure liquid chromatography (HPLC) seems to be most appropriate. After having extracted the soluble molecular components from the soot by soxhlet extraction in toluene, the sample was redissolved in benzonitrile and analyzed in our HPLC apparatus (Jäger *et al.*, in preparation). Figure 5 displays the chromatogram together with the assignments of most of the important peaks.

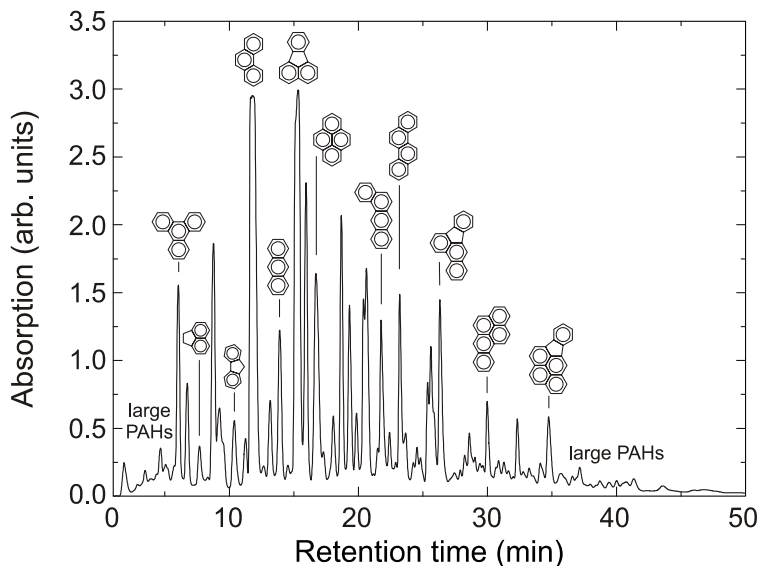


Fig. 5: High pressure liquid chromatogram of the extract of the carbonaceous powder produced by CO_2 laser pyrolysis of a $\text{C}_2\text{H}_4/\text{C}_6\text{H}_6$ mixture. Most of the peaks can be assigned to PAHs.

3.6 Zusammenfassung und Ausblick / Summary and future

Within the present project, we have studied electronic absorption spectroscopy of a few neutral and cationic PAHs in the gas phase at low temperature as provided by a supersonic jet. The method employed was cavity ring-down spectroscopy. In addition, some selected neutral PAHs were also investigated in superfluid helium droplets where the internal degrees of freedom are in equilibrium at 370 mK. For the cations of naphthalene and anthracene, we observed rather broad absorption bands around 671 and 709 nm, respectively. For the neutral species 2,3-benzofluorene and benzo[ghi]perylene, the vibrationless transitions to the lowest electronically excited state (S_1) were determined for the first time to be at 335 nm ($29\,894\text{ cm}^{-1}$) and at 400 nm ($25\,027\text{ cm}^{-1}$), respectively.

Up to now, none of the PAHs (neutral or cationic) studied by other groups or in our laboratory, showed any coincidence with astronomical observations. The cation bands are notoriously too broad. Part of the large bandwidth can be associated with the fact that the cations are not as cold as they are expected to be in astronomical environments. Therefore, experiments with vibrationally relaxed PAH cations (for example in ion traps) are urgently needed. Attempts to incorporate PAH cations into helium droplets were successful; but spectroscopic studies are still missing due to the difficulty to monitor the absorption of photons. Experiments in this direction should be pursued. In contrast, the absorption of neutral PAHs in helium droplets can be conveniently studied by monitoring the resulting evaporation of helium atoms. We studied the PAHs pyrene, anthracene, phenanthrene, and 2,3-benzofluorene. Although the measured bands are somewhat shifted and broadened due to the matrix effect, the data are very valuable especially if they can be compared to gas phase data. Note that the molecular vibrations are definitely cooled.

The experiments carried out so far dealt with PAH molecules that were synthesized by standard wet-chemical procedures. Such synthesis conditions are certainly not representative for astrochemical production routes. Therefore, we propose to use other production techniques which are more relevant for astrophysics. Laser pyrolysis of hydrocarbons could be a good example. Using this technique, we have produced carbonaceous powders with a high concentration of PAHs. The synthesis was performed by our partners in Romania. We were able to extract PAHs with molecular weights up to 600 amu. The first successful spectroscopic characterization was obtained for phenanthrene and anthracene, species which can also be purchased from chemical suppliers. In the future, it will be interesting to study the heavier species as well. However, it will be necessary

to have a means of efficient separation and to be able to collect enough material from the desired species. This should be most conveniently achieved with the high-pressure liquid chromatography (HPLC) apparatus that we have recently acquired.

Acknowledgments

This work was supported by a cooperation between the Max-Planck-Institut für Astronomie and the Friedrich-Schiller-Universität Jena as well as by the Deutsche Forschungsgemeinschaft in the frame of the Forschergruppe *Laborastrophysik*. We are grateful to I. Voicu (National Institute for Lasers, Plasma and Radiation Physics, Bukarest, Romania) for providing the carbonaceous soot.

3.7 Literatur / References

- Banisaukas, J., Szczepanski, J., Vala, M., Hirata, S.: *Vibrational and electronic absorption spectroscopy of 2,3-benzofluorene and its cation*, J. Phys. Chem. A **108** (2004) 3713-3722.
- Bernstein, M.P., Mattioda, A.L., Sandford, S.A., Hudgins, D.M.: *Laboratory infrared spectra of polycyclic aromatic nitrogen heterocycles: Quinoline and phenanthridine in solid argon and H₂O*, Astrophys. J. **626** (2005) 909-918.
- Biennier, L., Salama, F., Allamandola, L.J., Scherer, J.J.: *Pulsed discharge nozzle cavity ringdown spectroscopy of cold polycyclic aromatic hydrocarbon ions*, J. Chem. Phys. **118** (2003) 7863-7872.
- Biennier, L., Salama, F., Gupta, M., O'Keefe, A.: *Multiplex integrated cavity output spectroscopy of cold PAH cations*, Chem. Phys. Lett. **387** (2004) 287-294.
- Galazutdinov, G.A., Musaev, F.A., Krelowski, J., Walker, G.A.H.: *Narrow diffuse interstellar bands: A survey with precise wavelengths*, Publ. Astron. Soc. Pac. **112**, (2000) 648-690.
- Geigle, K.P., Hohlneicher, G.: *Franck-Condon/Herzberg-Teller interferences in weak electronic transitions*, J. Mol. Struct. **480-481** (1999) 247-251.
- Herbig, G.H.: *The diffuse interstellar bands*, Ann. Rev. Astron. Astrophys. **33** (1995) 19-73.
- Higgins, J.P., Reho, J., Stienkemeier, F., Ernst, W.E., Lehmann, K.K., Scoles, G.: *Spectroscopy in, on, and off a beam of superfluid helium droplets*, in: *Atomic and Molecular Beams, The State of the Art 2000*, ed. by R. Campargue (Springer-Verlag, Berlin, Heidelberg, 2001) pp. 723-754.
- Jäger, C., Mutschke, H., Huisken, F., Krasnokutski, S., Staicu, A., Henning, Th., Poppitz, W., Voicu, I.: *Identification and spectral properties of PAHs in*

- carbonaceous soot produced by laser pyrolysis*, *Astrophys. J. Suppl.* **166** (2006) 557-566.
- Jäger, C., Mutschke, H., Huisken, F., Henning, Th., Voicu, I., Poppitz, B.: *Spectral characterization of soot by-products obtained by CO₂ laser pyrolysis of benzene/hydrocarbon vapors*, *Phys. Chem. Chem. Phys.*, to be submitted.
- Jenniskens, P., Désert, F.-X.: *A survey of diffuse interstellar bands (3800 – 8680 Å)* *Astron. Astrophys. Suppl. Ser.* **106** (1994) 39-78.
- Krasnokutski, S., Rouillé, G., Huisken, F.: *Electronic spectroscopy of anthracene molecules trapped in helium nanodroplets*, *Chem. Phys. Lett.* **406** (2005) 386-392.
- Krelowski, J., Galazutdinov, G.A., Musaev, F.A., Nirski, J.: *Identification of the naphthalene cation in space?*, *Mon. Not. R. Astron. Soc.* **328** (2001) 810-914.
- Maier, J.P., Walker, G.A.H., Bohlender, D.A.: *On the possible role of carbon chains as carriers of diffuse interstellar bands*, *Astrophys. J.* **602** (2004) 286-290.
- Maier, J.P., Boguslavskiy, A.E., Ding H., Walker, G.A.H., Bohlender, D.A.: *The gas phase spectrum of cyclic C₁₈ and the diffuse interstellar bands*, *Astrophys. J.* **640** (2006) 369-372.
- Mattioda**, A.L., Hudgins, D.M., Bauschlicher, C.W., Rosi, M., Allamandola, L.J.: *Infrared spectroscopy of matrix-isolated polycyclic aromatic compounds and their ions. 6. Polycyclic aromatic nitrogen heterocycles*, *J. Phys. Chem. A* **107** (2005) 1486-1498.
- Mattioda**, A.L., private communication (2006).
- Motylewski, T., Linnartz, H.: *Cavity ring down spectroscopy on radicals in a supersonic slit nozzle discharge*, *Rev. Sci. Instrum.* **70** (1999) 1305-1312.
- O’Keefe, A., Deacon, D.A.G.: *Cavity ring-down optical spectrometer for absorption measurements using pulsed laser sources*, *Rev. Sci. Instrum.* **59** (1988) 2544-2551.
- Romanini, D., Biennier, L., Salama, F., Kachanov, A., Allamandola, L.J., Stoeckel, F.: *Jet-discharge cavity ring-down spectroscopy of ionized polycyclic aromatic hydrocarbons: progress in testing the PAH hypothesis for the diffuse interstellar band problem*, *Chem. Phys. Lett.* **303** (1999) 165-170.
- Rouillé, G., Sukhorukov, O., Staicu, A., Krasnokutski, S., Huisken, F., Henning, Th.: *Ultraviolet spectroscopy of pyrene in a supersonic jet and in liquid helium droplets*, *J. Chem. Phys.* **120** (2004) 028-6034.
- Rouillé, G., Arold, M., Staicu, A., Krasnokutski, S., Huisken, F., Henning, Th., Tan, X., Salama, F.: *The S₁ ← S₀ transition of benzo[ghi]perylene probed by cavity ring-down spectroscopy in supersonic jets*, *J. Chem. Phys.*, submitted for publication.

- Ruiterkamp, R., Halasinski, T., Salama, F., Foing, B.H., Allamandola, L.J., Schmidt, W., Ehrenfreund, P.: *Spectroscopy of large PAHs - Laboratory studies and comparison to the diffuse interstellar bands*, Astron. Astrophys. **390** (2002) 1153-1170.
- Salama, F., Allamandola, L.J.: *Electronic absorption spectroscopy of matrix-isolated polycyclic aromatic hydrocarbon cations. I. The naphthalene cation*, J. Chem. Phys. **94** (1991) 6964-6977.
- Snow, T.P., In: Tielens, A.G.G.M., Snow, T.P. (eds.): *The Diffuse Interstellar Bands* (Kluwer, Dordrecht, 1995) p. 379.
- Staicu, A., Sukhorukov, O., Rouillé, G., Huisken, F., Henning, Th.: *Cavity ring-down spectroscopy of carbon-containing molecules*, in: *ROMOPTO 2003: Seventh Conference on Optics*, edited by V. I. Vlad, Proc. SPIE **5581** (2004a) 670-676.
- Staicu, A., Rouillé, G., Sukhorukov, O., Henning, Th., Huisken, F.: *Cavity ring-down laser absorption spectroscopy of jet-cooled anthracene*, Molec. Phys. **102** (2004b) 1777-1783.
- Staicu, A., Krasnokutski, S., Rouillé, G., Henning, Th., Huisken, F.: *Electronic spectroscopy of polycyclic aromatic hydrocarbons (PAHs) at low temperature in the gas phase and in helium droplets*, J. Molec. Struct. **786** (2006) 105-111.
- Staicu, A., Krasnokutski, S., Rouillé, G., Huisken, F., Henning, Th., Scholz, R.: *Cavity ring-down spectroscopy of 2,3-benzofluorene in supersonic jets and liquid helium droplets*, Chem. Phys. Lett., to be submitted.
- Sukhorukov, O., Staicu, A., Diegel, E., Rouillé, G., Henning, Th., Huisken, F.: $D_2 \leftarrow D_0$ transition of the anthracene cation observed by cavity ring-down absorption spectroscopy in a supersonic jet, Chem. Phys. Lett. **386** (2004) 259-264
- Szczepanski, J., Vala, M., Talbi, D., Parisel, O., Ellinger, Y.: *Electronic and vibrational spectra of matrix isolated anthracene radical cations: Experimental and theoretical aspects*, J. Chem. Phys. **98** (1993) 4494-4511.
- Tan, X., Salama, F.: *Cavity ring-down spectroscopy and theoretical calculations of the $S_1(^1B_{3u}) \leftarrow S_0(^1A_g)$ transition of jet-cooled perylene*, J. Chem. Phys. **122** (2005a) 084318.
- Tan, X., Salama, F.: *Cavity ring-down spectroscopy and vibronic activity of benzo[ghi]perylene*, J. Chem. Phys. **123** (2005b) 014312.
- Tan, X., Salama, F.: *Cavity ring-down spectroscopy of jet-cooled 1-pyrenecarboxyaldehyde ($C_{17}H_{10}O$) and 1-methylpyrene ($C_{17}H_{12}$) cations*, Chem. Phys. Lett. **422** (2006) 518-521.
- Toennies, J.P., Vilesov, A.F.: *Superfluid helium droplets: A uniquely cold nanomatrix for molecules and molecular complexes*, Angew. Chem. Int. Ed. **43** (2004) 2622-2648.

- Tuairisg, S.Ó., Cami, J., Foing, B.H., Sonnentrucker, P., Ehrenfreund, P.: *A deep echelle survey and new analysis of diffuse interstellar bands*, Astron. Astrophys. Suppl. Ser. **142** (2000) 225-238.
- Van-Oanh, N.-T., Désesquelles, P., Douin, S., Bréchnignac, P.: *Photofragmentation of the fluorene cation: I. New experimental procedure using sequential multiphoton absorption*, J. Phys. Chem. A **110** (2006a) 5592-5598.
- Van-Oanh, N.-T., Désesquelles, P., Bréchnignac, P.: *Photofragmentation of the fluorene cation: II. Determination of the H-loss energy-dependent rate constant*, J. Phys. Chem. A **110** (2006b) 5599-5606.

3.1 Bericht Teilprojekt 12

3.1.1 Thema / Title

Silicium-Nanokristallite in Matrizen und ihre Beziehung zur Extended Red Emission

Silicon nanocrystals in matrices and their relation to the Extended Red Emission

3.1.2 Berichtszeitraum / Reported period

1.02.2004 – 31.12.2006

3.1.3 Projektleiter / Principal investigator

Friedrich Huisken, Prof. Dr.
Max-Planck-Institut für Astronomie, Heidelberg, und
Institut für Festkörperphysik, Universität Jena

Wolfgang Witthuhn, Prof. Dr.
Institut für Festkörperphysik, Universität Jena

3.2 Zusammenfassung / Abstract

3.2.1 Wortlaut des Antrags / Abstract of the proposal

Gegenstand des Projekts ist die Präparation von Silizium-Nanokristalliten in verschiedenen Festkörpermatrizen sowie die Untersuchung ihrer optischen Eigenschaften im sichtbaren und nahen infraroten Spektralbereich. Die Arbeiten sollen Auskunft darüber geben, ob im Festkörper eingebettete Silizium-Kristallite als Träger der Extended Red Emission in Frage kommen. Zur Herstellung der Analogmaterialien sollen im wesentlichen zwei Verfahren Anwendung finden: (1) Implantation von Silizium-Ionen in Quarz- und Silikatträgern und (2) Laserverdampfung von pulverisiertem Si, SiO, SiO₂ und Silikaten mit einem Überschuß an Silizium. Die Ausbildung der Silizium-Nanokristallite erfolgt durch anschließendes Tempern bei 1200 °C. Zur optischen Charakterisierung gehört die Aufnahme von Photolumineszenzspektren nach Anregung mit der vierten Harmonischen eines Nd:YAG-Lasers sowie die Erfassung der

Abklingzeiten. In einer weiteren Experimentreihe soll untersucht werden, inwieweit die Lumineszenz durch Ladungen auf der Oberfläche der Si-Nanoteilchen gequencht wird.

This project aims at preparing silicon nanocrystallites in various solid state matrices and investigating their optical properties in the visible and near infrared spectral regions. The studies will supply information on whether or not matrix-embedded silicon nanocrystallites are possible carriers for the Extended Red Emission. For the preparation of analogue materials, essentially two methods will be employed: (1) Implantation of silicon ions into quartz and silicate substrates, and (2) laser vaporization of Si, SiO, SiO₂ and silicate powders with an excess of silicon. The formation of silicon nanocrystallites is achieved by annealing at 1200 °C. Finally, the optical characterization is performed by recording photoluminescence (PL) spectra after excitation with the 4th-harmonic radiation of a Nd:YAG laser and studying the decay behavior of the PL. In another series of experiments, we will explore to what extend charges on the surface of the Si nanoparticles quench the luminescence.

3.2.2 Zusammenfassung des Berichts / Abstract of the report

Employing the accelerator facilities of the Institute of Solid State Physics of the University of Jena, we have implanted Si ions into quartz windows. By annealing the samples at temperatures around 1000 °C, silicon nanocrystals are formed within the SiO₂ matrix. Upon excitation with UV light, most samples reveal strong photoluminescence (PL) which is believed to result from quantum confinement. The optical properties of the matrix-embedded Si nanocrystals were studied as a function of the implantation conditions, the annealing parameters, and the temperature. The studies concentrated on the spectral and temporal behaviors (PL intensity vs. wavelength and PL intensity vs. time, respectively). In order to simulate matrix environments which resemble magnesium-rich silicates (forsterite and enstatite), we have also implanted magnesium ions at various fluences. It turned out that the PL originating from the silicon nanocrystals is severely quenched when the magnesium density is increased. Other elements (Ca, Na, and Ge) show the same trend. It is assumed that the quenching results from the positive charge (constituting a defect) that remains in the nanocrystal while the electron is trapped by an foreign ion residing at the interface between the Si nanocrystal and the matrix. It is only for Er where we observe an energy transfer giving rise to an enhanced emission of the erbium ion at 1536 nm. As far as the astrophysical implication is concerned, it is concluded that Si nanocrystals are

still promising candidates for the Extended Red Emission. They can be agglomerated to larger free-flying aggregates or they can be embedded in SiO₂ grains. In contrast, Si nanocrystals embedded in silicate grains cannot contribute to the emission due to the non-radiative recombination of the excitons at defects generated in the crystals upon the excitation.

3.3 Ausgangsfragen, neuester Stand der Forschung / Initial goals, current status of the field

Silicon nanocrystals are discussed as possible carriers of the Extended Red Emission (ERE), an astrophysical phenomenon observed in many stellar objects and clouds, and even in the Diffuse Interstellar Medium (Ledoux *et al.* 1998; Witt *et al.* 1998). Recently, our laboratory studies on oxygen-passivated silicon nanocrystals have shown that all ERE spectra known so far can be perfectly matched by laboratory spectra, suggesting that Si nanocrystals are responsible for this astrophysical luminescence phenomenon (Ledoux *et al.* 2001). However, more recent model calculations revealed that free-flying oxygen-passivated Si nanocrystals should give rise to an emission feature around 20 μm , which in fact is not observed in ERE regions (Li & Draine 2002). A possibility to satisfy this constraint is to assume that the Si nanocrystals are not individual free-flying nanoparticles, but instead agglomerated to clusters of nanoparticles or embedded in larger grains of some other material.

3.3.1 Initial Goals

To follow this idea, we have initiated a research program to study the photoluminescence (PL) of Si nanocrystals embedded in various solid matrices. The nanocrystals are generated by producing an excess concentration of silicon atoms in the respective material by ion implantation. Finally, the condensation of Si atoms to silicon nanoparticles and their crystallization is achieved by proper annealing at temperatures of 1000 °C and above (Cheylan & Elliman 1999).

As has been demonstrated by several authors (Garrido *et al.* 2004, Takeoka *et al.* 2000, Kahler & Hofmeister 2001), Si nanocrystals embedded in SiO₂ reveal strong photoluminescence (PL) the origin of which is still controversially discussed (quantum confinement or interface defects). It was planned to employ various implantation and annealing conditions to produce light-emitting samples and to study the spectral and temporal behaviors of this light emission as a function of the synthesis parameters, post-treatment conditions, and temperature. In a second step, it was

planned to dope the samples with Mg^{2+} ions with increasing concentration to simulate the conditions prevailing in magnesium-rich silicate grains (forsterite and enstatite) and to study the effect on the PL of the Si nanocrystals. Other dopants (Ca^{2+} , Na^+ , Ge^+ , Er^{3+} *etc.*) were considered as well. The investigations were aimed at contributing to the question whether Si nanocrystals embedded in Si-based grains were potential candidates for the Extended Red Emission.

3.3.2 Current status of the field

The issue of Si nanocrystals being responsible for the ERE was strongly supported by Witt *et al.* (1998) and Smith & Witt (2002). During the course of the present project, Witt and co-workers performed new observations in the Red Rectangle which is famous for its red luminescence. They discovered a new kind of luminescence in the blue (centered at 375 nm) that they associated with the emission from small neutral polycyclic aromatic hydrocarbons (PAHs) consisting of three to four aromatic rings such as anthracene and pyrene (Vijh *et al.* 2004). Following this study, Mulas *et al.* (2006) computed the phosphorescence emission fluxes for a few candidates and found that only anthracene appears compatible with the observations. On the other hand, Nayfeh *et al.* (2005) bring Si nanocrystals into play again. They suggest that ultrasmall Si nanoparticles with diameters of 1 nm could be the origin of the blue luminescence as well.

Very recent observations of NGC 7023 with the Hubble Space Telescope provided new constraints for the character of the ERE carrier (Witt *et al.* 2006). The authors suggest that the ERE carriers are produced by far-UV photons with energies in excess of 10.5 eV, probably through photoionization or photodissociation of an existing precursor and that the red luminescence results from the excitation of these carriers by near-UV/optical photons. Candidates compatible with this pictures would be doubly ionized PAH molecules (PAH dications). Unfortunately, no laboratory data is available for such exotic species so that the suggestion is difficult to prove. Summarizing the most recent results on the red and blue emissions in the Red Rectangle, it appears that PAHs and Si nanocrystals are at present the most widely discussed carrier candidates.

3.4 Angewandte Methoden / Experimental methods

3.4.1 Ion implantation

In the present study, we used two different kinds of substrates into which the Si ions were implanted: (1) 0.2-mm-thick quartz plates (Heraeus Suprasil 1) and (2) thermally oxidized Si wafers covered with a 300-nm-thick SiO₂ layer (Crystec). The ion implantation was performed employing the ion implanter ROMEO of the Institute of Solid State Physics, Jena. As ion energy, we chose 100 or 105 keV while the ion fluence was varied between 0.5×10^{17} and 2×10^{17} Si ions per cm². According to SRIM calculations carried out for this energy, a distribution of penetration depths with a maximum at 150 nm and a full width at half maximum of 100 nm was determined.

3.4.2 Annealing

The as-implanted samples were annealed for one hour at temperatures between 900 and 1100 °C. In all experiments discussed here, the annealing temperature was 1100 °C. To avoid any further oxidation, the annealing was carried in an atmosphere of nitrogen. When the samples are heated to such temperatures, the implanted Si ions diffuse within the matrix to nucleate and grow to clusters and small nanoparticles. While the melting point of bulk silicon is 1414 °C, Si clusters are expected to be in the liquid state. Upon slow cooling, the Si clusters crystallize to form defect-free Si nanocrystals concentrated in a layer 150 nm below the surface through which the ions were implanted.

3.4.3 Spectral and temporal photoluminescence studies

In contrast to bulk silicon, Si nanocrystals do emit light when they are excited by UV photons. This effect is attributed to the relaxation of the selection rules as a result of quantum confinement. The photoluminescence (PL) of the matrix-embedded Si nanocrystals has been studied in both the spectral and temporal domain using a dedicated self-made PL spectrometer. As excitation source, we used the fourth harmonic ($\lambda = 266$ nm) of a pulsed Nd:YAG laser (Continuum Minilite II, pulse width: 6 ns, maximum energy at 266 nm: 12 mJ per pulse). In order to avoid saturation effects, the UV laser beam is always attenuated to energy values below 15 μ J/pulse. Finally it is focused on the sample to a spot size of 1

mm diameter. The PL emanating from the excited spot is collected by a lens with a focal length of 70 cm and imaged by another lens ($f = 30$ cm) on the 3-mm-wide entrance slit of a 30-cm monochromator (McPherson, model 218-VUV-Vis-IR). The dispersed PL is detected by a l -N₂-cooled photomultiplier (Hamamatsu, model R5509-72) with high detection efficiency in the near-IR (up to 1.7 μ m). PL spectra are recorded by step-scanning the monochromator and collecting the signal in a computer-controlled gated integrator incorporated into a CAMAC module. The decay of the luminescence upon excitation is measured with a digital oscilloscope (Tektronix TDS320). During the decay measurement, the monochromator is parked at a distinct wavelength.

When we want to study the temperature dependence of the photoluminescence the sample is mounted on the cold finger of a closed-cycle helium cryostat (ADP DE-204-SL). The lowest temperature achieved is 6.5 K.

3.4.5 Implantation of foreign ions

After having characterized the samples regarding their optical properties, some of them were exposed to a beam of foreign ions (Mg, Ca, Na, Er). The energy was chosen such that the mean penetration depth was again 150 nm. To heal the defects originating from the second implantation, the samples were annealed at a temperature of 900 °C (post-annealing). The following characterization of the optical properties (PL frequency dependence and excited state lifetime measurements) yields valuable information on the interaction between the Si nanocrystals and the foreign atoms or, more specifically, between the exciton produced upon UV excitation and the foreign atoms in the surrounding SiO₂ matrix.

3.5 Ergebnisse und ihre Bedeutung / Results and their importance

3.5.1 Synthesis of nc-Si embedded in SiO₂ by ion implantation

Nanocrystalline silicon centers (nc-Si) are synthesized by the nucleation of excess silicon supplied by ion implantation in the SiO₂ matrix and by subsequent annealing generally performed at temperatures between 500 and 1200 °C. As shown by Garrido *et al.* (2004), the size of nc-Si depends on the concentration of the excess silicon and the duration of the annealing, but also on the annealing temperature (Cheylan *et al.* 2000). Ion irradiation generates defects in quartz that exhibits parasite luminescence around 650 nm, caused by non-bridging oxygen centers in the SiO₂ matrix. Cheylan *et al.* (2000) clearly demonstrated that an annealing treatment quenches this effect and, on the contrary, enhances the PL originating from the Si nanocrystals.

Figure 1 shows the PL spectra as a function of the excess of silicon for an annealing temperature of 1100 °C. It is seen that the PL maximum shifts to longer wavelengths (smaller energies) when the ion fluence is

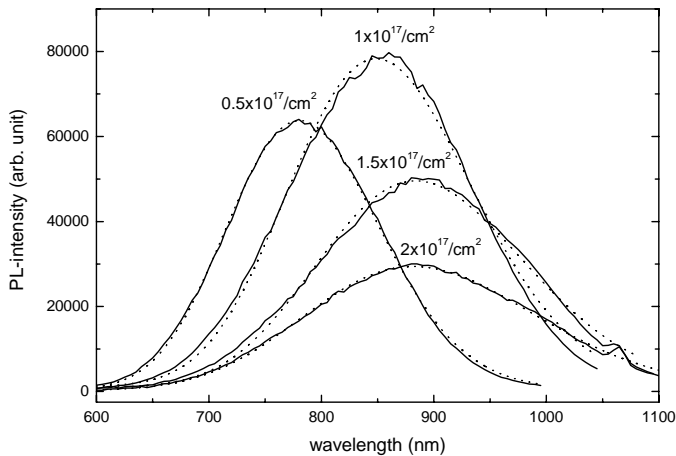


Fig. 1: PL spectra of quartz windows into which silicon was implanted at fluences of 0.5, 1, 1.5, and 2×10^{17} atoms per cm². Annealing at 1100 °C in N₂ was performed for one hour. The peak positions and halfwidths were evaluated by fitting log-normal distributions (dotted lines) to the data.

increased. This can be understood in view of the quantum confinement effect. According to the quantum confinement model, a PL maximum at larger (shorter) wavelength correlates with a larger (smaller) average size of the Si nanocrystals.

For large fluences, the red shift resulting from a further increase of the fluence becomes less pronounced. This is consistent with the asymptotic Ostwald ripening growth model of nc-Si (Garrido *et al.* 2004) where, for one annealing condition (temperature and duration), the size of nc-Si increases with the excess of silicon but to a lower extent.

Figure 1 also shows an increase of the PL intensity when the maximum position moves from 780 to 860 nm and a subsequent decrease for the spectra peaking above 860 nm. This is consistent with the PL yield measured by Ledoux *et al.* (2002) for free nc-Si covered by a SiO₂ layer produced by laser pyrolysis of silane. In their study, the maximum yield was found for an average size of 3.8 nm which corresponds to a PL emission wavelength of 840 nm for the same nc-Si diameter embedded in quartz. This behavior of the PL intensity can be explained by the concerted action of two effects: the decreasing PL efficiency as a result of reduced quantum confinement and the increased probability of encountering a defect in the nc-Si.

3.5.2 Temporal behavior of the photoluminescence from nc-Si

The multi-exponential behavior of the decay curves of an ensemble of nc-Si was observed before by other researchers (Linnros *et al.* 1997). The decay curves are usually fitted by a Kohlrausch function $I(t) = I_0 \exp[-(t/\tau)^\beta]$ where τ is the lifetime and β the dispersion factor. Analogous properties have been observed for the luminescence of CdSe quantum dots. Schlegel *et al.* (2002) and Fischer *et al.* (2003) showed that the multi-exponential feature is intrinsic of one single quantum dot. They noticed that the decay lifetimes correlated strongly with the luminescence intensity fluctuations where a high fluorescence yield is associated with a long fluorescence lifetime. In particular, at the highest fluorescence intensity, the decay curves were found to approach a single-exponential behavior.

In the main frame of Fig. 2, we have plotted the decay curves of the nc-Si PL as measured on a sample produced with an ion fluence of $1 \times 10^{17} \text{ cm}^{-2}$. From left to right, the emission wavelength varies from 675 to 1000 nm in steps of 25 nm, *i.e.* the lifetime increases as the emission wavelength becomes larger. The decay rates were evaluated by fitting

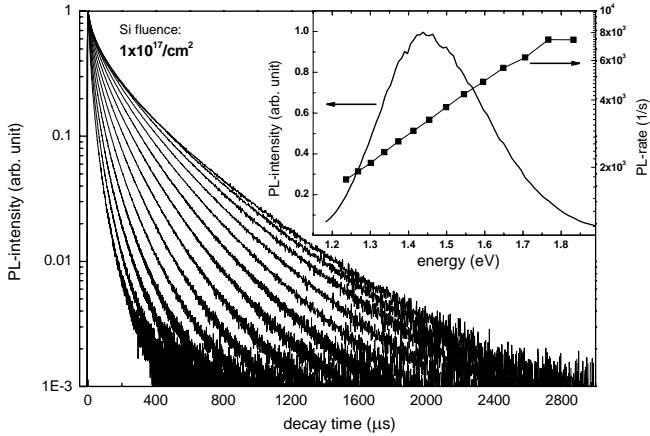


Fig. 2: PL decay curves of silicon quantum dots embedded in quartz recorded from 675 nm (left curve) to 1 μm (right curve) with a step of 25 nm. The inset shows the PL spectrum of the respective sample as well as the decay rates as a function of emission energy.

log-normal decay rate distributions to the measured data using the maximum entropy method of data analysis (Delerue *et al.* 2006). Log-normal rate distributions were also employed to fit the decay curves of CdSe nanocrystals, but with another method (Van Driel 2006). However, it must be underlined that there is by no means a unique solution and that the decay curves can be fitted by different distributions of rates.

In the inset of Fig. 2, it is seen that the decay rate increases exponentially with the emission energy. An exponential increase following an $\exp(-E/E^*)$ law, where E is the photon energy and the parameter E^* varies between 0.2 and 0.4 eV, has been observed by several authors. Here we found $E^* = 0.35$ eV which is similar to the 0.25 and 0.31 eV values, respectively, found by Huisken *et al.* (2002) and Delerue *et al.* (2006). This functional form has always been observed for quantum-confined nanostructures but its physical background still remains unexplained.

3.5.3 Temperature dependence of the PL of nc-Si embedded in SiO₂

Figure 3 shows PL spectra measured at 6.5, 12.5, 25, 50, 100, 200, and 300K in vacuum. As the temperature falls, the PL integrated intensity

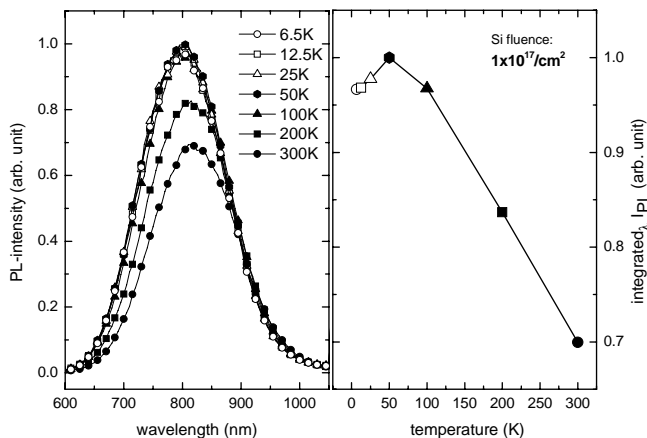


Fig. 3: Temperature dependence of PL emission spectra of nc-Si embedded in SiO₂.

increases and reaches a maximum at 50 K. At the same time, the spectra become broader and shift slightly to the blue.

This effect was also previously reported (Brongersma *et al.* 2000) and explained by a model introduced by Calcott *et al.* (1993) initially for porous silicon. In this model, the localized excitonic levels are split by an energy Δ , due to the exchange interaction between the electron and the hole. The lower level corresponds to a triplet state which has a radiative rate R_T . The upper level corresponds to a singlet state with a radiative rate R_S . The temperature dependence of the total radiative decay rate, R_R , can be evaluated by assuming thermal equilibrium between the two levels. Thus the rate becomes $R_R = [3R_T + R_S \exp(-\Delta/kT)]/[3 + \exp(-\Delta/kT)]$.

At low temperature, only the triplet state is occupied and the radiative decay rate is rather small. When the temperature is raised, the population of the upper level, which is characterized by a faster decay, becomes more important. The PL quantum yield η_{PL} is a function of the radiative and non-radiative rates and can be written as $\eta_{PL} = R_R/(R_R + R_{NR})$. This explains why the PL intensity increases when the temperature is raised from lower values to 75 K, typically reported. The decrease of the PL intensity for temperatures above 75 K can be explained by the fact that non-radiative processes between nc-Si and the SiO₂ matrix become more effective.

3.5.4 Quenching of the photoluminescence by magnesium doping

Quartz windows containing luminescent nc-Si were doped with magnesium by ion implantation with fluences from 3.2×10^{12} to $3.2 \times 10^{14} \text{ cm}^{-2}$ followed by an annealing at 900°C (post-annealing) in an oxygen-free atmosphere for one hour. The implantation energy was chosen such that the magnesium implantation depth coincides with the nc-Si layer location in the quartz window. Directly after implantation, no PL from nc-Si, or at best a very weak PL for the lowest doping ion concentration, was observed. This seems to prove that all or most of the nc-Si were irretrievably damaged as a result of the ion irradiation. The PL was partially recovered after the post-annealing treatment depending on the doping ion fluence, as illustrated in Fig. 4.

The figure illustrates that, as the magnesium fluence increases, the nc-Si PL intensity is more and more quenched. It was also noticed that the luminescence can be completely turned off with Mg fluences higher than $1 \times 10^{15} \text{ cm}^{-2}$. This could be expected by extrapolating the curve in the right panel that describes the PL quenching as a function of the magnesium fluence. The quenching effect is associated with a red shift, which continually increases with the concentration of the dopant. Such doping

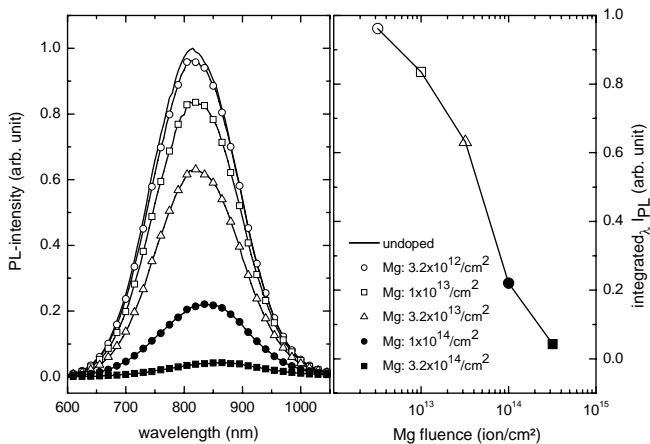


Fig. 4: Effect of Mg doping on the photoluminescence of nc-Si embedded in SiO_2 . Quartz windows containing luminescent nc-Si synthesized by ion implantation with a Si fluence of $1 \times 10^{17} \text{ cm}^{-2}$ and a subsequent annealing at 1100°C were implanted with Mg at different fluences and annealed at 900°C .

effects were also observed by Fujii *et al.* (2003) for nc-Si embedded in SiO₂ and boron as dopant. The samples were produced by co-sputtering using similar dopant concentrations. They could quench the PL down to 3% of the original value with a corresponding red shift of 70 nm. This is similar to our result yielding a maximum red shift of 42 nm in conjunction with a quenching of 4%.

The quenching of the PL can be explained by an interaction between the electron of the exciton with the positively charged Mg which we assume to reside outside the crystalline Si core. The electron is trapped and the hole remaining in the nanocrystal acts as a defect causing the non-radiative recombination of newly formed excitons. Smaller Si nanocrystals are expected to be more sensitive to this effect because the electron can be extracted more easily from the core. As smaller nanocrystals emit at shorter wavelengths, their enhanced quenching results in a red shift of the ensemble spectrum.

It seems that the order of the implantation phases – silicon implantation and magnesium implantation – does not play any role on the quenching of nc-Si PL. This was proved by another experiment, where Si nanocrystals were synthesized in previously doped quartz plates with the same concentrations and where no significant difference was observed. As a result, the PL quenching and the red shift should not be discussed in

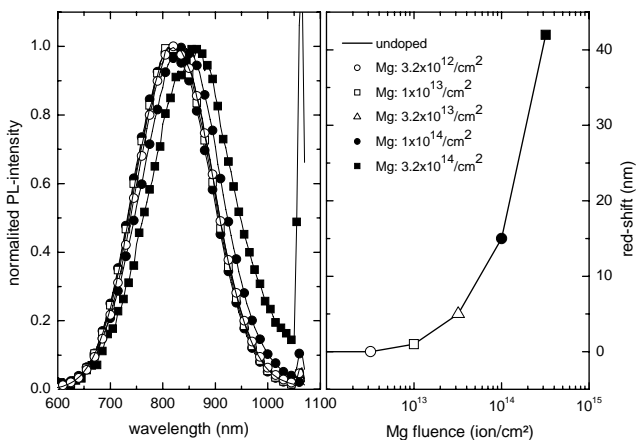


Fig. 5: Effect of magnesium doping on the maximum position of the PL of nc-Si synthesized by ion implantation (left: normalized spectra, right: red shift as a function of Mg fluence).

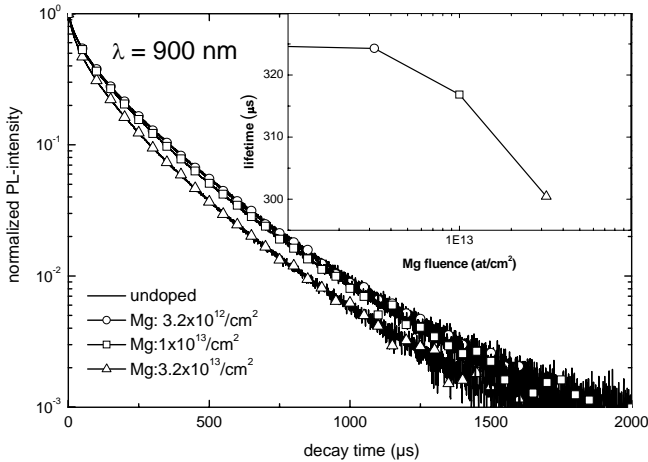


Fig. 6: Effect of magnesium doping on the PL decay of nc-Si synthesized by ion implantation.

terms of ion irradiation effects but in terms of doping and concentration effects.

PL measurements for doped and undoped nc-Si were performed from low temperatures (starting at 6.5 K) to room temperature. They showed that the relative quenching and the inherent red shift between doped and undoped nc-Si samples are independent of the temperature.

In the time domain, the registration of decay curves was performed at several wavelength positions of the PL spectra for undoped and doped samples. A shortening of the decay lifetime (increase of the decay rate) with the doping fluence was observed, as illustrated in the Fig. 6 for a wavelength position of 900 nm. The increase of the decay rate was independent of the emission energy of the PL spectra, and can thus not explain the small red shift observed in the frequency (or wavelength) domain. Such PL shortening behavior was also observed by other researchers for samples doped with B, P (Fujii *et al.* 2003), Au (Tchebotareva *et al.* 2005) and Er (Franzò *et al.* 2000), and were explained by an increase of the non-radiative rates caused by defects due to the presence of dopant ions.

3.5.5 Photoluminescence from erbium coupled with nc-Si in SiO₂

The enhancement of erbium emission coupled with nc-Si has already been studied by other researchers (Franzò *et al.* 2000, Kik *et al.* 2000) and is usually explained as follows. The Si nanoparticles serve as antenna for the erbium ions as they absorb in a broad frequency range as long as the photon energy is larger than the band gap. In the present system, due to the long lifetime of the nc-Si, the excitation energy (corresponding to the band gap) is transferred to the Er ions enabling them to emit at 1536 nm. The attractive feature of this mechanism is the possibility to build amplifiers for the 1536 nm radiation of erbium. Because of this interest, the PL of systems containing nc-Si doped with Er is well documented in the literature. Therefore, we found it interesting to study this interaction and to compare the measurements with our results obtained for other dopants (*e.g.* nc-Si doped with magnesium).

Samples were prepared as described in the preceding section by implanting erbium ions with fluences from 3.2×10^{13} to 3.2×10^{15} cm⁻². The left part of Fig. 7 displays the quenching effect caused by Er doping on the PL spectra of nc-Si when the Er implantation fluence increases, while the right part shows the situation in the wavelength range around 1525 nm where Er³⁺ has an emission band ($^4I_{13/2} \rightarrow ^4I_{15/2}$ at 1.536 μ m). The emission of erbium first increases with the concentration up to a fluence of 3.2×10^{14} cm⁻² and decreases for higher fluences. This can be

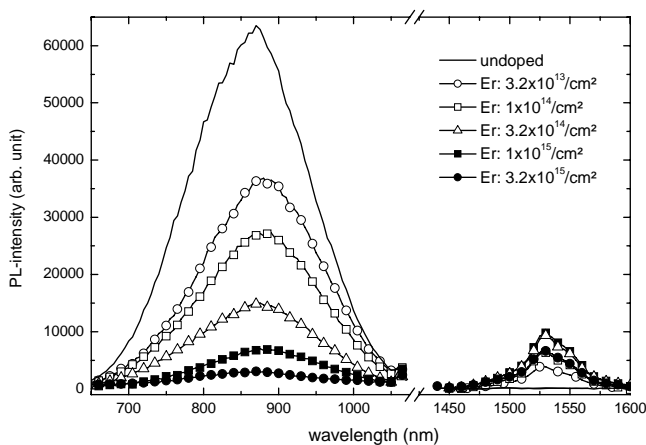


Fig. 7: Photoluminescence from nc-Si and erbium for samples produced with Er fluences between 3.2×10^{13} and 3.2×10^{15} cm⁻².

ascribed to the fact that, as the Er concentration is increased, the number of Er emission centers increases as well. However, when the concentration of damaged nc-Si becomes too important, the exciton concentration available for Er excitation is consequently reduced, resulting in a decrease of the erbium emission.

3.5.6 Other dopants

Similar experiments were carried out with other dopants such as calcium, sodium, and germanium. The effects on the photoluminescence of nc-Si – quenching of PL, shortening of decay lifetimes, and slight red shift – were very similar to those described for magnesium. The results are summarized in Fig. 8 where, for various dopants, the quenching of the nc-Si is plotted as a function of the relative concentration of the foreign atoms ($n_{\text{atom}}/n_{\text{nc-Si}}$).

The concentrations of foreign atoms in the samples investigated in the present study are much lower than those expected in silicate grains. Other experiments, not described here, revealed that, for even higher concentrations, the PL of embedded Si nanocrystals is totally quenched. Only some weak parasite luminescence at lower emission wavelengths, resulting from the presence of defects in the SiO_2 matrix could be de-

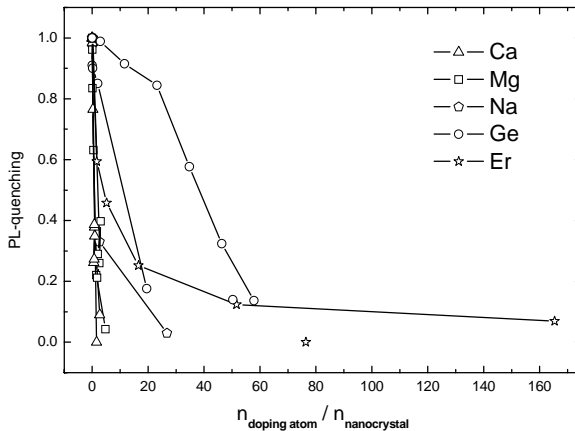


Fig. 8: Quenching of the photoluminescence of nc-Si plotted as a function of the number of foreign atoms per Si quantum dot. Here we have also included our results on calcium, sodium, and germanium which are not discussed in this report.

tected. But this PL is not compatible with astrophysical observations. In summary, the present studies show that silicon nanocrystals embedded in silicate grains cannot account for the Extended Red Emission while Si nanocrystals in SiO₂ grains would still be good candidates together with agglomerated oxidized nc-Si (clusters of Si nanoparticles).

3.5.7 Comparison with other experiments

In Fig. 9, we summarize the results of the PL of silicon nanocrystals as a function of particle size as obtained by various authors using various methods (laser pyrolysis, ion implantation, co-sputtering, reactive evaporation of SiO, and PECVD). The solid line corresponds to the theoretical tight-binding study of Delerue *et al.* (1993) which is considered to be the most accurate computation. This curve is represented by an inverse

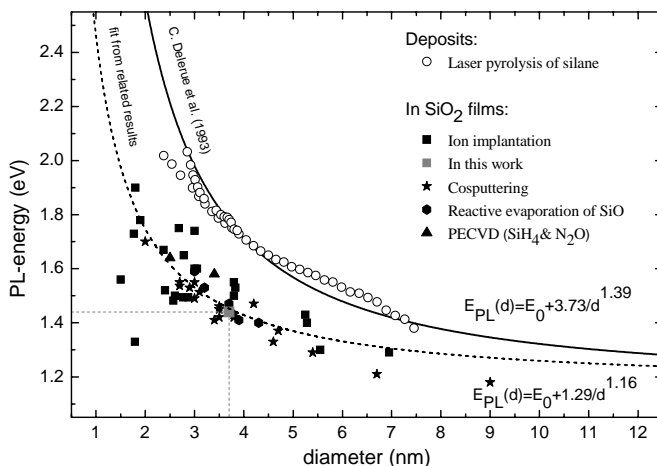


Fig. 9: Maximum positions of the PL curves, in terms of energy, as a function of the diameter of the crystalline core as obtained in various experiments. The open symbols correspond to laser pyrolysis experiments where the nanocrystals were produced as free particles in the gas phase (Ledoux *et al.* 2002). The solid symbols refer to Si nanocrystals in bulk SiO₂ or thin films (ion implantation: Guha *et al.* 2000, Garrido *et al.* 2000, Garrido *et al.* 2004, Hryciw *et al.* 2004, Sias *et al.* 2005, Franzò *et al.* 2001, and this work; co-sputtering: Fujii *et al.* 1998, Kanzawa *et al.* 1996, Mimura *et al.* 1999, Takeoka *et al.* 2000, Conibeer *et al.* 2006; reactive evaporation of SiO: Kahler and Hofmeister 2001; PECVD: Inokuma *et al.* 1997).

power law $E_{\text{PL}}(d) = E_0 + 3.73 d^{-1.39}$, where E_0 is the band gap of bulk silicon. It is seen that only the experimental data obtained for free oxygen-passivated Si quantum dots (Ledoux *et al.* 2002) comply with the theory. The other data points, corresponding to other synthesis methods, reveal smaller band gaps at a given diameter or smaller diameters at a given energy. For identical emission energies of 1.9 eV and 1.5 eV, silicon nanocrystals in a quartz matrix are, respectively, 49% and 43% smaller than free Si nanoparticles covered by a thin SiO₂ layer. The latter data points are best fitted by the power law $E_{\text{PL}}(d) = E_0 + 1.29 d^{-1.16}$.

From one of our samples discussed in the present report (having its PL maximum at $E = 1.44$ eV), we were recently able to obtain a HRTEM image and to determine the average size of the nanocrystals present in the sample ($d = 3.7$ nm). This data point agrees nicely with the other values obtained from ion-implanted samples.

The main difference between laser pyrolysis Si nanoparticles and the other Si nanocrystals is that the former nanoparticles were fully relaxed in the expansion of a supersonic helium jet before they were deposited on a substrate and subjected to a gentle oxidation. They are considered to be stress-free. In contrast, the nanocrystals synthesized by other methods are embedded in thin films or bulk SiO₂ matrices. It could be that they are subject to significant stress and that this is the reason for their different PL behavior. It is also possible that the PL in these systems is not of quantum-confined origin but defect-related as a result of the interaction between the exciton produced in the Si nanocrystal and the environment (matrix, film, or interface). The enhancement of the PL of erbium ions and the quenching of nc-Si PL by foreign ions supports the idea that there is a strong interaction between the Si nanocrystals and the surrounding.

3.6 Zusammenfassung und Ausblick / Summary and future

Within the present project, we have studied the photoluminescence properties of silicon nanocrystals embedded in SiO₂ matrices. The samples were prepared by Si ion implantation followed by an annealing treatment at 1100 °C. It is found that the silicon atoms condense to clusters and nanoparticles in the matrix giving rise to a strong photoluminescence response upon excitation with UV photons. Such systems can be considered as analog materials for astrophysical dust grains (SiO₂ grains containing Si nanocrystals). Comparing the results with those obtained earlier on free Si nanocrystals, which led to the proposal that Si nanocrysts-

tals could be the carriers of the Extended Red Emission (ERE), it is found that the PL of a Si nanocrystal of specific size is shifted to longer wavelength or smaller energy. As a result, if the ERE observations are to be explained by Si nanocrystals embedded in SiO₂ grains, the size regime (2.5 – 6.5 nm) postulated for free nanocrystals must be shifted to (1.5 – 4 nm). Unfortunately, it was not possible to determine the quantum efficiency of the PL of matrix-embedded nc-Si because the size distribution of the nanocrystals is not known with sufficient accuracy. Therefore, it is difficult to obtain quantitative information on the PL strength which would be required to discuss embedded Si nanocrystals in context with the ERE issue.

In order to simulate the situation encountered in magnesium-rich silicate grains, we have implanted Mg ions (and other ions such as Na, Ca, Ge, and Er) with various fluences into the samples containing the luminescent Si nanocrystals. It is found that doping with foreign ions significantly quenches the PL of the Si nanocrystals. In the case of erbium implantation, we could show (together with other researchers) that the excitation energy is efficiently transferred from the Si nanocrystals to the erbium ions. This proves that there is considerable interaction between the crystalline Si cores and the surrounding, raising the question whether this is consistent with a purely quantum-confined origin of the photoluminescence. As far as the astrophysical issue of the ERE is concerned, it is clear that silicate grains with silicon-rich cores cannot be efficient light emitters. Therefore, silicates can be discarded as candidates for ERE carriers.

Acknowledgments

This work was supported by a cooperation between the Max-Planck-Institut für Astronomie and the Friedrich-Schiller-Universität Jena as well as by the Deutsche Forschungsgemeinschaft in the frame of the Forschergruppe *Laborastrophysik*.

3.7 Literatur / References

- Brongserma, M.L., Kik, P.G., Polman, A., Min, K.S., Atwater, A.: *Size-dependent electron-hole exchange interaction in Si nanocrystals*, Appl. Phys. Lett. **76** (2000) 351.
- Calcott, P.D.J., Nash, K.J., Canham, L.T., Kane, M.J., Brumhead, D.: *Spectroscopic identification of the luminescence mechanism of highly porous silicon*, J. Lumin. **57** (1993) 257.

- Carrada, M., Wellner, A., Paillard, V., Bonafos, C., Coffin, H., Claverie, A.: *Photoluminescence of Si nanocrystal memory devices obtained by ion beam synthesis*, Appl. Phys. Lett. **87** (2005) 251911.
- Cheyman, S., Langford, N., Elliman: *The effect of ion-irradiation and annealing on the luminescence of Si nanocrystals in SiO₂*, Nucl. Instr. And Method. In Phys. Res. B **166-167** (2000) 851-856.
- Conibeer, G., Green, M., Corkish, R., Cho, Y., Cho, E.C., Jiang, C. W., Fangsuwannarak, T., Pink, E., Huang, Y., Puzzer, T., Trupke, T., Richards, B., Shalav, A., Lin, K L.: *Silicon nanostructures for third generation photovoltaic solar cells*, Thin Solid Films **511-512** (2006) 654.
- Delerue, C., Allan, G., Lannoo, M.: *Theoretical aspects of the luminescence of porous silicon*, Phys. Rev. B **48** (1993) 11024.
- Delerue, C., Allan, G., Reynaud, C., Guillois, O., Ledoux, G., Huisken, F.: *Multixponential photoluminescence decay in indirect-gap semiconductor nanocrystals*, Phys. Rev. B **73** (2006) 235318.
- Ding, L., Chen, T.P., Liu, Y., Ng, C.Y., Liu, Y.C., Fung, S.: *Thermal annealing effect on the band gap and dielectric functions of silicon nanocrystals embedded in SiO₂ matrix*, Appl. Phys. Lett. **87** (2005) 121903.
- Fisher, B.R., Eisler, H.G., Scott, N.E., Bawendi, M.G.: *Emission Intensity Dependence and Single-Exponential Behaviour In Single Colloidal Quantum Dot Fluorescence Lifetimes*, J. Phys. Chem. B **108** (2004) 143-148.
- Franzò, G., Pacifici, D., Vinciguerra, V., Priolo, F., Iacona, F.: *Er³⁺ ions-Si nanocrystals interactions and their effects on the luminescence properties*, Appl. Phys. Lett. **76** (2000) 2167.
- Franzò, G., Moreira, E.C., Pacifici, D., Priolo, F., Iacona, F., Spinella, C.: *Ion beam synthesis of undoped and Er-doped Si nanocrystals*, Nucl. Instr. and Meth. In Phys. Res. B **175-177** (2001) 140.
- Fujii, M., Toshikiyo, K., Takase, Y., Yamaguchi, Y., Hayashi, S.: *Below bulk-band-gap photoluminescence at room temperature from heavily P- and B-doped Si nanocrystals*, J. Appl. Phys. **94** (2003) 1990.
- Fujii, M., Yoshida, M., Hayashiand, S., Yamamoto, K.: *Photoluminescence from SiO₂ films containing Si nanocrystals and Er: Effects of nanocrystalline size on the photoluminescence efficiency of Er³⁺*, J. Appl. Phys. **84** (1998) 4526.
- Garrido, B., Lopez, M., Gonzalez, O., Perez-Rodriguez, A., Morante, J. R., Bonafos, C.: *Correlation between structural and optical properties of Si nanocrystals embedded in SiO₂: The mechanism of visible light emission*, App. Phys. Lett. **77** (2000) 3143.
- Garrido, B., Lopez, M., Perez-Rodriguez, A., Garcia. C., Pellegrino, P., Ferre, R., Moreno, J.A., Morante, J.R., Bonazos, C., Carrada, M., Claverie, A., de la Torre, J.,Souifiet, A.: *Optical and electrical properties of Si-nanocrystals ion beam synthesized in SiO₂*, Nucl. Instr. and Meth. In Phys. Res. B **216** (2004) 213.

- Guha, S., Qadri, S. B., Musket, R. G., Wall, M. A., Shimizu-Iwayama, T.: *Characterization of Si nanocrystals grown by annealing SiO₂ films with uniform concentrations of implanted Si*, J. App. Phys. **88** (2000) 3954.
- Hryciw, A., Meldrum, A., Buchanan, K.S., White, C.W.: *Effects of particle size and excitation spectrum on the photoluminescence of silicon nanocrystals formed by ion implantation*, Nucl. Instr. and Meth. in Phys. Res. B **222** (2004) 469.
- Huiskens, F., Ledoux, G., Guillois, O., Reynaud, C.: *Light-Emitting Silicon Nanocrystals from Laser Pyrolysis*, Adv. Mater. **14** (2002) 1861.
- Inokuma, T., Wakayama, Y., Muramoto, T., Aoki, R., Kurata, Y., Hasegawa, S.: *Optical properties of Si clusters and Si nanocrystallites in high-temperature annealed SiO_x films*, J. Appl. Phys. **83** (1998) 2228.
- Kahler, U., Hofmeister, H.: *Visible light emission from Si nanocrystalline composites via reactive evaporation of SiO*, Optical Materials **17** (2001) 83.
- Kanzawa, Y., Kageyama, T., Takeoka, S., Fujii, M., Hayashi, S., Yamamoto, K.: *Size-dependent near-infrared photoluminescence spectra of Si nanocrystals embedded in SiO₂ matrices*, Solid State Communication **102** (1997) 533.
- Kik, P.G., Brongersma, M.L., Polman, A.: *Strong exciton-erbium coupling in Si nanocrystal-doped SiO₂*, Appl. Phys. Lett. **76** (2000) 2325.
- Kik, P.G., Polman, A.: *Exciton-erbium energy transfer in Si nanocrystal-doped SiO₂*, Materials Science and Engineering B **81** (2001) 3-8.
- Ledoux, G., Guillois, O., Huiskens, F., Kohn, B., Porterat, D., Reynaud, C.: *Crystalline silicon nanoparticles as carriers for the Extended Red Emission*, Astron. Astrophys. **377** (2001) 707.
- Ledoux, G., Gong, J., Huiskens, F., Guillois, O., Reynaud, C.: *Photoluminescence of size separated silicon nanocrystals*, Appl. Phys. Lett. **80** (2002) 4834.
- Linnros, J., Galeckas, A., Lalic, N., Grivickas, V.: *Time-resolved photoluminescence characterisation of nm-sized silicon crystallites in SiO₂*, Thin Solid Films **297** (1997) 167-170.
- Mimura, A., Fujii, M., Hayashia, S., Yamamotoa, K.: *Quenching of photoluminescence from Si nanocrystals caused by Boron doping*, Solid State Communications **109** (1999) 561.
- Mulas, G., Mallocci, G., Joblin, C., Toublanc, D.: *Estimated IR and phosphorescence emission fluxes for specific polycyclic aromatic hydrocarbons in the Red Rectangle*, A&A **446** (2006) 537-549.
- Nayfeh, M.H., Shadia, R.H., Rao, S.: *Crystalline Si nanoparticles as carriers of the blue luminescence in the Red Rectangle nebula*, Astrophys. J. **621** (2005) L121-L124.
- Schlegel, G., Bohnenberger, J., Potapova, I., Mews, A.: *Fluorescence Decay Time of Single Semiconductor Nanocrystals*, Phys. Rev. Lett. **88** (2002) 137401-1.

- Smith, T.L., Witt, A.N.: *The photophysics of the carrier of the Extended Red Emission*, Astrophys. J. **565** (2002) 304-318.
- Sias, U. S., Amaral, L., Behar, M., Boudinov, H., Moreira, E.C., Ribeiro, E.: Photoluminescence behavior of Si nanocrystals as a function of the implantation temperature and excitation power density, J. Appl. Phys. **98** (2005) 034312.
- Takeoka, S., Fujii, M., Hayashi, S.: *Size-dependent photoluminescence from surface-oxidized Si nanocrystals in a weak confinement regime*, Phys. Rev. B **62** (2000) 16820.
- Tchebotareva, A.L., Michiel, J.A., Biteen, J.S., Atwater, H.A., Polman, A.: *Quenching of Si nanocrystal photoluminescence by doping with gold or phosphorous*, J. Lumim. **114** (2005) 137-144.
- Van Driel, A. F.: *PhD thesis: Light Sources in Semiconductor Photonic Materials*, Universiteit Utrecht (2006).
- Vijh, U.P., Witt, A.N., Gordon, K.D.: *Discovery of blue luminescence in the Red Rectangle: Possible fluorescence from neutral polycyclic aromatic hydrocarbon molecules?*, Astrophys. J. **606** (2004) L65-L68.
- Witt, A.N., Gordon, K.D., Furton, D.G.: *Silicon Nanoparticles: Source of Extended Red Emission?*, Astrophys. J. **501** (1998) L111-L115.
- Witt, A.N., Gordon, K.D., Vijh, U.P., Sell, P.H., Smith, T.L., Xie, R.-H.: *The excitation of Extended Red Emission: New constraints on its carrier from Hubble space telescope observations of NGC 7023*, Astrophys. J. **636** (2006) 303-315.

